

Effects of climate change on the urban drainage system of
Palermo

by Laura Bidera Miceli

February, 2017

*"Gutta cavat lapidem non vi,
sed saepe cadendo"*

(Lucrezio, *De Rerum Natura*, I 314 e IV 1281)

*A mia madre,
guida, complice e fidata consigliera.*

Acknowledge

I would like to express the deepest appreciation to my Advisor Professor Goffredo La Loggia, always available to listen to my needs and to help with suggestions, you have been a great mentor for me.

I would also like to give a special thanks to Professor Valerio Noto that has been more than guidance: always there when I needed, even during holidays or after 9 hours of jet lag. His contribution and feedback have been fundamental for this thesis: without his supervision and constant help this dissertation would not have been possible. Tough as a father and sympathetic as a friend, he is the Professor that every student would deserve.

I am sincerely grateful to my co-tutor Professor Erkan Istanbuluoglu for his hospitality at the University of Washington and for his guidance.

Many thanks also to Elisa Arnone, Domenico Caracciolo, Costanza Aricò, Antonia Incontrera, Fabio Corsino that gave me encouragement and suggestions throughout my Ph.D.

I would like to thank all my group members and friends during my stay at the University of Washington: Claire Beveridge, Ronda Strauch, Nicoleta Carina Cristea, Sai Siddhartha, Christina Bandaragoda and Hannah for their support concerning research matters and also because they made my experience in the USA being such a beautiful adventure!

Finally, the most important and biggest thank to my family that never stopped to be of support for me, especially my mother that accepted and shared all my choices.

Sommario

Questa ricerca mira a studiare la risposta al cambiamento climatico di un sistema di drenaggio urbano. Riconosciuto dal mondo scientifico come un delle più grandi sfide del XXI secolo, il cambiamento climatico rischia di mettere alla prova i centri abitati: più frequenti precipitazioni, alluvioni e ondate di calore saranno i problemi più impegnativi che le città dovranno affrontare.

Ciò potrebbe comportare serie conseguenze per le infrastrutture urbane come i sistemi di trasporto e le reti di drenaggio. Nello specifico, in caso di forti precipitazioni e alluvioni il pericolo è che i sistemi di drenaggio esistenti si rivelino inadeguati. In questo caso le strade vengono sommerse dall'acqua che defluisce sulla superficie impermeabile anche a causa del rigurgito dai pozzetti fognari.

Tuttavia, la bassa risoluzione temporale dei GCM unita alla necessità dei modelli afflusso-deflusso che in ambito urbano richiedono dati ad alta risoluzione, ha portato gli scienziati, da un lato, ad approfondire maggiormente gli effetti del cambiamento in aree extraurbane e, dall'altro, ad occuparsi della progettazione di nuovi sistemi di drenaggio urbano comprendenti strategie innovative di gestione delle acque piovane.

Questo studio vuole invece valutare gli effetti che il cambiamento climatico può provocare su un sistema di drenaggio urbano esistente, confrontando le criticità risultanti con quelle già presenti per stimarne l'eventuale aggravamento.

Abstract

The research here presented aims to investigate the response of an urban drainage system to the effects of climate change. Recognized by scientific world as one of the biggest challenge of the XXI century, climate change could create problems to the urban environments: more frequent rainfalls, floods and heat waves will be the most serious difficulties that cities will need to deal with.

Urban infrastructures, like transport and drainage systems, could be affected by effects of climate change. In detail, for heavy precipitations and floods current drainage system could be insufficient. This could cause waterlogged roads where water runs on the impervious surfaces even by overflowing manholes.

However, low time resolution of *General Circulation Models* together with the need of rainfall-runoff models that require high resolution data in urban environment drove researchers towards a dual approach. They indeed became more and more interested in analysing the effects of climate change in extra-urban areas and, at the same time, in designing new drainage systems including low impact developments (LIDs).

The purpose of this dissertation has been instead to study effects of climate change in a current urban drainage system, comparing its fails to those that already exist and evaluating the potential worsening.

Table of contents

Acknowledge.....	i
Sommario	ii
Abstract.....	iii
Table of contents	iv
List of Figures.....	ix
List of Tables.....	xiii
Introduction	1
PART I.....	5
THEORY	5
Chapter 1	6
Assessing of climate change in urban drainage systems	6
1.1 State of the art of the effects of climate change on urban drainage systems	10
1.1.1 Climate Change scenario generation.....	11
1.1.2 Approaches for Rainfall Disaggregation and Flood Analysis.....	12
1.1.2.1 Statistical downscaling	14
Empirical transfer function methods	15
Re-sampling or weather typing methods.....	16
Stochastic rainfall models.....	17
1.1.3 Hydrologic variability	18
1.2 Uncertainties in analysis of climate change impacts	19
1.2.1 Uncertainties associated to climate variability and its prediction.....	19

1.2.2 Sampling uncertainty	21
1.2.3 Uncertainties associated to hydrological models	21
1.3 Factors increasing impacts of climate change in urban drainage systems.....	22
1.3.1 Spatial structure and planning.....	23
1.3.2 Urbanization.....	24
1.3.2.1 Impacts of urban development on hydrology.....	26
1.4 Current design criteria of the urban drainage management infrastructures.....	27
1.4.1 Combined sewer overflow	30
1.5 Vulnerability of the urban drainage systems	32
1.5.1 Flooding	33
1.5.1.1 Flooding costs.....	33
1.6 Climate adaptation and mitigation measures for urban drainage systems.....	34
1.6.1 Flood risk and management	37
1.6.2 Adaptation Planning.....	39
1.6.2.1 Municipal Adaptation Planning Opportunities.....	40
1.6.2.2 Example of Adaptation Planning: Connecting Delta Cities	41
1.6.3 Sustainable stormwater system	43
1.6.4 Modeling water management.....	46
Chapter 2	48
Methods and models.....	48
2.1. AWE-GEN.....	50
2.1.1. Precipitation	51
2.1.1.1. Neyman-Scott Rectangular Pulse process	51
2.1.1.2. Low-frequency properties of precipitation process	52
2.1.2. Air temperature component.....	54
2.1.3. Cloud cover component	54
2.1.4. Shortwave incoming radiation component.....	55

2.1.5. Vapor pressure component.....	56
2.1.6. Wind speed and atmospheric pressure components.....	57
2.2. General Circulation Models (GCMs) and downscaling procedure	58
2.2.1. General Circulation Models	58
2.2.2. Description of Scenarios	59
2.2.2.1. Stylized Concentration Scenarios.....	60
2.2.2.2. The Socioeconomic Driven Scenarios from the Special Report on Emission Scenarios	60
2.2.2.3. New Concentration Driven Representative Concentration Pathway Scenarios, and Their Extensions	61
2.2.2.4. Comparison of Special Report on Emission Scenarios and Representative Concentration Pathway Scenarios	63
2.2.3. Stochastic downscaling procedure	67
2.2.3.1. Factor of change	69
2.2.3.2. Extension of precipitation statistics to finer time scales	71
2.3. Random cascade disaggregation model.....	72
2.3.1. Moment scaling.....	73
2.3.2. The canonical model	74
2.3.3. The microcanonical model.....	75
2.3.4. Parameter estimation.....	76
2.3.4.1. Parameter estimation-canonical model.....	76
2.4. EPA SWMM Model	77
2.4.1. Modeling Capabilities	77
2.4.2. Typical Applications of SWMM.....	79
2.4.3. SWMM'S CONCEPTUAL MODEL	79
2.4.3.1. Visual Objects	80
2.4.3.1.1. Subcatchments	81
2.4.3.1.2. Junction Nodes.....	82

2.4.3.1.3. <i>Outfall Nodes</i>	82
2.4.3.1.4. <i>Storage Units</i>	82
2.4.3.1.5. <i>Conduits</i>	83
2.4.3.1.6. <i>Pumps</i>	83
2.4.3.1.7. <i>Flow Regulators</i>	84
2.4.3.2. <i>Non-Visual Objects</i>	85
2.4.3.2.1. <i>Climatology</i>	86
2.4.3.2.2. <i>Unit Hydrographs</i>	86
2.4.3.2.3. <i>Time series</i>	86
2.4.3.3. <i>Computational Methods</i>	87
2.4.3.3.1. <i>Surface Runoff</i>	87
2.4.3.3.2. <i>Flow Routing</i>	88
2.4.3.3.3. <i>Surface Ponding</i>	90
PART II	91
STUDY CASE.....	91
Chapter 3	92
Study case: Palermo drainage system.....	92
3.1. The city of Palermo.....	93
3.2. Historic information of Palermo sewer system.....	93
3.3. Current assessment of the drainage system of Palermo.....	95
3.3.1. Separate system and pump station inside shipyard area	96
3.3.2. Pipe connecting shipyard area to the second pump station.....	97
3.3.3. Removal of discharge to the sea.....	97
3.3.4. Building of sewer networks	97
3.3.5. Wastewaters Treatment Plants	98
3.4. Recent flood events.....	98
3.5. Rainfall data.....	100

3.5.1. Data Analysis	100
3.5.2. Estimated Parameter by AWE-GEN	107
3.5.2.1. AWE-GEN results in stationary conditions and current climate.....	107
Chapter 4	112
Implementation, results and considerations	112
4.1. Applications of AWE-GEN: <i>Future runs</i> , weather forcing.....	113
4.1.1. Simulation and selection Series	115
4.2. Downscaling by Cascade Model	122
4.3. Impacts analysis.....	125
Conclusion.....	142
Bibliography	146

List of Figures

Figure 1.1. The difference between the natural ground cover and various types of impervious surfaces in urbanized areas.....	26
Figure 2.1. Schematic representation of the procedure applied on this study.....	49
Figure 2.2. Schematic representation of the procedure applied on this study including downscaling steps.....	50
Figure 2.3. Schematic representation of Neyman-Scott model with rectangular pulses.....	52
Figure 2.4. A flowchart of the used stochastic downscaling methodology (Fatichi et al., 2011).....	69
Figure 2.5. Example of the multiplicative random cascade with branching number $b = 2$ and cascade generator W for scales $n = 0, 1, \text{ and } 2$. (Molnar and Burlandot, 2005).....	73
Figure 2.6. Example of representation of visual objects in EPA SWMM (Rossman, 2010)..	80
Figure 2.7. Conceptual view of surface runoff (Rossman, 2010)	87
Figure 3.1. In blue the sea and the Kemonia and Papireto rivers, in orange the old town, in yellow the necropolis (Incontrera, 2014).....	93
Figure 3.2. Scheme about recovery plan to clean Palermo coast (Incontrera, 2014).....	96
Figure 3.3. Part of the drainage system of Palermo that is matter of this study. Black dots are studied manholes.	99
Figure 3.4. Monthly mean rainfall and temperature in the period 2002-2014 distinguished in wet and dry periods.	102
Figure 3.5. Percentages of wet and dry days for each year	103
Figure 3.6. Monthly rainfall depth for each year	104
Figure 3.7. Monthly average and variability of the rainfall depth.	105
Figure 3.8. Monthly average and variability of the rainfall intensity.	106

Figure 3.9. A comparison between observed (red) and simulated (green) monthly precipitation. The vertical bars denote the standard deviations of the monthly values.....	108
Figure 3.10. A comparison between observed (red) and simulated (green) monthly statistics of precipitation (mean, variance, lag-1 autocorrelation, skewness, frequency of non precipitation, transition probability wet-wet), for the aggregation period of 1 hour.....	108
Figure 3.11. A comparison between observed (red) and simulated (green) monthly statistics of precipitation (mean, variance, lag-1 autocorrelation, skewness, frequency of non precipitation, transition probability wet-wet), for the aggregation period of 24 hours.	109
Figure 3. 12. a) A comparison between observed (red) and simulated (green) fractions of time with precipitation larger than a given threshold [1–10–20mm] at different aggregation periods.	109
Figure 3. 12. b) The same comparison for dry spell length distribution, i.e. consecutive days with precipitation depth lower than 1 [mm]. E_{obs} and s_{obs} are the observed mean and standard deviation and E_{sim} and s_{sim} are the simulated ones.	110
Figure 3. 12. c) The same comparison for wet spell length distribution, i.e. consecutive days with precipitation depth larger than 1 [mm]. E_{obs} and s_{obs} are the observed mean and standard deviation and E_{sim} and s_{sim} are the simulated ones.	110
Figure 3. 13. A comparison between the observed (red crosses) and simulated values of extreme precipitation (green crosses) at (a) 1-hour and (b) 24-hour aggregation periods; (c) extremes of dry and (d) wet spell durations. Dry/wet spell duration is the number of consecutive days with precipitation depth lower/larger than 1 [mm].....	111
Figure 4.1. Average of annual precipitation calculated in 20 years for the three scenarios...	115
Figure 4.2. Average of the annual maximum for each 20-year long series (blue dots) and variability in terms of standard deviation of the maxima (blue bars) for <i>Current</i> scenario.	116
Figure 4.3. Average of the annual maximum for each 20-year long series (blue dots) and variability in terms of standard deviation of the maxima (blue bars) for <i>2100</i> scenario.	116
Figure 4.4. Median series for <i>Current</i> and <i>2100</i> scenarios: 20-year hourly rainfall depth for <i>2100</i> (blue line) and <i>Current</i> scenarios (red dots).....	117
Figure 4.5. 95° Percentile series for <i>Current</i> and <i>2100</i> scenarios: 20-year hourly rainfall depth for <i>2100</i> (blue line) and <i>Current</i> scenarios (red dots).....	117

Figure 4.6. Empirical cumulative distribution functions for <i>2100</i> (blue line) and <i>Current</i> (red dots) scenarios classified by percentile.	118
Figure 4.7. Empirical cumulative distribution functions of 50° percentile series for <i>2100</i> (blue line) and <i>Current</i> (red dots) scenarios considering only values >0.....	119
Figure 4.8. Empirical cumulative distribution functions of 95° percentile series for <i>2100</i> (blue line) and <i>Current</i> (red dots) scenarios considering only values >0.....	119
Figure 4.9. Number of dry and rainy days in median series of <i>Current</i> and <i>2100</i> scenarios.	120
Figure 4.10. Number of dry and rainy days in 95° Percentile series of <i>Current</i> and <i>2100</i> scenarios.	121
Figure 4.11. Mean intensities of rainy days for each series for both <i>Current</i> (blue bars) and <i>2100</i> (red bars) scenarios.....	121
Figure 4. 12. Scheme of aggregation data from 10-minute to 1-hour time step.	123
Figure 4.13. Hourly rainfall intensity of 10 days with time step equal to 1 hour.	124
Figure 4.14. Hourly rainfall intensity of 10 days with time step equal to 15 minutes.....	124
Figure 4.15. Flow from the street system into a partly full pipe (Mark et al., 2004).....	126
Figure 4.16. Flow to the streets from a pipe system with insufficient capacity (Mark et al., 2004).	126
Figure 4.17. Example of environment in which floods might occur. The blue hatching is set at 1.5m above the manhole and this is the threshold for which floods can be differentiated in ordinary and extraordinary.	128
Figure 4.18. Palermo centro storico sewer system. Dots are manholes, links are pipes, and cloud is the rain gage.....	129
Figure 4.19. Palermo centro storico drainage system under median rainfall series of <i>Current</i> scenario: red dots show <i>failures</i>	132
Figure 4.20. Palermo centro storico drainage system under 50° percentile rainfall series of future scenario: green dots show <i>failures</i>	132
Figure 4.21. Nodes in Palermo centro storico drainage system under 50° percentile series that flood in both scenarios.	134
Figure 4.22. Palermo centro storico drainage system under 95° Percentile rainfall series of <i>Current</i> scenario: red dots show every node that flooded.....	135

Figure 4.23. Palermo centro storico drainage system under 95° Percentile rainfall series of future scenario: green dots show every node that flooded..... 135

Figure 4.24. Nodes in Palermo centro storico drainage system under 95° percentile series that flood in both scenarios. 137

Figure 4.25. Nodes in Palermo centro storico drainage system under 50° percentile rainfall series. Comparison of flooding frequency of exceedance between both scenarios that flood in both scenarios. 139

Figure 4.26. Nodes in Palermo centro storico drainage system under 95° percentile rainfall series. Comparison of flooding frequency of exceedance between both scenarios that flood in both scenarios. 140

List of Tables

Table 2. 1. GCMs of the <i>IPCC 4AR</i> . (CMIP3)	64
Table 2. 2. GCMs of the <i>IPCC 5AR</i> (<i>CMIP5 and AMIP</i>)	65
Table 3. 1. Monthly mean rainfall and temperature in the period 2002-2014	101
Table 3.2. Monthly and annual rainfall depth analysis	104
Table 3.3. Monthly and annual rainfall intensity analysis	106
Table 4.1. Comparison of statistic indexes between observed and downscaled datasets	124
Table 4.2. Extract of number of occurrences and frequencies for each node.	131
Table 4.3. Summary of the flooded nodes for the median situation in both scenarios	132
Table 4.4 Summary of the flooded nodes for the 95° percentile situation in both scenarios.	132
Table 4.5. Classification of nodes that flood in both scenarios according to thresholds under the 50° percentile series.....	134
Table 4.6. Classification of nodes that flood in both scenarios according to thresholds under the 95° percentile series.....	137
Table 4. 7. Comparison of flooded nodes between both scenarios for 50° percentile series.	139
Table 4.8. Comparison between both scenarios for 95° Percentile series.....	139

Introduction

Climate change is currently viewed as one of the greatest challenge of the Earth (Adger et al., 2013). Cities have been identified as among the most vulnerable human habitats to the effects of climate change (Stern, 2007; Intergovernmental Panel on Climate Change (IPCC), 2007) because the fact that human induced climate change is inevitable and the impacts of this change pose a threat to populations, infrastructures, and the urban environment (IPCC 2013; Khedun et al., 2014; Wilby, 2007; Whitehead et al., 2009). In a world where the consensus view predicts substantial impacts of anthropogenic climate change on global water cycle in the near term and distant future (Kundzewicz *et al.*, 2007), hydrological impact analysis has become a thriving area of research.

On one hand, some studies have gone beyond asking merely what the potential hydrological impacts of future changes are likely to be, to attempting to model potential adaptation responses of water resource managers to these impacts; on the other hand, just few papers have researched about effects of climate change on urban wastewater by linking future precipitation with current drainage system.

For urban areas, in fact, some of the most significant potential impacts of climate change and further urban development are those related to stormwater management (Semadeni-Davies *et al.*, 2008). Indeed, climate change does not only involve an increase in average

temperature, but it also results in changes to natural phenomena such as extreme temperatures, wind, snowfall, rainfall, and an increase in sea level and, with growing urbanization leading to increasingly extensive impervious surfaces and enhanced climate change effects on urban drainage, changes in urban runoff are an issue of growing concern (Denault et al. 2006; Semadeni-Davies et al. 2008).

The aim of this dissertation is to assess the impacts of CC on urban areas starting from precipitations and ending to evaluate the effects of these rainfalls on the urban drainage systems.

The procedure used for this study includes, firstly, generation of time series. These, created by exploiting *General Circulation Models* (GCMs) simulations and calibrated by parameters from a real weather station, are used by rainfall-runoff model to evaluate the response of the urban drainage system.

One of the first issues to solve is related to the use of GCMs because, even if they are able to simulate globally the climate system of the Earth, they are complex numerical tools including five components: atmosphere, oceans, land surface, sea-ice and the biological and biogeochemistry cycles. Moreover, one of the most important drawbacks of GCMs is that GCMs realizations are only available at the daily or larger aggregation intervals.

This last point clashes with needs in modeling an urban drainage system because urban basins have sub-hourly lag time. It means that running an urban model with series at large time scales is useless and conceptually wrong.

In literature, there is not any procedure that downscale GCMs output at sub-hourly time scale and, for this reason, we have tried to solve this issue through two tools: *Advanced WEather GENerator* (AWE-GEN) (Fatichi et al., 2011) and Random Cascade model.

The *Advanced WEather GENerator* (AWE-GEN) (Fatichi et al., 2011) is an hourly stationary weather generator, capable of reproducing low and high-frequency characteristics of hydro-climatic variables and essential statistical properties of these variables, and its procedure is based on a stochastic downscaling of GCM predictions (Fatichi et al., 2011; 2013).

Since, as discussed, urban catchments require high resolution dataset, we have chosen to disaggregate from hourly to sub-hourly scale by Random Cascade model that is able to distribute rainfall on successive regular subdivisions in a multiplicative manner. This model has been successfully applied to rainfall modeling (Schertzer and Lovejoy, 1987; Over and Gupta, 1994, 1996; Olsson, 1998; Güntner et al., 2001).

Another important problem is that evaluating effects of climate change on an urban drainage system is not an easy issue because many matters are involved and several perspectives can be studied. This means that, in order to pursue the right path, specific goals need to be clear.

In detail, we are interested in investigating the distribution of the floods and their frequency along 20 years. It is important to clarify that this study considers floods just as water depths above the street caused by manhole overcoming and that only their depths above the manholes are going to be assessed, neglecting, for example, flow velocity over the street

For this purpose, we have tried to investigate two aspects of floods among the several impacts: the first related to the spatial distribution of floods and the second referred to their frequency of occurrence.

One of the main reasons why we focus on these effects is that the consequences of climate change in urban areas can affect directly or indirectly human life, also in drastic way: more rapid inputs to receiving water bodies and changes to their natural water balance (Carrière et al. 2007; Delpla et al. 2009) can cause enormous physical and psychological damages to inhabitants that must be prepared for facing first phases of emergency, post floods. Researches about climate change and its effects on urban areas show that intensive localized rainfall and extreme rainfall events could occur.

The described procedure has been applied to the Palermo urban catchment. The choice of using this case study is that, being created in 734 A.D., it can be defined as an ancient city and being its center, main part of this analyses, full of cultural and historic buildings, we are interested in investigating how its drainage system, designed in the 1930, could react under future possible climate condition.

In order to achieve the aim described above, we have decided to create two scenarios: the *baseline* representing the current climate and the *2100* scenario, referring the 2081-2100 period. For each scenario we have used the high resolution data provided by the weather station of *Palermo Uditore* as input, with an ensemble of 32 GCMs RCP 8.5, into AWE-GEN. Through this model, 50 hourly datasets 20-year long are generated and, after analyses for choosing the most characteristic time series, these are downscaled at 15-minute scale by Random Cascade Model and applied as input to Epa Swmm model.

In detail, the manuscript is divided into two main parts: a theoretical part which includes the description of the state of the art of the effects of climate change on urban drainage systems and the models used for the analyses (two chapters); and an experimental part in

which the case study is described and discussed (two chapters). A detailed description of each chapter is given below.

Chapter 1 will provide a description of the GCMs and the state of the art related to the impacts and mitigation measures for floods in urban areas. Chapter 2 will describe models and methods used in this thesis (i.e., AWE-GEN, the *General Circulation Models*, the downscaling procedure and Epa Swmm 5.0). Chapter 3 will present the study case, introducing Palermo, its drainage system and data used for this approach. Finally, Chapter 4 will show results and comments of the applied methodology to the study case.

PART I

THEORY

Chapter 1

Assessing of climate change in urban drainage systems

It is currently believed that the climate is changing largely because of anthropogenic activities that are increasing the amount of greenhouse gases (GHGs) in the atmosphere. The monthly average concentration of CO₂ in the atmosphere has increased from 280 ppm (parts per million; pre-1750 tropospheric concentration) to nearly 400 ppm (398.58 ppm in June 2013) (Tans et al., 2013; Blasing, 2013). The release of GHG and aerosols due to anthropogenic activities are changing the amount of radiation coming into and leaving the atmosphere. These are, in turn, changing the composition of atmosphere that may influence temperature, precipitation, storms and sea level. As the temperature gets warmer, it increases the amount of energy on the earth's surface which causes an intensification of the global water cycle: observed increases in global average air and ocean temperatures, melting of polar ice and significant increases in net anthropogenic radiative forcing revealed that our global climate system is undergoing substantial warming (IPCC, 2014) and rainfall patterns, evapotranspiration, tropospheric water content, and runoff changes are affecting water availability (Khedun et al., 2014). The frequency, intensity, spatial extent, duration, and

timing of extreme precipitation events are also changing (National Research Council 2011). Changes in extremes at both the lower end (e.g. reduction in precipitation leading to droughts) and upper end (e.g. high intensity rainfall resulting in floods) of the range of observed values can be expected and an increased intense of ‘dry and hot’ extremes for many regions around the world was revealed by a number of studies on different climate model projections (Christensen et al., 2003; Semmler et al., 2004; Kundzewicz et al., 2006; Beniston et al., 2007; Tsanis et al., 2011): it is well known that increasing temperatures tend to increase evaporation which leads to more precipitation. Changes in hydro-meteorological extremes can occur in three ways: (i) a shift in the mean, resulting in less low magnitude events and more high magnitude events; (ii) an increase in variability, i.e. more low and high magnitude events; and (iii) a change in the shape of the frequency distribution, i.e. near constant low magnitude events but an increase in high magnitude events (IPCC 2012). These changes will significantly affect frequency and severity of floods.

Deriving relevant precipitation data from climate models is a challenge. CC impact estimations on climatic variables including extreme rainfall, therefore, are most often based on the results of simulations with climate models (atmosphere–ocean circulation models: General Circulation Models (GCMs) and Regional Climate Models (RCMs)). RCMs can use initial and boundary conditions from the output of GCMs for selected time periods of the global simulation. This is commonly known as the nested regional climate modeling technique or dynamic downscaling. Up to now, this approach is one-way; there are no feedback mechanisms from the RCM simulation to the driving GCM. In this simulation scheme, the role of the GCM is to simulate the response of the global circulation to large scale forcing. The RCM accounts for finer scale forcing, like topographic features, in a physical manner, and enhances the simulation of the climatic variables at such space scales. However, at present the understanding of the processes involved in precipitation formation is limited, especially at high spatial and temporal resolution (Baker et al., 2008).

A wide range of global climate models (GCMs) predict key climate variables with fairly coarse temporal and spatial resolution using equations that describe the flow of energy and momentum and the conservation of mass and water vapour. Combinations of dynamic and stochastic downscaling techniques have been used (Onof et al., 2009) to extract the fine-resolution data needed for urban drainage simulations. In a first step, dynamic downscaling is performed by feeding the output from GCMs into a regional climate model (RCM) with the capability to refine the spatial scale of the data.

Hence our ability to model these processes in global and regional climate models is limited. Local, short duration precipitation generating mechanisms cannot be resolved because of numerical stability and computation efficiency considerations, hence limiting the time and space scales in the models. This means that at present there is a limit to how much dynamic downscaling can be applied and still yield realistic results. In any case the dynamic downscaling often results in systematic bias (underestimation) in the estimated extreme precipitation intensities (Dibike et al., 2008; Baguis et al., 2009).

So far, most regional climate model simulations are available at daily time scales and from 25 to 50 km space scales, some also at hourly time scales and 10 km space scales. Higher resolutions are sometimes available, but often these resolutions are a result of incorporating statistical downscaling methods into the dynamic simulations in order to make a bias correction as an inherent feature in the RCM simulation.

Some high resolution RCMs fail in describing the local surface processes over heterogeneous regions. In these cases, the better approach makes use of the lower resolution climate model results and an extra statistical downscaling step (Dibike et al., 2008).

Precipitation changes show substantial spatial and inter-decadal variability. Over the 20th century, precipitation has mostly increased over land in high northern latitudes, while decreases have dominated from 10°S to 30°N since the 1970s. The frequency of heavy precipitation events (or proportion of total rainfall from heavy falls) has increased over most areas (*likely*). Globally, the area of land classified as very dry has more than doubled since the 1970s (*likely*). There have been significant decreases in water storage in mountain glaciers and Northern Hemisphere snow cover. Shifts in the amplitude and timing of runoff in glacier- and snowmelt-fed rivers, and in ice-related phenomena in rivers and lakes, have been observed (*high confidence*).

Climate model simulations for the 21st century are consistent in projecting precipitation increases in high latitudes (*very likely*) and parts of the tropics, and decreases in some subtropical and lower mid-latitude regions (*likely*). Outside these areas, the sign and magnitude of projected changes varies between models, leading to substantial uncertainty in precipitation projections. Thus projections of future precipitation changes are more robust for some regions than for others. Projections become less consistent between models as spatial scales decrease (Bates et al.2008).

By the middle of the 21st century, annual average river runoff and water availability are projected to increase as a result of CC at high latitudes and in some wet tropical areas, and

decrease over some dry regions at mid-latitudes and in the dry tropics. Many semi-arid and arid areas (e.g., the Mediterranean Basin, western USA, southern Africa and northeastern Brazil) are particularly exposed to the impacts of CC and are projected to suffer a decrease of water resources due to CC (*high confidence*).

Increased precipitation intensity and variability are projected to increase the risks of flooding and drought in many areas. The frequency of heavy precipitation events (or proportion of total rainfall from heavy falls) will be *very likely* to increase over most areas during the 21st century, with consequences for the risk of rain-generated floods. At the same time, the proportion of land surface in extreme drought at any one time is projected to increase (*likely*), in addition to a tendency for drying in continental interiors during summer, especially in the sub-tropics, low and mid-latitudes.

Globally, the negative impacts of future CC on freshwater systems are expected to outweigh the benefits (*high confidence*). By the 2050s, the area of land subject to increasing water stress due to CC is projected to be more than double that with decreasing water stress. Areas in which runoff is projected to decline face a clear reduction in the value of the services provided by water resources. Increased annual runoff in some areas is projected to lead to increased total water supply. However, in many regions, this benefit is likely to be counterbalanced by the negative effects of increased precipitation variability and seasonal runoff shifts in water supply, water quality and flood risks (*high confidence*).

CC refers to ‘the variation of a zone’s weather pattern which is attributed directly or indirectly to human activity that alters the composition of the global atmosphere and which is, in addition to natural climate variability, observed over comparable periods of time’ (IPCC, 2014). This can be identified statistically by changes in mean (average) properties that persist over an extended period of time (decades or longer) (IPCC, 2014). CC is due to natural causes (variation in solar cycles, volcanic eruptions, etc.) and to persistent human-induced activities that cause (GHG) emissions such as industrial production, transport, construction, etc.

Current water management practices may not be robust enough to cope with the impacts of CC on water supply reliability, flood risk, health, agriculture, energy and aquatic ecosystems. In many locations, water management cannot satisfactorily cope even with current climate variability, so that large flood and drought damages occur. As a first step, improved incorporation of information about current climate variability into water-related management would assist adaptation to longer-term CC impacts. Climatic and non-climatic factors, such as

growth of population and damage potential, would exacerbate problems in the future (*very high confidence*).

CC challenges the traditional assumption that past hydrological experience provides a good guide to future conditions. The consequences of CC may alter the reliability of current water management systems and water-related infrastructure. While quantitative projections of changes in precipitation, river flows and water levels at the river-basin scale are uncertain, it is *very likely* that hydrological characteristics will change in the future. Adaptation procedures and risk management practices that incorporate projected hydrological changes with related uncertainties are being developed in some countries and regions.

Therefore, the standards concerning the design and management of storm-water infrastructures, such as storm drainage have to be adapted to the changing hydrologic processes under future climate.

1.1 State of the art of the effects of climate change on urban drainage systems

Evaluating regional impacts from possible CC on urban drainage requires a methodology to estimate extreme and short-duration rainfall statistics for the time period and the geographical region of interest. For historical conditions, CC effects can be investigated by analyzing trends in long-term historical records of rainfall. For future conditions, projected changes in rainfall statistics are based on future scenarios in GHG emissions simulated in climate models or statistical extrapolation based on historical observations. These changes need to be transferred to changes in the urban drainage model inputs.

Many researchers have examined the effects of CC on urban drainage infrastructure and municipal areas (Niemczynowicz, 1989; Waters et al., 2003; Papa et al., 2004; Ashley et al., 2004; Denault et al., 2006; Mailhot et al., 2006; Mailhot et al., 2007). Grum et al. (2006) simulated and analyzed the effects of extreme rainfall on an urban drainage system using the RCM model. Berggren et al. (2007) evaluated the overall effects of CC on urban areas. Olofsson (2007) analyzed the characteristics of urban drainage systems in consideration of B2 and A2 scenarios among the SRES scenario families. Willems et al. (2012) provided a critical review of the current state-of-the-art methods for assessing the impacts of CC on precipitation on the urban catchment scale. Arnbjerg-Nielsen et al. (2013) demonstrated that there are still many limitations in understanding how to describe precipitation in a changing climate in order to design and operate urban drainage infrastructure. Zhou (2014) suggested an integrated and trans-disciplinary approach for sustainable drainage design.

Semadeni-Davies et al. (2008) evaluated the effects on combined sewer systems in urban areas using the DHI MOUSE model. Berggren et al. (2011) investigated the hydraulic performance of urban drainage systems related to changes in rainfall and, through hydraulic parameters such as water levels in nodes (e.g., number of floods and frequency and duration of floods) and pipe flow ratio, described the impact of CC. Neumann et al. (2015) demonstrated a potential approach for estimating CC adaptation costs for urban drainage systems across the US. Semadeni-Davies et al. (2005) stated that there was lack of both tools and guidelines in the technical literature in order to assess CC impacts on hydrology. Furthermore, for urban areas, attention has generally focused on flood risk or water supply, rather than storm water drainage.

Many researchers predict that design intensities will increase due to CC. Arnbjerg-Nielsen (2013) suggested approaches to quantify the impact of CCs on extreme rainfall and projected that design intensities in Denmark are likely to increase by 10%–50% within the next 100 years. Ekström et al. (2005) suggested that the HadRM3H model can be used with some confidence to estimate extreme rainfall distributions and predicted that, for longer duration events (5–10 days), event magnitudes will show large increases in Scotland (up to +30%) using rational frequency analysis and individual grid box analysis. If we consider the impact of CC, the revised design criteria will stipulate greater capacity than current standards. Existing rainfall intensities do not reflect this issue (Berggren, 2008). New design criteria that account for rainfall intensities considering CC are necessary to prevent drainage system overload (Burrell et al., 2007; Mailhot et al., 2009).

Many other drivers will also have a large impact on the performance of the drainage system, particularly urbanization, changes in the drainage system, and changes in the performance criteria (Arnbjerg-Nielsen, 2010) and in practical applications these other drivers are often as important as the CC impacts (Semadeni-Davies et al., 2008).

1.1.1 Climate Change scenario generation

There are two general classes of CC impact studies, differing in the way in which the assumptions about the direction and magnitude of CC that may occur in the study area are generated. One approach is to use synthetic CC scenarios, in which the historical average temperature and precipitation are changed by fixed amounts at annual, seasonal, or monthly scales. This approach avoids the uncertainty associated with GCMs and allows for sensitivity analysis, an estimate of the amount of change in a hydrological variable resulting from a series of incremental changes in a climatic variable, which is a highly useful type of impact

analysis for the purpose of determining how much the climate must change in order for significant impacts to occur.

One disadvantage of synthetic scenario generation is that the chosen amounts of change in climatic variables are not necessarily realistic consequences of increased atmospheric GHG concentrations. This problem can be avoided by not selecting amounts of change arbitrarily, but instead by basing these on some other data, such as anomalies in the historical record or the range of changes predicted by climate models for the region. Another disadvantage of the synthetic approach is that, when the changes are applied to raw historical climate data, the range of variability in the scenario remains unchanged, which is problematic because CC is likely to alter variability, particularly in precipitation. To address this problem, Chiew *et al.* (2003) developed a refined method known as daily scaling, in which change factors are applied to ranked historical precipitation data. In this method, change factors are not constant across all years, seasons, or months, but are dependent on the relative magnitude of the event.

The alternative approach to CC scenario generation begins with one or more GHG emissions scenarios, usually from the IPCC's Special Report on Emissions Scenarios (SRES). These scenarios are used to drive GCMs, which rely on large-scale simulations of the coupled ocean-atmosphere system to predict the response of the climate to the projected increase in GHG concentrations. Because the outputs from these models are at too large a scale to be useful for most hydrological applications, they must be downscaled using either a regional climate model (RCM), which simulates local topographic and other influences on climate, or a statistical downscaling technique, which alters historic climate records according to the projected future change.

1.1.2 Approaches for Rainfall Disaggregation and Flood Analysis

To obtain CC impact estimates to urban drainage, CC scenarios have to be propagated through urban drainage models. This can be done using the output time series of the climate model as direct input for the drainage model. However, because local and small scale variables are required as input to the urban drainage model, statistical downscaling has to be applied. The bias correction will avoid that for the control simulations, drainage results will be obtained that systematically differ from the results obtained after drainage model calibration. A number of dynamical and statistical downscaling methods are available to downscale climate model gridded data at the target point locations (Prudhomme *et al.*, 2002; Dibike *et al.*, 2005; Fowler *et al.*, 2007; Praskievicz *et al.*, 2009; Kalra *et al.*, 2011). A simple method for transposing gridded climate projections to station scale is the use of delta change

factor (also called “perturbation factors”) (Zhu et al.,2012). In some studies delta change factors have been applied to precipitation time series (Prudhomme et al., 2002; Semadeni-Davies et al.,2008; Olsson et al.,2009; Berggren et al.,2012; Fortier et al.,2015), and in other studies it has been applied to design storm depth (Forsee et al.,2011 and Zhu et al.,2012). This method is to change or perturb the (historical observations or design storm based) input of the urban drainage model by means of climate factors (or “Delta Change (DC) factors”). The perturbation requires a change in both the number of rain storm events, and the probability distribution of the rain storm intensities.

In Quebec (Canada), Nguyen et al. (2008) have derived the IDF relations for the current period as well as for future periods under different CC scenarios given by the Canadian GCM and the UK Hadley Centre GCM. Furthermore, on the basis of the derived IDF relations, the design storms at a location of interest in the context of CC and the resulting runoff characteristics from typical urban areas with different sizes, shapes, and imperviousness levels can be estimated (Nguyen et al., 2010). While these studies have demonstrated the feasibility of linking GCM-based CC scenarios with short duration rainfall extremes and runoff processes from small urban catchments, the results have indicated the presence of high uncertainty in climate simulations provided by different GCMs.

In Sweden, Semadeni-Davies et al. (2008) applied their climate factors at 6-hour scale to rescale a 10-year tippingbucket series of observed 1-minute intensities. Later, Olsson et al. (2009) applied their continuous climate factor approach at 30-minutes scale to rescale a similar time series prior to climate effect simulations in the urban drainage model. Using that method, contrasting future precipitation trends, such as a decrease in total (seasonal) volume but an increase in the (short-term) extremes, were transferred to the observed series. Results show that the drainage impact results have strong regional differences (depending on the climate scenarios) but also strongly depend on the CC scenario considered.

A similar approach was followed by Ntegeka et al. (2008), who applied a perturbation approach to historical input time series of hydrological models. Both perturbations in the number of events and in the probability distribution of rainfall intensities were being made at the daily time scale. Per month of the year, the number of wet days in the rainfall series was calculated and perturbed by removing or adding wet days. Given that future climate for Belgium tends towards a smaller number of wet days in summer, wet days had to be removed in that season. A random removal operation was tested and compared with methods where by preference the isolated wet days that are situated in dry periods are turned into dry days. After

the wet day frequencies have been changed, the rainfall intensities of these wet days were changed following a quantile perturbation based method. This means that climate factors were applied depending on the cumulative probability or return period of the daily intensity. The changes to the sub-daily intensities were assumed identical to the daily changes.

Willems and Vrac (2010) perturbed the 10-minutes historical rainfall series at Uccle, Belgium, based on that quantile perturbation based method of Ntegeka et al. (2008) and compared the results with those obtained after applying an advanced weather typing based method. Interestingly, after simulating the impact on overflow frequencies of storage facilities to urban drainage systems, similar impact results were obtained for the two types of methods (which are based on largely different assumptions). The scenarios of future precipitation extremes should then be considered as well as scenarios of other key variables of change over time such as urban development, degree of imperviousness, local stormwater management, and other options in order to identify the best decisions about urban stormwater management.

An important issue for flood analysis is the time resolution and downscaling daily rainfall data to hourly rainfall data is needed. There are several methods for disaggregating daily time scale to hourly (Rodriguez-Iturbe et al., 1987; Rodriguez-Iturbe et al., 1988; Glasbey et al., 1995). Various stochastic downscaling techniques have been developed (Fowler et al., 2007) for the further temporal refinement of the RCM output and transfer to the spatial point-scale. Together, these nested models allow the impact of climate variability on sewer system performance with regard to flooding to be addressed. Other downscaling techniques such as weather typing or regression-based methods were found to be inadequate for this purpose due to their inability to reproduce extreme events (Wilby et al., 2002).

1.1.2.1 Statistical downscaling

The coarse scale and bias in the precipitation results of climate models require a statistical model (that both involve bias correction and statistical downscaling), which correlates the coarse scale (both in space and time) state of the atmosphere (the “predictor” variables) to the small scale rainfall (the “predictand” variable). The statistical model so far can only be based on historical data, thus assuming that the transfer from the predictors to the predictands will not significantly change under changing climatic conditions.

The statistical downscaling aims to scale the outputs from climate models down, both in space and time, to the scale of urban hydrological impact modeling, and even further to point rainfall in order to provide comparable values with historical rainfall series. Several statistical downscaling methods have been developed so far; they can be classified in: empirical transfer

function based methods; re-sampling methods or weather typing; and conditional probability-based or stochastic modeling methods.

Empirical transfer function methods

The empirical transfer function based methods make use of observed empirical relationships or transfer functions between the precipitation predictand and the predictors. A typical example of such methods is the popular regression-based statistical downscaling method (SDSM) proposed by Wilby et al. (2002). Predictors that have been found to correlate well with small scale (daily or sub-daily, point scale) precipitation are (mean) sea level pressure, geopotential height, zonal wind velocity speed and wind direction, specific or relative humidity, surface upward latent heat flux, temperature, dewpoint temperature and dewpoint temperature depression (representing the degree of saturation in water vapor in the atmosphere) (e.g. Vrac et al., 2007b; Dibike et al., 2008). Also geographical variables such as elevation, distance to the coast (diffusive continentality), advective continentality (which represents the degree at which incoming air mass paths traveled over land versus over the ocean) and topographical slope (given that this affects the degree of air mass going up, hence potentially cooling and precipitating, due to the presence of mountains) have been suggested (Vrac et al., 2007b).

Transfer functions considered so far took the form of a regression relation (Dibike et al., 2008), including generalized linear models (Vrac et al., 2007b; Leith et al., 2010), equations based on rainfall time-scaling laws (Nguyen et al., 2008) or artificial neural networks (Olsson et al., 2004). The predictor and predictand variables can be considered as time series, such that the value in each time step can be downscaled to obtain a time series of rainfall, to be used in urban drainage impact models that are based on continuous time series simulation and post-processing of simulation results (as typically done in impact analysis of sewer overflows on receiving rivers). Another approach is to preprocess the time series of the predictor and predictand variables, obtain statistics (e.g. empirical frequency distributions or calibrated probability distributions, at specific time and space scales), and derive transfer functions between these statistics or distributions. The latter approach is useful in impact analysis on sewer surcharging or flooding (using artificial storms for given storm frequencies or return periods).

Another method was based on the combination of a spatial downscaling technique to describe the linkage between large-scale climate variables as provided by GCM simulations with daily extreme precipitations at a local site using the popular Statistical Downscaling

Model (SDSM) (Wilby et al., 2002) and a temporal downscaling procedure to describe the relationships between daily extreme precipitations with sub-daily extreme precipitations using the scaling General Extreme Value (GEV) distribution (Nguyen et al., 2002). Nguyen et al. (2008) have shown the feasibility of this spatial–temporal downscaling method using GCM climate simulation outputs, NCEP re-analysis data, and daily and sub-daily rainfall data available at a number of rain gauges in Quebec (Canada). A bias-correction adjustment of the GCM-downscaled annual maximum daily rainfalls based on a second-order polynomial function was required to achieve good agreement with the observed at-site daily values. After obtaining the bias-corrected downscaled annual maximum daily rainfalls at a given site, further downscaling to sub-daily maximum rainfall intensities was required by means of a GEV distribution (Nguyen et al., 2002). Based on the concept of scaleinvariance, where moments of the rainfall distribution (GEV in this case) are a function of the time scale, which has scaling properties (Nguyen et al., 2007), probability distributions of sub-daily (hourly, 30-minutes, ...) rainfall intensities could accurately be obtained from the distribution of daily rainfall intensities.

Olsson et al. (2012) have shown that further advancements could be made by making the transfer function depends on RCM process variables characterizing the current weather situation such as cloud cover and precipitation type. They used 30-minute values of different cloud cover variables to estimate the wet fraction corresponding to the different precipitation types. These fractions were used to convert the gridbox average precipitation into a local intensity, with a corresponding probability of occurring in an arbitrary point inside the gridbox. It should be emphasized that RCMsimulated precipitation type and cloud cover are uncertain, and consequently also the estimated local intensity. Evaluation in Stockholm, Sweden, however showed a reasonable agreement with observations and theoretical considerations, which supports the approach (Olsson et al., 2012).

Re-sampling or weather typing methods

A second set of methods for statistical downscaling is based on re-sampling or weather typing. Downscaled future rainfall values are in these methods obtained from historical (observed) time series of the local rainfall predictand and coarse scale climatic predictor variables. For each future event (e.g. day) in the climate model output, a similar situation (analog event) is sought in the historical series of the climatic variables, and the small scale rainfall observation for that event considered as downscaled future rainfall. Pressure fields from climate models are typically used as predictor. Using a classification scheme, different

weather types are identified based on these pressure fields and relationships set between these weather types and the small scale rainfall predictand. This weather typing approach thus is based on synoptic similarity. Several references (although with application to other scales) exist that describe how to find robust weather types (e.g. Bárdossy et al., 1990; Benestad et al., 2008). Disadvantage of the technique is that no rainfall intensities that are more extreme than the most extreme event in the past will be considered for the future series; only the sequence and frequency of the events in the historical series will be modified.

To overcome that shortcoming, Willems et al. (2010) advanced the classical weather typing method by applying rainfall intensity changes to the 10-minutes rainfall intensities of each analog day depending on changes in daily temperature. They assumed that future rainfall changes are induced not only by changes in atmospheric circulation, but also by changes in temperature (due to the temperature dependence of the saturation value of precipitable water in the atmosphere). Instead of using climate analogs from the past, one can also consider climate analogs from other locations (for which it is expected – based on the results of climate models – that future climate conditions will become similar). This method has been tested by Arnbjerg-Nielsen (2008), assuming that the following 100 years the future climate in Denmark might become similar to the present climate in Northern France and Germany. Similar changes in precipitation quantiles were obtained as by the direct use of the precipitation results from a high resolution RCM.

Stochastic rainfall models

The third type of statistical downscaling can be seen as an extension of stochastic hydrology. It uses stochastic rainfall models, with parameters that have probability distributions, conditionally based on the coarse scale climatic predictor. The parameters of the stochastic model are to be obtained from statistical analysis of time series, and can be altered in accordance with climate model simulation results. Such types of stochastic rainfall models are also called “weather generators”. Onof et al. (2009) made use of a point rainfall generator, based on the Random Parameter Bartlett–Lewis Rectangular Pulse (BLRP) model, to generate rainfall at the hourly time scale. They basically followed a two-step approach where the rainfall generator captured the storm structure at the hourly time scale, and where in a second step a disaggregator was used (based on multiscaling) to bring hourly rainfalls down to finer scales. Such applications are often based on delta-change methods, i.e. identification of properties/variables that are believed or assumed to be scale invariant from the regional climate model scale to the urban catchment scale. The BLRP model was also applied by

Segond et al. (2007) to downscale daily rainfall, obtained with a generalized linear model, to hourly rainfall for an urban catchment in the UK. The hourly rainfall patterns were then interpolated (between rain gauges) linearly in space using inverse distance weighting to obtain hourly rainfall estimates over the whole catchment. Sunyer et al. (2009) compared 3 different stochastic rainfall models for downscaling of extreme rainfall events north of Copenhagen: based on Markov chain semi-empirical models and the Neyman–Scott Rectangular Pulses (NSRP) model. It was found that all 3 models represent well the increase in the number of extreme events, but only the NSRP model reflected well the change in variance.

In another study by Arnbjerg-Nielsen (2008), the usefulness of a stochastic point rainfall generator (BLRP in that case) for statistical rainfall downscaling was less convincing. He found that the rainfall changes obtained by that method lead to underestimations in comparison with two other methods, one that makes direct use of RCM precipitation results and one based on climate analogs. It was explained by the fact that changes in the BLRP model were estimated based on general rain storm properties (mean cell intensity, mean cell duration, rate of rain storm arrival, etc.), but with less emphasis on the changes in statistics of rainfall extremes.

1.1.3 Hydrologic variability

In addition to the previously discussed changes in mean hydrology, CC is also likely to affect hydrological variability. Even in areas where annual runoff changes only slightly, flow levels that are currently considered extremely low or high may become more common. For example, Arnell (2003b) examined the impacts of CC on hydrological variability in six basins in the United Kingdom during the twenty-first century, with results including a slight increase in mean monthly flow and a decrease in low flow amount of up to 40% by the 2080s, with a corresponding increase in inter-annual hydrological variability. In many world regions, particularly lower elevation tropical and humid mid-latitude areas, increased flooding is a significant risk of CC. Milly *et al.* (2002) found an increase in the observed frequency of large floods in major world river basins during the twentieth century. Kleinen et al. (2007) estimated, using statistically downscaled CC-driven alterations of a water balance equation, that up to 20% of the global population lives in river basins that may experience greater flooding as a result of CC by 2100. Palmer et al. (2002) predicted that heavy winter rainfall events in the United Kingdom and summer monsoons in Asia may increase by a factor of five during the twenty-first century.

In a continental-scale modelling study, Lehner *et al.* (2006) predicted increases in flood frequencies for northern Europe and drought frequencies for southern Europe.

Kundzewicz *et al.* (2005) found that past and projected future large floods in central Europe may be related to anthropogenic CC. Kay *et al.* (2006), using a conceptual model driven by high-resolution RCM outputs through the 2080s, found increases in flood frequency and magnitude for most of their 15 study basins in the United Kingdom. In six Australian basins, Evans *et al.* (2002), using a conceptual hydrological model driven by stochastic weather generator outputs, found an increase in the magnitude of floods, despite a decrease in mean annual runoff. Mote *et al.* (2003) also predicted increases in winter flooding in smaller rainfall-dominated and transient basins in the Pacific Northwest, because of increases in temperature and precipitation

1.2 Uncertainties in analysis of climate change impacts

Generally, the source of uncertainty involved in CC impact studies is resulted by climate model projections, the hydrologic model and data downscaling techniques. The main sources of uncertainty, climate model projections, are derived from three main sources: forcing, model response and internal variability (Deser *et al.*, 2012).

Together, the uncertainties associated to climate variability and its prediction are diverse and can be grouped into (i) the emission scenario uncertainty, (ii) GCM uncertainties, (iii) downscaling uncertainty, and (iv) internal climate variability (Tebaldi *et al.*, 2007; Wilby *et al.*, 2006). Since drainage system design relies on extreme precipitation observed within a short period, it is subject to sampling uncertainty. Drainage system design is further challenged by the uncertainty of future urban development. Thus the future runoff coefficient might change due to increased population densities.

1.2.1 Uncertainties associated to climate variability and its prediction

(i) Emission scenario uncertainty: The contributions of different sources of uncertainty to the overall uncertainty vary over the prediction lead time and depend on the climate variable of interest as well as on the temporal scale (Cox *et al.*, 2007). Hawkins *et al.* (2011) and Prein *et al.* (2011) conclude that with regard to precipitation the emission scenario uncertainty is negligible for prediction lead times of 40 years and less. Also according Wilby *et al.* (2006) the choice of emission scenario is less important for the near term, because most scenarios show very similar levels of emissions through the 2050s and it takes time for the atmosphere to respond (Wilby *et al.*, 2006). In basins where summer is the low flow period, the

uncertainty in GCM-derived river flows is greatest in summer (Wilby *et al.*, 2006), suggesting that changing precipitation and temperature patterns will alter seasonal water balance components in different ways.

(ii) Climate model uncertainty: This is clearly seen as one dominating factor for the overall uncertainty of climate projections (Hawkins *et al.*, 2011; Räisänen, 2007).

Studies indicate that the greatest source of uncertainty in the climate impact modelling chain is the GCM (Wilby *et al.*, 2006; Graham *et al.*, 2007). Because they all model atmospheric conditions and feedbacks differently, GCMs vary widely in their projections, particularly for precipitation. For this reason, Knutti (2008) and Räisänen (2007) suggest using the output from an ensemble of climate models as a probabilistic climate projection to account for climate model uncertainty.

(iii) Downscaling uncertainty: Further uncertainty is introduced by the downscaling techniques themselves. For dynamic downscaling, a multi-RCM approach can be applied analogously to the proposed multi-GCM approach. This was done by Fowler *et al.* (2009), who found that the RCM uncertainty is significant with regard to precipitation extremes.

Wood *et al.* (2004) compared three statistical downscaling methods, using the Variable Infiltration Capacity (VIC) macroscale hydrological model. The most accurate method was bias correction and spatial disaggregation. Dibike *et al.* (2005) used output from a GCM to compare two downscaling methods, regression analysis and a stochastic weather generator. The weather generator performed better when estimating the length of wet spells in the historical period. Salathé *et al.* (2007) found significant differences in regional climate response in the Pacific Northwest using statistical downscaling versus an RCM, with the RCM more accurately reproducing the historical climate. In comparing downscaling methods, RCMs and other dynamic techniques are generally more successful because they replicate regional climate systems, but also require more data and time to implement than the simpler statistical techniques. For dynamic downscaling, Fowler *et al.* (2009) applied a multi-RCM approach, analogously to the proposed multi-GCM approach and he found that the RCM uncertainty is significant with regard to precipitation extremes.

For stochastic downscaling, the uncertainty quantification is elusive due to the limited number of adequate techniques for downscaling extreme events at fine temporal and spatial scales (Maraun *et al.*, 2010; Sunyer *et al.*, 2012).

(iv) Internal climate variability: This uncertainty derives from the high sensitivity of the climate system to initial conditions which can never be reproduced perfectly. This is considered to be another key source of uncertainty, in particular when considering time horizons within the next few decades (Cox et al., 2007; Hawkins et al., 2011). This uncertainty could be reflected by running climate models with different initial conditions. In order to avoid the large computational expenses associated with this approach, internal climate variability could alternatively be reproduced by multiple realizations of stochastic downscaling. However, the ability of stochastic precipitation models to reproduce internal variability on an inter-annual scale is typically limited (Wilks et al., 1999). This ability has been enhanced by Fatichi et al. (2011) by explicitly accounting for precipitation inter-annual variability in the model structure.

1.2.2 Sampling uncertainty

As opposed to the aleatory uncertainty of climate variability as defined by IPCC (2013), the sampling uncertainty is of epistemic nature as it is reducible by additional information (Refsgaard et al., 2013; Walker et al., 2003). The stochastic downscaling methodology gives us the possibility to generate precipitation series of arbitrary length. Consequently, we are able to reduce the sampling error in sewer system design by using long stochastic precipitation series instead of short observed ones under the following assumptions:

(i) The stochastic downscaling model reproduces all statistical properties of precipitation correctly including those of extreme events.

(ii) The precipitation process is stationary on the yearly timescale (if inter-annual climate variability is not explicitly considered by the stochastic downscaling model).

(iii) The sampling error incurred when estimating the statistics used for calibration of the stochastic downscaling model from the observed precipitation series is negligible

1.2.3 Uncertainties associated to hydrological models

An additional source of uncertainty stems from the choice of a hydrological model in climate impact assessment. Different hydrological models vary in their parameters and assumptions and are suited to simulate runoff at certain spatial and temporal scales. In comparing the temperature-based potential evaporation (PE) with the physically based Penman-Monteith PE, Kay and Davies (2008) found that the temperature-based PE matched the observed PE better than did Penman-Monteith PE, for all the climate models studied for three catchments spread across Britain. The uncertainty introduced by the PE formulation was

less than that due to the climate model, but could still be important for some applications. Similarly, other studies have shown that results of climate impact studies are less sensitive to the hydrological model than the CC scenario (Graham *et al.*, 2007; Kay *et al.*, 2009). In other words, different hydrological models tend to produce similar outcomes, given the same climatic inputs, but the same hydrological model run under different GCM simulations may give widely differing results. Jiang *et al.* (2007) compared six conceptual water balance models and found that their simulations of observed conditions were similar, but there were greater differences when run under future climate simulations, particularly among those models that represented soil moisture differently.

The outputs from hydrological models can be further used in water resource management models to take the socio-economic aspects of the hydrological system into account (Christensen *et al.*, 2004), where additional uncertainty might occur. These may include models representing water demand (Groves *et al.*, 2008), dam and reservoir storage (Payne *et al.*, 2004), or conservation and efficiency policies (O'Hara and Georgakakos, 2008). At each stage of this modelling chain, assumptions must be made and error is inevitable, leading to amplified uncertainty throughout the modelling process (Wilby and Harris, 2006; Kay *et al.*, 2009).

1.3 Factors increasing impacts of climate change in urban drainage systems

Numerous studies involving CC predictions have indicated that heavy precipitation events will likely increase in frequency and intensity (Saraswat *et al.*, 2016). Semadeni-Davies *et al.* (2008) showed that the correlation between the increased intensity of rainfall and increased impervious surfaces cover is directly proportional to more extreme events, such as flooding, flash floods and greater peak flows. Hence, within the context of CC, a science-based system for evaluating the relative impacts of both urbanization and CC on stormwater runoff at a local scale is very much needed for better management policies. Stormwater management is planned based on local weather and climate. However, CCs, such as the amount, timing, and intensity of rain events, in combination with land development, can significantly affect the amount of stormwater runoff that needs to be managed. In some regions of the developing countries, the combination of climate and land use change may worsen existing stormwater-related flooding, whereas other regions in the world may be minimally affected. In the past, stormwater management was practiced in an anthropocentric, human-centric manner, and as a result, has had a profound effect on the environment. Along with CC, a suburban expansion has exploded over the last few years, thereby increasing impervious surface cover in place of

forests, pastures, and cropland. This has affected local hydrological cycles by producing more surface runoff and decreasing the base flow, interflow and depression storage (Davis et al., 2006). The impervious surfaces are directly responsible for the reduction in deep infiltration of water, and increase surface water runoff by at least 50% (https://www3.epa.gov/caddis/ssr_urb_is1.html).

1.3.1 Spatial structure and planning

Spatial structure refers to the way space is used in the city, including the size and spatial distribution inside the city, the daily flows of people, and network connections (Anas et al., 1998; Burger et al., 2012), as well as the changes in the use of urban space and its influence on a city's vulnerability; spatial planning strategies, that is, the frameworks for action which shape spatial structure (Albrechts, 2004) which in the case of climate adaptation have an important role in determining a city's resilience (de Vries, 2006). Understanding a city's form of spatial structure, the arrangement of urban public space (Anas et al., 1998), is crucial in developing spatial planning strategies for the benefit of people's socio-economic well-being as well as urban sustainability. The literature proposes two distinctive spatial structures: the 'polycentric city' characterised by a multitude of dispersed and interactive areas of employment, business and leisure (Hall et al., 2006), and the 'compact city', characterised by a highly contained urban development, high density, mixed land uses, high accessibility and continual intensification of development. In recent research relating spatial planning and sustainability (Harris, 2012), the question has been asked as to which type of spatial urban structure is sustainable in the long run suggesting the compact city is more sustainable than the polycentric city. Nevertheless, while urban intensification (compact city) delineates urban areas preserving green belts and rural zoning, reduces commuting and thus, emissions, and lowers costs of urban construction by reducing transportation of materials, it also drives up property costs, increases the heat-island effect through increased building density and the obstruction of wind corridors, and escalates the incidence of contagious diseases. These are a compact city's negative effects (Harris, 2012). On the one hand, the accumulation of populations and assets in cities exacerbates their vulnerability (Hallegatte et al., 2013) while, on the other hand, their compact characteristics, including the ability to promptly access emergency facilities, makes them better prepared to respond. Different types of political systems, of legal-administrative structures, governance types, and levels of socio-economic development render cities and their populations unequally exposed and vulnerable to climate-

related risks (Francesch-Huidobro et al., 2016). Substantial differences in approaches to dealing with CC and its consequences in cities are evident.

Once a city's spatial structure has been determined, strategic spatial planning influences its present management and future development. Strategic spatial planning is a public sector-led, social process through which a long-term vision is combined with short-term actions and means for implementation to shape what a place is and may become (Kaufmann et al., 1987). Revived in the 1990s after the neoconservative and postmodern disdain for planning prevalent in the 1980s became predominant again, spatial planning is a decisively normative approach to the organisation of space at different levels of geographical and political scale (Albrechts, 2004). A strategic spatial planning approach to the management and development of a city focuses on a limited number of key issues (priorities, feasible, etc.), takes account of context to determine opportunities and threats of decisions, studies external forces, identifies resources available, singles out relevant major stakeholders, allows for broad (multilevel) and sectoral (public, private, people) involvement, takes into account power structures, uncertainties, competing values, designs plans and decision frameworks for influencing spatial change, then decides, acts, checks results, implements plans, monitors, feed-backs and revises (Quinn, 1980; Barrett et al., 1981; Kaufmann et al., 1987; Benveniste, 1989; Friedmann et al., 1998; Albrechts, 1999; Hall et al., 2000). This implies that strategic planning is about institutional design, closely linked with the concept of sustainable planning, 'a positive-sum strategy combining economic, environmental, and social objectives in their spatial manifestation' (Albrechts, 2004). As such, strategic spatial planning purports integrated development, the management of change, stakeholder involvement, a negotiated form of governing and the effective connection between political authorities and implementation actors (Hillier, 2002). These ideas resonate with the governance approach to governing (integration, stakeholder involvement, negotiation).

1.3.2 Urbanization

The world is currently undergoing a period of rapid urbanisation largely due to population growth and rural to urban immigration. However, in much of Europe population growth is slowing and demographics point to an aging society; thus urbanisation has been largely driven by the trend towards smaller households. Increased urbanisation in some towns can partly be attributed to the high number of immigrants.

The impacts of urbanization on the water cycle are essentially related to surfaces becoming impervious, resulting in a marked reduction in the infiltration capacity of soils and more

vulnerable drainage systems subjected to larger and faster water inputs (Bi et al., 2015). Unless urban planning measures are developed to counter these historic trends, the percentage of rain that runs off will increase with urban development, inexorably leading to higher runoff flows and volumes (Braud et al. 2013; Chocat 1997). This situation, when it happens, will have various repercussions on humans and infrastructures, from complaints and claims to political and social pressure put on urban drainage system managers, in addition to resulting in costs in damages for municipalities (Kunkel et al. 1999; Watt et al. 2003). Moreover, anticipated changes in air temperature and precipitation could affect flow in receiving watercourses, alter sediment morphology and transport, and change the kinetics of chemical reactions and, hence, the mobility and dilution of pollutants discharged by wastewater systems and storm drains in urban settings (Burton et al., 2002; Caissie et al. 2014; Casadio et al. 2010; Chocat et al. 2007; Gooré Bi et al. 2014; Whitehead et al. 2009).

In the context of urbanization, we can accurately define stormwater as the runoff from pervious and impervious surfaces in predominantly urban environments (Saraswat et al., 2016). Impervious surfaces can be defined as concrete charcoal roads, highways, roofs, pavements and footpaths. The land cover and precipitation relationship pathways have created a state in which the watersheds and their streams and channels are adversely impacted (Frazer, 2005).

In *Figure 1.1*, from the centre of watershed protection, we can see the relation between urbanized areas covered with impervious roads and streams. The figure demonstrates that increasing impervious surfaces alters the hydrologic cycle and creates conditions that no longer can support the diversity of life. The problems that urbanized watersheds face include flooding, stream bank erosion and pollutant export. The receiving streams of these intensified storm flows alter hydraulic characteristics due to peak discharges several times higher than pre-development or even rural land cover characteristics (LeRoy et al., 2006). Improving the water quality of runoff entering receiving waters and reducing pressure on existing water supply systems are thus major goals of urban water management.

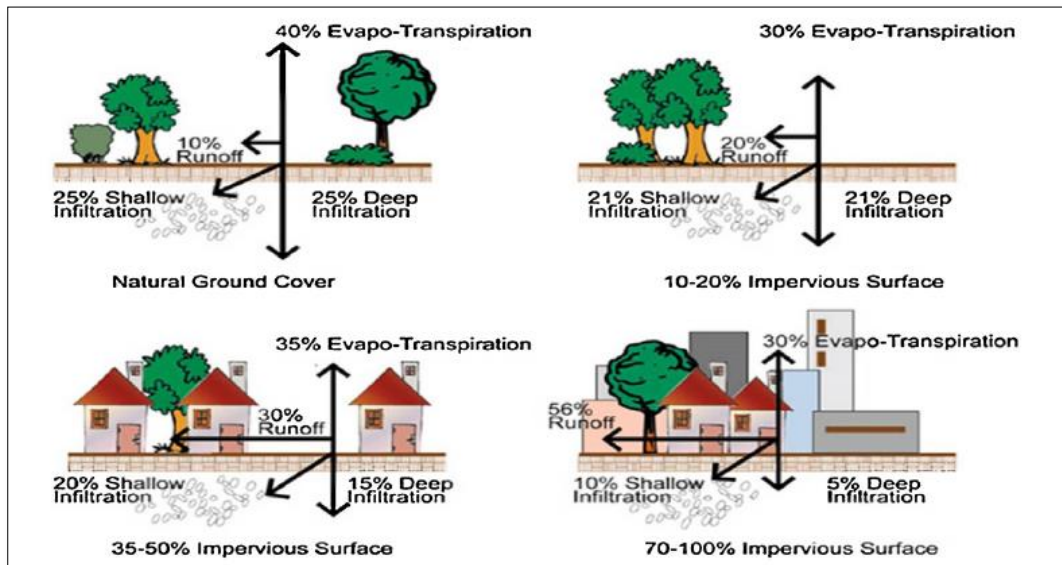


Figure 1.1. The difference between the natural ground cover and various types of impervious surfaces in urbanized areas.

One of the most comprehensive studies to determine socio-economic storylines for CC impact assessment has been undertaken as part of the UK Climate Impacts Programme (UKCIP, 2001; Berkhout et al., 2002; Shackley et al., 2002).

Understanding potential climate-related impacts is especially necessary given that these changes may interact in complex ways with other elements of global change (Clifford, 2009), notably urban development. These two driving forces of future hydrological change are likely to affect both water quantity and quality, at global, continental, regional, and basin scales, in geographically disparate areas around the world. Not only are changes in mean hydrology expected, but also changes in hydrological variability, which are particularly significant for water resource management. Further complicating these issues is the inherent uncertainty present at every stage in the methods and techniques used by researchers to predict future changes.

1.3.2.1 Impacts of urban development on hydrology

It is well known that an increase in impervious surface area accompanied by urban development significantly alters hydrological response, in particular by increasing the ‘flashiness’ or quickness to and magnitude of peak flow from rainfall events (Dunne et al., 1978). As impervious surface area increases, the entire water balance of the basin is altered, with increased surface runoff and decreased groundwater recharge and evapotranspiration.

Several studies have modeled the hydrological response of basins to historical or potential future urban development.

One major research question that has been explored is whether there exist thresholds of impervious surface area above which the hydrological response is characteristically urban. Wang (2006) conducted a retrospective analysis of the impacts of urban development on flood risk in an approximately 400 km² Texas basin, using both 30 m digital elevation models and high-resolution Light Detection and Ranging (LiDAR) data. He found that, from 1974 to 2002, the basin impervious surface area increased from approximately 10% to over 38%, with an accompanying increase in the 100-year flood peak of 20%. In another retrospective analysis, Nirupama et al. (2007) used data on land use, meteorology, and hydrology to estimate the increase in flood risk caused by urban development in London, Ontario. This study demonstrates that approximately 15% impervious surface area may be a threshold above which basin hydrology exhibits the typical urban flashiness. Also, basin size influences hydrological sensitivity to urban development, with smaller basins experiencing relatively greater impacts than larger ones. Runoff does not increase linearly with rainfall, and the amount and location of basin impervious surfaces affects the relation between these variables (Dunne et al., 1978).

1.4 Current design criteria of the urban drainage management infrastructures

Water is the lifeblood of an ecosystem, but when it falls on a city of impervious surfaces, it is called stormwater and regarded a liability (Stephens et al., 2002). Traditional development and stormwater management practices have resulted in buried streams, polluted waterways, and flooded neighbourhoods creating a deficit of the natural spaces well documented to promote human health and wellbeing (Spirn 1984; Kaplan, 1995; Pinkham, 2000; Roy et al., 2010).

CC affects the function and operation of existing water infrastructure – including hydropower, structural flood defences, drainage and irrigation systems – as well as water management practices.

Sewer systems are designed to remove sewage and drain stormwater in order to limit flooding. Wastewater is collected from various sectors and transferred to a wastewater treatment plant for treatment to meet environmental water quality standards before it is returned to the environment (e.g., waterway, ocean, or aquifer). In some cases, a portion of

the wastewater could be recycled—treated to a higher standard—and reused by a prospective end-user (Ajami et al., 2014).

As it is not realistic to provide protection from every rainstorm, the probability that flooding will occur is limited by an acceptable level. National standards recommend maximum permissible frequencies of exceeding critical reference water levels at every manhole (DWA, 2006; IDA Spildevandskomiteen, 2005). DWA (2006) suggests using one historical high-resolution point-precipitation series representative for the location of the sewer system as the input for precipitation-runoff simulations to predict the relevant exceeding frequencies. As opposed to design storms, historical precipitation series allow the intra-storm variability to be addressed. Today, high-resolution precipitation series are typically available with durations of 30/40 years (Egger et al., 2015). However, by definition, only very rare precipitation events induce critical runoff events in more or less well-designed drainage systems. We must consider these precipitation events as highly random due to the large variability of sub-daily precipitation intensities. Therefore, the available series are just single random samples of precipitation series under the climatic conditions prevailing during the observation (Egger et al., 2015). In consequence of this short observation periods, exceeding frequencies derived from hydraulic calculations with such short series must be considered as very uncertain estimates of the true exceeding rates even under a stationary climate (Egger et al., 2015).

The storm-water infrastructures in an urban area are usually designed based on the rainfall depth calculated employing statistical analyses of observed precipitation data. The rainfall depths are calculated from the historic rainfall time series without considering CC impact i.e., based on the assumption of a stationary climate. Existing urban drainage systems are designed to cope with weather conditions in specific areas (Berggren et al., 2012). The ages of systems vary and, in some places, can be quite old (e.g., in many old city centers). This means that existing urban drainage systems were designed for past climate conditions and might not be suitable for current circumstances or able to accommodate future changes (Berggren, 2008). But, the climate is now non-stationary (Karla et al., 2009 and Brown C., 2010) because of the anthropogenic force. So, the designing of storm-water management infrastructure based on design storm considering the assumption of non-stationary climate will not be able to manage extreme events in future climate (Milly et al., 2008) and for this reason to move to design specifications accounting for uncertainties associated to climate variability and its projection

is becoming a need (Fatichi et al., 2012). Questioning current design practice is also very timely in view of the growing demand for sewer rehabilitation (Maurer et al., 2006).

Although the effects of CC at the local level are poorly understood and appear to be gradual, their potential cumulative impact over the service life of drainage infrastructure warrants a change in the basic philosophy of hydrotechnical designs (Arisz et al., 2006). In practice, engineers have no choice but to consider CC in order to adapt and serve the public interest (Lapp, 2005): the design criteria of the urban drainage management infrastructure must be revised with the consideration of possible impact of CC (Mailhot et al., 2010).

Examples of propagations of CC impacts based on single design events can be found in Niemczynowicz (1989), Waters et al. (2003), and Grossi et al. (2008). Examples of propagations of continuous simulations of precipitation time series can be found in Semadeni-Davies et al. (2008), Arnbjerg-Nielsen et al. (2009), Olsson et al. (2009), Schreider et al. (2000), and Willems (2011).

Moglen et al. (2014) examined the changes in detention basin performance under several CC scenario at a study location north of Washington, DC, and indicated that in most cases, the performance of detention basin would be inadequate under future climate condition. Forsee et al. (2011) also revealed the inadequate performance of detention basin under future climate condition in a watershed in Las Vegas Valley, Nevada. There are other studies showing inadequate performance of storm sewer and combined sewer under future climate condition (Semadeni-Davies et al., 2008; Berggren et al., 2012; Fortier et al., 2015).

While the necessity of improving the urban drainage system to accommodate CC has been recognized, few studies have put forward an approach for conducting such research. This is probably due to the complexities involved in incorporating CC in urban flood analysis in order to evaluate alternative flood control projects. The importance of developing design standard for addressing the CC was indicated by many researchers (Guo YP., 2006; Mailhot et al., 2010; Moglen et al., 2014). Forsee et al. (2011) explored the projected changes in design-storm depths for Pittman watershed in Las Vegas using five NARCCAP data sets, and they showed a significant increase in case of three GCM+RCM pairs. Zhu et al. (2012) investigated the potential changes in IDF curve due to CC impact for six regions in the United States. They found strong regional patterns and increase in the intensity of extreme events under future climate for most of the study sites. Mailhot et al. (2007) investigated the CC impact in IDF curves for Southern Quebec using the Canadian Regional Model projections. The study results show that return period of 2 hour and 6 hour storm events will be

approximately halved and return period of 12 hour and 24 hour storm events will decrease by one third. Coulibaly et al. (2005) found significant increases in storm depth in 2050s and 2080s in Grand River, Kenora and Rainy River region in Canada by analyzing the storm depth calculated from climate simulations. In most of the studies, frequency analysis was performed on the annual maximum precipitation time series by fitting only one to three distributions for design storm depth calculations. For example, the Log-Pearson Type III for NARCCAP future precipitation time series was used by Moglen et al.(2014), generalized extreme value was used by some studies (Mailhot et al., 2007; Forsee et al.,2011; Zhu et al., 2012), Extreme value type I (EV I) was used by Zhu et al. (2012), Gumbel and generalized extreme value were used by Zhu (2013). Ahmed et al. (2016) explored the CC impact on design storm depth calculated by employing frequency analyses of NARCCAP precipitation data sets, testing:a) twenty seven distributions for the observed, NARCCAP current and future dataset, and the best among the fitted distribution was used for frequency analysis to calculate design storm depths; b) two statistical tests for goodness of fit at a 95% confidence level.

1.4.1 Combined sewer overflow

Prior to the late-2000s, studies on the effects of CC on urban areas exclusively focused on adjacent river systems and watershed drainage rather than stormwater or wastewater systems (Ashley et al., 2005). However, in recent years, there have been significant gains in modeling the impact of changing extreme precipitation patterns on urban stormwater, particularly in combined sewer systems.

When a combined sewer network is overwhelmed by stormwater, the excess water will overflow to adjacent water bodies in order to relieve the system and prevent flooding in manholes. Combined sewer overflow (CSO) is a common event in cities with inadequate capacity of sewer systems, and this overflow is likely to be more intense during heavy rainfall events. CSOs taint water bodies with untreated wastewater coming from residential, commercial and industrial units (U.S. EPA 1999) causing significant water quality and public health concerns due to the high concentration of pathogens, toxic pollutants, debris and solids (U.S. EPA 1999, Walsh et al. 2005; Passerat et al. 2011; Holeyton et al. 2011). On the other hand, combined sewer systems have been traditionally used. For example, currently, in areas around the Northeast, Pacific Northwest and Great Lakes in the U.S., combined sewer systems are being used for a total population of more than 40 million people residing in more than 700 communities (U.S. EPA 2008). Although these communities are required to control such impacts in accordance with the Clean Water Act, they discharge more than 3000 MCM

of untreated or partially untreated sewage into receiving waterways annually (U.S. EPA 2004).

In addition, even for a system that has a satisfactory performance under the current climate condition, CC can affect precipitation patterns and subsequently CSO events (Fortier et al., 2014).

In other words, the main negative impacts of such changes might be more frequent and severe sewer overloading and flooding in urban areas (Nilsen et al. 2011). The reason for this lies under the fact that CSOs are affected by changes in rainfall intensity, frequency and duration (Arnbjerg-Nielsen 2008), especially changes which lead to extreme precipitation events may have more significant impacts on CSOs characteristics (Arnbjerg-Nielsen 2008; Nilsen et al. 2011; Rose et al. 2001). However, since CSOs can happen even for moderate and small rainfalls, it would be more realistic to assume that an increase in rainfall total depth, increases the probability of having a CSO (Fortier et al., 2014). Therefore, for robust CSO control plan (including those that are planning to eliminate CSOs under the current climate conditions), future precipitation scenarios under CC must be a particular concern (Tavakol-Davani et al., 2016).

When the impact on urban runoff is studied (e.g. through runoff peak flows, floods, surcharge frequencies, and CSO frequencies and volumes), the projected impacts are uncertain, not only due to the uncertainties in the climate projections, but also due to uncertainties in the hydrological and hydraulic models (Arnbjerg-Nielsen et al., 2013). Care is required when predicting the impacts of more extreme conditions. The hydrological and hydraulic models are often calibrated and validated against historical time series of limited lengths, which may have included only a few extreme events. Extension of the model simulations to future conditions should therefore be made with caution, especially when considering system performance under extreme events that might become more common under future CC conditions.

In one of the pioneering efforts, a variety of CC and urbanization scenarios were explored using the Danish Hydrological Institute (DHI) MOUSE (MOdel of Urban SEwers) (Semadeni-Davies et al. 2008). Such comparisons allowed for exploration of the system sensitivity to evolve, and to better describe the range of likely future performance. Moreover, other studies have used U.S. Environmental Protection Agency Stormwater Management Model (SWMM) and stochastic methods to explore the range of possible performance under

CC and system operation (Kleidorfer et al. 2009). It has been found that, such applications provide a high flexibility to understand various system responses under climate variability.

Regarding the future rainfall projection, some studies have used a range of Global Circulation Models (GCM) to account for uncertainty (Semadeni-Davies et al. 2008). However, other studies have used a more appropriate method for smaller scales of urban water system, which is downscaling projections to remove the bias between global and local projections (Arnbjerg-Nielsen 2008; Nasserri et al. 2013; Nilsen et al. 2011; Rose et al. 2001; Tavakol-Davani et al. 2013). The latter technique has had a satisfactory performance in providing the precipitation time-series to run different rainfall-runoff models, including urban stormwater models.

1.5 Vulnerability of the urban drainage systems

Sewer flooding, urban surface water flooding and wet weather pollution are already recognised as significant issues in the world, and CC impacts on rainfall will likely exacerbate these problems (Arnbjerg-Nielsen et al., 2013; Ashley et al., 2005, 2007; Berggren, 2014; Mott Macdonald, 2011). For more than a century sewer systems have been constructed at large scale across cities worldwide. These drainage systems have reduced the vulnerability of the cities in general, but at the same time could make them more vulnerable to rainfall extremes, partly due to the lack of consideration to what occurs when the design criteria are exceeded. Next to this increase in the vulnerability, there is strong evidence that due to the global warming the probabilities and risks of sewer surcharge and flooding are changing.

Nevertheless, the number of CC studies dealing with urban drainage impacts is still rather limited, partly because they require a specific focus on small urban catchment scales (usually less than 500 km²) and short duration precipitation extremes (normally less than 1 day)(Willems, et al., 2009). Despite the significant increase in computational power in recent years, climate models still remain relatively coarse in space and time resolution and are unable to resolve significant features at the fine scales of urban drainage systems. They also have limitations in the accuracy of describing precipitation extremes due to a poor description of the non-stationary phenomenon during a convective storm leading to the most extreme events on a local scale (Willems, et al., 2009). To bridge the gaps between the climate model scales and the local urban drainage scales and to account for the inaccuracies in describing precipitation extremes, downscaling methods and bias-correction methods are commonly used in practice.

1.5.1 Flooding

Floods are one of the most devastating natural hazards. Floods, like tornadoes, are traumatic events. They happen with relatively short warning, and can lead to tremendous loss of life and property and can disrupt the lifestyle and balance of a whole community. Material damage resulting from a flood event may include damage to buildings, equipment, roads and transport system, drainage, sewage and water supply networks. Associated costs can range from a few million dollars to several billion dollars (Khedun et al., 2014).

Flooding can occur in various forms, such as coastal, river and surface water flooding (sometimes known as ‘urban’ or ‘storm water’ flooding). Surface water flooding occurs due to a complex interplay of factors, including the precise location, intensity and duration of rainfall, the characteristics of urban land surfaces and the engineering design of the surface drainage and sewer system. Surface water flooding tends to be most severe during intense rainfall downpours, which are often, but not exclusively, associated with convective rainfall events.

Surface water flood risk emerges from the interplay between biophysical and human factors (Hall et al., 2003b). Biophysical factors determine the frequency, duration and intensity of rainfall, and the runoff that occurs when rain hits the ground. Rainfall may be infiltrated into the ground, but in urban areas with impermeable surfaces rain water will flow on the surface in directions modified by the form of buildings and streets and will accumulate at locations with low topographical elevation. These processes are modified by drains that are designed to convey water away from urban areas on the surface or in pipes (Blanc et al., 2012). Risk will also be dependent on the vulnerability of the area and population exposed to the event (Hall et al., 2005) and, where in place, the effectiveness of surface water management interventions.

1.5.1.1 Flooding costs

Preliminary estimates of recovery cost for the flood that devastated large swaths of Alberta, Canada, for example, are between 3 and 5 billion Canadian dollars. Reconstruction efforts to revert back the effect of a flood and restore the feeling of normalcy within the community can take several years. The trauma resulting from a calamitous flood does not subside once the water retreats.

Long term impacts may include mental disorders, such as anxiety and depression related to economic and property loss, that may linger for several years (Haines et al. 2006). Such

problems may be even more acute within communities in low-income countries where relief and reconstruction efforts are not always readily available.

According to records kept by the International Disaster Database (www.emdat.be), there have been over four thousand flood events across the world since 1900 causing an estimated US\$ 595 billion in damage. Nearly 7 million people have lost their lives and over 88 million have been left homeless as a result of floods. Asia, followed by the Americas, has endured the highest number of flood events with an associated estimated damage of over US\$ 362 billion for Asia and nearly US\$ 100 billion for the Americas.

The southern, eastern, and southeastern Asian region, home to half of the world's population, has witnessed some of the disastrous floods. The deadliest flood in history occurred in China in 1931—3.7 million people perished due to drowning and ensuing disease and starvation and 51 million people were affected. Global warming is expected to accelerate the hydrological cycle and consequently affect precipitation depth, intensity and frequency, timing of snowmelt, soil moisture, infiltration and evapotranspiration. Combined with ongoing land use changes, it may lead to an increase in the number and impact of devastating floods (Khedun et al., 2014). A number of regional and global studies (e.g. the Ganges, Brahmaputra and Meghna basin in Asia (Mirza et al. 2003), Europe (Christensen et al., 2003; Kundzewicz et al., 2005), Canada (Loukas et al., 1999)) show that mean discharge may be affected and the risk of flooding may increase. Using both recorded streamflow measurements and simulated flow from coupled global atmospheric and hydrological models Milly et al. (2002) showed that the frequency of great floods, i.e. floods with a return period of 100 years or more, is projected to increase while floods with shorter return periods may not be significantly affected.

1.6 Climate adaptation and mitigation measures for urban drainage systems

In most cases the impact analyses of urban runoff indicate that in regions where CC occurs a systematic adaptation effort should be undertaken to minimize the impacts on the performance of the drainage systems. This need is further amplified by a range of other drivers, including increased urbanization, wealth, and drainage boundary conditions such as increased risk of extreme sea surges and fluvial flooding (Tait et al., 2008; Olsson et al. 2010; Huong et al. 2011; Pedersen et al. 2012). Some of these studies suggest that, regardless of the importance of CC impacts, systematic adaptation can mitigate the impacts to an acceptable

level through implementation of reasonable measures (Semadeni-Davies et al. 2008; Zhou et al. 2012).

While *climate mitigation* – the actions taken to reduce net GHG emissions – has historically been the main focus of policy attention (Mai et al., 2015), *climate adaptation* – the process of adjustment to actual or expected climate and its effects (IPCC 2014) – is becoming more prominent as a means to moderate or avoid harm from existing emissions. Climate adaptation is of particular relevance to cities as past experiences with climate-induced natural disasters (Rosenzweig et al., 2001; Aerts et al., 2012), as well as climate changeability and long-term CC demonstrate that vulnerability (the propensity to be adversely affected) and its causes are location-specific (Naess et al., 2005). These explanations resonate with the fact that spatial structure, spatial planning strategies, flood risk and management are also location-specific (IPCC, 2014). They also raise questions about the need to identify dominant institutional characteristics of the governance arrangements in given localities, and about the constraining and enabling factors influencing them (institutions and governance arrangements). Dominant institutional characteristics can be observed in the institutional configurations and mechanisms of cooperation among actors and how these affect the steering capacity of organisations (including their coordination capacity) to address climate-related flood risks (Naess et al., 2005).

With regard to drainage systems, the effectiveness of potential adaptation measures varies due to the magnitude of flooding and regional features. Therefore, system improvement should be preceded by an evaluation of drainage system capacity. Mitigation measures should be identified within a range where the effects of CC on the drainage system can be evaluated and accommodated, and an economic analysis is necessary for efficient determination.

Urban planners and designers of urban drainage infrastructure can use the projected changes in extreme rainfall and other key inputs to start accounting for the effects of future CC. Sections of the urban drainage system with insufficient capacity to convey future design flows can be upgraded over the next few decades as part of a programme of routine and scheduled replacement and renewal of ageing infrastructure. Optimization methods for CC adaptation are currently emerging (Zhou et al. 2012). However, current urban drainage practices are increasingly being challenged. In Australia, a persistent drought period has recently led to increased demand for retaining the precipitation in urban areas through implementation of water sensitive urban design (WSUD) principles for urban water management (Wong et al., 2009; Beecham, 2012). Study case projects that meet both urban

drainage criteria for CC adaptation and other objectives are often collected and recorded in national repositories to inspire other stakeholders to consider multifunctional use of urban spaces. Examples of such repositories are UKCIP (2013) and Climate Change Adaptation (2013).

An adaptive approach has to be established that provides flexibility and reversibility but also avoids closing off options. This is different from the traditional engineering approach, which can be static and is often based on design rules set by engineering communities without much public debate. An adaptive approach involves active learning that recognizes that flexibility is required as understanding increases (Arnbjerg-Nielsen et al., 2013). Essentially two paradigms are being questioned. First, the recent focus on optimization of infrastructure has led to reduced investment and to reduced operational costs. This in turn has led to ageing and deteriorating infrastructure with lower service levels. Secondly, the concept of urban drainage as a well defined and relatively static scientific discipline is being challenged (Arnbjerg-Nielsen et al., 2013). The implications of urban drainage design decisions are intricately connected to other decisions about the well-being of the city in the same way that decisions about the well-being of the city have a major influence on the ability of the urban drainage system to deliver the essential services in an affordable and efficient way.

Adaptation options designed to ensure water supply during average and drought conditions require integrated demand-side as well as supply-side strategies. The former improve water-use efficiency, e.g., by recycling water. An expanded use of economic incentives, including metering and pricing, to encourage water conservation and development of water markets and implementation of virtual water trade, holds considerable promise for water savings and the reallocation of water to highly valued uses. Supply-side strategies generally involve increases in storage capacity, abstraction from water courses, and water transfers. Integrated water resources management provides an important framework to achieve adaptation measures across socio-economic, environmental and administrative systems. To be effective, integrated approaches must occur at the appropriate scales.

Mitigation measures can reduce the magnitude of impacts of global warming on water resources, in turn reducing adaptation needs. However, they can have considerable negative side effects, such as increased water requirements for afforestation/reforestation activities or bio-energy crops, if projects are not sustainably located, designed and managed. On the other hand, water management policy measures, e.g., hydrodams, can influence GHG emissions. Hydrodams are a source of renewable energy. Nevertheless, they produce GHG emissions

themselves. The magnitude of these emissions depends on specific circumstance and mode of operation.

Water resources management clearly impacts on many other policy areas, e.g., energy, health, food security and nature conservation. Thus, the appraisal of adaptation and mitigation options needs to be conducted across multiple water-dependent sectors. Low-income countries and regions are *likely* to remain vulnerable over the medium term, with fewer options than high income countries for adapting to CC. Therefore, adaptation strategies should be designed in the context of development, environment and health policies.

Several gaps in knowledge exist in terms of observations and research needs related to CC and water. Observational data and data access are prerequisites for adaptive management, yet many observational networks are shrinking. There is a need to improve understanding and modelling of CCs related to the hydrological cycle at scales relevant to decision making. Information about the water related impacts of CC is inadequate – especially with respect to water quality, aquatic ecosystems and groundwater – including their socio-economic dimensions: current tools to facilitate integrated appraisals of adaptation and mitigation options across multiple water-dependent sectors are inadequate.

1.6.1 Flood risk and management

Flood risk and management is concerned with the probability (risk), strategies and measures (management) aimed at mitigating or preventing urban flooding (Albrechts, 2004). One of the ‘wicked problems’ facing politicians and strategic planners in the context of CC is the risk of flooding. This problem is even more acute given the transboundary nature of flooding which exposes the mismatch between problem characteristics, dominant institutional characteristics, and organisational forms. As previously explained, flooding is the temporary covering of land by water outside its normal confines (Flood-Site Consortium, 2015). It may be caused by rainfall (pluvial), sea and tidal surges (coastal), river discharges (fluvial), among others, with each flood having its own characteristics with regards water depth, flow velocity, matter fluxes, temporal and spatial dynamics (Schanze, 2006). The probability of a potentially damaging flood occurring is called flood hazard as damage depends on the vulnerability of the asset exposed to it. CC results in the increased flood hazards caused by all of the abovementioned phenomena, with the raising sea level, more rainfall, and increased frequency and intensity of extreme weather events. Vulnerability is measured by the loss of cultural and social attributes (life, cultural-historical, personal, and sentimental assets), economic attributes (property, means of livelihood), and/or ecological attributes (pollution of

ecosystems such as soil, rivers and their biota) caused by the flood hazard. Flood risk then emerges as the interrelation of flood hazard and flood vulnerability (Schanze, 2006). CC increases the complexity of flood risks.

Flood risk management, is the ‘holistic (comprehensive) and continuous societal analysis, assessment and reduction of flood risk’ (Flood-Site Consortium, 2015). Conventionally, flood risk management is considered as hydraulic engineers’ responsibility. Managing floods may include or not include a risk analysis.

The former entails checking whether the flood protection infrastructure (hydrological) is reliable, making decisions and taking actions to mitigate the remaining risk above protection. The latter entails taking decisions and actions that reduce flood risk. In structuring risk management activities three tasks are undertaken: risk analysis (previous, current and future risk); risk assessment (perception and evaluation of risk); risk reduction (interventions that can potentially decrease risk). Linking these tasks is the process of collective decision-making (Hall, Meadowcroft, Sayers, & Bramley, 2003) often influenced by dominant institutional characteristics (visions, norms, practices) and decision-making processes.

Governance refers to ‘an arrangement where one or more public agencies directly engage non-state stakeholders in a collective decision-making process that is formal, consensus-oriented, and deliberative and that aims to make or implement public policy or manage public programs or assets’ (Ansell et al., 2008). As a process, governance is ‘the procedures and structures of public policy decision making and management that engage people constructively across the boundaries of public agencies, levels of government, and/or the public, private and civic sphere to carry out a public purpose that could not otherwise be accomplished’ (Emerson et al., 2012). In the context of the governance of flooding in the face of CC, governance is the institutional configuration (including norms and values) and mechanisms of cooperation allowing for coordination between spatial planning strategies and flood-risk management actions (Francesch-Huidobro, 2015a,b).

Institutions refer to the system of rules (professional approaches, beliefs, values), decision-making procedures, and programmes that impact social practices, define roles to the participants of these practices, and guide interactions among them (Young, 1999; Steimo, 2001). As such, they underpin political behaviour. Formal (constitutional rules) or informal (cultural norms), institutions tend to be entrenched in particular organisations. Moreover, institutions impact an organisation’s steering and coordinating capacities often enabling and/or constraining their functioning.

1.6.2 Adaptation Planning

The impacts of CC are occurring around the world and planners, policy makers, and engineers face the challenge of preparing appropriate plans to mitigate the effects of CC on the built environment.

There are two fundamental responses to anthropocentric CC: mitigation and adaptation. Mitigation refers to lessening global CC by either reducing and/or eliminating GHG emissions or enhancing GHG sinks (Fussel, 2007). Adaptation, as defined by the Intergovernmental Panel on Climate Change (IPCC), is “actions that reduce the negative impact of CC and/ or take advantage of new opportunities. It involves making adjustments in our decisions, activities and thinking because of observed or expected changes in climate” (IPCC, 2007).

Nelson *et al.* (2007) defined adaptation to environmental change as "an adjustment in ecological, social, or economic systems in response to observed or expected changes in environmental stimuli and their effects and impacts in order to alleviate adverse impacts of change". The related concept of resilience refers to the ability of a system to withstand change. Different regions and different sectors vary in their resilience, and therefore in their capacity for adaptation (Arnell, 2000).

Milly *et al.* (2008) argued that CC has undermined the principle of stationarity, a central concept in water resource management which holds that future hydrological events will be within the range of past variability. Currently, water managers make decisions based on probability density functions, which are generated with observed data on the inverse relation between the frequency of an occurrence and its magnitude. Because CC is likely to change both the mean conditions and the variability of hydrological regimes, basing long-term management decisions on these functions is highly problematic, a reality increasingly acknowledged by water resource managers (Praskievicz *et al.*, 2009).

Fussel (2007) identifies several reasons why adaptation is important today and will continue to be important in the future. First, Fussel (2007) notes that anthropocentric GHG emissions are affecting the global climate. NASA and NOAA both found 2014 to be the hottest year on record, which resulted in extreme heat and flooding in many parts of the world (NASA, 2015). The average global temperature was approximately “0.57° Centigrade (1.03 Fahrenheit) above the average of 14.00°C (57.2 °F) for the 1961-1990 reference period. This is 0.09°C (0.16 °F) above the average for the past ten years (2004-2013)” (WMO, 2014). Fussel (2007) also notes that due to the accumulation of GHGs already in the atmosphere, the

climate will continue to change regardless whether GHG emissions ceased today (Fussel, 2007). The effects of emission reductions have a significant lag time, meaning, the positive impacts will not be felt for many decades after the reductions are made. The impacts of adaptation are experienced at the local and/or regional scale, whereas mitigation requires collective global action. Last, Fussel (2007) describes the important ancillary benefits of adaptation, namely reducing climate-sensitive risks.

For the reasons identified by Fussel (2007), adaptation planning has become more mainstream in recent years. Local governments will necessarily be at the forefront of this study, as many of the impacts of CC will affect infrastructure within their jurisdiction.

Adaptation planning typically incorporates “hard” and “soft” approaches. Soft approaches are usually employed first and refer to policy and behavioural changes (Clark et al, nd; Jones et al, 2012); hard infrastructure refers to manmade infrastructure. (Clark et al, nd).

1.6.2.1 Municipal Adaptation Planning Opportunities

Municipal governments provide services that reflect the needs and desires of their constituents. Under provincial legislation, municipal governments have the authority to provide, but are not limited to, the following services:

- General government
- Transportation – streets and roads, in some cases urban transit
- Protection – police, fire
- Environment – water treatment and supply, waste water treatment, refuse collection/disposal
- Recreation and culture – recreation centres, playing fields, parks, libraries
- Land use planning and regulation, building regulation, zoning
- Regulation – animal control, public health, signs, business licensing, municipal services (BC Ministry of Culture, Sport, and Community Development, 2014)

CC adaptation does not fit neatly into any one of these categories but it would be necessary to address CC at the local scale for two main reasons: a) the impacts of CC are directly experienced at the local level (Richardson et al., 2012) and, therefore, adaptation responses must account for geographic variability and downscaled climate vulnerability analysis (Measham, et al., 2011); b) the apparent lack of success at the international and national level to achieve meaningful reductions in GHG reductions has left municipal governments needing to prepare for anticipated climate impacts.

Municipal governments have three critical roles in CC adaptation: develop adaptation responses to local impacts, mediate between individual and collective responses to vulnerability, and govern the delivery of resources to facilitate adaptation (Measham et al., 2011). Effective adaptation responses require strong leadership at the local level to ensure integration into the existing policy and planning processes (ICLEI, 2015). In addition, responses must be measurable, reflective, prioritized, and cost effective in the long term (Travers et al., 2012).

In many respects, municipal governments already have the necessary tools to address CC. Existing tools include Official Community Plans (OCPs), zoning bylaws, development permits, design guidelines, and master infrastructure plans. Despite these tools, barriers to adaptation at the municipal level remain.

The unknown risks of CC impacts to individual infrastructure components, and determining the adaptive capacity of these components. The development of effective knowledge and capacity among municipal staff to maintain infrastructure at a sustainable level of service that is resilient to CC impacts (Feltmate et al, 2012).

Feltmate et al. (2012) recommend cities embrace a “no regrets” approach to climate policy and aim to improve infrastructure resilience and generate community benefits that extend beyond mitigating CC impacts. In fact, sustainable rainwater infrastructure is often used in the literature as a means to integrate green infrastructure into urban areas and receive multiple benefits from the infrastructure. Receiving multiple benefits from a single infrastructure investment allows planners, city officials, and engineers to implement “no-regrets” infrastructure. The idea behind “no-regrets” infrastructure for adaptation is that a single infrastructure investment will provide multiple benefits, which help to justify a certain type of adaptation infrastructure over another. For instance, implementing sustainable rainwater measures provides stormwater management, economic, social and environmental benefits, as well as acting as a CC adaptation measure. Alternatively, “hard” infrastructure such as a reservoir to catch and store excess stormwater only provides stormwater management services and can prove expensive over the long-term due to maintenance costs and inability to efficiently be upgraded for increased storage capacity.

1.6.2.2 Example of Adaptation Planning: Connecting Delta Cities

Cities around the world are on the front lines in the battle against CC. Delta cities, however, confront a particularly urgent challenge, as Hurricanes Katrina (New Orleans) and Sandy (New York), the flash flood in Buenos Aires, the cloudburst in Copenhagen, and the

annual flooding inundation in Ho Chi Minh and Jakarta have shown. Situated where rivers meet larger bodies of water, delta cities must safeguard urban populations and infrastructure from the potentially devastating impacts of CC and severe weather, such as storm surge, flooding, and sea level rise.

Delta cities, in fact, are particularly vulnerable to the consequences of CC such as floods (Nicholls et al., 2007; Aerts et al., 2012; Hallegatte et al., 2013). Before the urbanization of deltas, floods were not a threat but the driving force of the process of making delta landscapes. Today, urban infrastructures such as drainage systems, dikes and dams, together with accelerated processes of land reclamation and the training of rivers have disrupted the natural process of land-making, decreasing the capacity of delta cities to cope with excessive water (Meyer et al., 2010). These infrastructural-induced problems are compounded by CC-related impacts such as sea level rise, rainfall, and increasing ratio of extreme weather events, such as storms, typhoons, tsunamis, and intense precipitation. Together, infrastructural and climate-related problems threaten the urban development and spatial quality of delta cities. The transition to climate-adaptive urban development is, thus, a major challenge facing delta cities across the globe, and one that urban planners, civil engineers and policy-makers need to address (Carter et al., 2015).

These urgent challenges sparked the first conversations between Rotterdam and other megacities during a 2007 C40 Cities Climate Leadership Group meeting in Tokyo, leading to the formation of the C40 Connecting Delta Cities (CDC) network. Today there are ten global cities in the CDC network: Ho Chi Minh City, Hong Kong Jakarta, London, Melbourne, New Orleans, New York, Rotterdam, Copenhagen and Tokyo – all committed to sharing knowledge about policies, planning measures, and technologies that reduce the impact of climate risks. The success of the CDC network has become a proof point for what is now an organizing principle of C40: the formation of working groups of cities focused on common challenges and opportunities (Aerts et al., 2009).

As previously explained, one of the conclusions of the fifth global climate report ‘Climate Change 2013: The Physical Science Basis’ (IPCC, 2013) is that continued emissions of GHG will cause further warming and changes in all components of the climate system. This century the sea level will keep on rising and the contrast in precipitation between wet and dry regions and between wet and dry seasons will increase: extreme precipitation events over most of the mid-latitude land masses and over wet tropical regions will very likely become more intense and more frequent by the end of this century. At the same time, many delta cities suffer from

severe land subsidence. As a consequence of these urban developments, and projections for land subsidence and CC, the vulnerability of delta cities is expected to increase in the decades to come. All this may well be the future scenario, but CC is already occurring, with extreme events happening more frequently and cities already facing flood losses. New Orleans, New York, Bangkok, Manila, Jakarta and many others all faced severe flooding, losses and damage in recent years. The current climate risks and the projected increase in climate risk and other trends create an urgency for cities to act. It is for this reason that in 2008 several delta cities joined forces and, initiated by the City of Rotterdam, set up the network called Connecting Delta Cities (CDC). Connecting Delta Cities (CDC) CDC is a sub network within the framework of the C40 Cities Climate Leadership Group (C40), a network of the world's mega cities committed to addressing CC. C40 was created in 2005 by former Mayor of London Ken Livingstone, and forged a partnership in 2006 with the Cities Programme of President Clinton's Climate Initiative (CCI). Sharing knowledge and working together on adaptation to CC is what these cities practise within the CDC-network. Cities play an important role in the climate adaptation process since they have already developed the ability to adapt continuously to change and attract economic activity and investment. One could say cities have already been adapting to changing conditions for many years or even centuries, and CC is an additional challenge that needs to be addressed in cities' planning, investments and regulations. With the CDC network, the member cities have shown for five years now leadership in the field of adaptation to CC.

1.6.3 Sustainable stormwater system

The world's population has reached 7.2 billion, and more people live in cities than in rural areas (UNDESA, 2014). Water is a very critical natural resource for the world's fastest growing urban areas. Commercial, residential, and industrial users already place considerable demands on cities' water resources and supply, which often require water treatment (Bahri, 2012). The demand of water resources in urban areas is approaching the capacity of the water supply and, in many cases, the limits of sustainable water use are being exceeded (Hatt et al., 2004; Mitchell et al., 2003). In some cases, water scarcity is leading to conflict over water rights. In urban watersheds, competition with agriculture and industry is intensifying as cities expand in size and political influence (Bahri, 2012). With industrial and domestic water demand expected to double by 2050 (UNDP, 2006), competition among urban, peri-urban, and rural areas will likely worsen. A critical challenge to newly developed urban cities is design for resilience to the impact of CC with regards to sustainable management of water

resources. It is currently well accepted that the conventional urban water management approach is highly unsuited to addressing current and future sustainability issues (Ashley et al., 2005; Wong et al., 2008). The conventional approach to urban water systems around the world involves the use of a similar series of systems for drainage of stormwater, potable water and sewerage. As explained by Bahri (2012), the unsustainable nature of this approach is highlighted by the current ecosystem-related problems and degraded environment in urban areas due to changes in the hydrology of catchments and quality of runoff, leading to modified riparian ecosystems (Bahri, 2012). United Nations Agenda 21 (1992) stated that achieving sustainable urban water systems and protecting the quality and quantity of freshwater resources are key components of ecologically sustainable development.

Because of CC and the spread of urbanization, the negative impacts are intensifying, resulting in increasing runoff, pollutant loads and pressure on existing systems, with a significant economic cost required to augment conventional systems. Alternative approaches are required to develop sustainable water systems in urban environments, and Integrated Urban Water Management (IUWM) is one such approach, which views the water supply, drainage and sanitation as components of an integrated physical system within an organizational and natural landscape (Mitchell et al., 2007a, 2007b). It is an integrated system that seeks to reduce the inputs and outputs to decrease the inefficiencies of water resources that are associated with the traditional practices of urbanization (Hardy et al., 2005). Although this incorporation and diversification of urban water systems increase the complexity of urban water systems, they also provide more opportunities to attain sustainable water use and increase the overall water system resilience (Mitchell et al., 2005; Mitchell et al., 2007b). The identified key components of the IUWM system are the methods and measures to capture and utilize urban stormwater, that is defined stormwater as precipitation, such as rain or melting snow (Saraswat et al., 2016). In a natural environment, a small percentage of precipitation becomes surface runoff; however, as urbanization increases, the amount of surface runoff drastically increases. Surface runoff is created when pervious or impervious surfaces are saturated from precipitation or snow melt (Durrans, 2003). Pervious surface areas naturally absorb water to the saturation point, after which, rainwater becomes runoff and travels via gravity to the nearest stream. This point of saturation is dependent on the landscape, soil type, evapotranspiration and biodiversity of the area (Pierpont, 2008). In the urban environment, due to the impervious surfaces that cover the natural environment, the hydrological processes

of surface water runoff become more unnatural, causing damage to infrastructure and contamination of water by pollutants (Ragab et al., 2003).

The need for stormwater runoff management capture and transportation systems developed as a result of human experiences with various challenges due to destructive floods. The sustainable stormwater runoff management target is to understand the changes in the urban landscape, in which the addition of vegetation is not widely observed, with the aim of devising approaches to limit certain undesirable effects and to take advantage of the new opportunities (Huang et al., 2007). A sustainable stormwater system is not a system to address runoff problems and avoid unwanted contaminants in the water, but rather, it is a system to increase the potential usability of water resources in society (Sundberg et al., 2004). Stormwater capture and drainage may be considered not only as systems to divert undesired water from urban areas but also as valuable elements for landscaping the surroundings of buildings and roads (Boller, 2004). In general, to control surface runoff, flood control agencies have constructed large centralized facilities, such as culverts, detention basins and sometimes re-engineered natural hydrologic features, including the paving of city river channels to quickly convey runoff to receiving water bodies. These large-scale facilities are required to handle the massive amounts of runoff generated by the largest storm events, as it would be impractical to handle this runoff on a decentralized parcel-by-parcel basis with small-scale infiltration devices. The current trend is toward a more overall integrated approach to manage stormwater runoff as an integrated system of preventive and control practices to accomplish stormwater management goals. The first principle is to minimize the generation of runoff and pollutants through a variety of techniques, and the second principle is to manage runoff and its pollutants to minimize their impacts on humans and the environment in a cost effective manner (EPA, 2007).

There will frequently be decisions made in stormwater management that reflect the economic, political, social, and aesthetic components that may be influenced by a range of factors, including knowledge of urban water problems, frequency and water restrictions, familiarity with use of alternative water sources, and either positive or negative support from water authorities, government agencies and researchers.

Stormwater management in Japan and Thailand has always aimed to control stream flow for municipal and commercial use while preventing water-related disasters in cities (Saraswat et al., 2016). City stormwater management policies were based on flood control and, in recent years, shifted from the exclusive use of structural approaches to using a combination of

structural and non-structural approaches. Thailand has focused more on structural measures in addressing stormwater issues, including aggressive implementation of measures involving the general public and the private sector (Chiplun-kar et al., 2012). In Vietnam, an integrated design of surface runoff infiltration, storage and transportation of stormwater was applied. The country has focused on increasing the groundwater levels by increasing the stormwater percolation rates through enhanced infiltration (Werner et al., 2011).

1.6.4 Modeling water management

High-intensity precipitation associated with CC, combined with higher impervious surface area accompanying urban development, increases surface runoff and creates flashy storm discharge, which has negative hydrological and water quality impacts. Waters *et al.* (2003) used the water resource model Personal Computer – Storm Water Management Model (PCSWMM), driven by a synthetic CC scenario, to simulate the management actions needed to maintain peak discharge at current levels under a 15% increase in rainfall intensity in an urban basin in Ontario. The most effective methods were downspout disconnection, increased depression storage, and increased street detention storage. Such sustainable stormwater management techniques may become increasingly necessary to avoid the worst impacts of CC and urban development. A further consequence of the increased flashiness of urban runoff resulting from higher-intensity precipitation and higher impervious surface area is that dry periods may be more severe (Meehl *et al.*, 2007).

The increased surface runoff and reduced groundwater recharge associated with some scenarios of CC and urban development not only mean higher floods, but also more frequent and severe droughts, because of the reduction in water storage. Fowler et al. (2007) used the Mospa water management model, driven by a regional CC scenario based on the HadCM3 GCM, to determine twenty-first century impacts of CC on the water supply system of northwestern England. They found that overall available yield will decrease by 18%, but that existing water infrastructure and management practices should be sufficient to meet future demand. Problems with increased hydrological variability associated with CC and urban development are likely to be more severe in regions with pronounced seasonal variability in flows. O'Hara et al. (2008) assessed the water supply system in San Diego, California, as a study case to develop a methodology for evaluating the need for changes in water storage capacity as a result of CC, finding an increase in future storage costs under CC, exacerbated by population growth.

These combined pressures may force some urban water utilities to limit demand through conservation measures or to seek alternative sources of supply, such as groundwater reserves or interbasin transfers. Finally, in addition to the direct impacts on urban water supplies, CC is also likely to exacerbate conflicts over competing uses for water resources, such as extraction for municipal and agricultural use, hydropower, and environmental flows (Praskievicz et al., 2009). This problem is likely to be especially severe in regions like the mountains of the western United States, where increased temperatures will diminish the snowpack and shift the timing of peak runoff to earlier in the spring, leaving lower flows available during the high-demand summer (Praskievicz et al., 2009).

VanRheenen et al. (2004) used a water resource model, driven by outputs from a macroscale hydrological model perturbed by statistically downscaled GCM scenarios, to examine the impacts of CC on water management in California's Sacramento and San Joaquin basins. They found that the modeled adaptation measures could meet only up to 96% of environmental flow requirements in the Sacramento River Basin and less than 80% in the San Joaquin River Basin by 2099. These findings illustrate the potential exacerbation of water resource conflicts under future CC and urban development and the impossibility of meeting all demand for water in some regions.

Chapter 2

Methods and models

The goals of this study are to analyze CC's effects on a urban drainage system and suggest some methods of mitigation. This kind of investigations requires a procedure that starts from storms and ends to floods as conceptualized in *Figure 2.1*.

However, it is important to consider that in that schematic representation two important downscaling steps need to be added as shown in *Figure 2.2*: the first downscaling is required because *General Circulation Models* (GCMs) are able to provide monthly data and, for this study, the least time scale for rainfalls needs to be hourly time steps to compare observed statistics of precipitation to the simulated ones; the second downscaling needs to be applied to achieve sub-hourly rainfalls from simulated hourly datasets because urban catchments require a sub-hourly time scale to make outputs being closer to the thru and to point out all different finer steps in the rainfall-runoff simulations.

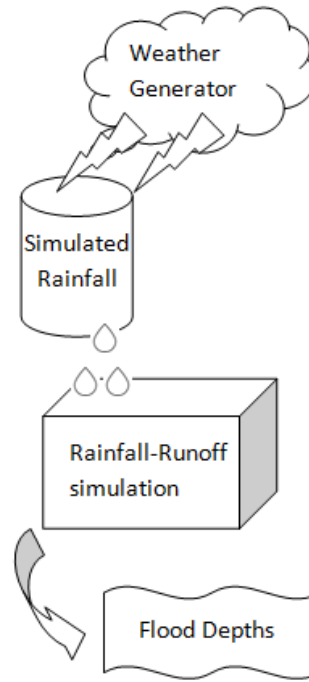


Figure 2.1. Schematic representation of the procedure applied on this study.

This chapter provides an overview about methods and models used for the illustrated procedure in *Figure 2.1* and *Figure 2.2*: the chosen weather generator model is AWE-GEN by Fatichi et al. (2011), see section 2.1 for the description; inputs of this weather generator model are data from both weather station and GCMs, as explained in section 2.2, in which the downscaled procedure is also clarified; while section 2.3 describes the random cascade disaggregation model that is needed to obtain sub-hourly datasets used as input of rainfall-runoff model; in section 2.4, the Storm Water Management Model by EPA (EPA SWMM) is introduced as a valid model to obtain estimation of flood depths and, deductively, consequent and possible flood damages.

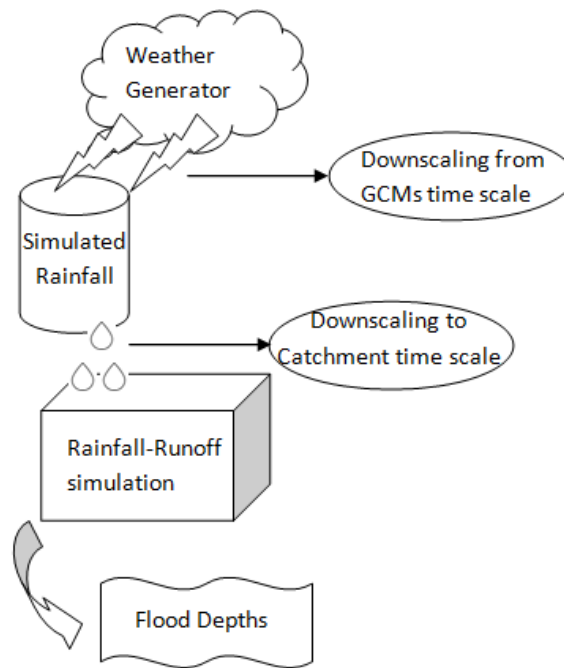


Figure 2.2. Schematic representation of the procedure applied on this study including downscaling steps.

2.1. AWE-GEN

Advanced WEather GENerator (AWE-GEN) (Fatichi et al., 2011) is an hourly stationary weather generator. The generator is capable of reproducing low and high-frequency characteristics of hydro-climatic variables and essential statistical properties of these variables. The weather generator employs both the physically-based and stochastic approaches and can be considered a substantial evolution of the model presented by Ivanov et al. (2007).

The main modules of the model are the following: the precipitation module based on the *Poisson-Cluster* process, the module simulating vapor pressure, the wind speed module, the shortwave radiation module, the cloudiness and air temperature components, and the atmospheric pressure module. Furthermore, a procedure to take into account non-stationary change of climate has been incorporated in the AWE-GEN framework. The procedure is based on a stochastic downscaling of GCM predictions (Fatichi et al., 2011; 2013).

The variables simulated by the weather generator at hourly scale are precipitation, cloud cover, shortwave radiation with partition into various type and spectral bands, air temperature, vapor pressure, wind speed, and atmospheric pressure.

Interested readers are referred to Fatichi et al. (2011; 2013) and to the on-line technical documentation available at <http://www.umich.edu/ivanov> for details concerning the model

structure and parameterization. A brief description of each one of the model components is provided in the following sections.

2.1.1. Precipitation

The precipitation component of the AWE-GEN is based on the Poisson-cluster rainfall model (Onof et al., 2000) that was originally introduced by Rodriguez-Iturbe et al. (1987) and Rodriguez-Iturbe and Eagleson (1987) and was further developed by Rodriguez-Iturbe et al. (1988), Entekhabi et al. (1989), Cowpertwait (1991) and Cowpertwait et al. (1996). Recently, this type of precipitation occurrence has been extended to the two-dimensional space; a third moment theoretical function of the rainfall process has been developed to better fit extreme values; and an overlapping model of two rectangular pulse processes has been proposed to enhance the capability in reproducing finer structure of the process (Cowpertwait, 1994; Cowpertwait, 1995; Cowpertwait, 2003; Cowpertwait, 2007; Leonard et al., 2008).

2.1.1.1. Neyman-Scott Rectangular Pulse process

The *Neyman-Scott Rectangular Pulse* (NSRP) approach (Figure 2. 3) is used in AWE-GEN to generate the internal structure of precipitation process. The model is primarily based on the approach of Cowpertwait (1998), Cowpertwait et al. (2002), and Cowpertwait (2004). The storm time origin occurs as a Poisson process with the rate λ [h^{-1}]. A random number of cells C is generated for each storm according to the geometrical distribution with the mean μ_c [-]. Cell displacement from the storm origin is assumed to be exponentially distributed with the mean β^{-1} [h]. A rectangular pulse associated with each precipitation cell has an exponentially distributed life time with the mean η^{-1} [hr] and intensity X [$\text{mm}\cdot\text{h}^{-1}$]. The latter is distributed according to the Gamma distribution with the parameters α and θ . The distributions adopted for the random process within the NSRP model fully define the statistical properties of the aggregated process over an arbitrary time-scale h (Cowpertwait, 1998).

The parameter estimation procedure follows that of Cowpertwait et al. (2002), Cowpertwait (2006), Cowpertwait et al. (2007), i.e., an objective function containing statistical properties of precipitation at different aggregation times is used. After a large number of tests using available data, the following properties are used in the objective function: the coefficient of variation $C_v = \sqrt{\gamma_{h,0}} / \mu_h$; the lag-1 autocorrelation $\rho(h) = \gamma_{h,1} / \gamma_{h,0}$; the skewness $k(h) = \xi_h / \gamma_{h,0}^{3/2}$; and the probability that an arbitrary interval of length h is dry,

$\Phi(h)$. The parameters μ_h , $\gamma_{h,l}$, and ζ_h represent the mean, the covariance, and the third moment of precipitation process at a given aggregation time interval h and lag-1. The utilized fitting procedure assumes that hourly rainfall time series are available as the coarsest temporal resolution. The procedure specifically uses the above statistical properties of the rainfall process at four different time scales h : 1, 6, 24, and 72 h. The simplex method (Nelder and Mead, 1965) is used as a minimization method for the imposed objective function. The method has been previously employed by Cowpertwait (1998), Cowpertwait et al. (2007) with good performance in terms of its convergence characteristics. In order to take into account the seasonality of site climatology, the parameters are estimated on a monthly basis, i.e., six parameters for each month need to be inferred to completely define the NSRP model: λ , μ_c , β , η , α , and θ .

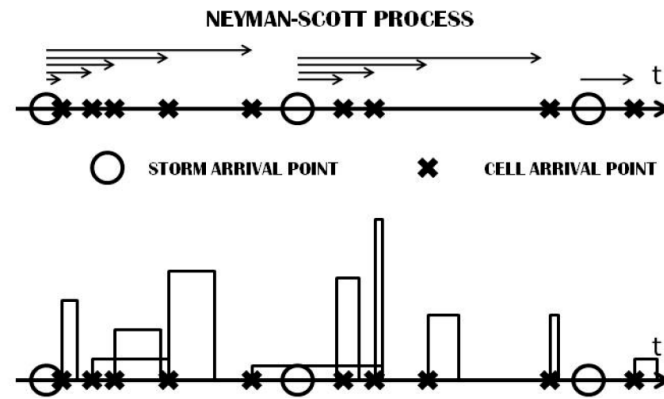


Figure 2. 3. Schematic representation of Neyman-Scott model with rectangular pulses.

2.1.1.2. Low-frequency properties of precipitation process

Previous efforts of validation of the NSRP model at larger time intervals, for instance, at the yearly time scales, have indicated that the variance of the simulated process was smaller than the one inferred from observed data (Wilks and Wilby, 1999). This underestimation, sometimes referred to as “overdispersion” (Katz and Parlange, 1998; Wilks, 1999), is probably because of the underlying stationarity assumption of weather generators (Wilks and Wilby, 1999).

In order to introduce the capability for reproducing low-frequency properties of the precipitation process and overcome the problem of “overdispersion”, a numerical procedure of external selection of hourly precipitation series generated with the NSRP model on the basis of the annual precipitation series generated with the model is implemented in the AWE-GEN (Bates et al., 2008). The approach therefore aims to preserve the variance and the

autocorrelation properties of the precipitation process at the annual scale, rather than at the monthly scale. It does not undermine the capability of the model to preserve the intra-annual precipitation statistics. The latter is guaranteed by the NSRP model, which is applied seasonally at the hourly scale.

Markov-type models have been commonly used to reproduce annual time series of precipitation (Srikanthan and McMahon, 1982; Srikanthan and McMahon, 2001), though they neglect the possible long term persistency of the process (Wilson and Hilferty, 1931). The inter-annual variability of precipitation at the annual time scale is simulated using an autoregressive order-one model, AR(1), with the skewness modified through the Wilson-Hilferty transformation (Wilson and Hilferty, 1931; Fiering and Jackson, 1971):

$$P_{yr}(i) = \overline{P_{yr}} + \rho_{P_{yr}}(P_{yr}(i-1) - \overline{P_{yr}}) + \eta(i)\sigma_{P_{yr}}\sqrt{1 - \rho_{P_{yr}}^2} \quad (2.1)$$

where $\overline{P_{yr}}$ is the average annual precipitation, $\sigma_{P_{yr}}$ is the standard deviation, and $\rho_{P_{yr}}$ is the lag-1 autocorrelation of the process. The term $\eta(i)$ represents the random deviate of the process, which is transformed according to the Wilson and Hilferty (1931) approach. The parameters $\overline{P_{yr}}$, $\sigma_{P_{yr}}$, $\rho_{P_{yr}}$, and $\gamma_{P_{yr}}$ are determined from annual observations.

The NSRP model that captures intra-annual precipitation regime (the high-frequency properties) is coupled with the AR(1) model (Bates et al., 2008) that reproduces precipitation inter-annual variability (the low-frequency properties) in the following manner. First, the NSRP model is used to simulate precipitation series at the hourly time scale for the period of one year. The obtained total precipitation is then compared with the annual value estimated with the autoregressive model (Bates et al., 2008). If the difference between the two values is larger than a certain percentage \tilde{p} of the measured long-term mean annual precipitation, the simulated one-year long hourly series are rejected; a new series is generated and the above comparison is repeated. Once the difference between the two values is below the \tilde{p} threshold, the NSRP model simulated time series of precipitation are accepted. The entire procedure is repeated until all annual values generated with the model (Bates et al., 2008) have matching hourly series generated with the NSRP model. The rejection threshold \tilde{p} can be chosen according to the information about observational errors of annual precipitation.

Given the stationary nature of the NSRP model, the search of ‘‘suitable’’ years can be computationally exhaustive for locations characterized by a high variance of annual precipitation. In order to reach the convergence in a reasonable computational time, an adjustment procedure similar to that proposed by Kysely and Dubrovsky (2005) is introduced

after a pre-defined number of iterations without a satisfactory match. Specifically, discarded one-year long hourly NSRP precipitation series are first selected that have the closest match to the precipitation simulated with the AR(1) model. These series are subsequently multiplied by a correction factor to match the annual precipitation simulated with the AR(1) model.

2.1.2. Air temperature component

Air temperature is simulated with a mixed physics-based, stochastic approach developed by Curtis and Eagleson (1982) and Ivanov et al. (2007). AWE-GEN utilizes the same approach with further improvements.

The generation of air temperature $T(t)$ [$^{\circ}\text{C}$] is simulated as the sum of a stochastic component $dT(t)$ and a deterministic component $\tilde{T}(t): T(t) = \tilde{T}(t) + dT(t)$. The deterministic component of air temperature $d\tilde{T}(t)/dt$ is assumed to be directly related to underlying physical processes such as the divergence of radiative and eddy heat fluxes. The deterministic time-gradient of temperature $d\tilde{T}(t)/dt$ is a function of the air temperature itself, and of the incoming long-wave radiation (which exhibits a dependence on cloud cover). It is further related to the site geographic location and Sun's hourly position, used as a proxy for shortwave irradiance (Curtis and Eagleson, 1982).

The stochastic temperature component $dT(t) = T(t) - \tilde{T}(t)$, is estimated through an autoregressive model. The random deviate exhibits a significant dependence on the hour of the day, with differences noticeable in various statistics of $dT(t)$ for morning, midday, afternoon, evening, and night. Consequently, the average of the stochastic component $\overline{dT_h}$ and its standard deviation $\sigma_{dT,h}$ are estimated differently for each hour of the day.

The coefficients and the parameters used to estimate the deterministic and stochastic components are evaluated at the monthly scale. Ivanov et al. (2007) describe the procedure for estimation of the coefficients. The parameters $\overline{dT_h}$, $\sigma_{dT,h}$, and ρ_{dT} (the lag-1 autocorrelation of the stochastic component) are estimated from $dT(t)$ using conventional techniques.

2.1.3. Cloud cover component

The cloud cover simulated in AWE-GEN is based on the framework first developed by Curtis and Eagleson (1982) and Ivanov et al. (2007). Cloud cover $N(t)$ is the fraction of the celestial dome occupied by clouds. In the model of Ivanov et al. (2007), $N(t)$ [-] is considered to be a random variable that has different dynamics during intra-storm and inter-storm periods. During an intra-storm period, the value of cloudiness is assumed to be equal to 1.

During an inter-storm period, the existence of the “fair weather” region, R_0 , is assumed. The region is sufficiently distant from storms, thus the cloud cover can be assumed stationary and fully characterized by the first two statistical moments: the mean $E\{N(t)\}_{t \in R_0} = M_0$ and the variance $VAR\{N(t)\}_{t \in R_0} = \sigma_M^2$ of the process. T_R [h] is the length of the post-storm period after which the cloud cover process can be considered stationary. The second assumption is that the transition of the cloud process between the boundary of a storm and the fair weather period is described through an exponential function $J(t)$. The latter is characterized by two coefficients controlling the transition rates ζ and γ [h^{-1}], and by the average cloud cover of the first hour after a storm and of the last hour of an inter-storm, J_1 .

The parameters required for the model are $M_0, \sigma_m^2, \rho_m(1)$ (lag-1 autocorrelation value for the fair weather region), $\gamma = \zeta, J_1$, and 11 parameters of the Beta distribution that are used to generate random variables.

2.1.4. Shortwave incoming radiation component

In weather generators, shortwave radiation, R_{sw} [$\text{W} \cdot \text{m}^{-2}$], is commonly estimated through regression with other variables (Richardson, 1984; Parlange and Katz, 2000). The likely reason for such an approach is a lack of a conventional methodology for direct estimation of cloudiness and optical properties of the atmosphere. Once the site geographic location and cloudiness are known, several deterministic models with different degrees of complexity can be used to calculate the incoming shortwave radiation for clear-sky and overcast conditions (Gueymard, 1989; Freidenreich and Ramaswamy, 1999; Muneer et al., 2000; Gueymard, 2001; Gueymard, 2008; Ineichen, 2006). These methods use empirical coefficients to determine the atmospheric transmittances and the scattering fractions for direct and diffuse shortwave radiation. The incoming shortwave radiation is estimated with the model *REST2* developed by Gueymard (Gueymard, 2008) for clear sky conditions.

The parameterizations of Stephens (1978) and Slingo (1989) are used to compute transmittances for arbitrary cloudy conditions. The simulation of cloud cover, directly affects the computed shortwave fluxes. The partition of the incoming energy into different spectral bands could be useful for several purposes, such as ecological or eco-hydrological simulations that require the photosynthetically active radiation, PAR, as input. The discussed weather generator considers two bands K : the ultraviolet/ visible UV/VIS band, with wavelengths within the interval [0.29-0.70 μm], and the near infrared NIR band, with wavelengths within the interval [0.70-4.0 μm] (Gueymard, 2008). In the first band, ozone, nitrogen dioxide

absorption, and Rayleigh scattering are concentrated; the absorption by water vapor and uniformly mixed gases is concentrated in the second band.

The output of the radiation component of the weather generator contains the direct beam, $R_{Bn,A}$ [$\text{W}\cdot\text{m}^{-2}$], and diffuse, $R_{D,A}$ [$\text{W}\cdot\text{m}^{-2}$], radiation fluxes for the ultraviolet/visible UV/VIS [0.29-0.70 μm] and the near infrared NIR [0.70-4.0 μm] bands. PAR is also explicitly computed in AWE-GEN: conversion factors are applied to the first radiation band UV/VIS to compute PAR (Gueymard, 2008). The same factors are applied for both clear and cloudy sky conditions.

The spatial distribution of solar radiation over a terrain is a function of surface geometry: site slope β_T [rad] and aspect ζ_T [rad] alter the daily distribution of incoming energy at the ground. Furthermore, the reflection and shadow effects of the surrounding terrain can strongly influence site radiation fluxes (Dubayah and Loechel, 1997; Rigon and Bertoldi, 2006; Ivanov et al., 2007; Fatichi, 2010).

2.1.5. Vapor pressure component

The vapor pressure is not commonly simulated by weather generators (Semenov et al., 1998). Some weather generators, for instance, include relative humidity (Sharpley and Williams, 1990) or dew point temperature (Parlange and Katz, 2000; Ivanov et al., 2007). While the conversion of relative humidity or dew point temperature into vapor pressure is mathematically straightforward, it involves non-linearity. Because of that, an accurate simulation of dew point temperature or relative humidity does not necessary imply a good fit for vapor pressure. Dew point or relative humidity outputs of weather generators should therefore be checked before asserting their suitability for applications that require vapor pressure.

This model approaches the simulation of air humidity via the simulation of vapor pressure deficit, Δe [Pa], i.e., the difference between the vapor pressure at saturation e_{sat} [Pa], and the ambient vapor pressure e_a [Pa]. Following Bovard et al. (2005), who pointed out a correlation between vapor pressure deficit Δe and PAR during daylight time, the correlation of vapor pressure deficit with shortwave radiation and temperature has been analyzed. The possibility of such a linkage stems from the observation that specific humidity and vapor pressure, e_a , remain almost constant throughout the day, especially in dry climates. Therefore, the variations of Δe should be well explained by the diurnal cycle of air temperature. The assumption is primarily valid when the atmosphere is stable and the exchange between air masses with different characteristics is limited.

In order to simulate vapor pressure, a framework similar to the one used to model air temperature is used: Δe is simulated as the sum of the deterministic component, Δe , and the stochastic component, $d\Delta e$: $\Delta e(t) = \Delta e(t) + d\Delta e(t)$. The term Δe is related to air temperature through a cubic function, which is essentially an approximation of the commonly used exponential relation between T_a and e_{sat} (Dingman, 2002). From observational data, a significant correlation was also detected with global shortwave radiation, R_{sw} [W m^{-2}], at the lag of one and two hours:

$$\Delta e(t) = a_0 + a_1 T_a^3(t) + a_2 R_{sw}(t-1) + a_3 R_{sw}(t-2) \quad (2.2)$$

where a_i ($i = 0, 1, \dots, 3$) are the regression coefficients. The deterministic component Δe usually shows a minor hourly variance when compared to $\Delta e(t)$. The residuals $d\Delta e(t)$ are modeled with the AR(1) approach. Finally, the ambient vapor pressure e_a is calculated as the difference between e_{sa} and $\Delta e(t)$.

The parameters a_i ($i = 0, 1, \dots, 3$) are estimated on a monthly basis using conventional regression techniques, for example, the least squares approach. The parameters of the stochastic component: the average vapor pressure deficit deviations, $\overline{d\Delta e}$, the standard deviation, $\sigma_{d\Delta e}$, and the lag-1 autocorrelation of the process, $\rho_{d\Delta e}$, are evaluated using the time series of $d\Delta e(t)$ after removing the deterministic component from the observed series of $\Delta e(t)$.

2.1.6. Wind speed and atmospheric pressure components

Several studies highlight that cross-correlation between wind speed and other variables is typically very weak (Curtis and Eagleson, 1982; Ivanov et al., 2007) and thus wind speed is usually modeled as an independent variable.

Fatichi et al. (2011) observed that wind speed exhibits a marked daily cycle in some locations and therefore the assumption of independence may need to be questioned. From a physical point of view, the wind speed daily cycle is related to turbulent fluxes occurring in the surface boundary layer that are enhanced during the daytime by the dissipation of sensible heat. The wind daily cycle is thus more pronounced in dry climates. Starting from this concept, a relation between the global solar radiation and wind speed has been investigated. As found, the maximum correlation between the two cycles is usually shifted by several hours, possibly due to the difference in thermal properties of the ground surface and air.

The method adopted to simulate the wind speed, W_s [$\text{m}\cdot\text{s}^{-1}$], is based on representing the process as a sum of the deterministic component W_s and the stochastic component dW_s . This is a new approach as compared to methods developed previously. The deterministic component relates wind speed to the incident global shortwave radiation. The correlation is shifted by several hours (up to 3 h) and the shift strongly depends on the site location, as inferred from our tests:

$$W_s(t) = c_0 + c_1 R_{sw}(t) + c_2 R_{sw}(t-1) + c_3 R_{sw}(t-2) + c_4 R_{sw}(t-3) \quad (2.3)$$

where c_i ($i = 0, 1, \dots, 4$) are the regression coefficients. The stochastic component $dW_s(t) = W_s(t) - W_s(t-1)$ is modeled with the autoregressive AR(1) model including the Wilson–Hilferty transformation (Wilson and Hilferty, 1931; Fiering and Jackson, 1971). This transformation is necessary to represent the generally positive skewness exhibited by hourly wind speed data (Takle and Broen, 1978; Deaves and Lines, 1997).

The parameters c_i are estimated with conventional regression techniques. The parameters of the stochastic component: the average wind speed deviation, $\overline{dW_s}$, the standard deviation, σ_{dwd} , the lag-1 autocorrelation, ρ_{dws} , and the skewness of the process, γ_{dws} , are evaluated using time series of $dW_s(t)$ after removing the deterministic component from the observed series of $W_s(t)$. Wind speed generally does not present marked differences throughout the year, therefore the parameters are derived and assumed to be valid for all months.

The atmospheric pressure P_{atm} [mbar] is generally neglected in weather generators, given its low impact on hydrological and ecological processes. However, it is used in many non-linear equations describing physical phenomena, such as evaporation. This observation implies that using a constant value of atmospheric pressure is theoretically incorrect. In the AWE-GEN, a simple autoregressive model AR(1) is employed with parameters valid for the entire year. It has been observed that AR(1) model is suitable for reproducing hourly atmospheric pressure dynamics in several different climates.

2.2. General Circulation Models (GCMs) and downscaling procedure

2.2.1. General Circulation Models

The *General Circulation Models* (GCMs) are complex numerical tools able to simulate globally the climate system of the Earth. GCMs include five components: atmosphere, oceans, land surface, sea-ice and the biological and biogeochemistry cycles. There is a

disagreement with regards to the reliability of GCMs skill to reproduce much more than global averages of climatic variables within the Earth system. Since GCMs realizations are the foundation of any climate change prediction study, questioning the reliability of GCMs means questioning the overall possibility of making inferences about future climate and consequently whatever scientific discussion about climate change predictions must be looked as biased from the beginning. But, while climate models provide information that may not be exact in the absolute sense, yet due to their physically-based nature and their global scale of application, they still provide a robust prediction of a tendency, or at least they identify the emergence of a climate change signal. Nonetheless, the possibility that model artifacts can undermine the credibility of the study could not be totally dismissed but currently few alternatives, if any, are available. Moreover, GCMs have two important drawbacks: 1) the realizations spatial resolution is too coarse to be used directly in local studies (each model has a different pixel dimension that range from 130 to 550 km), 2) GCMs realizations are only available at the daily or larger aggregation intervals.

In this thesis, we used the GCMs (atmospheric component) employed in the *Intergovernmental Panel on Climate Change - Fifth Assessment Report (IPCC 5AR)* (IPCC, 2013). Specifically, in the *Chapter XI* (Meehl et al., 2007) of the Working Group I, climate models are assessed and their projections discussed. An overview of availability of GCM outputs used in the 5AR of the IPCC, can be found on the website of the *Coupled Model Intercomparison Project (CMIP)* (<http://cmip-pcmdi.llnl.gov/cmip5/index.html?submenuheader=0>).

Since projections of climate change depend upon future human activity, climate models are run assuming different scenarios.

2.2.2. Description of Scenarios

Long-term climate change projections reflect how human activities or natural effects could alter the climate over decades and centuries. In this context, defined scenarios are important, as using specific time series of emissions, land use, atmospheric concentrations or radiative forcing (RF) across multiple models allows for coherent climate model intercomparisons and synthesis. Some scenarios present a simple stylized future (not accompanied by a socioeconomic storyline) and are used for process understanding. More comprehensive scenarios are produced by Integrated Assessment Models (IAMs) as internally consistent sets of emissions and socioeconomic assumptions (e.g., regarding population and socioeconomic development) with the aim of presenting several plausible future worlds. In general it is these

scenarios that are used for policy relevant climate change, impact, adaptation and mitigation analysis. It is beyond the scope of this report to consider the full range of currently published scenarios and their implications for mitigation policy and climate targets—that is covered by the Working Group III contribution to the AR5. RCP scenarios are used within the CMIP5 intercomparison exercise (Taylor et al. 2012) along with the SRES scenarios (IPCC, 2000) developed for the IPCC Third Assessment Report (AR3) but still widely used by the climate community.

2.2.2.1. Stylized Concentration Scenarios

A 1% per annum compound increase of atmospheric CO₂ concentration until a doubling or a quadrupling of its initial value has been widely used since the second phase of CMIP (Meehl et al., 2000) and the Second Assessment Report (Kattenberg et al., 1996). This stylized scenario is a useful benchmark for comparing coupled model climate sensitivity, climate feedback and transient climate response, but is not used directly for future projections. The exponential increase of CO₂ concentration induces approximately a linear increase in RF due to a ‘saturation effect’ of the strong absorbing bands (Augustsson and Ramanathan, 1977; Hansen et al., 1988; Myhre et al., 1998). Thus, a linear ramp function in forcing results from these stylized pathways, adding to their suitability for comparative diagnostics of the models’ climate feedbacks and inertia. The CMIP5 intercomparison project again includes such a stylized pathway, in which the CO₂ concentration reaches twice the initial concentration after 70 years and four times the initial concentration after 140 years (IPCC,2013). The corresponding RFs are 3.7 W m⁻².(Ramaswamy et al., 2001) and 7.4 W m⁻² respectively with a range of ±20% accounting for uncertainties in radiative transfer calculations and rapid adjustments, placing them within the range of the RFs at the end of the 21st century for the future scenarios (IPCC, 2013). The CMIP5 project also includes a second stylized experiment in which the CO₂ concentration is quadrupled instantaneously, which allows a distinction between effective RFs and longer-term climate feedbacks (Gregory et al., 2004).

2.2.2.2. The Socioeconomic Driven Scenarios from the Special Report on Emission Scenarios

The climate change projections undertaken as part of CMIP3 and discussed in AR4 were based primarily on the SRES A2, A1B and B1 scenarios (IPCC, 2000). These scenarios were developed using IAMs and resulted from specific socioeconomic scenarios, that is, from storylines about future demographic and economic development, regionalization, energy

production and use, technology, agriculture, forestry, and land use. All SRES scenarios assumed that no climate mitigation policy would be undertaken. Based on these SRES scenarios, global climate models were then forced with corresponding WMGHG and aerosol concentrations, although the degree to which models implemented these forcings differed (Meehl et al., 2007b). The resulting climate projections, together with the socioeconomic scenarios on which they are based, have been widely used in further analysis by the impact, adaptation and vulnerability research communities.

2.2.2.3. New Concentration Driven Representative Concentration Pathway Scenarios, and Their Extensions

A new parallel process for scenario development was proposed in order to facilitate the interactions between the scientific communities working on climate change, adaptation and mitigation (Hibbard et al., 2007; Moss et al., 2008, 2010; van Vuuren et al., 2011). These new scenarios, Representative Concentration Pathways, are referred to as pathways in order to emphasize that they are not definitive scenarios, but rather internally consistent sets of time-dependent forcing projections that could potentially be realized with more than one underlying socioeconomic scenario. The primary products of the RCPs are concentrations but they also provide gas emissions. They are representative in that they are one of several different scenarios, sampling the full range of published scenarios (including mitigation scenarios) at the time they were defined, that have similar RF and emissions characteristics. They are identified by the approximate value of the RF (in $W m^{-2}$) at 2100 or at stabilization after 2100 in their extensions, relative to pre-industrial (Moss et al., 2008; Meinshausen et al., 2011c). RCP2.6 (the lowest of the four, also referred to as RCP3-PD) peaks at $3.0 W m^{-2}$ and then declines to $2.6 W m^{-2}$ in 2100, RCP4.5 (medium-low) and RCP6.0 (medium-high) stabilize after 2100 at 4.2 and $6.0 W m^{-2}$ respectively, while RCP8.5 (highest) reaches $8.3 W m^{-2}$ in 2100 on a rising trajectory (IPCC, 2013). The primary objective of these scenarios is to provide all the input variables necessary to run comprehensive climate models in order to reach a target RF. These scenarios were developed using IAMs that provide the time evolution of a large ensemble of anthropogenic forcings (concentration and emission of gas and aerosols, land use changes, etc.) and their individual RF values (Moss et al., 2008, 2010; van Vuuren et al., 2011). Note that due to the substantial uncertainties in RF, these forcing values should be understood as comparative ‘labels’, not as exact definitions of the forcing that is effective in climate models. This is because concentrations or emissions, rather than the RF itself, are prescribed in the CMIP5 climate model runs.

Various steps were necessary to turn the selected ‘raw’ RCP scenarios from the IAMs into data sets usable by the climate modelling community (IPCC, 2013). First, harmonization with historical data was performed for emissions of reactive gases and aerosols (Lamarque et al., 2010; Granier et al., 2011; Smith et al., 2011), land use (Hurtt et al., 2011), and for GHG emissions and concentrations (Meinshausen et al., 2011c). Then atmospheric chemistry runs were performed to estimate ozone and aerosol distributions (Lamarque et al., 2011). Finally, a single carbon cycle model with a representation of carbon–climate feedbacks was used in order to provide consistent values of CO₂ concentration for the CO₂ emission provided by a different IAM for each of the scenarios. This methodology was used to produce consistent data sets across scenarios but does not provide uncertainty estimates for them. After these processing steps, the final RCP data sets comprise land use data, harmonized GHG emissions and concentrations, gridded reactive gas and aerosol emissions, as well as ozone and aerosol abundance fields. These data are used as forcings in individual climate models. The number and type of forcings included primarily depend on the experiment (IPCC, 2013). For instance, while the CO₂ concentration is prescribed in most experiments, CO₂ emissions are prescribed in some others. During this development process, the total RF and the RF of individual forcing agents have been estimated by the IAMs and made available via the RCP database (Meinshausen et al., 2011c). Each individual anthropogenic forcing varies from one scenario to another. The total anthropogenic RF estimated by the IAMs in 2010 is about 0.15 W m⁻² lower than ERF in 2010 (2.2 W m⁻²), the difference arising from a revision of the RF due to aerosols and land use in the current assessment compared to AR4. All the other individual forcings are consistent to within 0.02 W m⁻². The change in CO₂ concentration is the main cause of difference in the total RF among the scenarios. In 2010, the relative contribution of CO₂ to the total anthropogenic forcing is about 80 to 90% and does not vary much across the scenario, as was also the case for SRES scenarios (Ramaswamy et al., 2001). Aerosols have a large negative contribution to the total forcing (about –40 to –50% in 2010), but this contribution decreases (in both absolute and relative terms) in the future for all the RCPs scenarios (IPCC, 2013). This means that while anthropogenic aerosols have had a cooling effect in the past, their decrease in all RCP scenarios relative to current levels is expected to have a net warming effect in the future (Levy II et al., 2013). The 21st century decrease in the magnitude of future aerosol forcing was not as large and as rapid in the SRES scenarios. However, even in the SRES scenarios, aerosol effects were expected to have a diminishing role in the future compared to GHG forcings, mainly because of the accumulation of GHG in the atmosphere (Dufresne et al., 2005). Other forcings do not change much in the future,

except CH₄ which increases in the RCP8.5 scenario (IPCC, 2013). Estimates of all of these individual RFs are subject to many uncertainties. The conversion to RF uses the formula:

$$RF = 3.71/\ln(2) * \ln(CO_{2eq}/27.8) Wm^{-2} \quad (2.4)$$

where CO_{2eq} is in ppmv.

The four RCPs (Meinshausen et al., 2011c) are based on IAMs up to the end of the 21st century only. In order to investigate longer-term climate change implications, these RCPs were also extended until 2300. The extensions, formally named Extended Concentration Pathways (ECPs) but often simply referred to as RCP extensions, use simple assumptions about GHG and aerosol emissions and concentrations beyond 2100 (such as stabilization or steady decline) and were designed as hypothetical ‘what-if’ scenarios, not as an outcome of an IAM assuming socioeconomic considerations beyond 2100 (Meinshausen et al., 2011c). In order to continue to investigate a broad range of possible climate futures, RCP2.6 assumes small constant net negative emissions after 2100 and RCP8.5 assumes stabilization with high emissions between 2100 and 2150, then a linear decrease until 2250 (IPCC, 2013). The two middle RCPs aim for a smooth stabilization of concentrations by 2150. RCP8.5 stabilizes concentrations only by 2250, with CO₂ concentrations of approximately 2000 ppmv, nearly seven times the pre-industrial level. As RCP2.6 implies net negative CO₂ emissions after around 2070 and throughout the extension, CO₂ concentrations slowly reduce towards 360 ppmv by 2300 (IPCC, 2013).

2.2.2.4. Comparison of Special Report on Emission Scenarios and Representative Concentration Pathway Scenarios

The four RCP scenarios used in CMIP5 lead to RF values that range from 2.3 to 8.0 W m⁻² at 2100, a wider range than that of the three SRES scenarios used in CMIP3 which vary from 4.2 to 8.1 W m⁻² at 2100 (IPCC, 2013). The SRES scenarios do not assume any policy to control climate change, unlike the RCP scenarios. The RF of RCP2.6 is hence lower by 1.9 W m⁻² than the three SRES scenarios and very close to the ENSEMBLES E1 scenario (Johns et al., 2011). RCP4.5 and SRES B1 have similar RF at 2100, and comparable time evolution (within 0.2 W m⁻²). The RF of SRES A2 is lower than RCP8.5 throughout the 21st century, mainly due to a faster decline in the radiative effect of aerosols in RCP8.5 than SRES A2, but they converge to within 0.1 W m⁻² at 2100 (IPCC, 2013). RCP6.0 lies in between SRES B1 and SRES A1B. Results obtained with one General Circulation Model (GCM) (Dufresne et al., 2013) and with a reduced-complexity model (Rogelj et al., 2012) confirm that the

differences in temperature responses are consistent with the differences in RFs estimates. RCP2.6, which assumes strong mitigation action, yields a smaller temperature increase than any SRES scenario. The temperature increase with the RCP4.5 and SRES B1 scenarios are close and the temperature increase is larger with RCP8.5 than with SRES A2 (IPCC, 2013).

The spread of projected global mean temperature for the RCP scenarios is considerably larger (at both the high and low response ends) than for the three SRES scenarios used in CMIP3 (B1, A1B and A2) as a direct consequence of the larger range of RF across the RCP scenarios compared to that across the three SRES scenarios.

An overview of the Atmosphere-Ocean General Circulation Models (AOGCMs) and Earth System Models (ESMs) participating in Coupled Model Intercomparison Project Phase 5 (CMIP5), and a comparison with Coupled Model Intercomparison Project Phase 3 (CMIP3), can be found in *Table 2. 1* and *Table 2. 2*.

Table 2. 1. GCMs of the *IPCC 4AR*. (CMIP3)

	Group	Country	Model
CMIP3	Beijing Climate Center	China	BCC-CM1
	Bjerknes Centre for Climate Research	Norway	BCCR-BCM2.0
	National Center for Atmospheric Research	USA	CCSM3
	Canadian Centre for Climate Modelling and Analysis	Canada	CGCM3.1 (T47)
	Canadian Centre for Climate Modelling and Analysis	Canada	CGCM3.1 (T63)
	Centre National de Recherches Meteorologiques	France	CNRM-CM3
	CSIRO Atmospheric Research	Australia	CSIRO-Mk3.0
	CSIRO Atmospheric Research	Australia	CSIRO-Mk3.5
	Max Planck Institute for Meteorology	Germany	ECHAM5/MPI-OM
	Meteorological Institute of the University of Bonn, Meteorological Research Institute of KMA, and Model and Data group	Germany-Korea	ECHO-G
	LASG / Institute of Atmospheric Physics	China	FGOALS-g1.0
	US Dept. of Commerce- NOAA - Geophysical Fluid Dynamics	USA	GFDL-CM2.0

	Laboratory		
	US Dept. of Commerce- NOAA - Geophysical Fluid Dynamics Laboratory	USA	GFDL-CM2.1
	NASA Goddard Institute for Space Studies	USA	GISS-AOM
	NASA Goddard Institute for Space Studies	USA	GISS-EH
	NASA Goddard Institute for Space Studies	USA	GISS-ER
	Instituto Nazionale di Geofisica e Vulcanologia	Italy	INGV-SXG
	Institute for Numerical Mathematics	Russia	INM-CM3.0
	Institut Pierre Simon Laplace	France	IPSL-CM4
	Center for Climate System Research, National Institute for Environmental Studies, and Frontier Research Center for Global Change (JAMSTEC)	Japan	MIROC3.2 (hires)
	JAMSTEC	Japan	MIROC3.2 (medres)
	Meteorological Research Institute	Japan	MRI-CGCM2.3.2
	National Center for Atmospheric Research	USA	PCM
	Hadley Centre for Climate Prediction and Research Met Office	UK	UKMO-HadCM3
Hadley Centre for Climate Prediction and Research Met Office	UK	UKMO-HadGEM1	

Table 2. 2. GCMs of the IPCC 5AR (CMIP5 and AMIP)

	Group	Country	Model
CMIP5	CSIRO Atmospheric Research	Australiaa	ACCESS1.0,ACCESS1.3
	Beijing Climate Center	China	BCC_CSM1.1, BCC-CSM1.1(m)
	Beijing Normal University Earth System Model	China	BNU-ESM
	Canadian Centre for Climate Modelling and Analysis	Canada	CanCM4 CanESM2
	National Science Foundation,	USA	CSM4

	Department of Energy, National Center for Atmospheric Research		CESM1(BGC) CESM1(WACCM) CESM1(FASTCHEM) CESM1(CAM5) CESM1(CAM5.1-FV2)
	Centro Euro-Mediterraneo per I Cambiamenti Climatici	Italy	CMCC-CM,CMCC- CMS CMCC-CESM
	Centre National de Recherches Meteorologiques / Centre Europeen de Recherche et Formation Avancees en Calcul Scientifique	France	CNRM-CM5
	Commonwealth Scientific and Industrial Research Organisation in collaboration with the Queensland Climate Change Centre of Excellence	Australia	CSIRO-Mk3.6.0
	EC-EARTH consortium	Europe	EC-EARTH
	LASG, Institute of Atmospheric Physics, Chinese Academy of Sciences; and CESS, Tsinghua University	China	FGOALS-g2 FGOALS-s2
	The First Institute of Oceanography, SOA, China	China	FIO-ESM v1.0
	Geophysical Fluid Dynamics Laboratory	USA	GFDL-ESM2M GFDL-ESM2G GFDL-CM2.1 GFDL-CM3
	NASA Goddard Institute for Space Studies	USA	GISS-E2-R,GISS-E2-H GISS-E2-R-CC, GISS- E2-H-CC
	Met Office Hadley Centre (additional HadGEM2-ES realizations contributed by Instituto Nacional de Pesquisas Espaciais)	UK	HadmGEM2-ES HadGEM2-CC HadCM3
	National Institute of Meteorological Research/Korea Meteorological Administration	Korea	HadGEM2-AO
	Institute for Numerical Mathematics	Russia	INM-CM4

	Institut Pierre-Simon Laplace	France	IPSL-CM5A-LR/- CM5A-MR/ -CM5B-LR
	Japan Agency for Marine- Earth Science and Technology, Atmosphere and Ocean Research Institute (The University of Tokyo), and National Institute for Environmental Studies	Japan	MIROC4h.MIROC5 MIROC-ESM MIROC-ESM-CHEM
	Max Planck Institute for Meteorology (MPI-M)	Germany	MPI-ESM-LR/-ESM- MR/-ESM-P
	Meteorological Research Institute	Japan	MRI-ESM1 MRI-CGCM3
	National Center Environmental Prediction	USA	NCEP-CFSv2
	Norwegian Climate Centre	Norway	NorESM1-M NorESM1-ME
AMIP	Geophysical Fluid Dynamics Laboratory	USA	GFDL-HIRAM C180/- HIRA; C360
	Meteorological Research Institute	Japan	MRI-AGCM3.25/ -AGCM3.2H

2.2.3. Stochastic downscaling procedure

In the presented approach of stochastic downscaling only precipitation and air temperature are directly considered. But, once precipitation and temperature factors of change are introduced into AWE-GEN, the other variables might be affected as a result of linkages considered by the weather generator.

Various GCMs multi-model ensemble and probabilistic approaches to the analysis of climate projections have been recently proposed, like the Bayesian methods (Tebaldi and Knutti, 2007). The underlying idea is that a performance forecast can be improved by weight-averaging results from multiple models. The multi-model ensemble approach realized in this thesis follows that of Tebaldi et al. (2005) where model combines information coming from several GCMs and observations to determine the *probability density functions* (PDFs) of future changes of different certain climatic variables at the regional scale (Fatichi et al., 2011). In the Bayesian framework, all uncertain quantities are modeled as random variables, with a prior probability distributions. The method assigns weights to climate models, according to two criteria: the *bias* and the *convergence*. The *bias* measures the difference between GCM simulations and the best approximation of the “truth” value of a certain variable for the control scenario, μ . The *convergence* criterion measures the distance between the GCM

simulations and the “true” value of a certain variable of the future realizations, v . Note that for each statistic v represents the expected value of the PDF for the future.

The multi-model ensemble approach of inference is used for all statistical properties of climatic variables that are part of stochastic downscaling, i.e., the mean, the variance, the frequency of non precipitation, and the skewness of fine-scale precipitation (for each month), the coefficient of variation and the skewness of annual precipitation, and the mean monthly air temperature (Fatichi et al., 2011; 2013). Long-term statistics of present climate X_0 are calculated from observed values based on point measurements, which therefore represent a much smaller area as compared to a typical GCM grid cell size. The difference between observations and climate model realizations is accounted for by the bias criterion used to weight different GCM realizations in getting proper downscaling information. This implies that the shape of the probability density functions of the factors of change is somewhat dependent on the observed climate.

In *Figure 2. 4* a flowchart of the used stochastic downscaling methodology is presented (Fatichi et al., 2011). More specifically, a set of factors of change is computed to reflect changes in the mean monthly air temperature and several statistics of precipitation (e.g., mean, variance, skewness, frequency of no-precipitation) at different aggregation periods (24, 48, 72, 96 h), as a result of comparing historical and projected climate model outputs. The factors of change derived from the ensemble of GCM realizations are subsequently applied to a set of statistics of the observed climate in order to obtain statistics representative of the future climate. Using these statistical properties, an updated set of AWE-GEN parameters can be estimated. Each of these AWE-GEN parameters set is calculated assuming stationary climate for any considered period. Finally, the re-parameterized weather generator is used to simulate hourly time series of hydro-climatic variables that are considered to be representative of the predicted climate. For a more detailed description of the procedure, interested readers are referred to Fatichi et al. (2011) and Fatichi et al. (2013).

It is important to remind that the uncertainties captured by the proposed procedure and quantified by the *PDFs* are only a part of the total uncertainty of climate change predictions. The *PDFs* of factors of change are the result of climate model differences in predicting future; these *PDFs* do not contain any information about other sources of uncertainty (e.g., model structure, different CO₂ emission scenarios, etc.). However, the variation of climate change predictions between different models is probably the most meaningful measure of uncertainty that is presently available, although, this measure is more likely to underestimate than overestimate the total uncertainty.

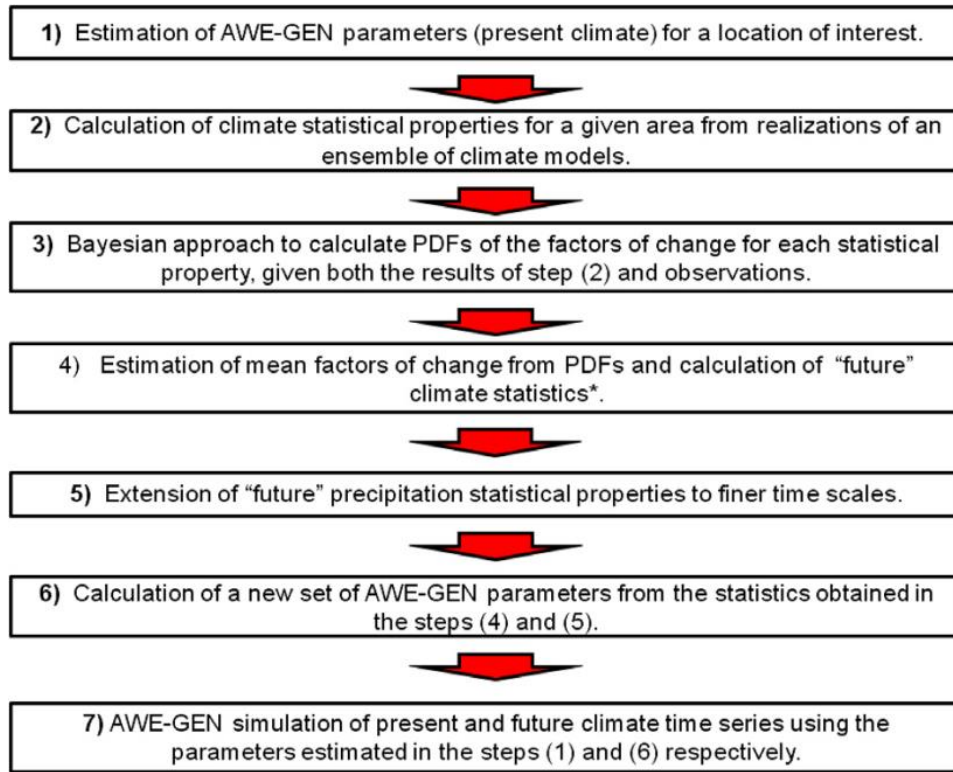


Figure 2. 4. A flowchart of the used stochastic downscaling methodology (Fatichi et al., 2011).

2.2.3.1. Factor of change

The factors of change for precipitation (Pr) are calculated for each statistic used by the weather generator: the mean $E_{Pr}(h)$, the variance $VAR_{Pr}(h)$, and the skewness $SKE_{Pr}(h)$, where h is the aggregation interval (24, 48, 72, 96 h). The product factor is also applied to the frequency of non-precipitation Φ_{Pr} , following a logit-like transformation: $f(\Phi_{Pr}) = \Phi_{Pr} / (1 - \Phi_{Pr})$, as proposed by Kilsby et al. (2007). This transformation allows the linearization of Φ_{Pr} across a wide range of values, reducing inaccuracies in the computation of the product factor. The downscaling of the lag-1 autocorrelation $\rho_{Pr}(h)$ is neglected due to difficulties in finding a proper relationship for the factor of change of this statistic, and due to the weaker sensitivity of weather generator realizations to $\rho_{Pr}(h)$ variations.

The stochastic downscaling uses a Bayesian approach to weight climate model realizations (Tebaldi et al., 2004, 2005; Fatichi et al., 2011) which allows one to derive the probability distributions of factors of change (FOC) representative of the ensemble of GCM projections. FOC from single climate models can be calculated as ratios ($FOCR$) or “delta” ($FOCD$), i.e., differences of climate statistics for historical and future periods. The general equation, which using $FOCR$ provides the statistical properties S at the time aggregation h in the future scenario reads:

$$S(h)^{FUT} = \frac{S(h)^{GCM,FUT}}{S(h)^{GCM,CTS}} \cdot S(h)^{OBS} = FOCR \cdot S(h)^{OBS} \quad (2.5)$$

where the superscript *FUT* denotes the future scenario, *OBS* denotes observations, and *CTS* denotes the control scenario, which is the GCMs run representing the current climate. The notation GCM implies *General Circulation Models* outputs. The sought statistical property for future climate, S^{FUT} , is then calculated from the observed statistics of present climate, S^{OBS} , and the product factor of change computed using statistics derived from the control and the future scenarios, $S^{GCM,FUT}/S^{GCM,CTS}$ (obtained from GCM outputs).

In order to include the effects of intra-annual seasonality, the factors of change are calculated on a monthly basis.

Low-frequency effects are important in the detection of climate change impacts, especially when long-term variations in the occurrence and duration of drought or wet periods are likely to be encountered. AWE-GEN is capable of taking into account such features of precipitation regime. Therefore, statistical properties describing the inter-annual variability of precipitation are also downscaled using the derived factors of change from GCM realizations. Specifically, once downscaling is carried out for the mean precipitation at finer aggregation intervals and realized independently for each month, the total annual precipitation \bar{P}_{yr}^{FUT} is obtained as the sum of modified monthly precipitation. The application of independent factors of change on a monthly basis, however, has a not immediately apparent implication: \bar{P}_{yr}^{FUT} may not be exactly equal to $\bar{P}_{yr}^{OBS} \cdot \left[\bar{P}_{yr}^{GCM,FUT} / \bar{P}_{yr}^{GCM,CTS} \right]$, where the expression in the brackets is the factor of change estimated at the annual scale. This outcome is due to the fact that applying the factors of change at the monthly scale is different from applying a factor of change at the annual scale. However, in order to account for seasonality and to be coherent with the factors of change calculated at the aggregation periods smaller than 1 year, \bar{P}_{yr}^{FUT} is used as the mean annual precipitation of the *FUT* scenario. Furthermore, the coefficient of variation and the skewness of annual precipitation must be downscaled using (3.62): the downscaling of the former is necessary in order to introduce changes in the variance of precipitation annual time series. It is necessary to compute a factor of change for the coefficient of variation and not directly for the variance because of the issue of the mean annual precipitation. The autocorrelation property of annual precipitation process is not directly downscaled. The value inferred from observations is kept for simulations of future climate.

With regard to the mean monthly temperature, its statistical properties S , is obtained by the following equation, which uses the “delta” factor of change $FOCD$:

$$S(h)^{FUT} = S(h)^{OBS} + [S(h)^{GCM,FUT} - S(h)^{GCM,CTS}] = S(h) + FOCD \quad (2.6)$$

Correcting only the mean does not permit to infer changes of higher order statistics and thus to capture the changes in the daily cycle or frequency of extremes. This limitation is related to the procedure adopted for the estimation of the parameters of the air temperature model. Nevertheless, in many cases intra-daily variation of changes can be considered to have a fairly minor effect on the hydrological dynamics. The correction $FOCD = T_{mon}^{GCM,FUT} - T_{mon}^{GCM,CTS}$ is applied on a monthly basis to air temperature simulated by the weather generator at the hourly scale.

2.2.3.2. Extension of precipitation statistics to finer time scales

Since, several statistics of precipitation in the weather generator are required at the aggregation intervals of 1 h and 6 h, a methodology to infer the factors of change for these periods is necessary. The extension to shorter time scales is straightforward for the mean, i.e., given the linearity of the mean operation, the factors of change are equal at each aggregation period. The extension to shorter time scales is not such a trivial task for the other statistical properties, such as the variance $VAR_{Pr}(h)$, the frequency of non-precipitation $\Phi_{Pr}(h)$, and the skewness $SKE_{Pr}(h)$.

In order to infer VAR_{Pr} at 1 h and 6 h aggregation intervals, a theoretical derivation of Marani (Marani, 2003; Marani, 2005) is applied. The parameters for the $VAR_{Pr}(h)$ of Marani (2003) are estimated from the variance $VAR_{Pr}^{FUT}(h)$ at different aggregation periods equal to or larger than 24 hours (24, 48, 72, and 96 h). The values of $VAR_{Pr}^{FUT}(h)$ are thus calculated once $VAR_{Pr}^{OBS}(h)$ and the factors of change for precipitation variance are known at the aggregation period $h \geq 24h$.

The extension to 1 h and 6 h aggregation periods of the frequency of non-precipitation $\Phi_{Pr}(h)$ is realized through an exponential function $\Phi_{Pr}(h) = e^{-\gamma h}$, that links $\Phi_{Pr}(\geq 24)$ to $\Phi_{Pr}(<24)$, considering that $\Phi_{Pr}(0) = 1$, by definition. The exponential decay of the frequency of non-precipitation $\Phi_{Pr}(h)$ has been observed in practically all of the analyzed time series. The parameter γ is estimated from $\Phi_{Pr}(24)^{FUT}$ and $\Phi_{Pr}(48)^{FUT}$. The values of $\Phi_{Pr}(h)^{FUT}$ are calculated from the observed $\Phi_{Pr}(h)^{OBS}$ using the factors of change FC for logit transformed

frequency of non-precipitation. Since the fitting of $\Phi_{Pr}(h < 24)$ is carried out with two values of $\Phi_{Pr}(\geq 24)$, γ is determined using the least squares method.

Skewness $SKE_{Pr}(h)$ is not extended to 1 h and 6 h aggregation periods since no suitable relationship was found for this statistic. The factors of change for 1 h and 6 h skewness are taken equal to one. This implies that the values obtained from observations are employed for generating future scenarios.

2.3. Random cascade disaggregation model

Following up to the procedure, already known by *Figure 2.2*, the hourly rainfall data, obtained by the stochastic downscaling procedure (see section 2.2), still remain difficult to apply for a rainfall- runoff model on an urban catchment because rapid/large inputs, with growing urbanization leading to increasingly extensive impervious surfaces and enhanced CC effects on urban drainage, show durations of these events are often shorter than 1 hour, so large time scales do not help to achieve good flooding results needed to estimate flood depths and to deduct possible flood damages.

However, going from hourly to sub-hourly time step is not an easy operation and, in literature, valid methods that are able to go to finer levels well preserving statistic parameters are not so many, but one of the most popular is the Random Cascade model.

In this study, Random cascade disaggregation model was determined to be one of the best choice, also according analysis, shown in section 4.2.

Discrete multiplicative random cascade models distribute mass on successive regular subdivisions of an interval in a multiplicative manner. This dissipative process is reminiscent of rainfall disaggregation and multiplicative random cascade models were successfully applied to rainfall modelling (Schertzer and Lovejoy, 1987; Over and Gupta, 1994, 1996; Olsson, 1998; Güntner et al., 2001). There are two conceptually different but very simple versions of a random cascade—a canonical model, which preserves mass on the average in disaggregation, and a microcanonical model, which preserves mass exactly in disaggregation. This section summarizes the basic theory behind random cascade models. We use the notation of Gupta and Waymire (1993) and Over and Gupta (1994, 1996) throughout this section. For further details, the reader should refer to the original papers.

The basic cascading structure of the multiplicative random cascade model distributes rainfall on successive regular subdivisions with b as the branching number. The i th interval after n levels of subdivision is denoted D_n^i (there are $i=1, \dots, b^n$ intervals at level n). The dimensionless spatial scale is defined as $\lambda_n = b^{-n}$, i.e., $\lambda_0=1$ at the 0 th level of subdivision.

The distribution of mass occurs via a multiplicative process through all levels n of the cascade, so that the mass in subcube D_n^i is:

$$\mu_n(D_n^i) = r_0 \lambda_n \prod_{j=1}^n W_j(i) \quad \text{for } i = 1, 2, \dots, b^n; \quad n > 0 \tag{2.7}$$

Here r_0 is an initial rainfall depth at $n = 0$ and W is the so-called cascade generator. The substantial difference between the two cascade models we test here is in how they treat the cascade generator. The basic structure of the discrete multiplicative random cascade model as used in this study is illustrated in *Figure 2. 5*, with $b = 2$ as the branching number and $n = 0, 1,$ and 2 .

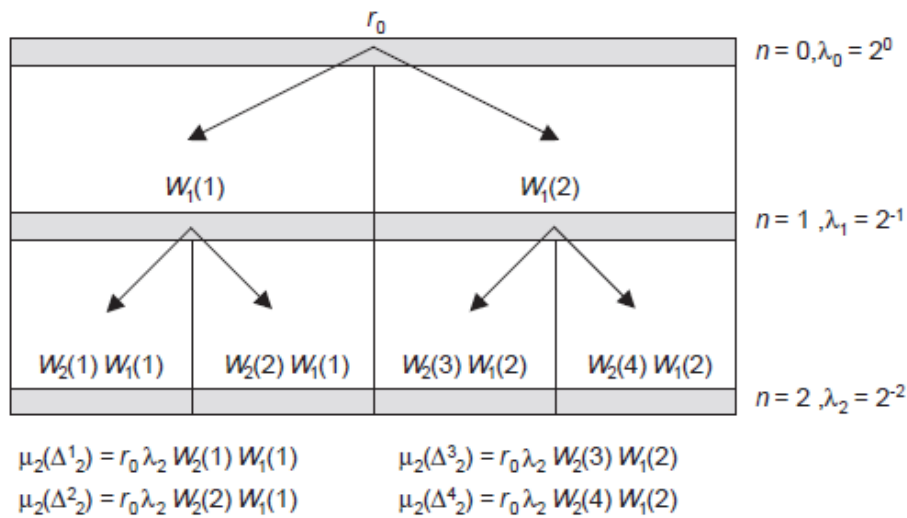


Figure 2. 5. Example of the multiplicative random cascade with branching number $b = 2$ and cascade generator W for scales $n = 0, 1,$ and 2 . (Molnar and Burlandot, 2005).

2.3.1. Moment scaling

Properties of the cascade generator W can be estimated from the moment scaling behaviour across scales. Sample moments are defined as:

$$M_n(q) = \sum_{i=1}^{b^n} \mu_n^q(D_n^i) \tag{2.8}$$

where q is the moment order ($q \geq 0$). For large n , the sample moments should converge to the ensemble moments. However, because the ensemble moments diverge to infinity or converge to zero as $n \rightarrow \infty$, the (rate of) convergence/divergence of the moments with scale is considered. In a random cascade, the ensemble moments are shown to be a log–log linear

function of the scale of resolution λ_n . The slope of this scaling relationship is known as the Mandelbrot–Kahane–Peyriere (MKP) function (Mandelbrot, 1974; Kahane and Peyriere, 1976):

$$\chi_b(q) = 1 - q + \log_b E(W^q) \quad (2.9)$$

The MKP function contains important information about the distribution of the cascade generator W , and thus determines the scaling properties of rainfall. The slope of the sample moment scaling relationship can be found as:

$$\tau(q) = \lim_{\lambda_n \rightarrow 0} \frac{\log M_n(q)}{-\log \lambda_n} \quad (2.10)$$

For large n (as $\lambda_n \rightarrow 0$) and for a specific range of q , slopes of the moment scaling relationships for sample and ensemble moments converge, i.e.,

$$\chi_b(q) = \tau(q) \quad (2.11)$$

In data analysis, the scaling of the sample moments is used to estimate $\tau(q)$, and assuming a distribution for the cascade generator W , the parameters of the cascade model can then be estimated.

2.3.2. The canonical model

The canonical model used in this study is the intermittent lognormal β -model (Gupta and Waymire, 1993; Over and Gupta, 1994, 1996). In this model, the cascade generator W is treated as an independent and identically distributed (*iid*) random variable. The distribution of W is non-negative with $E(W)=1$, so that mass is, on the average, conserved at all levels in the cascade development (Molnar and Burlandot, 2005).

Intermittency in rainfall is preserved by defining a probability that $W=0$ exists. The generator is written as a composite variable $W=BY$, where B is an intermittency factor and Y is a strictly positive random variable.

The intermittent model divides the domain into rainy and nonrainy fractions based on the following probabilities:

$$P(B = 0) = 1 - b^{-\beta} \text{ and } P(B = b^\beta) = b^{-\beta} \quad (2.12)$$

where β is a parameter and $E(B)=1$. Variability in the positive part of the generator is obtained from Y . The distribution of Y is arbitrary, but it has to be positive, and $E(Y)=1$. For rainfall modeling, good results have been obtained with Y lognormal (Over and Gupta, 1996), and this is the model used here. If we take $Y = b^{\gamma + \sigma X}$, where X is a normal $N(0,1)$ random variable, the condition $E(Y)=1$ gives:

$$Y = b^{-\left(\frac{\sigma^2 \ln b}{2} + \sigma X\right)} \quad (2.13)$$

where σ^2 is a parameter defining the variance of Y . The composite generator W is then distributed as:

$$P(W = 0) = 1 - b^{-\beta} \text{ and } P(W = b^\beta Y) = b^{-\beta - \frac{\sigma^2 \ln b}{2} + \sigma X} = b^{-\beta} \quad (2.14)$$

and the MKP function of W is (e.g., Over and Gupta, 1994):

$$\chi_b(q) = \tau(q) = (\beta - 1)(q - 1) + \frac{\sigma^2 \ln b}{2}(q^2 - q) \quad (2.15)$$

The canonical model has two parameters, β and σ^2 , which are related to the intermittency and variability of the generator W , respectively.

2.3.3. The microcanonical model

The microcanonical model preserves mass exactly between levels n in the cascade development (as opposed to the canonical model). The cascade generator W is a random variable, which is constrained so that in every subdivision into b subintervals at level n , the following holds:

$$\sum_{K=1}^b W_n(b(i-1) + k) = 1 \quad \text{for } i = 1, 2, \dots, b^{n-1} \quad (2.16)$$

The distribution of W in this case is identical to that of the breakdown (or partition) coefficients (e.g., Menabde and Sivapalan, 2000). Intermittency in the microcanonical model is preserved by allowing

$$W_n(i) = 0 \quad (2.17)$$

Assuming symmetry in the breakdown coefficients, the microcanonical model disaggregates every nonzero rainfall amount in the interval i at scale $n-1$ into $b=2$ intervals (j

and $j+1$) at scale n . In this case, two situations may occur. First is that intermittency emerges in one interval only at the scale n with probability $p_{0,w}$, i.e.,

$$P(W_n(j) = 0 \text{ or } W_n(j+1) = 0) = p_{0,w} \quad (2.18)$$

Second is that intermittency does not emerge, and both intervals j and $j+1$ have $0 < W < 1$.

A particularly suitable probability density function for W under the symmetric case is the Beta distribution with the parameter a governing the variance of W :

$$f(w) = \frac{1}{B(a)} w^{a-1} (1-w)^{a-1} \quad (2.19)$$

where $B(a)$ is the Beta function. This distribution has a mean $E(W)=0.5$ and variance $\text{Var}(W)$. For $a=1$, this distribution is exactly uniform; for $a>1$, it is bell-shaped symmetrically around $E(W)$. In generation, if we take the branching number $b=2$, we need to generate two values of W (w_1 and w_2) which satisfy Eq. (2.16) and are distributed according to Eq. (2.18). This can be done by generating two independent gamma-distributed numbers x_1 and x_2 with parameter a . Then their ratios $w_1=x_1/(x_1+x_2)$ and $w_2=x_2/(x_1+x_2)$ will satisfy both requirements. The parameter a can be estimated by the method of moments:

$$a = \frac{1}{8\text{Var}(W)} - 0.5 \quad (2.20)$$

The non-intermittent part of the microcanonical model is identical to that of Menabde and Sivapalan (2000) where it was used to disaggregate rainfall during storm periods. The microcanonical model also has two parameters, $p_{0,w}$ and a , which are related to the intermittency and variability of the generator W , respectively.

2.3.4. Parameter estimation

2.3.4.1. Parameter estimation-canonical model

The parameters of the canonical model are estimated from the MKP function. First, the sample moments $M_n(q)$ are computed at all scales n according to Eq. (2.8), and the slope $\tau(q)$ of the relationship with the scale λ_n is determined by linear regression on log-transformed data according to Eq.(2.10).

The two parameters of the canonical model can be directly estimated from the $\tau(q)$ function given in Eq. (2.15).

These parameters are estimated from all data and are constant. The model using these estimates will be referred to as the canonical model with constant parameters, C(CT).

Another possible approach is to estimate β and σ^2 for each nonzero rainfall interval at scale $n = 0$, and to relate the parameters to the rainfall rate r_0 at the $n = 0$ scale: this might be called the large scale forcing (LSF) relation, following Over and Gupta (1994).

2.4. EPA SWMM Model

The EPA Storm Water Management Model (SWMM) is a dynamic rainfall-runoff simulation model used for single event or long-term (continuous) simulation of runoff quantity and quality from primarily urban areas. The runoff component of SWMM operates on a collection of subcatchment areas that receive precipitation and generate runoff and pollutant loads. The routing portion of SWMM transports this runoff through a system of pipes, channels, storage/treatment devices, pumps, and regulators. SWMM tracks the quantity and quality of runoff generated within each subcatchment, and the flow rate, flow depth, and quality of water in each pipe and channel during a simulation period comprised of multiple time steps. SWMM was first developed in 1971 and has undergone several major upgrades since then. It continues to be widely used throughout the world for planning, analysis and design related to storm water runoff, combined sewers, sanitary sewers, and other drainage systems in urban areas, with many applications in non-urban areas as well. The current edition, Version 5, is a complete re-write of the previous release. Running under Windows, SWMM 5 provides an integrated environment for editing study area input data, running hydrologic, hydraulic and water quality simulations, and viewing the results in a variety of formats. These include color-coded drainage area and conveyance system maps, time series graphs and tables, profile plots, and statistical frequency analyses.

2.4.1. Modeling Capabilities

SWMM accounts for various hydrologic processes that produce runoff from urban areas. These include:

- * time-varying rainfall;
- * evaporation of standing surface water ;
- * snow accumulation and melting;
- * rainfall interception from depression storage;
- * infiltration of rainfall into unsaturated soil layers;
- * percolation of infiltrated water into groundwater layers;

- * interflow between groundwater and the drainage system;
- * nonlinear reservoir routing of overland flow;
- * capture and retention of rainfall/runoff with various types of low impact development (LID) practices.

Spatial variability in all of these processes is achieved by dividing a study area into a collection of smaller, homogeneous subcatchment areas, each containing its own fraction of pervious and impervious sub-areas. Overland flow can be routed between sub-areas, between subcatchments, or between entry points of a drainage system. SWMM also contains a flexible set of hydraulic modeling capabilities used to route runoff and external inflows through a drainage system network of pipes, channels, storage/treatment units and diversion structures. These include the ability to:

- * handle networks of unlimited size;
- * use a wide variety of standard closed and open conduit shapes as well as natural channels;
- * model special elements such as storage/treatment units, flow dividers, pumps, weirs, and orifices;
- * apply external flows and water quality inputs from surface runoff, groundwater interflow, rainfall-dependent infiltration/inflow, dry weather sanitary flow, and user-defined inflows;
- * utilize either kinematic wave or full dynamic wave flow routing methods;
- * model various flow regimes, such as backwater, surcharging, reverse flow, and surface ponding;
- * apply user-defined dynamic control rules to simulate the operation of pumps, orifice openings, and weir crest levels.

In addition to modeling the generation and transport of runoff flows, SWMM can also estimate the production of pollutant loads associated with this runoff. The following processes can be modeled for any number of user-defined water quality constituents:

- * dry-weather pollutant buildup over different land uses;
- * pollutant washoff from specific land uses during storm events;
- * direct contribution of rainfall deposition;
- * reduction in dry-weather buildup due to street cleaning;
- * reduction in washoff load due to BMPs;

- * entry of dry weather sanitary flows and user-specified external inflows at any point in the drainage system;
- * routing of water quality constituents through the drainage system;
- * reduction in constituent concentration through treatment in storage units or by natural processes in pipes and channels.

2.4.2. Typical Applications of SWMM

Since its inception, SWMM has been used in thousands of sewer and stormwater studies throughout the world. Typical applications include:

- * design and sizing of drainage system components for flood control;
- * sizing of detention facilities and their appurtenances for flood control and water quality protection;
- * flood plain mapping of natural channel systems;
- * designing control strategies for minimizing combined sewer overflows;
- * evaluating the impact of inflow and infiltration on sanitary sewer overflows;
- * generating non-point source pollutant loadings for waste load allocation studies;
- * evaluating the effectiveness of BMPs for reducing wet weather pollutant loadings.

2.4.3. SWMM'S CONCEPTUAL MODEL

SWMM conceptualizes a drainage system as a series of water and material flows between several major environmental compartments. These compartments and the SWMM objects they contain include:

- * the *Atmosphere* compartment, from which precipitation falls and pollutants are deposited onto the land surface compartment. SWMM uses Rain Gage objects to represent rainfall inputs to the system;
- * the *Land Surface* compartment, which is represented through one or more Subcatchment objects. It receives precipitation from the Atmospheric compartment in the form of rain or snow; it sends outflow in the form of infiltration to the Groundwater compartment and also as surface runoff and pollutant loadings to the Transport compartment;
- * the *Groundwater* compartment receives infiltration from the Land Surface compartment and transfers a portion of this inflow to the Transport compartment. This compartment is modeled using Aquifer objects;

- * the *Transport* compartment contains a network of conveyance elements (channels, pipes, pumps, and regulators) and storage/treatment units that transport water to outfalls or to treatment facilities. Inflows to this compartment can come from surface runoff, groundwater interflow, sanitary dry weather flow, or from user-defined hydrographs. The components of the Transport compartment are modeled with Node and Link objects.

Not all compartments need appear in a particular SWMM model. For example, one could model just the transport compartment, using pre-defined hydrographs as inputs.

2.4.3.1. Visual Objects

Figure 2. 6 depicts how a collection of SWMM's visual objects might be arranged together to represent a stormwater drainage system. These objects can be displayed on a map in the SWMM workspace. The following sections describe each of these objects.

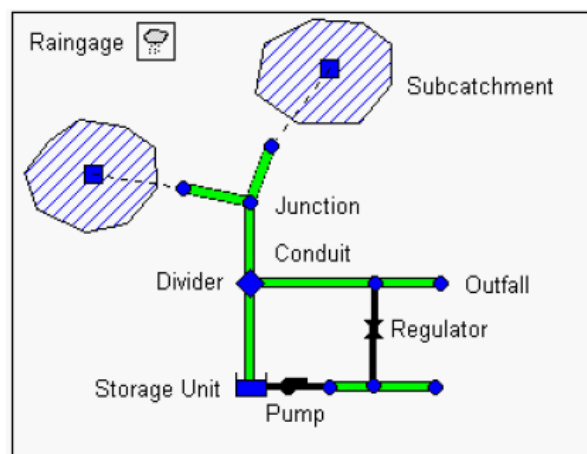


Figure 2. 6. Example of representation of visula objects in EPA SWMM (Rossman, 2010)

The difference between the natural ground cover and various types of impervious surfaces in urbanized areas.

Rain Gages supply precipitation data for one or more subcatchment areas in a study region. The rainfall data can be either a user-defined time series or come from an external file. Several different popular rainfall file formats currently in use are supported, as well as a standard user-defined format. The principal input properties of rain gages include:

- * rainfall data type (e.g., intensity, volume, or cumulative volume);
- * recording time interval (e.g., hourly, 15-minute, etc.);
- * source of rainfall data (input time series or external file);
- * name of rainfall data source.

2.4.3.1.1. Subcatchments

Subcatchments are hydrologic units of land whose topography and drainage system elements direct surface runoff to a single discharge point. The user is responsible for dividing a study area into an appropriate number of subcatchments, and for identifying the outlet point of each subcatchment. Discharge outlet points can be either nodes of the drainage system or other subcatchments.

Subcatchments can be divided into pervious and impervious subareas. Surface runoff can infiltrate into the upper soil zone of the pervious subarea, but not through the impervious subarea. Impervious areas are themselves divided into two subareas - one that contains depression storage and another that does not. Runoff flow from one subarea in a subcatchment can be routed to the other subarea, or both subareas can drain to the subcatchment outlet.

Infiltration of rainfall from the pervious area of a subcatchment into the unsaturated upper soil zone can be described using three different models:

- * Horton infiltration;
- * Green-Ampt infiltration;
- * SCS Curve Number infiltration;

To model the accumulation, re-distribution, and melting of precipitation that falls as snow on a subcatchment, it must be assigned a Snow Pack object. To model groundwater flow between an aquifer underneath the subcatchment and a node of the drainage system, the subcatchment must be assigned a set of Groundwater parameters. Pollutant buildup and washoff from subcatchments are associated with the Land Uses assigned to the subcatchment.

The other principal input parameters for subcatchments include:

- * assigned rain gage;
- * outlet node or subcatchment;
- * assigned land uses;
- * tributary surface area;
- * imperviousness;
- * slope;
- * characteristic width of overland flow;
- * Manning's n for overland flow on both pervious and impervious areas;
- * depression storage in both pervious and impervious areas;
- * percent of impervious area with no depression storage.

2.4.3.1.2. Junction Nodes

Junctions are drainage system nodes where links join together. Physically they can represent the confluence of natural surface channels, manholes in a sewer system, or pipe connection fittings. External inflows can enter the system at junctions. Excess water at a junction can become partially pressurized while connecting conduits are surcharged and can either be lost from the system or be allowed to pond atop the junction and subsequently drain back into the junction.

The principal input parameters for a junction are:

- * invert elevation;
- * height to ground surface;
- * ponded surface area when flooded (optional);
- * external inflow data (optional).

2.4.3.1.3. Outfall Nodes

Outfalls are terminal nodes of the drainage system used to define final downstream boundaries under Dynamic Wave flow routing. For other types of flow routing they behave as a junction. Only a single link can be connected to an outfall node. The boundary conditions at an outfall can be described by any one of the following stage relationships:

- * the critical or normal flow depth in the connecting conduit;
- * a fixed stage elevation;
- * a tidal stage described in a table of tide height versus hour of the day;
- * a user-defined time series of stage versus time.

The principal input parameters for outfalls include:

- * invert elevation;
- * boundary condition type and stage description;
- * presence of a flap gate to prevent backflow through the outfall.

2.4.3.1.4. Storage Units

Storage Units are drainage system nodes that provide storage volume. Physically they could represent storage facilities as small as a catchbasin or as large as a lake. The volumetric properties of a storage unit are described by a function or table of surface area versus height.

The principal input parameters for storage units include:

- * invert elevation;

- * maximum depth;
- * depth-surface area data;
- * evaporation potential;
- * ponded surface area when flooded (optional);
- * external inflow data (optional).

2.4.3.1.5. Conduits

Conduits are pipes or channels that move water from one node to another in the conveyance system. Their cross-sectional shapes can be selected from a variety of standard open and closed geometries. Irregular natural cross-section shapes are also supported.

SWMM uses the Manning equation to express the relationship between flow rate (Q), cross-sectional area (A), hydraulic radius (R), and slope (S) in open channels and partially full closed conduits. For standard U.S. units,

$$Q = \frac{1.49}{n} AR^{2/3}\sqrt{S} \quad (2.21)$$

where n is the Manning roughness coefficient. For Steady Flow and Kinematic Wave flow routing, S is interpreted as the conduit slope. For Dynamic Wave flow routing it is the friction slope (i.e., head loss per unit length).

The principal input parameters for conduits are:

- * names of the inlet and outlet nodes;
- * offset heights of the conduit above the inlet and outlet node inverts;
- * conduit length;
- * Manning's roughness;
- * cross-sectional geometry;
- * entrance/exit losses;
- * presence of a flap gate to prevent reverse flow.

2.4.3.1.6. Pumps

Pumps are links used to lift water to higher elevations. A pump curve describes the relation between a pump's flow rate and conditions at its inlet and outlet nodes.

The on/off status of pumps can be controlled dynamically through user-defined Control Rules.

The principal input parameters for a pump include:

- * names of its inlet and outlet nodes;
- * name of its pump curve;
- * initial on/off status.

2.4.3.1.7. Flow Regulators

Flow Regulators are structures or devices used to control and divert flows within a conveyance system. They are typically used to:

- * control releases from storage facilities;
- * prevent unacceptable surcharging;
- * divert flow to treatment facilities and interceptors.

SWMM can model the following types of flow regulators:

a) Orifices

Orifices are used to model outlet and diversion structures in drainage systems, which are typically openings in the wall of a manhole, storage facility, or control gate. They are internally represented in SWMM as a link connecting two nodes. An orifice can have either a circular or rectangular shape, be located either at the bottom or along the side of the upstream node, and have a flap gate to prevent backflow.

Orifices can be used as storage unit outlets under all types of flow routing. If not attached to a storage unit node, they can only be used in drainage networks that are analyzed with Dynamic Wave flow routing.

The flow through a fully submerged orifice is computed as

$$Q = CA\sqrt{2gh} \quad (2.22)$$

where Q = flow rate, C = discharge coefficient, A = area of orifice opening, g = acceleration of gravity, and h = head difference across the orifice. The area of an orifice's opening can be controlled dynamically through user-defined Control Rules.

The principal input parameters for an orifice include:

- * names of its inlet and outlet nodes;
- * configuration (bottom or side);
- * shape (circular or rectangular);
- * height above the inlet node invert;
- * discharge coefficient.

b) Weirs

Weirs, like orifices, are used to model outlet and diversion structures in a drainage system. Weirs are typically located in a manhole, along the side of a channel, or within a storage unit. They are internally represented in SWMM as a link connecting two nodes, where the weir itself is placed at the upstream node. A flap gate can be included to prevent backflow.

Weirs can be used as storage unit outlets under all types of flow routing. If not attached to a storage unit, they can only be used in drainage networks that are analyzed with Dynamic Wave flow routing.

The height of the weir crest above the inlet node invert can be controlled dynamically through user-defined Control Rules. This feature can be used to model inflatable dams.

The principal input parameters for a weir include:

- * names of its inlet and outlet nodes;
- * shape and geometry;
- * crest height above the inlet node invert;
- * discharge coefficient.

c) Outlets

Outlets are flow control devices that are typically used to control outflows from storage units. They are used to model special head-discharge relationships that cannot be characterized by pumps, orifices, or weirs. Outlets are internally represented in SWMM as a link connecting two nodes. An outlet can also have a flap gate that restricts flow to only one direction.

Outlets attached to storage units are active under all types of flow routing. If not attached to a storage unit, they can only be used in drainage networks analyzed with Dynamic Wave flow routing.

A user-defined function or table of flow versus head difference determines the flow through an outlet.

The principal input parameters for an outlet include:

- * names of its inlet and outlet nodes;
- * height above the inlet node invert;
- * function or table containing its head-discharge relationship.

2.4.3.2. Non-Visual Objects

In addition to physical objects that can be displayed visually on a map, SWMM utilizes several classes of non-visual data objects to describe additional characteristics and processes within a study area. In the following section, some of the units are analyzed.

2.4.3.2.1. Climatology

In this section some of the objects are described.

Temperature

Air temperature data are used when simulating snowfall and snowmelt processes during runoff calculations. If these processes are not being simulated then temperature data are not required.

Air temperature data can be supplied to SWMM from one of the following sources:

- * a user-defined time series of point values (values at intermediate times are interpolated);
- * an external climate file containing daily minimum and maximum values (SWMM fits a sinusoidal curve through these values depending on the day of the year).

Evaporation

Evaporation can occur for standing water on subcatchment surfaces, for subsurface water in groundwater aquifers, and for water held in storage units. Evaporation rates can be stated as:

- * a single constant value;
- * a set of monthly average values;
- * a user-defined time series of daily values;
- * daily values read from an external climate file.

2.4.3.2.2. Unit Hydrographs

Unit Hydrographs (UHs) estimate rainfall-derived infiltration/inflow (RDII) into a sewer system. A UH set contains up to three such hydrographs, one for a short-term response, one for an intermediate-term response, and one for a long-term response. A UH group can have up to 12 UH sets, one for each month of the year. Each UH group is considered as a separate object by SWMM, and is assigned its own unique name along with the name of the rain gage that supplies rainfall data to it.

2.4.3.2.3. Time series

Time series can be used to describe:

- * temperature data;
- * evaporation data;
- * rainfall data;
- * water stage at outfall nodes;

- * external inflow hydrographs at drainage system nodes;
- * external inflow pollutographs at drainage system nodes.

Each time series must be given a unique name and can be assigned any number of timevalue data pairs. Time can be specified either as hours from the start of a simulation or as an absolute date and time-of-day.

For rainfall time series, it is only necessary to enter periods with non-zero rainfall amounts. SWMM interprets the rainfall value as a constant value lasting over the recording interval specified for the rain gage that utilizes the time series. For all other types of time series, SWMM uses interpolation to estimate values at times that fall in between the recorded values.

For times that fall outside the range of the time series, SWMM will use a value of 0 for rainfall and external inflow time series, and either the first or last series value for temperature, evaporation, and water stage time series.

2.4.3.3. Computational Methods

SWMM is a physically based, discrete-time simulation model. It employs principles of conservation of mass, energy, and momentum wherever appropriate. This section briefly describes some methods SWMM uses to model stormwater runoff quantity.

2.4.3.3.1. Surface Runoff

The conceptual view of surface runoff used by SWMM is illustrated in *Figure 2. 7* below. Each subcatchment surface is treated as a nonlinear reservoir. Inflow comes from precipitation and any designated upstream subcatchments. There are several outflows, including infiltration, evaporation, and surface runoff.

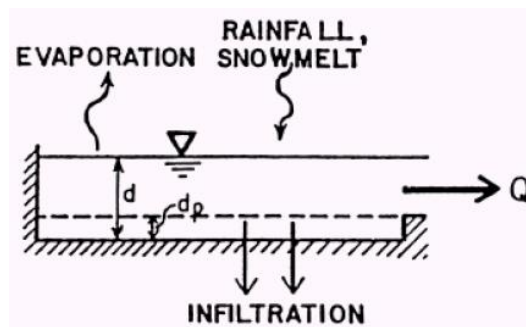


Figure 2. 7. Conceptual view of surface runoff (Rossman, 2010)

The capacity of this "reservoir" is the maximum depression storage, which is the maximum surface storage provided by ponding, surface wetting, and interception. Surface runoff per unit area, Q , occurs only when the depth of water in the "reservoir" exceeds the maximum

depression storage, dp , in which case the outflow is given by Manning's equation. Depth of water over the subcatchment (d in feet) is continuously updated with time (t in seconds) by solving numerically a water balance equation over the subcatchment.

Infiltration

Infiltration is the process of rainfall penetrating the ground surface into the unsaturated soil zone of pervious subcatchments areas. SWMM offers three choices for modeling infiltration:

* *Horton's Equation*

This method is based on empirical observations showing that infiltration decreases exponentially from an initial maximum rate to some minimum rate over the course of a long rainfall event. Input parameters required by this method include the maximum and minimum infiltration rates, a decay coefficient that describes how fast the rate decreases over time, and a time it takes a fully saturated soil to completely dry;

* *Green-Ampt Method*

This method for modeling infiltration assumes that a sharp wetting front exists in the soil column, separating soil with some initial moisture content below from saturated soil above. The input parameters required are the initial moisture deficit of the soil, the soil's hydraulic conductivity, and the suction head at the wetting front;

* *Curve Number Method*

This approach is adopted from the NRCS (SCS) Curve Number method for estimating runoff. It assumes that the total infiltration capacity of a soil can be found from the soil's tabulated Curve Number. During a rain event this capacity is depleted as a function of cumulative rainfall and remaining capacity. The input parameters for this method are the curve number, the soil's hydraulic conductivity (used to estimate a minimum separation time for distinct rain events), and a time it takes a fully saturated soil to completely dry.

2.4.3.3.2. Flow Routing

Flow routing within a conduit link in SWMM is governed by the conservation of mass and momentum equations for gradually varied, unsteady flow (i.e., the Saint Venant flow equations). The SWMM user has a choice on the level of sophistication used to solve these equations:

a) **Steady Flow Routing**

Steady Flow routing represents the simplest type of routing possible (actually no routing) by assuming that within each computational time step flow is uniform and steady. Thus it simply translates inflow hydrographs at the upstream end of the conduit to the downstream

end, with no delay or change in shape. The Manning equation is used to relate flow rate to flow area (or depth).

This type of routing cannot account for channel storage, backwater effects, entrance/exit losses, flow reversal or pressurized flow. It can only be used with dendritic conveyance networks, where each node has only a single outflow link (unless the node is a divider in which case two outflow links are required). This form of routing is insensitive to the time step employed and is really only appropriate for preliminary analysis using long-term continuous simulations.

b) Kinematic Wave Routing

This routing method solves the continuity equation along with a simplified form of the momentum equation in each conduit. The latter requires that the slope of the water surface equal the slope of the conduit.

The maximum flow that can be conveyed through a conduit is the full-flow Manning equation value. Any flow in excess of this entering the inlet node is either lost from the system or can pond atop the inlet node and be re-introduced into the conduit as capacity becomes available.

Kinematic wave routing allows flow and area to vary both spatially and temporally within a conduit. This can result in attenuated and delayed outflow hydrographs as inflow is routed through the channel. However this form of routing cannot account for backwater effects, entrance/exit losses, flow reversal, or pressurized flow, and is also restricted to dendritic network layouts. It can usually maintain numerical stability with moderately large time steps, on the order of 5 to 15 minutes. If the aforementioned effects are not expected to be significant then this alternative can be an accurate and efficient routing method, especially for long-term simulations.

c) Dynamic Wave Routing

Dynamic Wave routing solves the complete one-dimensional Saint Venant flow equations and therefore produces the most theoretically accurate results. These equations consist of the continuity and momentum equations for conduits and a volume continuity equation at nodes.

With this form of routing it is possible to represent pressurized flow when a closed conduit becomes full, such that flows can exceed the full-flow Manning equation value.

Flooding occurs when the water depth at a node exceeds the maximum available depth, and the excess flow is either lost from the system or can pond atop the node and re-enter the drainage system.

Dynamic wave routing can account for channel storage, backwater, entrance/exit losses, flow reversal, and pressurized flow. Because it couples together the solution for both water

levels at nodes and flow in conduits it can be applied to any general network layout, even those containing multiple downstream diversions and loops. It is the method of choice for systems subjected to significant backwater effects due to downstream flow restrictions and with flow regulation via weirs and orifices. This generality comes at a price of having to use much smaller time steps, on the order of a minute or less (SWMM will automatically reduce the user-defined maximum time step as needed to maintain numerical stability).

2.4.3.3.3. Surface Ponding

Normally in flow routing, when the flow into a junction exceeds the capacity of the system to transport it further downstream, the excess volume overflows the system and is lost. An option exists to have instead the excess volume be stored atop the junction, in a ponded fashion, and be reintroduced into the system as capacity permits. Under Steady and Kinematic Wave flow routing, the ponded water is stored simply as an excess volume. For Dynamic Wave routing, which is influenced by the water depths maintained at nodes, the excess volume is assumed to pond over the node with a constant surface area. This amount of surface area is an input parameter supplied for the junction.

Alternatively, the user may wish to represent the surface overflow system explicitly. In open channel systems this can include road overflows at bridges or culvert crossings as well as additional floodplain storage areas. In closed conduit systems, surface overflows may be conveyed down streets, alleys, or other surface routes to the next available stormwater inlet or open channel. Overflows may also be impounded in surface depressions such as parking lots, back yards or other areas.

PART II

STUDY CASE

Chapter 3

Study case: Palermo drainage system

In order to conduct a careful analysis of the study case, it is important to know problems associated with crisis events and socio-economic situation about population.

The studied basin is the center of the city of Palermo. Palermo has been for many years subject to overload phenomena and surface runoff (Incontrera, 2014). There are several papers that have dealt with the problem. The University of Palermo and especially the Department of Hydraulic and Environmental Application (now Department of Civil, Environmental, Aerospace, Materials Engineering - DICAM) has been involved in activities to protect the territory of the city of Palermo many times. For examples in 1999 AMAP (Azienda Municipalizzata Acquedotti Palermo), company that manages water resources in Palermo, entrusted the updating and integrating knowledge about sewer network in the historical part of the city to the Department of Civil, Environmental, Aerospace, Materials Engineering of the University of Palermo.

In this chapter a brief introduction about the city, with particular regard to characteristics of the drainage system is described.

3.1. The city of Palermo

Palermo is a city with 671696 (Istat, 2016) habitants in the north-east of Sicily Island. Founded by the Phoenicians in 734 BC, the city has undergone several changes as a result of the numerous settlements over the time. The city was a plain with many marshy areas. Now the plain is almost completely urbanized and surrounded by mountains with a predominantly limestone. The climate is Mediterranean, characterized by hot – dry summers and cool-rainy winters.

Palermo is divided into 8 districts, defined *circostrizioni*. The historic district of the city is called *First-Palazzo Reale-Monte di Pietà*. Over the past 30 years, this district has gone through a radical change of his employment (Busetta, 2013). The lack of building renovation has created a first abandonment of the district and a subsequent repopulation by foreigners. About a quarter of all foreign residents in the city actually lives inside only this district and the measures for ancient buildings are very scarce. The population density is still very high, about 8000 inh/km² compared to average population density in the city, about 3000 inh/km².

3.2. Historic information of Palermo sewer system

The construction of the sewage of Palermo has gone hand in hand with the evolution of the city. During the Arab settlement, the city was enclosed by two rivers called "Kemonia" and "Papireto" who received all discharges of the city and representing a perennial hygienic danger (*Figure 3.1*).



Figure 3.1. In blue the sea and the Kemonia and Papireto rivers, in orange the old town, in yellow the necropolis (Incontrera, 2014).

Felice Giarrusso writes that as a result of epidemics and floods caused by the Kemonia River in 1557 and 1575, the Senate dealt with the problem of drainage of the two streams by adopting some solutions: about the Kemonia River, it was decided to divert the water coming from the mountain regions, corresponding to the avenues today called *viale delle Scienze*, *corso Pisani* and *Fossa della Garofala* into the Oreto River and lowest spring waters were conveyed to the harbor area through a covered channel with a vaulted roof that ran under the old course; about the Papireto River, it was decided to fill the pit called "Danisinni" from which originated the river with a covered canal that served as a disposer of water draining to the harbor area.

However these works were not revealed sufficient to eliminate the dangers of floods, perhaps due to insufficient collectors. In fact, soon after heavy rainfall the filled area is transformed back into the swamp and in the following time intensive rainfall has continued to generate floods with damage and many casualties. It is interesting to note that, at that time, the roads were built as a cradle, accepting the notion that the road had turned into collector during rainfall event. The drainage system continued to be one of the so-called bells, shafts or pipes, made by individuals without a comprehensive plan, which discharged in two covered streams. These pipes are made of clay. They broke often for brittleness of the material and sewage was going to soak the soil. At the same time many aqueducts, also made of clay, suffered the same fate with constant dangers of drinking water contamination and cholera epidemics, as in 1837 and in 1854.

Meanwhile, the city began to expand, it was realized *via Maqueda* and extended up to the countryside, a project for the reconstruction of *Corso Vittorio Emanuele* was designed by Torregrossa R. and Ampulla M. in 1858. Those engineers renovated the sewer system, providing for the construction of the road with culverts, sidewalks and pronounced slope as to convey the rain water through the culverts. These notions were soon accepted by the Technical Department of the Municipality and implemented in the new city sewers.

Before 1886, the city sewer network had a total length of approximately 70 km of canals and 26 outfalls into the sea, 11 discharges to *Cala* (the harbor), 5 along the beach at the *Foro Italico* and 10 distributed among *Piazza S. Muzzo*, in front of the existing commercial harbor, and *Piazza Ucciardone*. Following the expansion of the city, which extended in principle by the river Oreto to Via Notarbartolo, in 1930 the Municipality of Palermo decided to draw up a general plan of the sewer system (Incontrera, 2014).

The city was divided into three basins with independent collection and sewer systems: a) the first one was bounded by the Oreto River, *corso Olivuzza*, *Via Cavour* and *Via Volturmo*;

b) the second one was bounded by *Via F. Crispi*, PA-TP railway, *Via Volturmo* and the *Passo di Rigano* channel; c) the third one was bounded by PA-TP railway, *Passo di Rigano* channel, *Via Principe di Scalea* and *Piazza Libertà-Piazza Leoni*. In turn, the city area was protected by appropriate stormwater channels.

3.3. Current assessment of the drainage system of Palermo

The current sewer system has been drawn in the 1930, but, the urban expansion without adequate extension of sewage, the inadequacy of existing hydraulic infrastructures, the non-realization of part of the channels that allow the diversion of rainwater from the mountains that surround the city, still now amount to situations of discomfort which in some cases can cause severity damage (Incontrera, 2014).

With the adoption of the Merli law (No. 319/05.10.1976) and the drafting of the new program for the implementation of the drainage system for the city of Palermo (*PARF-Programma di Attuazione della Rete Fognaria*) by the Division of Public Works, after approved by the Land and Environment Regional Department in 1987, problems related to the disposal of rainwater, even if partially, find a proper solution.

In summary, the characteristic features of the solutions outlined by the PARF can be summarized as follows:

1. Subdivision of the entire urbanized area into two basins:
 - a) a main basin called the *South-Eastern* with an expected population equivalent of 880,000 inhabitants gravitating to the water treatment plant located in *Acqua dei Corsari* area;
 - b) a secondary basin called *North-Western* with an expected population equivalent of 100,000 people gravitating to the water treatment plant located in the *Fondo Verde* area;
2. Construction of two main pipes (*South-Eastern and North-Western* pipes) at the service of the two mentioned above basins;
3. Realization of the two named wastewater treatment plants serving the two basins;
4. Elimination of all discharges inshore with the exception of those emissaries in relation to surplus flows and stormwater for the areas served by separated system;
5. Building of an offshore pipes to carry the water from the two wastewater treatment plan;
6. Reuse of treated water for irrigation or for groundwater recharge;
7. Reorganization of the main stormwater channels to protect urban area.

Currently only some works, mentioned in the PARF, have been realized. The 5 lots already banned are shown below, pointing out the state of realization of the work.

3.3.1. Separate system and pump station inside shipyard area

This first lot deals with the reorganization of *Cantieri Navali* discharge area with separation of wastewater, (up to a dilution equal to 3 times the average flow rate Q_m) from stormwater, the removal of stormwater through a channel, out of the shipyard area and the building of a pump station lifting for wastewater (*Figure 3.2* in red).

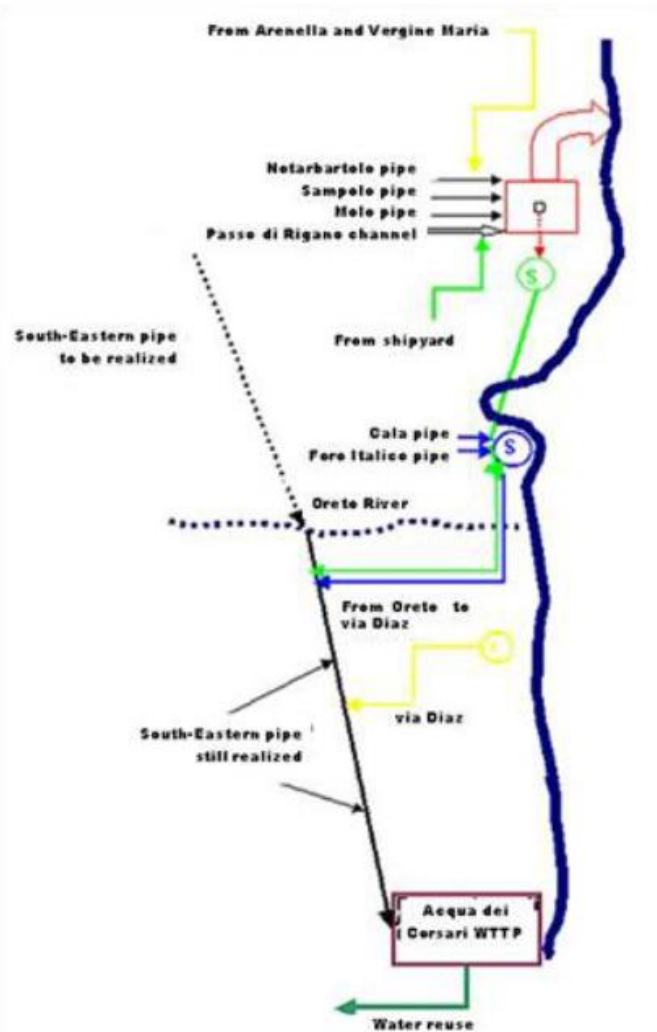


Figure 3.2. Scheme about recovery plan to clean Palermo coast (Incontrera, 2014).

From technical point of view limited executive changes must be made to connect these works with the sewage pumping station. Its final design is almost ready, because most of these works are realized during the intervention funded by the Portual Authority Agency.

3.3.2. Pipe connecting shipyard area to the second pump station

It connects to lot n.1 and concerns the wastewater flow. It consists of feeding the —*Acqua dei Corsari* wastewater treatment with a channel from harbor area to sewage pump station of *Porta Felice* (Figure 3.2 in light green). For this work the municipality of Palermo and the company which deals with water management have already prepared the preliminary project but nothing has been realized.

3.3.3. Removal of discharge to the sea

This program work concerns the interception of pipes, the sewage pumping in *Porta Felice* plant and the adduction to the *South-Eastern* collector of the group of discharges present along the *Foro Italico*, the *South Quay* and within the *Cala* area (Figure 3.2 in blue). The works for the construction of the pumping station and its pipes were made in 2007. However, it was expected a updating of this system due to the construction of other works included in the *PARF*, which will bring additional flows: the construction of a pipe through *piazza della Pace*, *corso Scinà*, *Via Quintino Sella* and *via Puglisi* and the construction of another pipe, which will pass under *via Roma* and *via Cavour* to reconnect to the *Cala* pipe.

3.3.4. Building of sewer networks

As part of this lot two interventions aimed at the elimination of secondary discharges are grouped here (Figure 3.2 in yellow), with less importance than in harbor area, but with strategic importance for the achievement of coastal waters quality:

- a) Construction of the sewer network for *Arenella* and *Vergine Maria* suburbs, with adduction to the shipyard. This intervention aims to regulate discharges of 9,500 residents in *Arenella* and *Vergine Maria* that currently end up into the sea and puts them in the sewer network. The work has been completed in 2012.
- b) Interception of discharges from *Via Diaz* to the *Oreto River* and adduction to the *South-Eastern* Emissar. The *South-Eastern* emissary has been realized only for the final path between the right bank of the *Oreto River* and the sewage treatment plant. It is long 6.5 kilometers and has a circular diameter of 3.7 m. For now it collects the wastewater from *Sperone*, *Ciaculli*, *Brancaccio*, *Oreto*, *Guadagna*, *Villagrazia*, *Bonagia*, *Falsomiele* and part of *Villaggio Santa Rosalia*.

So that it may come into operation lacks the construction of approximately 3100 m of new pipeline near *via Uditore* and the area between *Piazza Principe di Camporeale* and *via del Vespro*. A spillway system and a siphon in correspondence of the *Oreto River* are also provided. The realized works have been financed because have been included in the three-year program of public works of the Palermo Municipality (2007-2009).

3.3.5. Wastewaters Treatment Plants

These interventions on the *Acqua dei Corsari* wastewater treatment plant bring the capacity from the current 440,000 population equivalent to the capacity provided for *PARF* (Figure 3.2 in purple). This expansion is necessary because with the implementation of the measures referred to lots no. 2, 3 and 4 is to complete the adduction to the purifier of the whole wastewater for *South-West* basin required by *PARF*. About this it should be noted that the wastewater treatment plant was built with the general hydraulic parts sized for its final structure (880,000 habitants) and the enhancement involves the construction of new tanks for grit removal, primary and secondary sedimentation and oxidation. However these new contributions of wastewater will allow the completion of the overall project of reuse of treated water for irrigation, which was first funded a lot of 300 l/sec potential in 1997 (Figure 3.2 in dark green).

The *Fondo Verde* wastewater treatment plant has been completed and is currently in operation at full load. It is located in *via Olimpo* and treats the wastewaters flow down *Mondello, Valdesi, Partanna Mondello, ZEN I, Z.E.N. II, Pallavicino* and *Villaggio Ruffini*. However the purified wastewater is fed back into the sewer system that revolves on the *South-Eastern* basin because of not completed *North-Western* Emissary and the offshore pipe in *Cala D'Isola*. In fact, the *North-Western* Emissary has been achieved without the final stretch between *Tommaso Natale* and *Cala D'Isola* (Incontrera, 2014).

3.4. Recent flood events

In Palermo, phenomena of overflowing were always recorded, mainly due to flood of underground channels. To alleviate these episodes additional infrastructure for preservation of the town and in particular the old center of the city were built. The first measure, which was adopted as a result of flooding in 1931, during which the city was fully involved, was the construction of the *Passo di Rigano* channel. Although it is now transformed in a sewer pipe, this work has proved useful in preventing flood damage effects of previous centuries. However the construction of the channel *Passo di Rigano* was not sufficient to protect certain areas of the city, especially the deeper ones in the old town that became flooded for events with very low return period, equal to 2-3 years (Freni, 1996).

Following further investigations, even by the local Civil Protection Agency, the channel that collects the *Papireto* River has been designed, in order to prevent any rising during rainy periods. Even this action has improved the efficiency of the drainage system in the old town of Palermo, but overflowing continue to occur.

It is possible to note that since 2007, the year in which the last major changes to the sewer system were made, overflowing events mainly occur along the coastline, from *Sferracavallo* to *Acqua dei Corsari* and along the surrounding highway areas, nearby the axes of the main crossing (*viale Michelangelo*, *viale Lazio*, *via Pitrè*, *corso Calatafimi*, *via Oreto*). The causes of these inefficiencies, resulting in traffic inconveniences of course, because they involve the principal street of the long-distance traffic, are difficult to understand, although some assumptions can be done. For example, it can be assumed that the waterproofing of additional areas below the hills of Palermo has caused a higher flow rate to discharge. This is very clear in at least two critical events. The first event was the construction of a large shelter for emigrate in *via Belmonte Chiavelli*: the impermeable surface has created a slide, almost a preferential channel, with the outlet in a narrow street. The result has been to channel the water directly in the residential area. The second recently occurred example is a major quantity of water in the pipes along the streets *viale Michelangelo* and *viale Lazio*: even in this case it is expected a growing urbanization in that areas.

After this complete explanation of the drainage system of Palermo, it is important to remark that this study focuses only on the center of Palermo and *Figure 3.3* points out location of studied manholes (black dots).

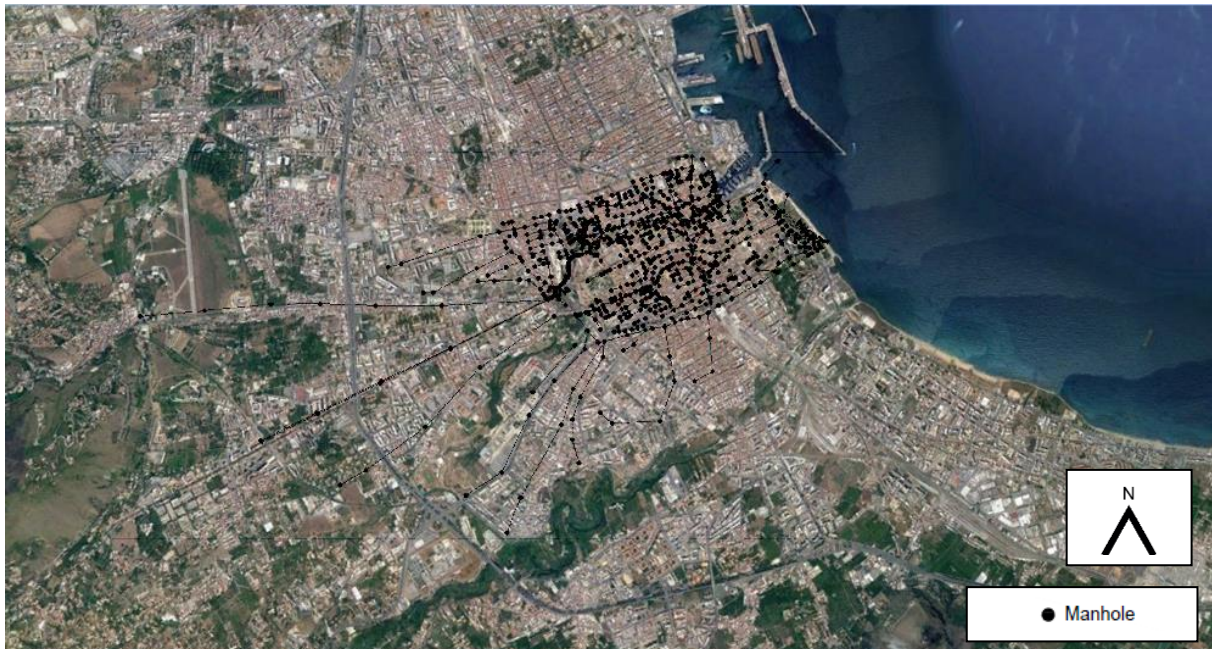


Figure 3.3. Part of the drainage system of Palermo that is matter of this study. Black dots are studied manholes.

3.5. Rainfall data

For this study about CC's effects on Palermo urban drainage system, rainfall data information were collected using gauge networks.

Rain gauges within the city belong to:

- Osservatorio delle Acque;
- Sicilian agro-meteorological information service (Servizio informativo Agro-meteorologico della Sicilia- SIAS);

The network of Osservatorio consists of 255 rain gauges and , for the city of Palermo, currently three rain gauge are available: *Osservatorio delle Acque* (coordinates UTM ED50 354093E, 4220253N, 57 m a.s.l.), *Istituto Zootecnico* (coordinates 351007E, 4220156N, 110 m a.s.l.) and *Osservatorio Astronomico* (coordinates UTM ED50, 355705E, 4219648N, 80 m a.s.l.). Temporal resolution about rainfall data is related to the type of rain gauge. Base available product of this Agency is 1 hour cumulative precipitation and for this reason, these data are not considered for this study.

The regional Agency SIAS has a gauge network with 96 on line stations, scattered throughout Sicily. There is only one rain gauge In Palermo city and it is part of the station called *Uditore* (coordinates UTM ED50 353448E, 4221667N, 50 m a.s.l.).

This station has been chosen as weather data source for this study because is the only one on Palermo able to record high resolution data at 10 minutes scale.

3.5.1. Data Analysis

Climate data are essential to this study to estimate parameter useful to calculate the climate factor for the future weather generated by AWE-GEN.

We used weather data collected by SIAS on the Palermo Uditore rain gage station. These data are observations during the period 2002-2014 of several hourly variables: atmospheric pressure, solar radiation, air temperature, relative humidity, wind speed and precipitation, that is available in a 10 minutes time step. Compliance of these 13-year rainfall data with the historical data has been proven to be sure that running these data as input of AWE-GEN, simulated rainfall series in output are a good likely description of the weather in Palermo.

Palermo has a typical Mediterranean climate that is the climate of the lands in the Mediterranean Basin. The lands around the Mediterranean Sea form the largest area where this climate type is found, but it also is found in most of coastal California, in parts of Western and South Australia, in southwestern South Africa, sections of Central Asia, and in central Chile.

In order to better understand Palermo weather, studying observed data has been necessary. The average of annual precipitation is 700 mm/year and the monthly average rainfall and temperature values in the period 2002–2014 have been calculated, and reported in *Table 3. 1*.

Table 3. 1. Monthly mean rainfall and temperature in the period 2002-2014

Month	AVG monthly temp [°C]	AVG monthly depth [mm]
Jan	11,8	92,5
Feb	11,5	89,8
Mar	13,5	75,5
Apr	16,4	64,3
May	19,9	20,3
Jun	24,0	12,0
Jul	26,8	5,4
Aug	27,0	8,6
Sep	24,0	79,4
Oct	20,5	104,3
Nov	16,7	59,0
Dec	13,4	118,3

Table 3. 1 shows that the minimum average of monthly temperature is in February and its value is 11.5 °C, while the maximum average value is referred to August (27 °C). Regarding depth of precipitation, December has been the wettest month, on average, during the 2002-2014 period and its depth has been 118.3 mm, while July has been the driest month with 5.4 mm.

There are several type of Mediterranean climate and Sicily has a *hot-summer Mediterranean climate* that is the most common subtype of the Mediterranean climate, also known as “typical Mediterranean climate”. Regions with this form of climate experience average monthly temperatures in excess of 22.0 °C during its warmest month and an average in the coldest month between 18 to –3 °C or, in some applications, between 18 to 0 °C. Also, at least four months must average above 10 °C. Regions with this form of the Mediterranean climate typically experience hot, sometimes very hot and dry summers and mild, wet winters. In a number of instances, summers here can closely resemble summers seen in arid and semiarid climates. However, high temperatures during summers are generally not quite as high as those in arid or semiarid climates due to the presence of a large body of water. All areas with this subtype have wet winters. However, some areas with a hot Mediterranean subtype can actually experience very chilly winters, with occasional snowfall. Precipitation is heavier during the colder months. However, there are a number of clear, sunny days during the wetter months.

This study recognizes only two "seasons" during the year: identifying the 4 months with the highest temperature and the lowest rainfall depth from May to August (dry season), wet season goes from October to April.

Following this distinction between dry and wet season, *Figure 3.4* shows both the average of rainfall depth (blue bars) and the average of temperatures (red curve) for each month.

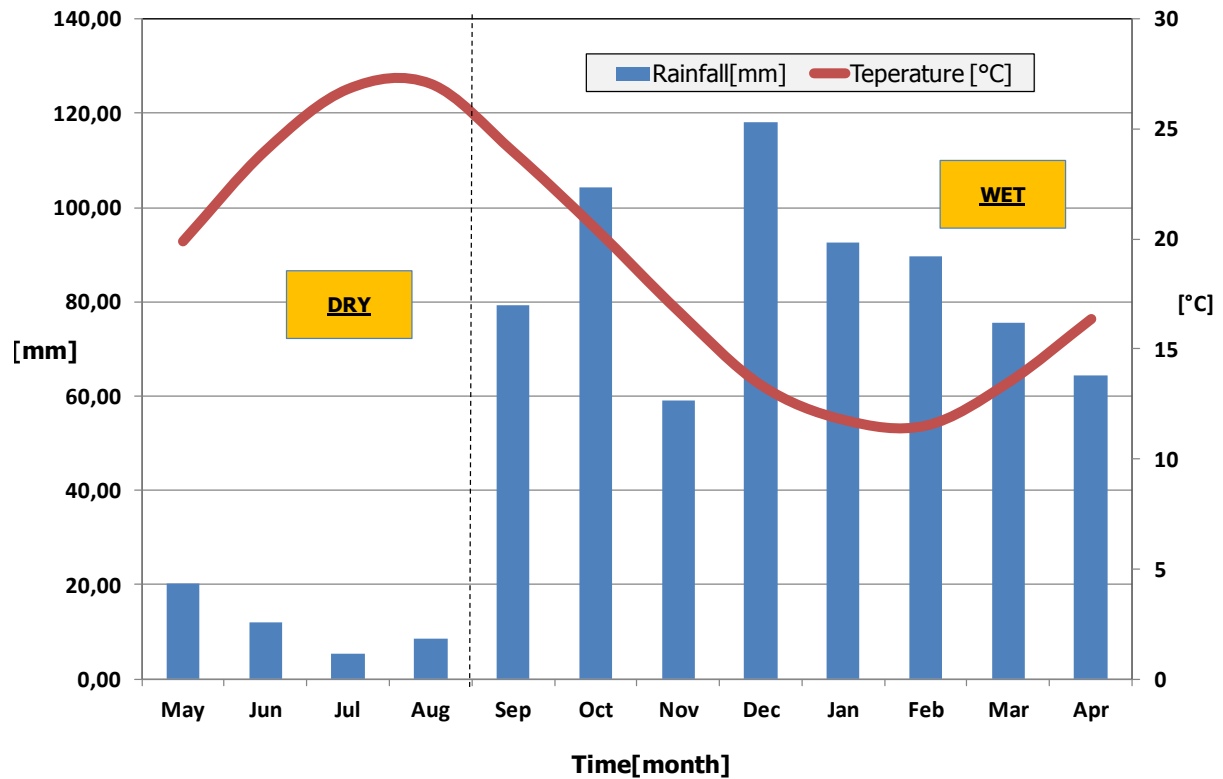


Figure 3.4. Monthly mean rainfall and temperature in the period 2002-2014 distinguished in wet and dry periods.

Figure 3.4 reports the same information of *Table 3.1* but it points out that the distinction between dry and wet period is clear for both variables: in fact, the peak of temperature and the lowest value of precipitation is in the dry season, and vice versa for the wet season.

In order to underline the clear difference between the two seasons, it is needed to remark that the highest monthly depth is about 20 mm in May, during the dry season, while, during the wet season, the lowest value of monthly rainfall depth is about 59 mm in November, about 3 times the value of May.

In agreement with aims of this dissertation, we decided that precipitation data requires to be shown more extensively than temperature and for this reason following analysis are dedicated only to precipitation data.

In order to analyze the percentage of wet and dry days for each year, it is important to study **Errore. L'origine riferimento non è stata trovata..**

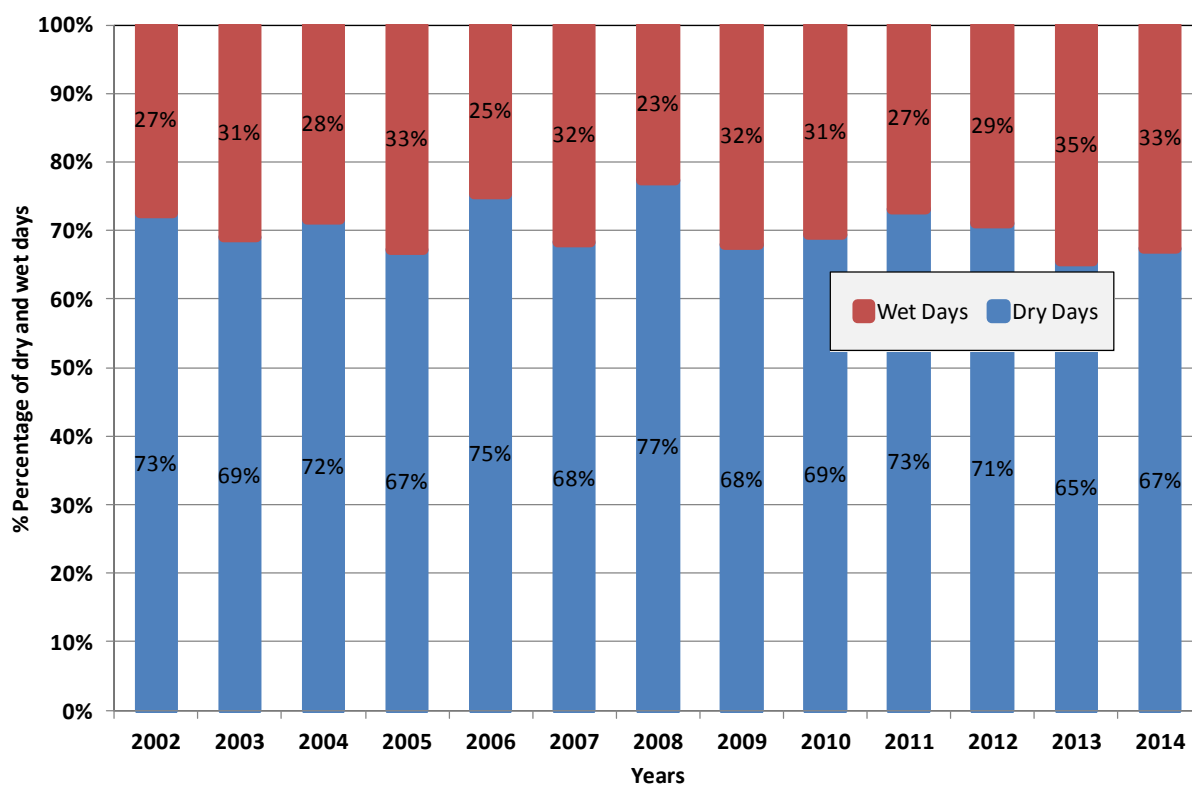


Figure 3.5. Percentages of wet and dry days for each year

Errore. L'origine riferimento non è stata trovata. displays percentages of wet (red bars) and dry (blue bars) days for each year: the percentage of wet days in 2008 has been the lowest during the period 2002-2014, while 2013 has had 35% of the year rained and this is the highest percentage in this dataset. By this plot, it is clear that the mean of number of rainy days is about 30%.

Moreover, analysis of monthly precipitation depth (*Table 3.2*) and intensity (*Table 3.3*) has been studied. In detail, *Table 3.2* shows, for each year, the monthly depths of precipitation and it is possible to notice that during 2008 it has rained 443 mm/year, the lowest value between 2002 and 2014, while the highest annual depth is about 1268 mm/year in 2009. This table is also able to point out information month by month: for example, January 2008 has been the driest January with about 22 mm/month while January 2010 has rained 187 mm/month; June 2013 has been dry while there has been about 43 mm/month in June 2005; also, about 35 mm/month of rain fell in October 2004 while about 294 mm/month in October 2009.

Between 2002 and 2014, it has been rained about 729 mm/year with a variability in terms of standard deviation equal to about 209 mm, and by *Table 3.2* it is possible to read average of monthly precipitation for each month and its standard deviation.

Table 3.2. Monthly and annual rainfall depth analysis

Year	Depth [mm]												
	Total Precip [mm]	Jan	Feb	Mar	Apr	May	Jun	Jul	Aug	Sep	Oct	Nov	Dec
2002	514	35,0	13,6	19,0	44,8	68,8	7,0	10,0	31,0	65,0	50,0	59,6	110,2
2003	873,8	146,4	100,4	26,4	111,0	19,0	6,4	1,2	32,4	137,2	127,2	43,2	123,0
2004	790	67,4	49,6	96,8	78,0	19,2	41,8	14,0	0,0	116,8	35,0	126,6	144,8
2005	809,6	70,8	102,6	80,2	122,6	12,6	43,2	7,4	16,4	24,0	87,4	46,0	196,4
2006	500,2	93,8	79,2	42,8	20,8	0,0	21,2	27,0	11,4	75,8	37,8	20,0	70,4
2007	664,2	12,8	60,6	114,0	61,0	16,0	13,4	0,0	0,0	42,6	149,0	110,0	84,8
2008	443	22,2	17,2	94,0	8,4	13,6	0,4	0,0	0,0	62,0	48,4	34,2	142,6
2009	1268,4	185,0	180,8	79,6	96,4	1,0	11,0	0,0	1,6	241,8	294,0	52,0	125,2
2010	762	187,4	104,0	76,0	61,0	8,6	6,8	3,2	0,0	93,8	115,8	56,2	49,2
2011	630,2	47,4	131,0	33,2	34,8	30,2	0,4	3,6	0,2	75,6	133,0	49,4	91,4
2012	692,6	77,2	126,0	71,0	58,8	25,4	0,0	1,8	0,0	66,6	68,0	79,2	118,6
2013	731,4	122,6	103,0	134,0	30,0	13,0	1,8	0,0	18,4	15,2	127,2	43,2	123,0
2014	800	134,2	99,0	114,0	108,4	36,0	2,2	1,4	0,8	16,0	82,8	47,4	157,8
Average	729,2	92,5	89,8	75,5	64,3	20,3	12,0	5,4	8,6	79,4	104,3	59,0	118,3
ST. DEV.	209,0	58,5	46,3	36,2	36,8	17,8	14,8	7,8	12,2	61,0	69,1	29,8	38,8

By this table it is possible to create a first plot that show the monthly depths for each year (Figure 3.6) that points out how the seasonal trend is evident with May, June, July and August that have the lowest values.

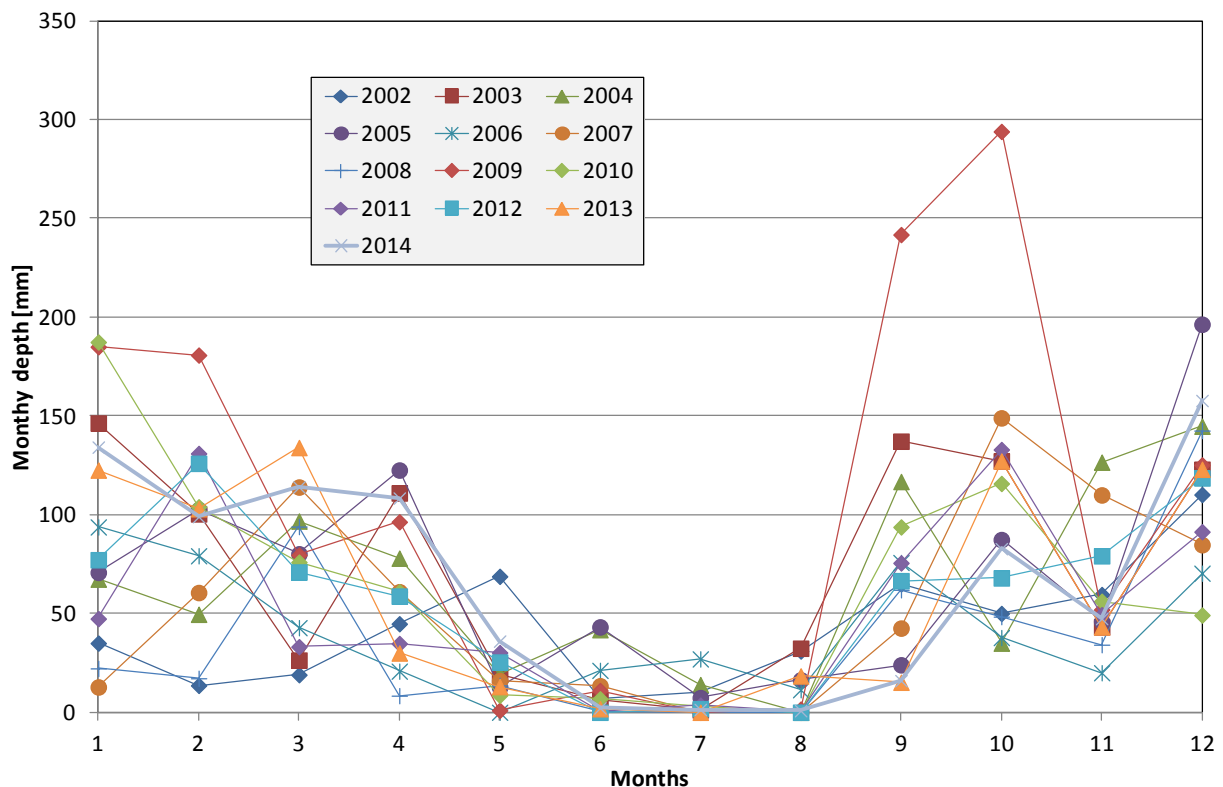


Figure 3.6. Monthly rainfall depth for each year

Figure 3.6 shows all the years from 2002 and 2014, month by month, remarking that October 2009 has been the month with the highest rainfall depth, while the differences

between others values are low. It is possible to plot information about the averages of monthly rainfall and their variability, in terms of standard deviation, as shown in *Figure 3.7*.

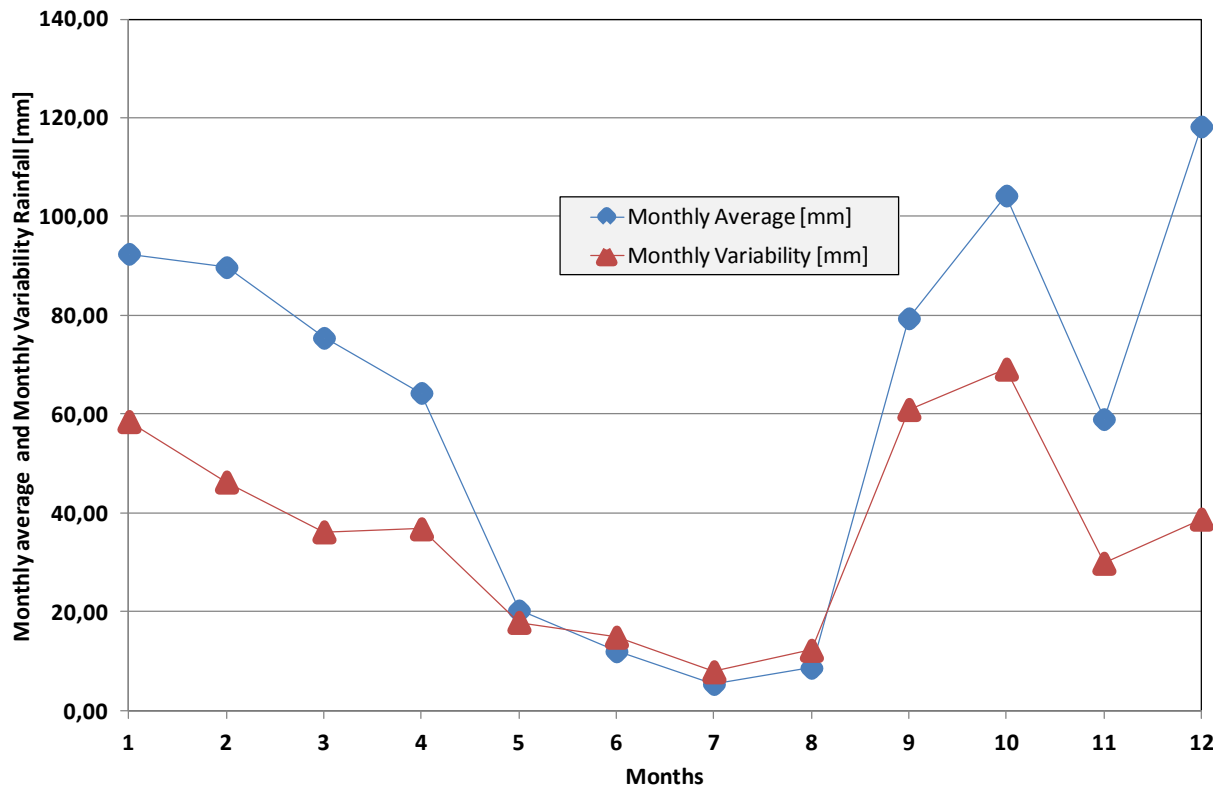


Figure 3.7. Monthly average and variability of the rainfall depth.

By *Figure 3.7* it is possible to state that December has been the month with the highest rainfall depth, on average, while July has been the one with less rain. Also, the months, that have been classified as in the dry season, show to have the lowest depth, on average, and the lowest standard deviation. The highest standard deviation is in October, and it can be justified by the high rainfall depth recorded in October 2009.

Calculating rainfall intensities, some considerations can be stated by *Table 3.3* that shows for each month of the period 2002-2014 average of monthly intensity. By these values, it has been possible to calculate the average of both monthly intensity in mm/hr for each year and monthly intensity in mm/hr for each month. For each month, the coefficient of variation has been calculated to measure the dispersion of these values around the mean value. Regarding the average of intensities calculated for each year (from left to right), it is evident that the minimum average of intensity is about 2.3 mm/hr in 2007 and the maximum has been in 2003 equal to about 4.4 mm/hr.

Table 3.3. Monthly and annual rainfall intensity analysis

Year	Depth [mm]	Intensity[mm/hr]												
	Total Precip [mm]	Jan	Feb	Mar	Apr	May	Jun	Jul	Aug	Sep	Oct	Nov	Dec	Average
2002	514	2,3	2,0	2,4	2,6	3,4	2,0	7,5	3,6	7,6	5,6	3,8	2,9	3,81
2003	873,8	2,9	2,8	2,5	2,8	2,7	4,8	7,2	7,5	7,4	7,3	2,6	2,5	4,43
2004	790	2,5	3,6	2,5	2,9	2,7	5,3	4,7	0,0	6,5	4,2	3,2	2,7	3,41
2005	809,6	2,3	2,3	2,6	2,5	2,9	13,6	1,9	1,9	3,5	5,0	2,3	3,5	3,70
2006	500,2	2,3	2,5	2,1	1,7	0,0	3,1	18,0	4,9	5,4	3,5	2,8	2,7	4,09
2007	664,2	1,8	3,1	2,0	2,3	3,1	2,0	0,0	0,0	3,8	4,4	3,1	2,5	2,34
2008	443	2,8	2,5	2,8	2,3	2,5	1,2	0,0	0,0	6,0	4,5	2,3	3,8	2,55
2009	1268,4	2,7	3,2	2,7	2,8	2,0	4,1	0,0	2,4	6,7	6,1	4,5	3,1	3,36
2010	762	2,7	2,3	1,9	2,7	2,2	3,1	2,7	0,0	4,5	3,6	2,6	2,3	2,55
2011	630,2	1,9	3,1	2,5	2,8	2,3	1,2	3,6	1,2	5,7	6,0	8,5	3,0	3,47
2012	692,6	3,1	2,3	2,8	2,5	4,1	0,0	1,5	0,0	5,7	3,8	3,3	4,1	2,77
2013	731,4	3,0	2,5	3,0	2,3	2,3	1,8	0,0	4,4	3,5	7,3	2,6	2,5	2,94
2014	800	3,1	2,4	2,7	3,3	3,8	4,4	1,2	4,8	4,0	7,5	3,9	3,4	3,71
Average	729,18	2,58	2,66	2,49	2,57	2,63	3,59	3,72	2,36	5,40	5,28	3,51	3,01	
CV	0,29	0,17	0,17	0,14	0,15	0,38	0,95	1,35	1,05	0,27	0,27	0,47	0,18	

Regarding monthly analysis(from up to down), the maximum value of average intensity is about 5.4 mm/hr for September, while the minimum is in August and it is about 2.4 mm/hr. Plotting monthly average along the years and their coefficient of variation, *Figure 3.8* shows that maximum variability, in terms of coefficient of variation, is related to the hottest months, while the lowest value of coefficient of variation is in March.

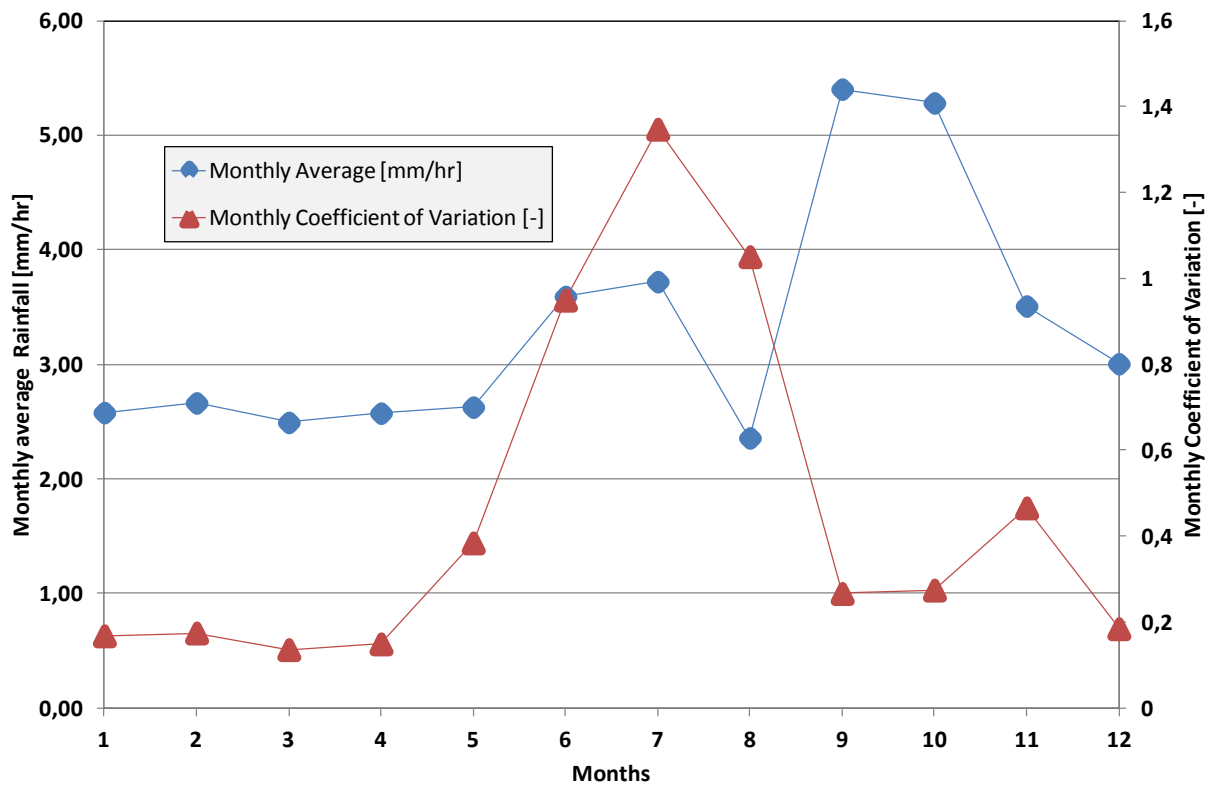


Figure 3.8. Monthly average and variability of the rainfall intensity.

3.5.2. Estimated Parameter by AWE-GEN

Aim of this study is to investigate the effects of CC on the urban drainage system of Palermo comparing these to those caused by current climate.

The adopted method requires a control period, usually representative of the present climate, for which both meteorological observations and climate model simulations are available. To this aim, a *Baseline* scenario for the basin, representative of the *Current* conditions, has been opportunely generated by the AWE-GEN starting from hourly data from 2002 to 2014 derived by the Palermo Uditore SIAS meteorological station.

On the total, three climate scenarios, including 50 realizations of rainfall, temperature, solar radiation, relative humidity and wind speed, have been created and investigated for the basin: namely the *Baseline (Current scenario)* and two climate projections for the RCP 8.5, based on GCM projections over the periods 2045–2065 (*2050 scenario*) and 2081–2100 (*2100 scenario*), respectively (see chapter 4).

In details, regarding *2050 scenario* and *2100 scenario*, 50 series 20-year long have been generated, while, regarding the *current scenario*, the 50 series are 50-year long. This choice has been necessary in order to test and compare outputs from the weather generator model to the observed data, as shown in section 3.5.2.1.

Further impact analysis include, for each scenario, a set of 50 generations 20-year long; it is important to clarify that, regarding the *Baseline*, each series, that is generated as 50-year long, has been randomly cut in a 20-year long series to make the three scenarios being equal in terms of length of the series.

3.5.2.1. AWE-GEN results in stationary conditions and current climate

In order to test the AWE-GEN model the current climate has been simulated in stationary conditions using data of the SIAS weather station in Palermo with 13 years of hourly weather data (2002-2014). Following results are related to the generated fifty 50-year long series.

The first analysis has included a comparison between observed and simulated monthly precipitation, as shown in *Figure 3.9*. This plot points out that the model is able to respect the monthly averages with some differences about variability in terms of standard deviations; in details, variability of simulated series is frequently lower than that related to the observed data, except that variability of July and December when it is larger. This first result prove that the model is able to well maintain rainfall characteristics because outcomes of simulated series are not fare from those of observed data.

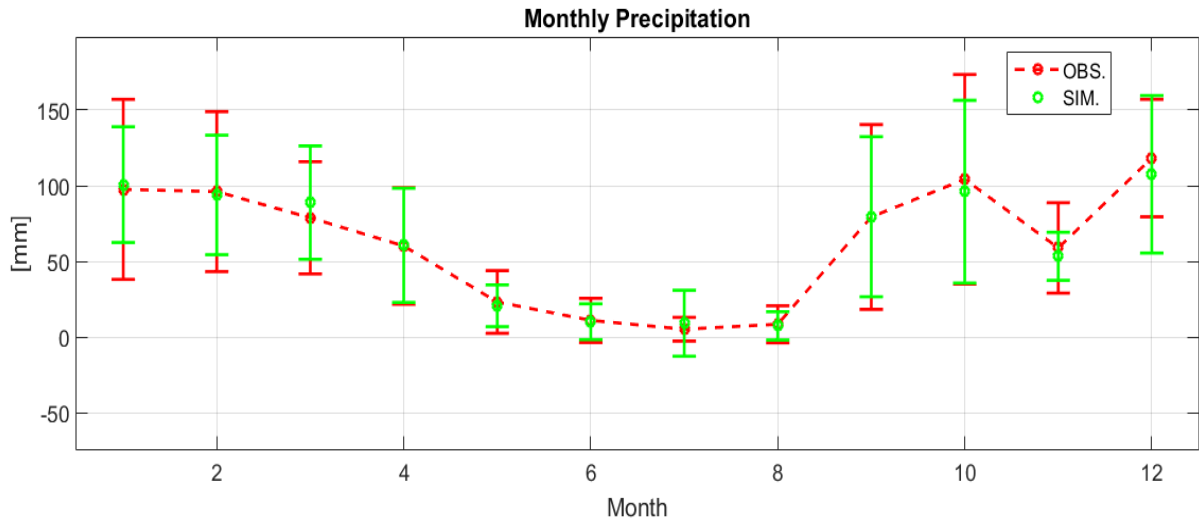


Figure 3.9. A comparison between observed (red) and simulated (green) monthly precipitation. The vertical bars denote the standard deviations of the monthly values.

Going through other statistic analysis, *Figure 3.10* and *Figure 3.11* show a comparison between observed and simulated monthly statistics of precipitation (mean, variance, lag-1 autocorrelation, skewness, frequency of non precipitation, transition probability wet-wet), for the aggregation period of 1 hour and 24 hours, respectively, are shown.

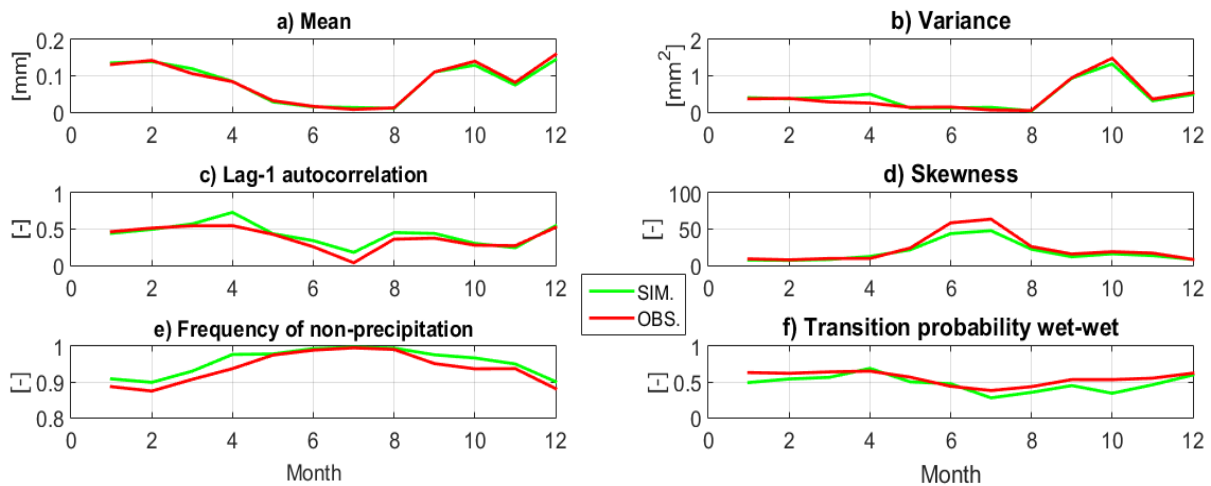


Figure 3.10. A comparison between observed (red) and simulated (green) monthly statistics of precipitation (mean, variance, lag-1 autocorrelation, skewness, frequency of non precipitation, transition probability wet-wet), for the aggregation period of 1 hour.

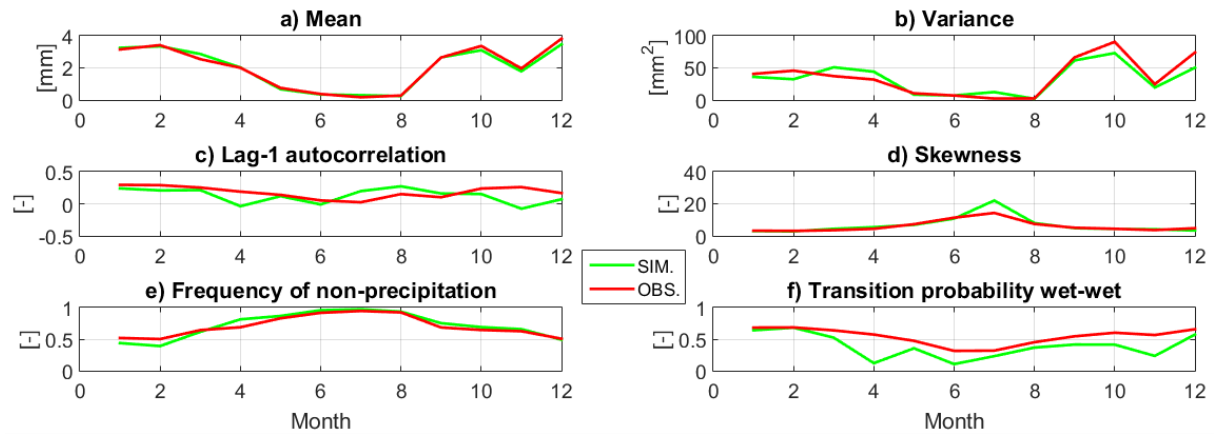


Figure 3.11. A comparison between observed (red) and simulated (green) monthly statistics of precipitation (mean, variance, lag-1 autocorrelation, skewness, frequency of non precipitation, transition probability wet-wet), for the aggregation period of 24 hours.

Even these analysis show that there is a correspondence between the two datasets and, even if statistics related to the aggregated period of 1 hour are better than those of aggregated period of 24 hours, it is still possible to state that results are good in order to the aim of this dissertation.

Moreover, fractions of time with precipitation larger than 1mm, 10mm and 20mm at different aggregation periods can be studied as shown in *Figure 3. 14*.

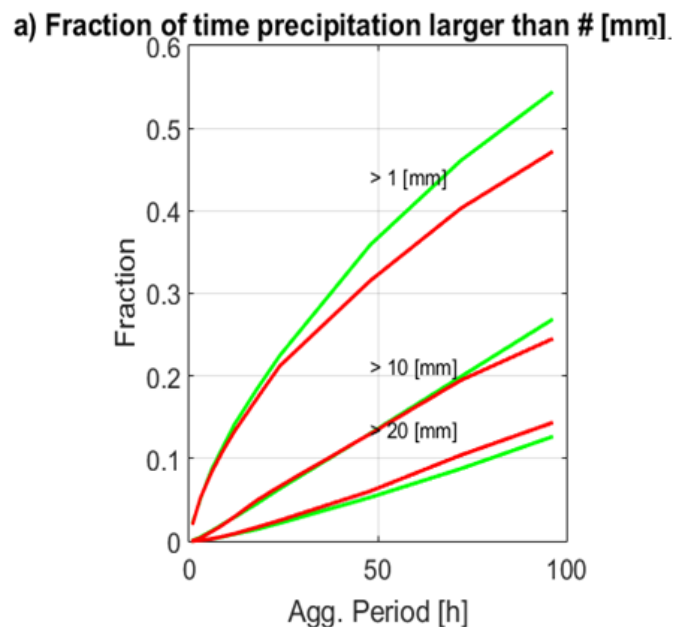


Figure 3. 12. a) A comparison between observed (red) and simulated (green) fractions of time with precipitation larger than a given threshold [1–10–20mm] at different aggregation periods.

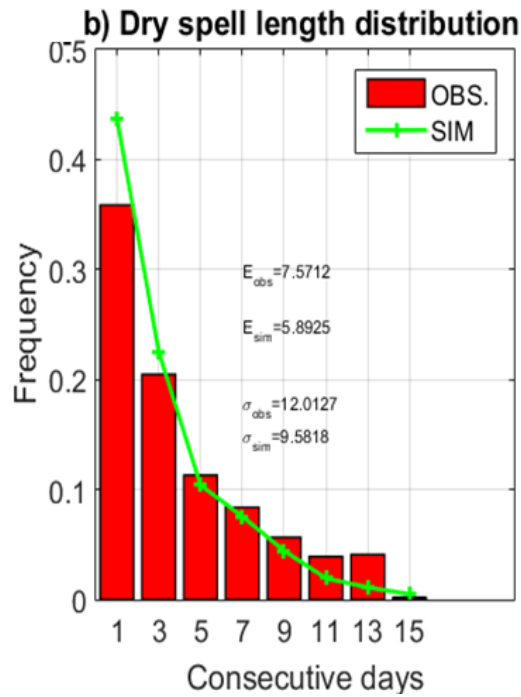


Figure 3. 13. b) The same comparison for dry spell length distribution, i.e. consecutive days with precipitation depth lower than 1 [mm]. E_{obs} and σ_{obs} are the observed mean and standard deviation and E_{sim} and σ_{sim} are the simulated ones.

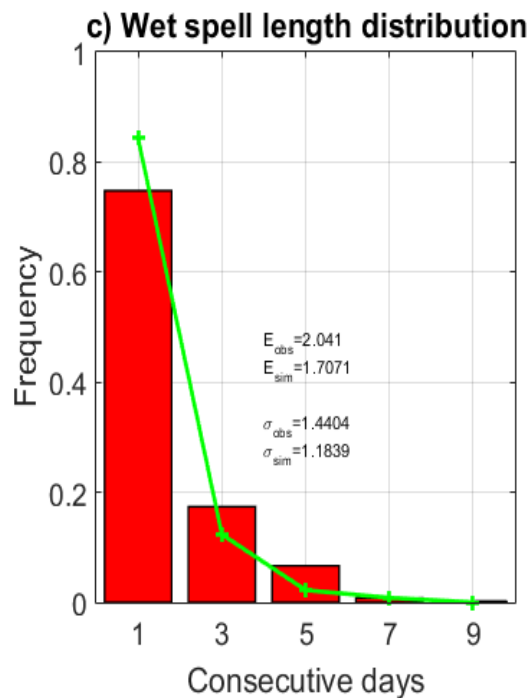


Figure 3. 14. c) The same comparison for wet spell length distribution, i.e. consecutive days with precipitation depth larger than 1 [mm]. E_{obs} and σ_{obs} are the observed mean and standard deviation and E_{sim} and σ_{sim} are the simulated ones.

Figure 3. 14 shows that the better comparison is related to the fractions of time with precipitation larger than 10 mm, while the worst is related to the one larger than 1mm. Also, the plot about dry spell length distribution shows that the mean coming from the observed data is about 7.5 while it is about 5.9 from the simulated and standard deviation is respectively about 12 and 9.6. These values can still be a sign of good generations by a model that well simulated observed data. Regarding the wet spell length distribution, mean and standard deviation are respectively about 2 and 1.4 for the observed data and about 1.7 and 1.2 for the simulated series. Even extremes of precipitation are been respected by the simulated generations as shown in

Figure 3. 15 where it is possible to notice that, except that some values, simulated rainfalls well reproduce highest extremes of observed data.

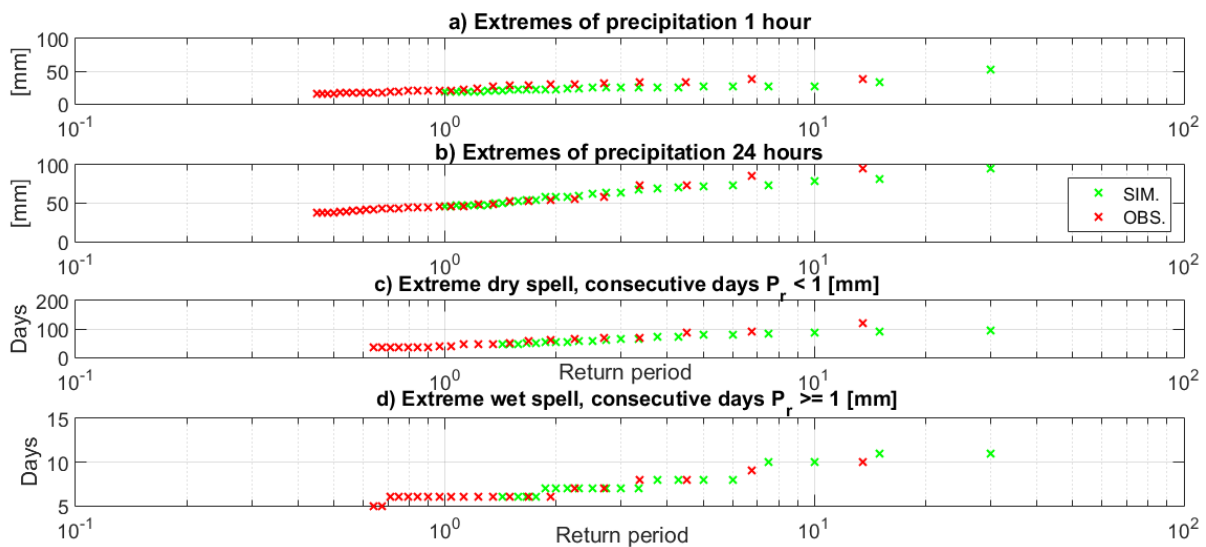


Figure 3. 15. A comparison between the observed (red crosses) and simulated values of extreme precipitation (green crosses) at (a) 1-hour and (b) 24-hour aggregation periods; (c) extremes of dry and (d) wet spell durations. Dry/wet spell duration is the number of consecutive days with precipitation depth lower/larger than 1 [mm].

Chapter 4

Implementation, results and considerations

Over the past century, cities have become increasingly urban societies. The changes in land use associated with urban development affect flooding in many ways. Removing vegetation and soil, grading the land surface, and constructing drainage networks increase runoff to streams from rainfall and snowmelt.

Rainfall in urban areas is typically more problematic than in rural areas, because of impervious surfaces such as roofs, parking lots and roads. These collect the flow and direct it into the urban drainage system, causing rapid runoff and higher peak flows.

The aim of this dissertation is to study effects of CC on the sewer system of Palermo. Studying GCMs and using a weather generator it is possible to simulate rainfall that will affect Palermo in the future. These precipitations will be transformed in runoff by a stormwater manager model (Epa Swmm 5.0) and floods are calculated above each manhole. This chapter wants to show both the procedure that has been used to achieve results and analysis of main outcomes.

In detail, synthetic series are generated to simulate the *Current* climate and for modeling future climate conditions, according to climate change: section 4.1 describes and shows series

generated by the weather generator AWE-GEN. These series are at hourly scale and need to be disaggregated by a downscaling model because in urban catchment, where concentration times are often short, the shape, timing and peak flow of hydrographs are significantly influenced by the time resolution of the rainfall: it has been proved that a too coarse temporal resolution of rainfall data causes a systematic underestimation of peak runoff (Gujer and Krejci, 1988). The temporal resolution of the recorded rain data is often lower than the data needed for rainfall– runoff simulations; if the rainfall time series with low resolution are sufficiently long for statistical analyses, different disaggregation procedures may be developed to generate high-resolution rainfall time series and section 4.2 illustrates application and results of Random Cascade Model. Then, the series are at 15-minutes scale and are applied into Epa Swmm 5.0 as input and, by that, the sewer system behavior and overflows may be investigated under *Current* and future climate, as discussed in section 4.3.

4.1. Applications of AWE-GEN: *Future runs*, weather forcing

Downscaling of GCM-based data is a key aspect in climatologically driven hydrological simulations (e.g., Wilby and Wigley, 1997; Fowler et al., 2007; Chen et al., 2011), since the GCMs typically have a temporal (e.g., daily or even monthly) and spatial (e.g., from 100 to 300 km) resolution inadequate to represent hydrological processes at scales smaller than the continental scale. In this study, different climatic scenarios are generated by the hourly Advanced WEather GENerator, AWE-GEN, (Ivanov et al., 2007; Fatichi et al., 2011) based on a stochastic downscaling of an ensemble of GCMs realizations (Fatichi et al., 2011, 2013). More specifically, for generating the *future runs* climate, realizations from a subset of 32 GCMs by the IPCC-5AR (Moss et al., 2010; IPCC, 2013) have been considered. The IPCC-AR5 analyzed four greenhouse gas concentration trajectories (i.e., Representative Concentration Pathways: RCP 2.6, RCP 4.5, RCP 6, and RCP 8.5), corresponding to four possible hypotheses about the rise of greenhouse gas emission in the years to come. The four RCPs are related to the possible radiative values increase in the year 2100 with respect to the pre-industrial values (+2.6, +4.5, +6.0, and +8.5 W/m², respectively). The GCM realizations corresponding to the most “pessimistic”, i.e. RCP 8.5, IPCC-AR5 scenarios have been here considered.

The adopted method requires a control period, usually representative of the present climate, for which both meteorological observations and climate model simulations are available. To this aim, a *Baseline* scenario for the basin, representative of the *Current* conditions, has been opportunely generated by the AWE-GEN starting from hourly data from 2002 to 2014 derived by the Palermo Uditore SIAS meteorological station (see Section 3.5.1).

On the total, three climate scenarios, including 50 stationary 20 years long time series of rainfall, temperature, solar radiation, relative humidity and wind speed, have been created and investigated for the basin: namely the *Baseline (Current scenario)* and two climate projections for the RCP 8.5, based on GCM projections over the periods 2045–2065 (*2050 scenario*) and 2081–2100 (*2100 scenario*), respectively.

Regarding the Mediterranean areas, previous studies have found an annual decreases in precipitation (Cannarozzo et al., 2006): eastern part (Amanatidis et al., 1993 and Kutiel et al., 1996), central part (Giuffrida and Conte, 1989 and Piervitali et al., 1998) and western part (Esteban-Parra et al., 1998 and De Luis et al., 2000). Different previous studies analyzed trend of hydrological variables for the island of Sicily (Italy—Southern-center of Mediterranean sea). Among these Cannarozzo (1985) found a generalized decrease of annual rainfall while a decreasing trend has been detected for some rain gauges around Palermo area (Aronica et al., 2002). Bonaccorso et al. (2005) analyzed the trends in annual maximum rainfall series finding different behaviors according to the different time scale. In particular for shorter durations the rainfall series generally exhibit increasing trends while for longer duration more and more series exhibit decreasing trends. Following analysis focus on rainfall, neglecting others variables.

As stated, each scenario is composed of 50 series and each series is 20 years long. Data included in each series are hourly precipitation depth in mm.

It is possible to calculate the average of annual precipitation depth for each year and, averaging along each series, to obtain fifty series representing the average of the annual precipitation. Using this procedure for each scenario and plotting results, as shown in *Figure 4.1*, it is easy to notice that every scenario is fully discerned by others and that average of annual depths in *Current* generation are the highest while the ones in *2100* scenario are the lowest.

Figure 4.1 shows values of average of annual depth precipitation for each series and each scenarios. The *Current* scenario is represented by the blue dashed line and average of all these 50 values is 728 mm/y: this value is calculated as average of the annual average of the fifty series. The *2050* scenario is represented by the red dotted line and, following the same procedure explained before, it has an average value equal to 647 mm/y. Finally, the *2100* scenario is the black continuous line and its average annual depth is 559 mm/y.

Analysis prove a decreasing of the average values: *2050* and *2100* scenarios decrease of about 12% and 23% , respectively, as compared with *Current* scenario, in term of annual average precipitation depth.

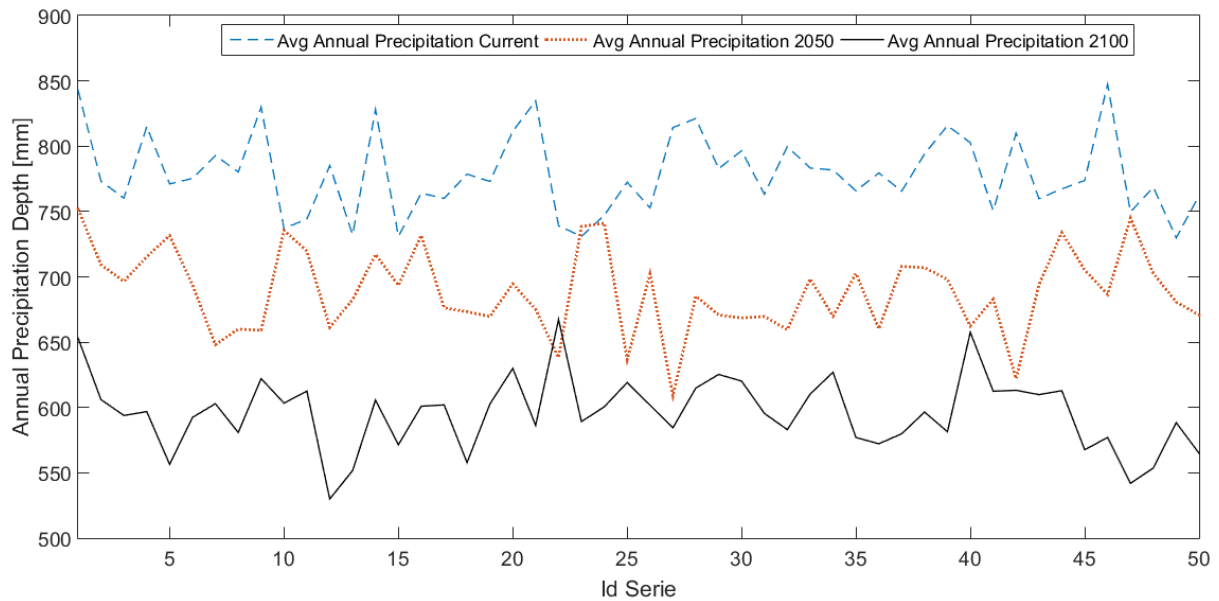


Figure 4.1. Average of annual precipitation calculated in 20 years for the three scenarios

Since the highest decreasing is in the precipitation relative to the 2100 scenario, this study is going to analyze the impact that rainfalls in 2100 scenario will probably cause on the drainage system of Palermo and the differences of these impacts from those caused by *Current* climate.

4.1.1. Simulation and selection Series

Synthetic precipitation series generated by AWE-GEN are hourly data and each scenario is composed by 50 generations. Analysis focuses on running in continuous the series that are 20 year-long. This means that investigating every series for each scenario would constitute a computational burden disproportionate to the aim of this dissertation and, for this reason, selection becomes a central issue of the study.

Many papers explain which are eligibility criteria in a decision process: some of them are easy and others are complicated, but none of those has been used for goals similar to this thesis. In this context, to be able to estimate climate change effects on urban drainage system and, consequently, floods that occur in an urban area during future conditions, series are analyzed and chosen by calculating their annual maximum hourly depths.

In details, in each series, annual maximum hourly depth is calculated and the average of these maxima are evaluated along the 20 year long. Each scenario has fifty values that represent the average values of the maximum annual depth in every series and outcomes are plotted in *Figure 4.2* and *Figure 4.3*.

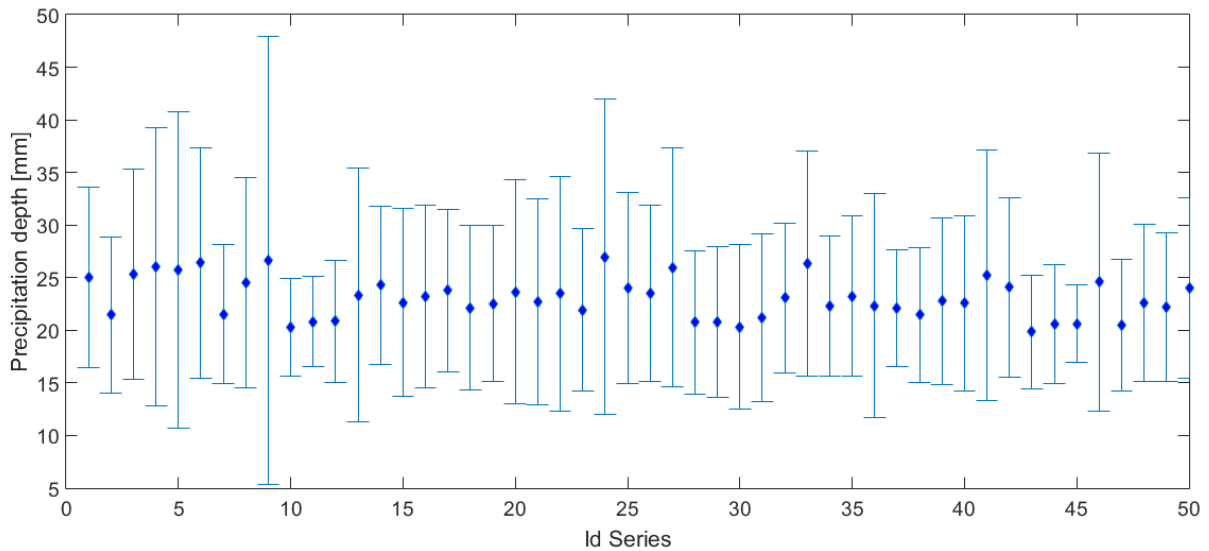


Figure 4.2. Average of the annual maximum for each 20-year long series (blue dots) and variability in terms of standard deviation of the maxima (blue bars) for *Current* scenario.

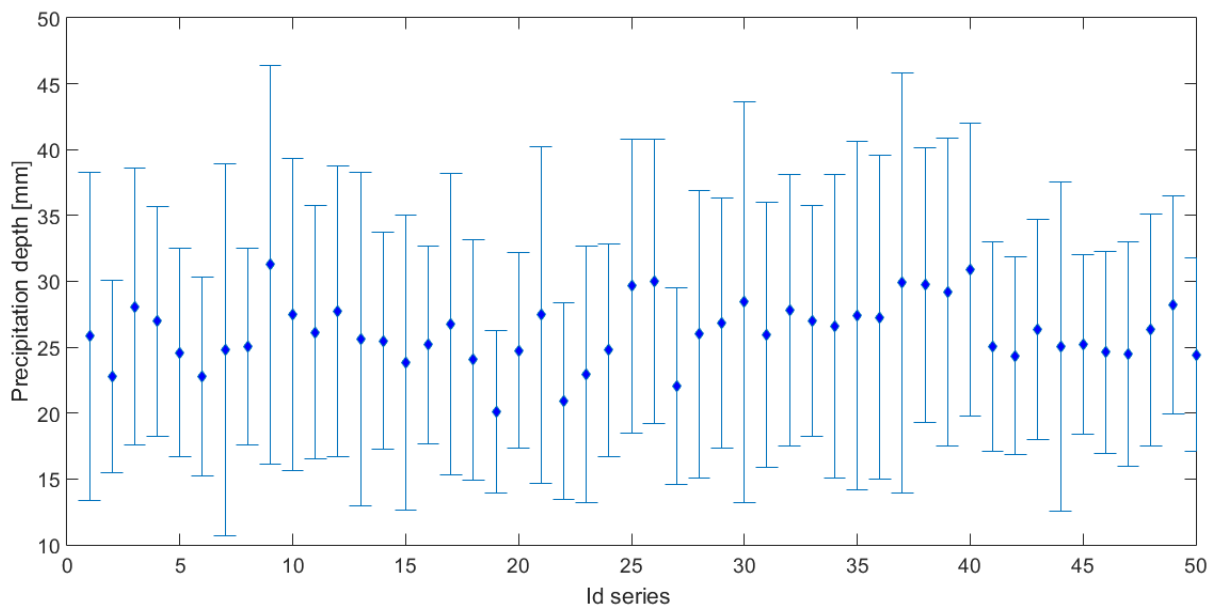


Figure 4.3. Average of the annual maximum for each 20-year long series (blue dots) and variability in terms of standard deviation of the maxima (blue bars) for *2100* scenario.

Figure 4.2 and *Figure 4.3* point out that variability in terms of standard deviation around average of maxima values is higher in 2100 scenario.

Characterizing each series by the annual maximum hourly depth calculated along the 20 years, percentiles are estimated for each scenario. We decide to chose those series for which the annual maximum hourly depth represents the 95° percentiles of the fifty series, as harder situation, and 50° percentile, as median case. It is possible in this way to select four series, 2 for each scenarios.

Plotting hourly precipitation depth along 20 years, *Figure 4.4* and *Figure 4.5* are obtained: in those red dots represent *Current* scenario and blue lines are *2100* scenario. These series are directly provided by AWE-GEN. Looking at those plots, it is clear that median precipitation depths show peaks that are, in general, smaller than those from 95° percentile series, and, in both cases, it is possible to state that peaks of the future (*2100*) are higher than the *Current* scenario.

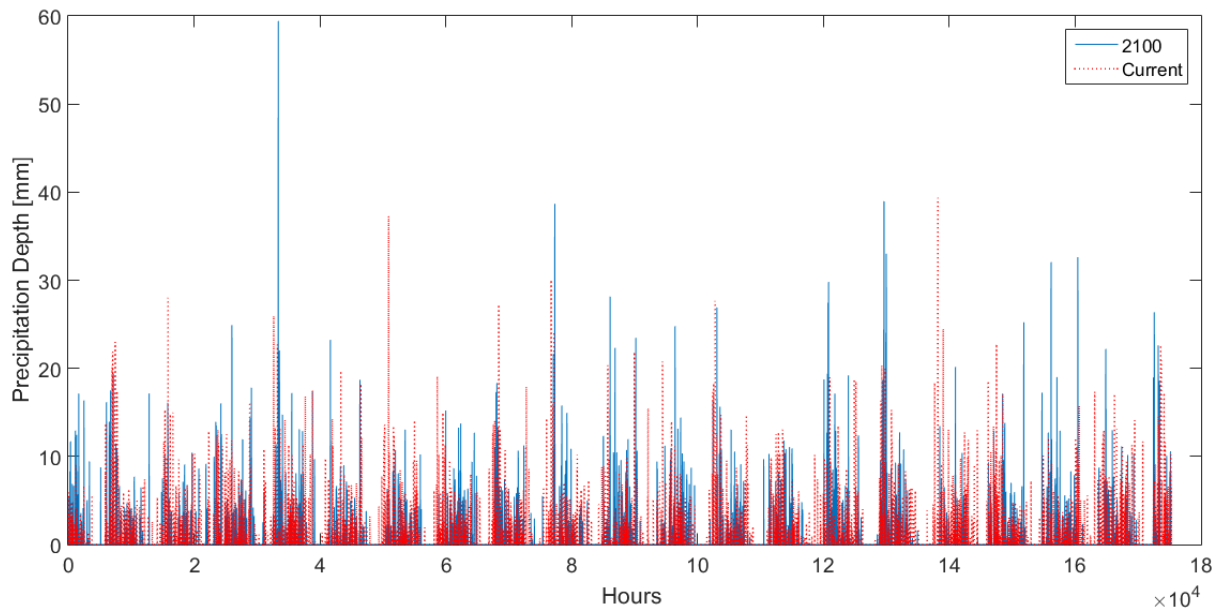


Figure 4.4. Median series for *Current* and *2100* scenarios: 20-year hourly rainfall depth for *2100* (blue line) and *Current* scenarios (red dots).

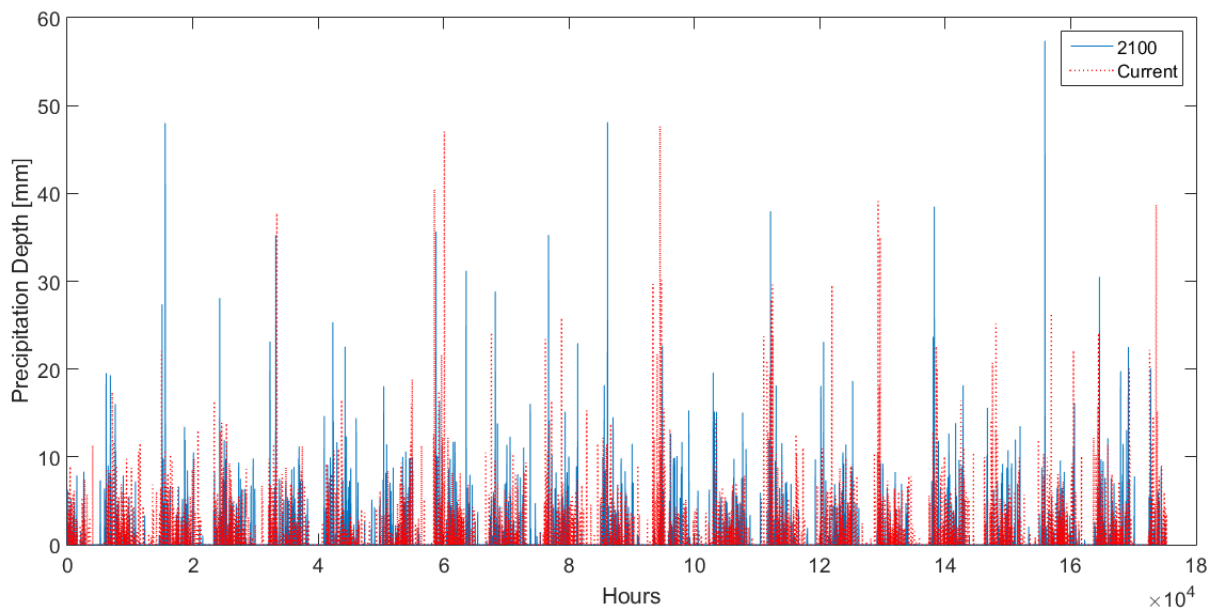


Figure 4.5. 95° Percentile series for *Current* and *2100* scenarios: 20-year hourly rainfall depth for *2100* (blue line) and *Current* scenarios (red dots).

In order to better understand the differences between those series of different scenarios, the analysis of the empirical cumulative distribution functions can be useful. *Figure 4.6* shows *ecdfs* for both percentiles in both scenarios.

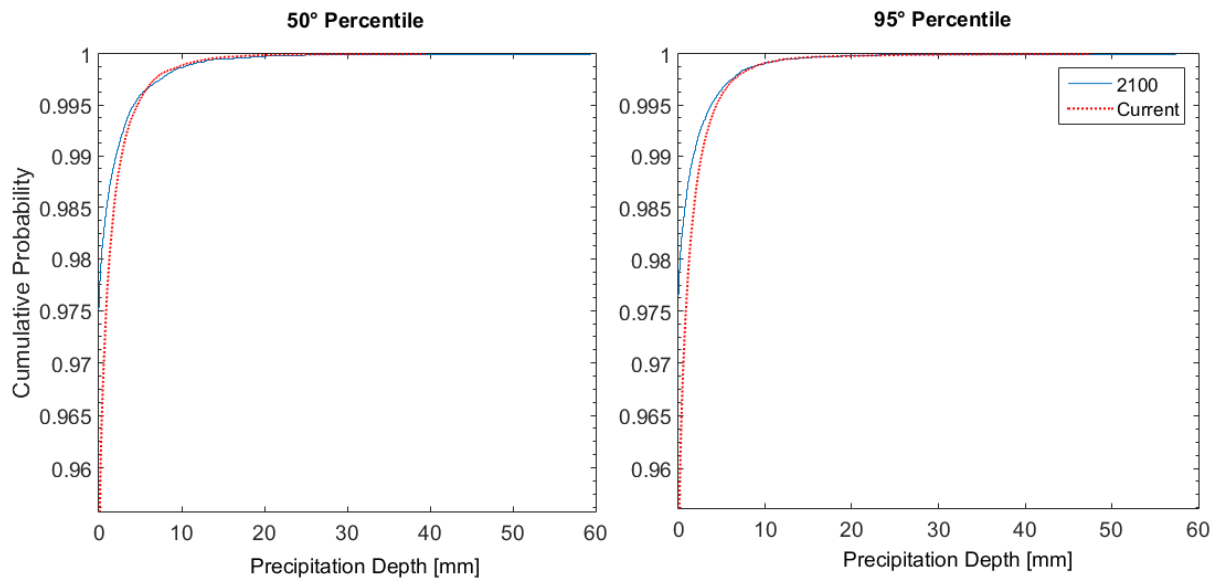


Figure 4.6. Empirical cumulative distribution functions for *2100* (blue line) and *Current* (red dots) scenarios classified by percentile.

By *Figure 4.6*, for the same cumulative probability the *2100* scenario show a lower precipitation depth in mm in both percentiles, up to very high probability where the situation is the opposite.

Calculating the same *ecdfs* with the same data but without zero values, plots become *Figure 4.7* and *Figure 4.8*. In these plots, looking at the same cumulative probability, the precipitation depth in mm in *2100* scenario is higher than that in the *Current* scenario.

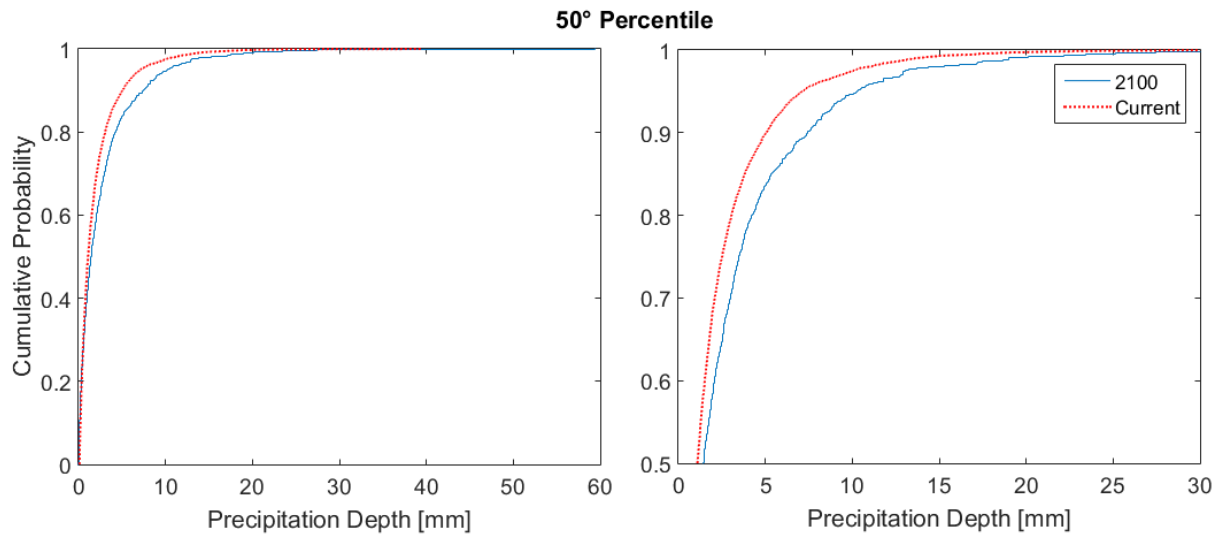


Figure 4.7. Empirical cumulative distribution functions of 50° percentile series for 2100 (blue line) and *Current* (red dots) scenarios considering only values >0 .

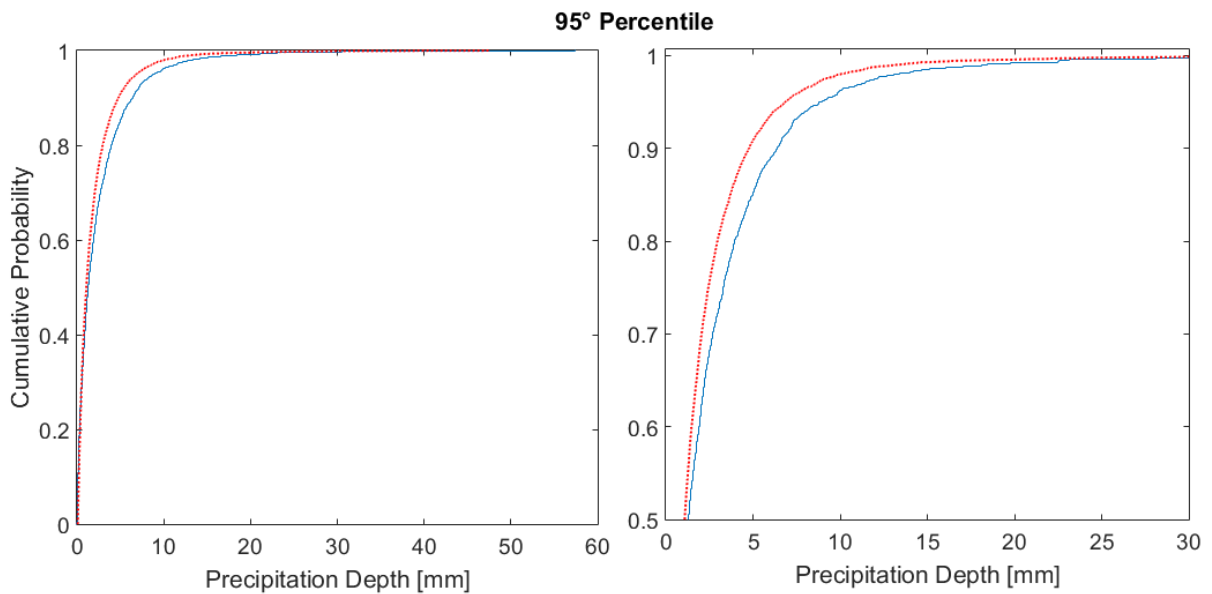


Figure 4.8. Empirical cumulative distribution functions of 95° percentile series for 2100 (blue line) and *Current* (red dots) scenarios considering only values >0 .

The differences between *Figure 4.6* and *Figure 4.7* (or *Figure 4.8*) are caused by the number of wet and dry time -steps: it proves that *Current* climate is wetter than the future one, in terms of number of time-steps.

Therefore, defining *Rainy* days as sequence of 24 hourly values whose sum is larger than zero and *dry* days the others, it is crucial to calculate the number of *dry* and *rainy* days in the 50° (*Figure 4.9*) and 95° percentile (*Figure 4.10*) series.

In details, regarding 50° percentile series, *Figure 4.9* shows that the percentage of number of rainy days in the 2100 scenario is 19% and this value is lower than the same in the *Current* scenario (28%).

In details, *Figure 4.9* shows that the percentage of number of rainy days in the 2100 scenario is 19% and this value is lower than the same in the *Current* scenario (28%). This comparison of the 50° percentile series proves that future climate is going to be drier than the *Current* one.

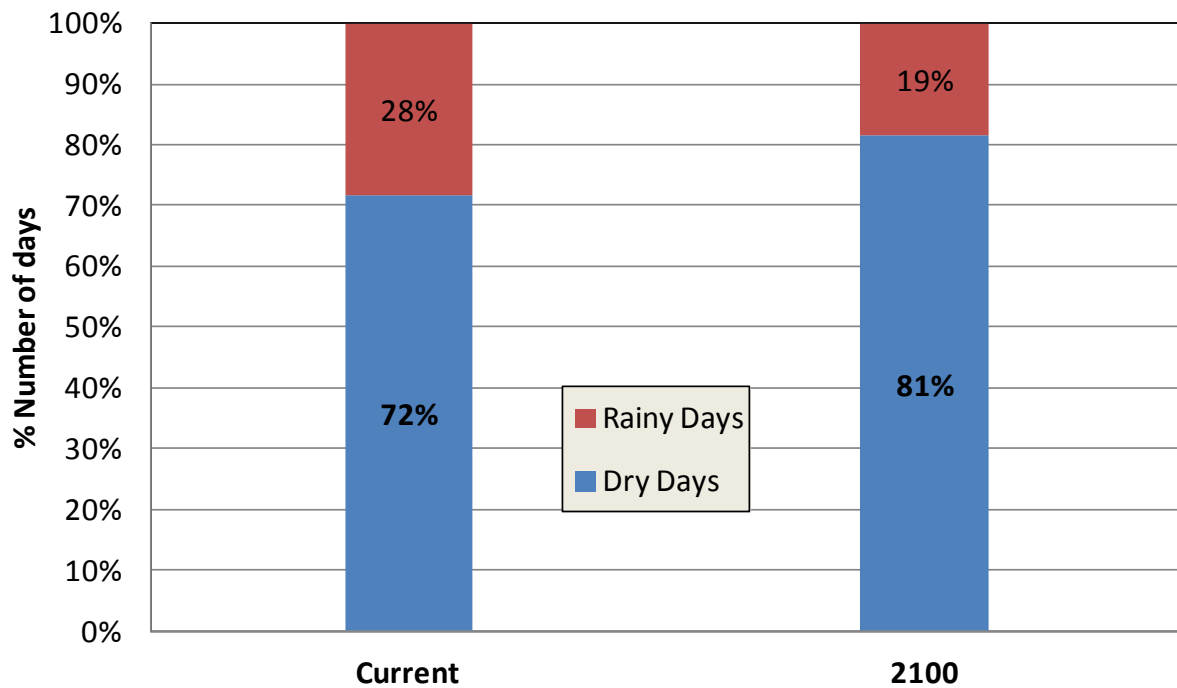


Figure 4.9. Number of dry and rainy days in median series of *Current* and 2100 scenarios.

Figure 4.10, that plots information coming from 95° percentile series, shows that, even in this circumstance, future scenario has a percentage of rainy days (18%) that is lower than that coming from *Current* scenario (27%). Both these values, referred to 95° percentile, are lower than the same in 50° percentile.

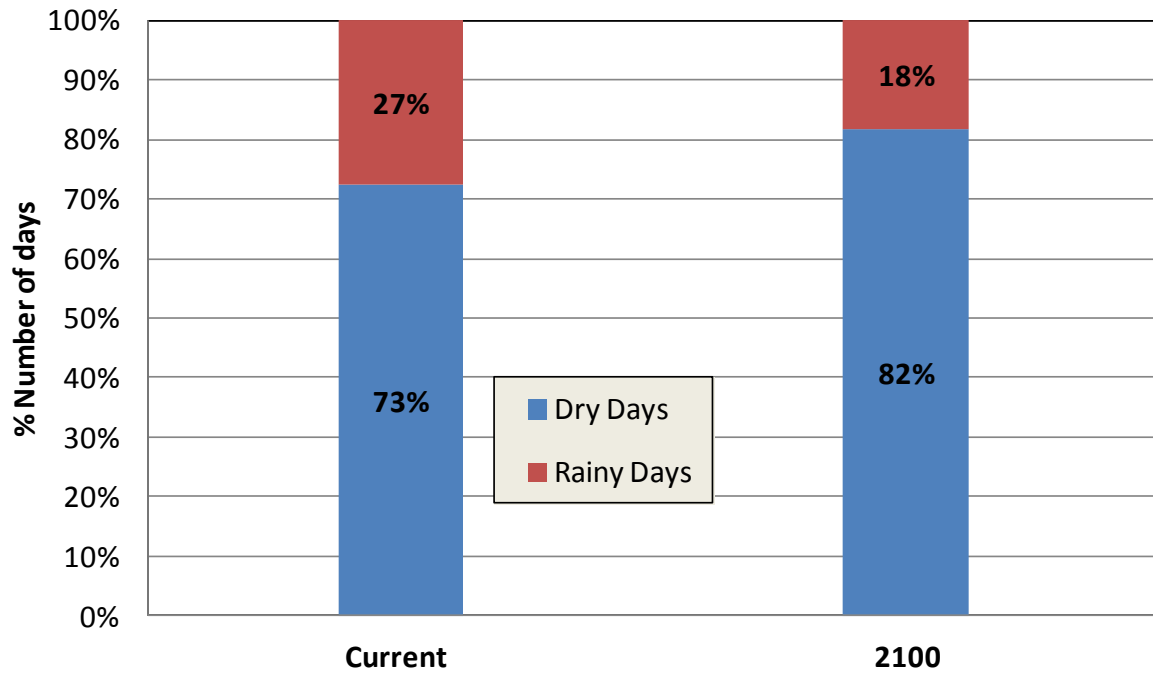


Figure 4.10. Number of dry and rainy days in 95° Percentile series of *Current* and *2100* scenarios.

It is possible to study the average of maximum intensities [mm/hr] along each series, in which the maximum intensities are calculated as maximum hourly value in the series 20-year long, and plotting this information outcomes can be shown (*Figure 4.11*).

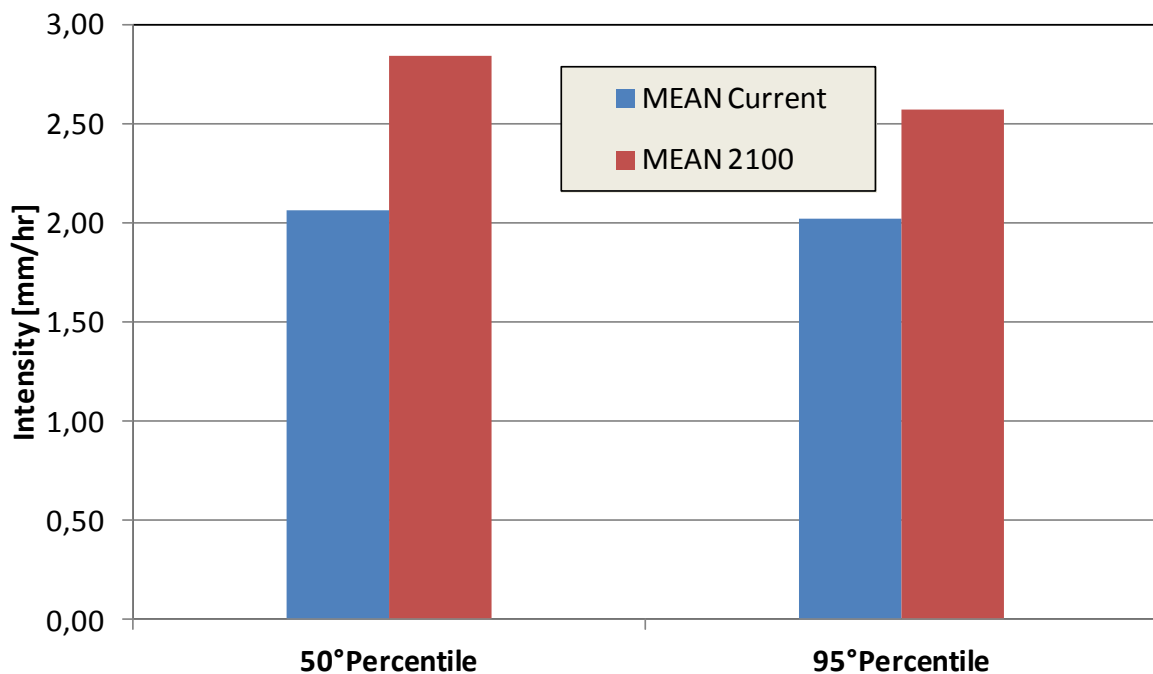


Figure 4.11. Mean intensities of rainy days for each series for both *Current* (blue bars) and *2100* (red bars) scenarios.

Figure 4.11 shows that in both percentiles the higher value of average of maxima intensities [mm/hr] is related to the 2100 scenario.

4.2. Downscaling by Cascade Model

General effect of urbanization on the hydrological characteristics of a catchment is to reduce the amount of infiltration into the ground and to increase the runoff velocity. If the temporal resolution of rainfall data is too coarse systematic underestimation of peak runoff are expected (Gujer and Krejci, 1988). The lag time between precipitation peak and discharge peak can be reduced by a factor of up to 8 in urban areas (Wohl, 2000). The effect of urbanization on the overall response of a catchment tends to be greater for small, frequent floods rather than more extreme events. It is also commonly assumed that rainfall loss in urban areas are less than those from adjacent rural areas because of the lower infiltration. For all these reasons, temporal resolution of input data should be fine enough to study an urban catchment like Palermo center and to obtain good results.

As stated, the four chosen series that come from AWE-GEN are represented at hourly scale. In order to increase the time resolution of these series, this study apply a *Random Cascade Model* that, as explained in section 2.3, is able to go from hourly to sub-hourly time step; in detail, this method is able to break each hourly data in four 15-minute time step data.

To be sure that this model can be useful for the aim of this dissertation, it is important to verify how it works and how acceptable its outcomes can be, but, since the finest resolution of generated series is at hourly scale, it is not possible to prove this model on these series.

Data from weather station are available at time step suitable to use Cascade model that can be applied to downscale series, once aggregated. Statistics from downscaling are compared to those resulting from aggregated dataset to make sure that, during the downscaling process, characteristics of precipitation are preserved.

In detail, observed rainfall depths, coming from SIAS (see section 3.5 for more details), are high resolution data and their time step is equal to 10-minute. First of all, to apply the random cascade model, observed dataset is aggregated at 30-minute scale and then in hourly data as shown in *Figure 4. 12*.

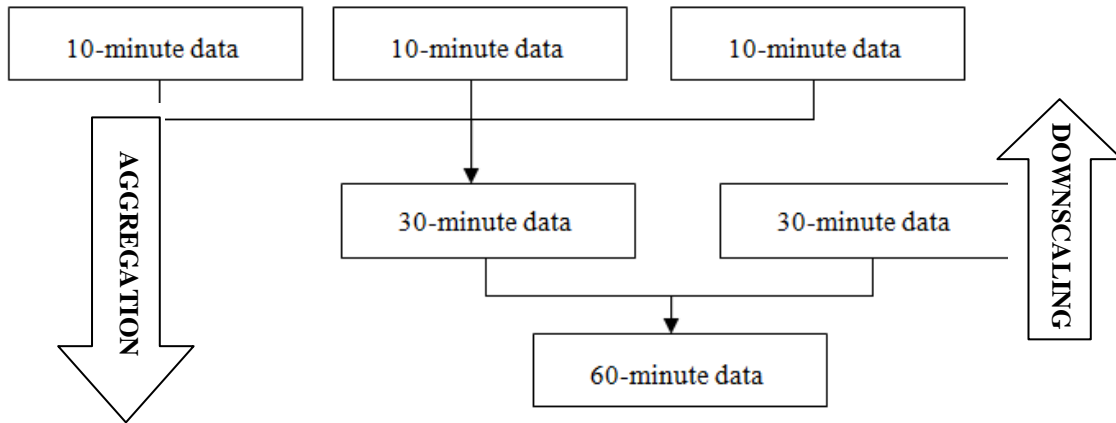


Figure 4. 12. Scheme of aggregation data from 10-minute to 1-hour time step.

Obtaining 1-hour time step data, it has been possible to apply random cascade model to downscale time series from hourly to 30-minute scale.

Now on, in order to compare results at the 30-minute time step, and to clarify following analysis, *observed* refers to 30-minute data coming from aggregation, *downscaled* alludes to 30-minute data coming from downscaling by random cascade approach.

To study how model works, it is essential to compare statistic indexes in these two datasets. Neglecting explanation about sum and mean that must be the same in both datasets for definition, standard deviation (*St.Dev.*), coefficient of variation (*CV*), Skewness, Kurtosis and percentage of number of wet time steps coming from the *observed* dataset can be compared to the ones coming from *downscaled* data as shown in *Table 4.1*.

By this comparison, it is possible to note that this model is able to well maintain characteristics of the dataset downscaled by this procedure because indexes of outcomes are very close to the same indexes of the *observed* dataset.

This verification allows to use random cascade model for the four chosen time series, needed to analyze impact on the urban drainage system of Palermo.

Table 4.1. Comparison of statistic indexes between observed and downscaled datasets

	Observed	Downscaled
Sum [mm]	9480	9480
Mean [mm]	0,0416	0,0416
St.Dev [mm]	0,367	0,375
CV[-]	8,819	9,019
Skewness [-]	26,228	26,800
Kurtosis [-]	1226,080	1255,064
Wet timesteps [%]	6,045	4,319

In order to show effects of downscaling during 10 days, *Figure 4.13* and *Figure 4.14* present rainfall intensity [mm/hr] for the dataset with 1 hour time step and the same period of the same variable coming from disaggregating model with time step equal to 15 minutes, respectively.

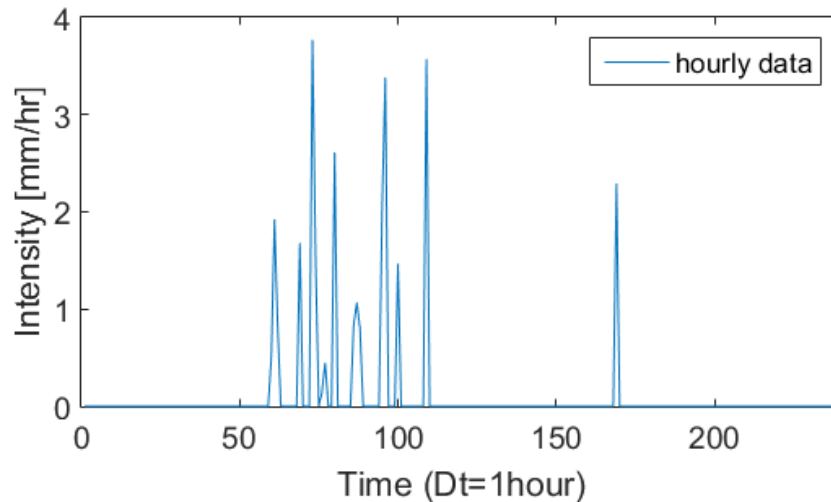


Figure 4.13. Hourly rainfall intensity of 10 days with time step equal to 1 hour.

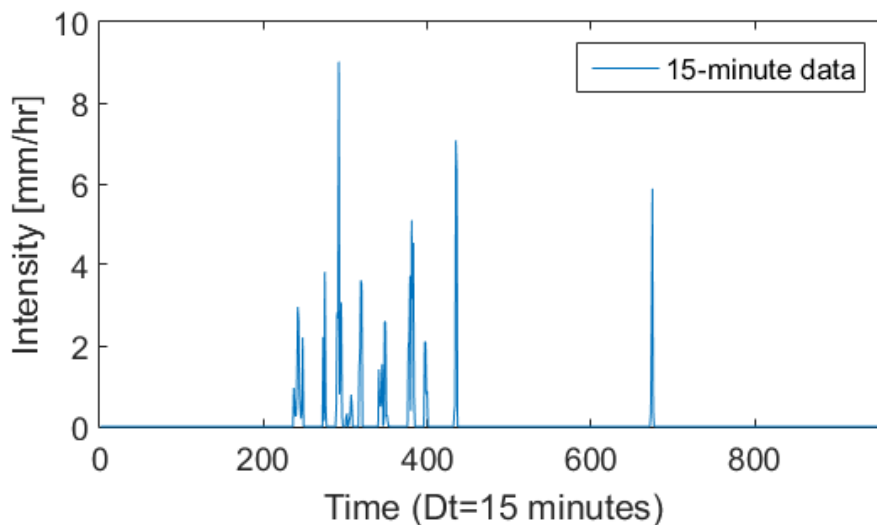


Figure 4.14. Hourly rainfall intensity of 10 days with time step equal to 15 minutes.

Comparison between *Figure 4.13* and *Figure 4.14* proves that this approach is able to respect the shape of the event and characteristics of the precipitation because from the *Figure 4.13* it is possible to understand the likeness with the *Figure 4.14*. Intensities in the series at 15-minute scale are about 2.5 times higher than those from series at hourly time step. Looking at the ten days plotted at hourly scale, maximum intensity is about 3.8 mm/h, while the same series at 15-minutes time steps shows that the highest intensity is about 9.1 mm/h. The

intensity related to the last peak in the plots is equal to 2.3 mm/h for the series at hourly scale and it is about 6 mm/h for that at 15-minute scale.

These higher resolution time series will be used as meteoric forcing for the storm water manager model (Epa Swmm 5.0) and derived floods will be studied.

4.3. Impacts analysis

Floods can influence many aspects of human life due to their destructive effects and create significant expenses on mitigation efforts. Heavy rains and urban development have led to the increasing in the frequency of flood, that is caused by: the accumulative impervious areas, the reducing of the flow capacity by the canals silting, the infrastructure deficit of micro and macro drainage facilities that are undersized to the *Current* demands (Tucci and Collischonn, 2000).

The classification of damages in floods, *flash floods* and *overflow* is not simple. Urban *flash floods* are flood events which cause damages in small catchment areas of less than 100 km² (and even less than 10 km²) and are caused by small-scale rain events with volumes that far exceed the rainfall predictions and considerations originally factored into the design of local hydrological structures.

Flash floods, especially in urban areas, may contain hazardous materials, broken electric lines, sewage, etc. Explosions and fires during flash floods are not uncommon. In urban areas, the impacts caused by floods can be very high because the areas affected are densely populated and contain vital infrastructure.

The runoff generate by *overflow* starts as overland flow on the street before entering the underground pipe system through manholes.

If the intake capacity of the drainage system is limited, only a fraction of the water can flow into the pipes and a large runoff volume will be transported on the surface during and after a heavy rainfall (Mark et al., 2004). This may happen even if the underground pipe system has sufficient capacity, see *Figure 4.15*.

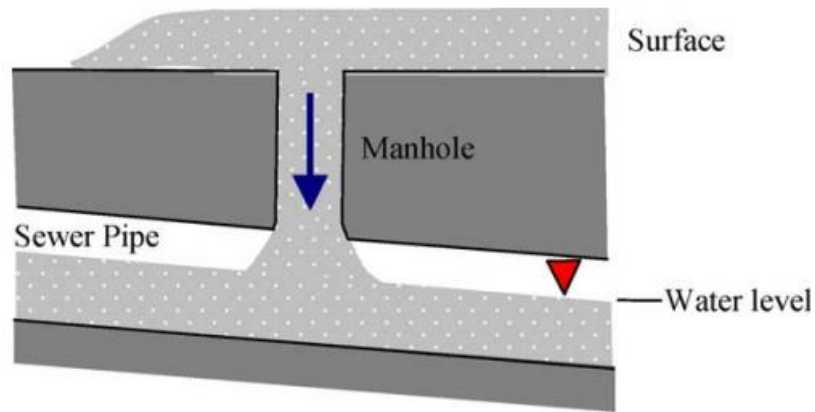


Figure 4.15. Flow from the street system into a partly full pipe (Mark et al., 2004).

The water in the pipe system may return to the street system if the capacity of the pipe system is insufficient. In this case the water will flow from the pipe system to the street system, causing surface flooding, see *Figure 4.16*.

The duration of flooding on the street depends on the intake capacity of the catch pits, the drainage capacity of the pipe system, infiltration and evaporation in the catchment area.

Even if, in this modeling approach, the urban drainage system consists of two networks, one representing the free surface flow in the streets and one for the pipe network, the modeling proposal of this study is to use a 1D model to flow routing along the underground drainage features (pipe networks). The hydrodynamic model is based on an implicit solution of the St Venant equations. Manholes (network nodes) function as points where water from the street can enter the pipe system and vice versa.

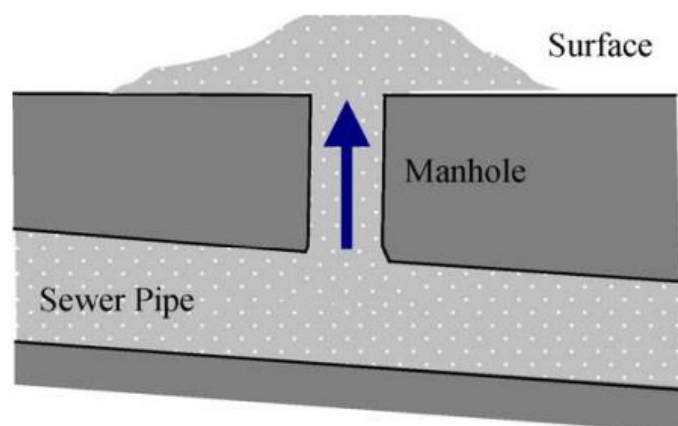


Figure 4.16. Flow to the streets from a pipe system with insufficient capacity (Mark et al., 2004).

Therefore, this dissertation neglects runoff due to the direct pathway of the water on the street and analyzes only floods caused by *overflows*. These are linked to the drainage system deficit and correspond to a momentary accumulation of water in urban area.

Defining *critical points* of the drainage system those where water comes out from manholes, in this study we consider only floods on the street and in the city originated by *critical points* and we ignore velocity of the runoff and propagation of floods on the streets.

Overall, aim of this dissertation is to analyze impacts that CC causes on the drainage system of Palermo, namely if, in future, rainfalls will put the drainage system through the wringer, causing more floods or higher flooding depths than the *Current* climate. To figure out what will be going on, it is important to solve two issues :

- I. Distribution of *critical points* of the drainage system of Palermo caused by future climate may be different from the one caused by the *Current* precipitation: are these differences going to be remarkable, in terms of number of failing manholes?
- II. Looking at the *critical points* that fail in both scenarios, are floods going to be more frequent in the future than in the *Current* conditions, or *vice versa*?

With today's advances in computer technology, many cities in the developed part of the world manage local and minor flooding problems using computer-based solutions. This involves building computer models of the drainage/sewer system, for instance by using software like MOUSE (Lindberg et al., 1989); InfoWorks (Bouteligier et al., 2001) and the SWMM models (EPA SWMM, MIKE SWMM, and XP SWMM), (Huber and Dickinson, 1988). These types of models are used to understand the frequently complex interactions between rainfall and flooding. Once the existing conditions have been analyzed and understood, alleviation schemes can be evaluated and the optimal scheme implemented.

The chosen software for this dissertation is Epa Swmm 5.0. As explained in section 2.4, Epa Swmm allows to have the excess volume be stored above the junction, and be reintroduced into the system as capacity permits. Flow routing set in this study is the dynamic wave routing, which is influenced by the water depths maintained at nodes, while the excess volume is assumed to pond over the node with a constant surface area. This amount of surface area is an input parameter supplied for the junction and, for each node, it has been considered equal to the floodable area of the street above each manhole.

Defining *failure* as the deficit of the drainage system, namely when water overcomes the street level by the manhole under pressure, it is important to set thresholds that allow to distinguish flood in *ordinary* and *extraordinary* as shown in *Figure 4.17*: when water goes out

of the manhole, it is defined *ordinary* flood up to 1.5m above the street; if water exceed 1.5m above the head of the manhole, it is an *extraordinary* flood.

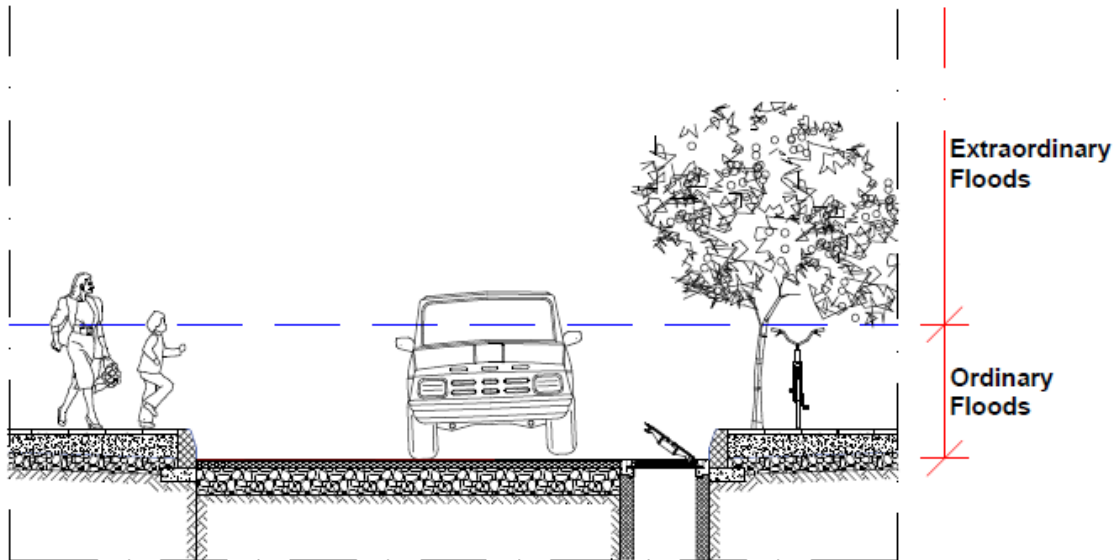


Figure 4.17. Example of environment in which floods might occur. The blue hatching is set at 1.5m above the manhole and this is the threshold for which floods can be differentiated in ordinary and extraordinary.

Uploading Palermo Centro storico drainage system into Epa Swmm 5.0, map area (*Figure 4.18*) creates a scheme including 833 nodes into 296 sub-catchments. Driving forces of this model are the 4 time-series 20-year long 15- minutes time step discussed early that are input into rain gage.

Epa Swmm allows the user to select different mathematical models to describe the runoff formation and propagation in pipe systems, and also different solving methodologies for the resulting equations, according to the peculiarities of the study case.

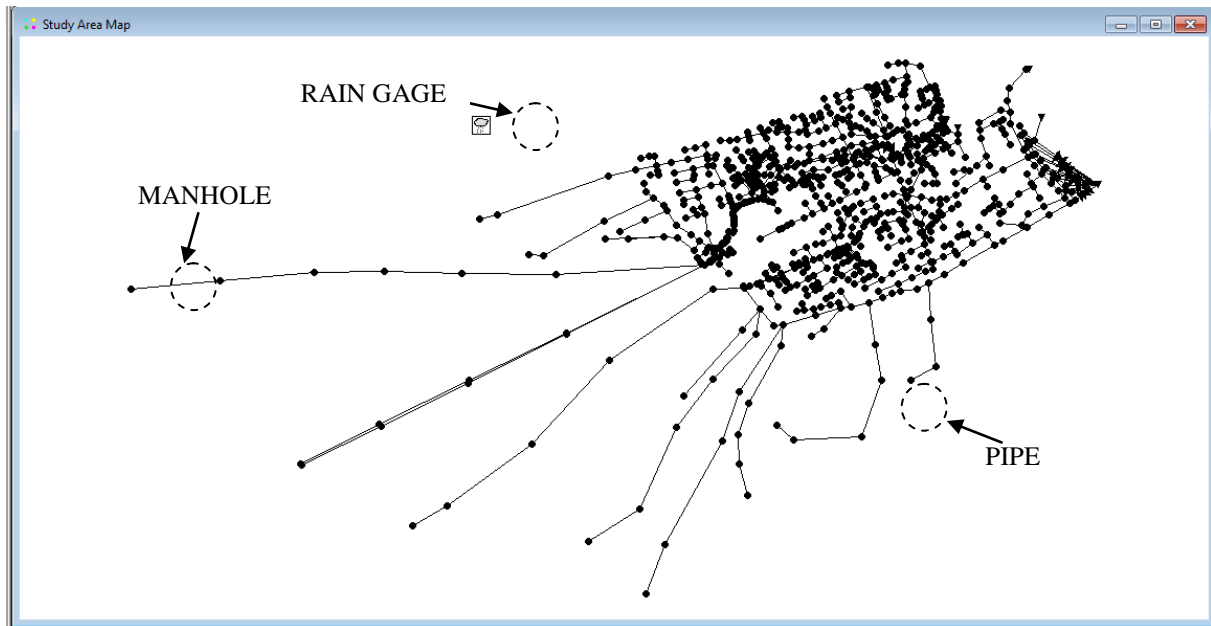


Figure 4.18. Palermo centro storico sewer system. Dots are manholes, links are pipes, and cloud is the rain gage.

For the purpose of this study, outputs of these simulations are four continuous 20-year rainfall with a routing time equal to 1 second and results from running two 50° percentile series are compared to each other, and the same procedure has been repeated for the two 95° percentile series.

In this context, simulations give several output, but analysis of this study focuses only on node flooding that is calculated with time step equal to the rainfall time series (15 minutes). In detail, defining *flood depth* as the water depth [m] measured above the manhole, it is possible to name *number of occurrence* as time step in which flood depth is higher than zero (threshold 1) or higher than 1.5m above the street (threshold 2), and *frequency* as the number of occurrences divided by the total number of time steps present in 20 years.

By this way, a table can be created to list, for each node, number of occurrences and frequencies, as shown in *Table 4.2*.

In this case, the drainage system under 50° percentile series will produce floods and maximum flood depth in '10.100' node does not rise the street level in 20 years for the *Current* scenario and it does 5 time steps for the 2100 scenario: in this case, frequency is equal to 0.0007%. In this node there is not any excess of the second threshold and it means that this node is not affected by extraordinary floods in *Current* or future climate.

Table 4.2. Extract of number of occurrences and frequencies for each node.

50° ID node	Number of Occurrence				FREQUENCY			
	h>street		h>street+1,5		h>street		h>street+1,5	
	Current	2100	Current	2100	Current	2100	Current	2100
'10.100'	0	5	0	0	0,0000%	0,0007%	0,0000%	0,0000%
'10.110'	0	11	0	0	0,0000%	0,0016%	0,0000%	0,0000%
'10.120'	0	8	0	0	0,0000%	0,0011%	0,0000%	0,0000%
'10.130'	0	12	0	0	0,0000%	0,0017%	0,0000%	0,0000%
10.140'	1	18	0	0	0,0001%	0,0026%	0,0000%	0,0000%
'10.150'	0	5	0	0	0,0000%	0,0007%	0,0000%	0,0000%
'10.170'	1	7	1	0	0,0001%	0,0010%	0,0001%	0,0000%
'10.180'	1	8	1	0	0,0001%	0,0011%	0,0001%	0,0000%
'10.190'	0	6	0	0	0,0000%	0,0009%	0,0000%	0,0000%
'10.200'	0	2	0	0	0,0000%	0,0003%	0,0000%	0,0000%
'10.290'	0	14	0	0	0,0000%	0,0020%	0,0000%	0,0000%
'10.300'	3	107	3	29	0,0004%	0,0153%	0,0004%	0,0041%
'10.310'	2	114	2	53	0,0003%	0,0163%	0,0003%	0,0076%
'10.320'	764	870	604	303	0,1089%	0,1241%	0,0861%	0,0432%
'10.330'	697	806	553	271	0,0994%	0,1149%	0,0789%	0,0386%
'11'	81	129	54	24	0,0116%	0,0184%	0,0077%	0,0034%
'50'	0	34	0	12	0,0000%	0,0048%	0,0000%	0,0017%
'50.060'	6	19	2	0	0,0009%	0,0027%	0,0003%	0,0000%
'50.070'	0	2	0	0	0,0000%	0,0003%	0,0000%	0,0000%

Reading information about '10.330' node, for example, it is possible to note that maximum flood depth is higher than zero during 697 time steps under the *Current* scenario and 806 under *2100* scenario and relative frequencies are 0.0994% and 0.1149%, respectively. Furthermore, under *Current* scenario, this node has 553 time steps in which maximum flood depth is higher than 1.5m (frequency 0.0798%) and it means that just 144 time steps (of the 697 recorded) report ordinary floods indicated by flood depths that are higher than zero and lower than 1.5m. Regarding *2100* scenario, '10.330' node reports 271 time steps exceeding threshold 2 and 553 time steps with depths ranging between zero and 1.5m.

Studying flood depth of nodes in this way, it is possible to produce two table, similar to the *Table 4.2*: one for comparison between the 50° percentile series (*Current* Vs. *2100*) and one for the 95° percentile series (*Current* Vs. *2100*).

By these tables it is possible to make one first remark about location and distribution of these *critical manholes* that flood creating other tables showing how many nodes flood in both scenarios and how many of them are in common in the two scenarios as shown in *Table 4.3* and *Table 4.4*.

Table 4.3. Summary of the flooded nodes for the median situation in both scenarios

Number of nodes	h>Street		h>Street+1,5		Street>h>1,5	
	Current	2100	Current	2100	Current	2100
#flooded nodes	94	214	83	86	11	128
#future flooded nodes merged with current ones	-	94	-	58	-	8

Table 4.4 Summary of the flooded nodes for the 95° percentile situation in both scenarios

Number of nodes	h>Street		h>Street+1,5		Street>h>1,5	
	Current	2100	Current	2100	Current	2100
#flooded nodes	172	180	54	53	118	127
#future flooded nodes merged with current ones	-	170	-	53	-	116

Table 4.3, that refers to the comparison between the two 50° percentile series, points out that there are 94 nodes in which water rises at least the street level, under the *Current* scenario, and 214 nodes for the *2100* scenario. Common nodes are 94 and it means that all the nodes that flood in *Current* scenario will flood also in the *2100* one. Among these 94 nodes, that flood in *Current* scenario, 83 manholes show exceeding threshold 2 and 11 nodes generate ordinary flood. Regarding the *2100* scenario, water overcomes threshold 2 in 86 nodes while 128 nodes show ordinary flood. Number of nodes in common in both scenarios are 58 with water depth higher than the threshold 2 and 8 that climb the street but their maximum flood depths do not rise 1.5m.

Table 4.4 is able to explain how the drainage system acts under 95° percentile series. This comparison shows that 172 nodes flood in the *Current* scenario: 170 of them are affected also by flood in the *2100* scenario. In detail, common nodes exceeding threshold 2 are 53 while 116 generate ordinary floods.

In order to answer to the first issue that questions about the distribution of *critical points* that, caused by future climate, may be different from those caused by the *Current* precipitation, maps are needed. These need to point out the differences about distribution of *failures* in the system.

Regarding *Current* scenario, Figure 4.19 shows location of nodes that are affected by floods caused by median series, and Figure 4.20 is the product of the *2100* scenario.

Looking at the two maps, the study proves that future rainfall will probably create a larger number of failures of the drainage system that will occur in parts of the city that are not affected by floods in the *Current* scenario.

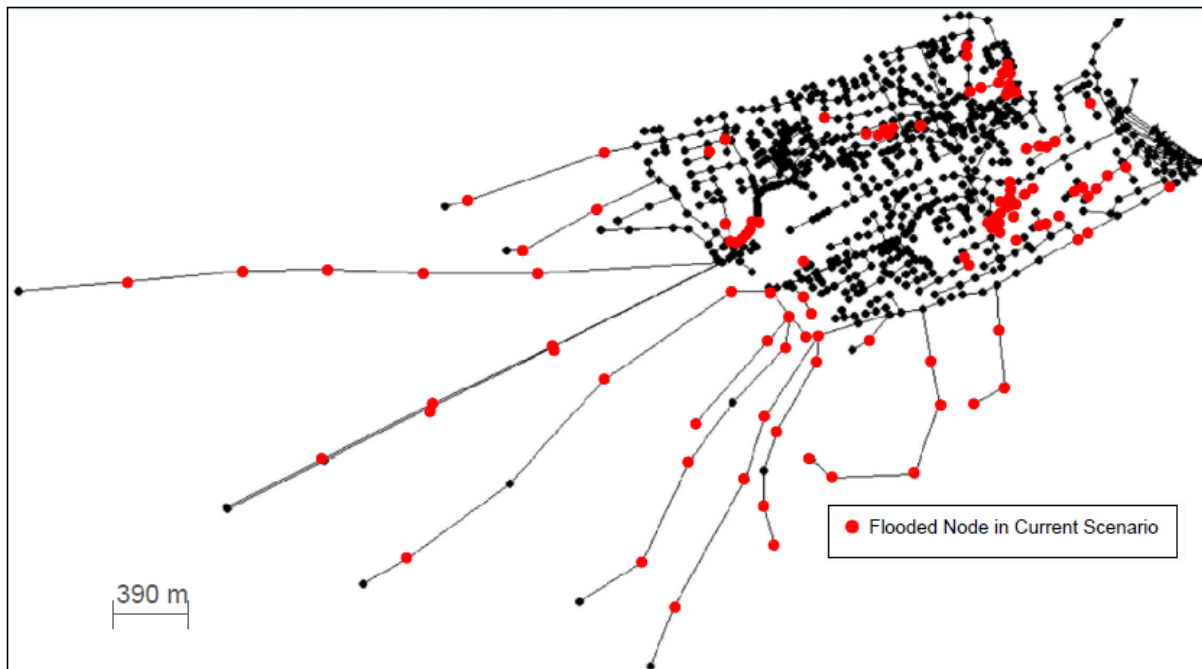


Figure 4.19. Palermo centro storico drainage system under median rainfall series of *Current* scenario: red dots show *failures*.

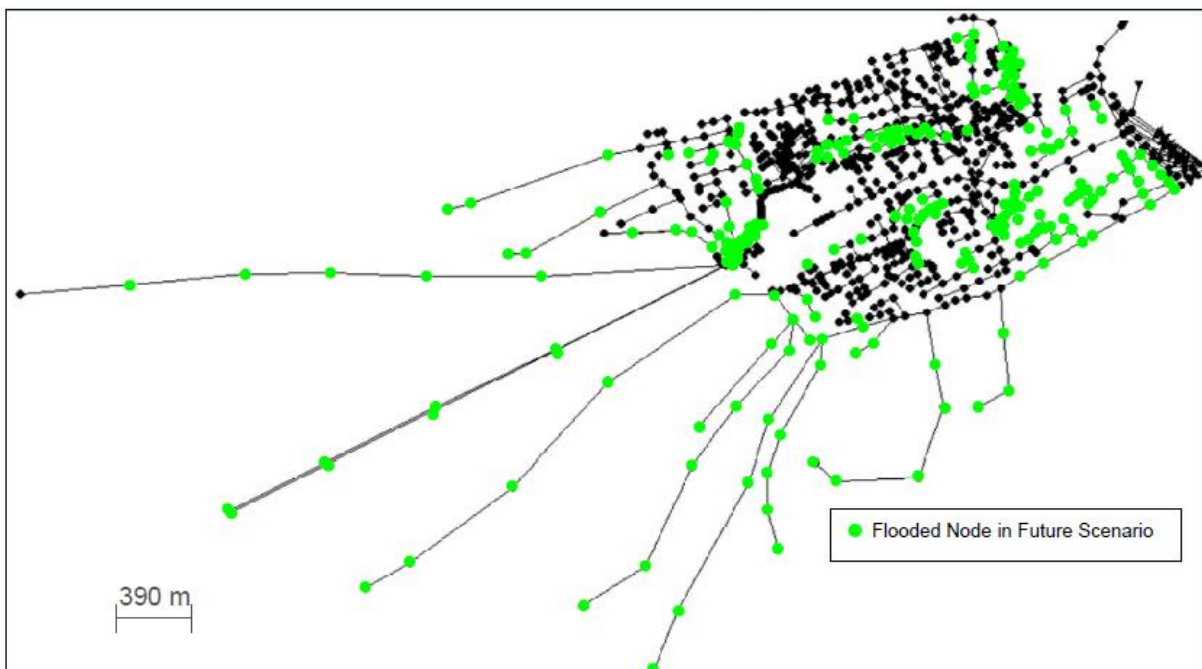


Figure 4.20. Palermo centro storico drainage system under 50° percentile rainfall series of future scenario: green dots show *failures*.

Furthermore, it is possible to notice that those parts affected by floods in both scenarios, future rainfall will probably cause more *failures*, in terms of number of *critical point*. In fact, the map referred to 2100 scenario shows denser areas where floods occur than the same map of the *Current* scenario.

Table 4.3 allows to make other remarks about common nodes; in fact even if flooded nodes in both scenarios are 94, only 8 nodes overcome the first threshold and 58 the second one. In order to explain these numbers, Table 4.5 shows the classification of *critical* nodes in both scenarios according to fixed thresholds from the comparison of the 50° percentile series.

Reading this table from left to right, it explains that, among the 94 *critical* nodes, *Current* scenario causes rising of threshold 2 in 83 nodes while 11 are those manholes where water depth crosses only threshold 1.

Regarding 2100 scenario, 61 *critical* nodes produce extraordinary floods while 33 produce water depths overcoming only threshold 1.

Studying Table 4.5 from up to down, 94 *failures* are in common in both scenarios; regarding threshold 2, current climate causes floods in 83 *critical point* while 2100 scenario will probably produce extraordinary floods in 61 manholes: 58 *critical* nodes are those that cross threshold 2 in both scenarios; on the other hand, threshold 1 is overcome in 11 and 33 failing manholes, under, respectively, *Current* and 2100 scenario: 8 manholes are common *critical* nodes in both scenario.

Table 4.5. Classification of nodes that flood in both scenarios according to thresholds under the 50° percentile series.

Scenarios	h>Street	h>Street+1,5	Street<h<1,5
Current	94	83	11
2100	94	61	33
#Common nodes	94	58	8

In order to analyze properly differences between two scenarios, it is needed to focus only on the 66 *critical* nodes (58+8) that are affected by failures in both scenarios, under the same thresholds: Figure 4.21 shows the map that points out locations of these 66 *failures*.

This map, generated by the previous table, adds information about distribution, allowing to state that ordinary floods (green dots) are related to few strewn locations, while aggregation of

red dots (extraordinary floods) shows that there are *critical* parts of the center of the city, in terms of drainage system, where water overcoming the streets rises with significant depth.

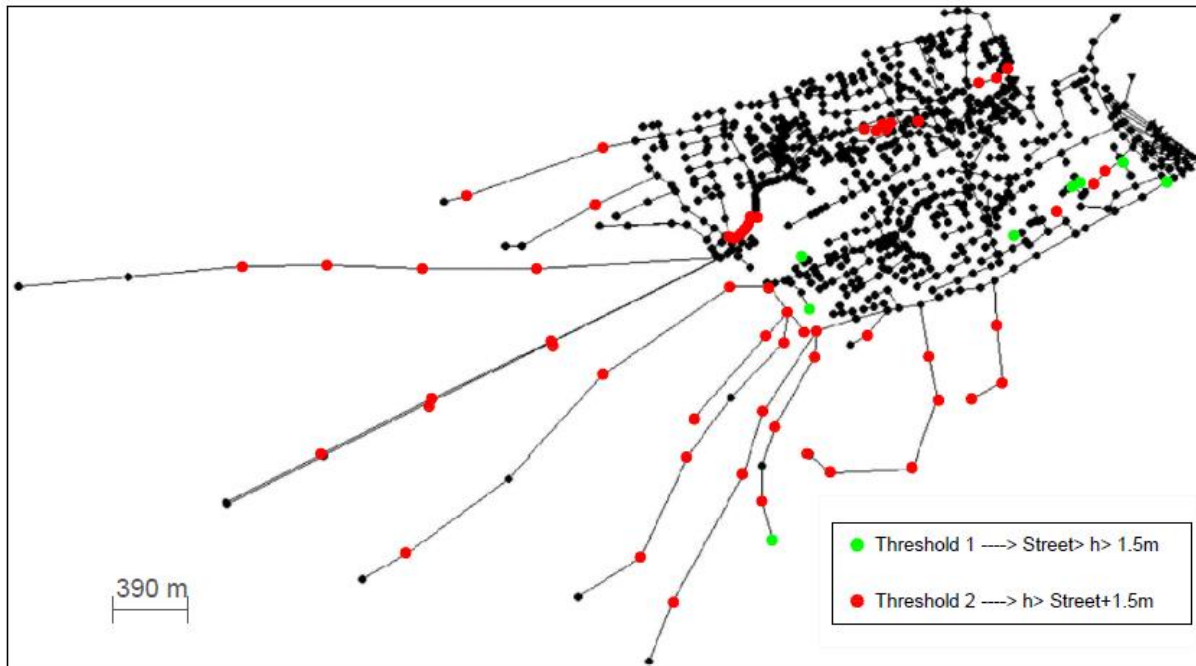


Figure 4.21. Nodes in Palermo centro storico drainage system under 50° percentile series that flood in both scenarios.

Regarding comparison of 95° percentile series coming out from both scenarios, *Table 4.4* shows that failures are different from previous comparison, and in order to visualize failures on the drainage system, it is possible generate maps (*Figure 4.22* and *Figure 4.23*) as well as produced for the 50° percentile series.

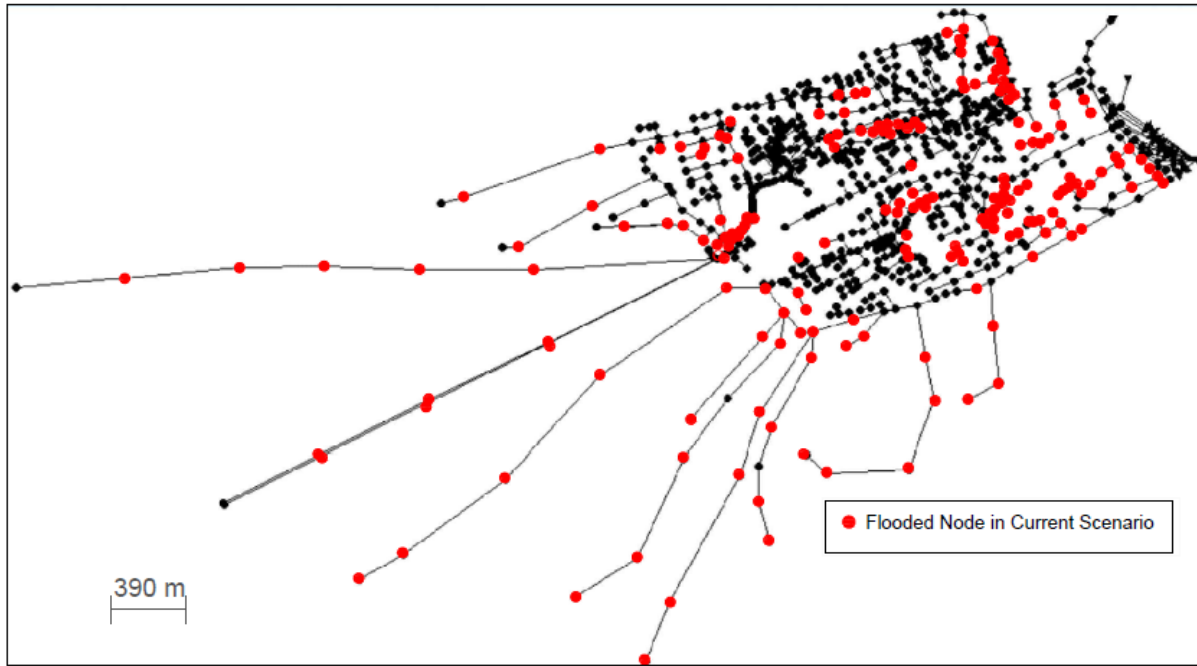


Figure 4.22. Palermo centro storico drainage system under 95° Percentile rainfall series of *Current* scenario: red dots show every node that flooded

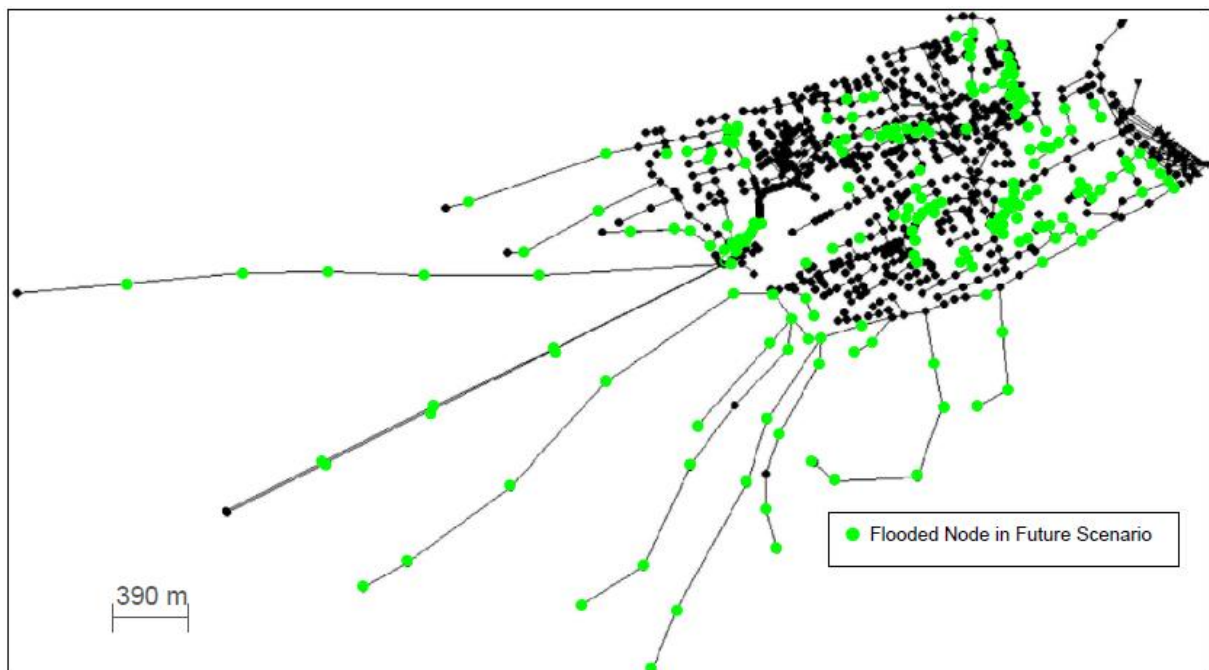


Figure 4.23. Palermo centro storico drainage system under 95° Percentile rainfall series of future scenario: green dots show every node that flooded

By looking at these two maps, it is clear that there is not an obvious difference between two scenarios because, even if flooded manholes in future will be numerically more than those in the *Current* scenario, this divergence is relative only to few nodes.

A good explanation about why, in this case, scenarios are so similar, it is possible to be found in the selection way of these series, as discussed in section 4.2. It is important to recall that series have been chosen according to the average of the annual maximum depth during 20 year. In detail, these 50 values, one for each series, have been sorted and, as usual in statistic, 95° percentile refers to a value very close by the maximum. In this case the series have an average of annual maximum depth is just a little lower than the maximum value of the sample (50 series). This means that precipitation are hard and in both scenarios are close by the hardest in the 50 generations.

In fact, analyzing *Table 4.4*, it reports 172 flooded nodes for the *Current* scenario and 180 for the *2100* scenario. This is a first index that shows similarity in the working of the drainage system in both scenarios.

As discussed above, for a fair comparison it is essential looking at those nodes that are affected by the same kind of flood because not all 170 *critical* nodes have the same behavior under the two scenarios. In detail *Table 4.6* shows that 116 nodes are affected by ordinary floods under *Current* scenario and 117 manholes under *2100* one; extraordinary floods are caused by 54 and 53 *critical* nodes, respectively, in *Current* and *2100* scenario.

Table 4.6. Classification of nodes that flood in both scenarios according to thresholds under the 95° percentile series.

Scenarios	$h > \text{Street}$	$h > \text{Street} + 1,5$	$\text{Street} < h < 1,5$
Current	170	54	116
2100	170	53	117
#Common nodes	170	53	116

Again, this table proves that rainfalls coming by the two scenarios lead sewer system to act and respond to the events in the similar way, producing similar *failures*. This is more clear by the map, in *Figure 4.24*, where green dots refer to nodes that in both scenarios overcome the threshold 1 and red dots are those that cross the threshold 2.

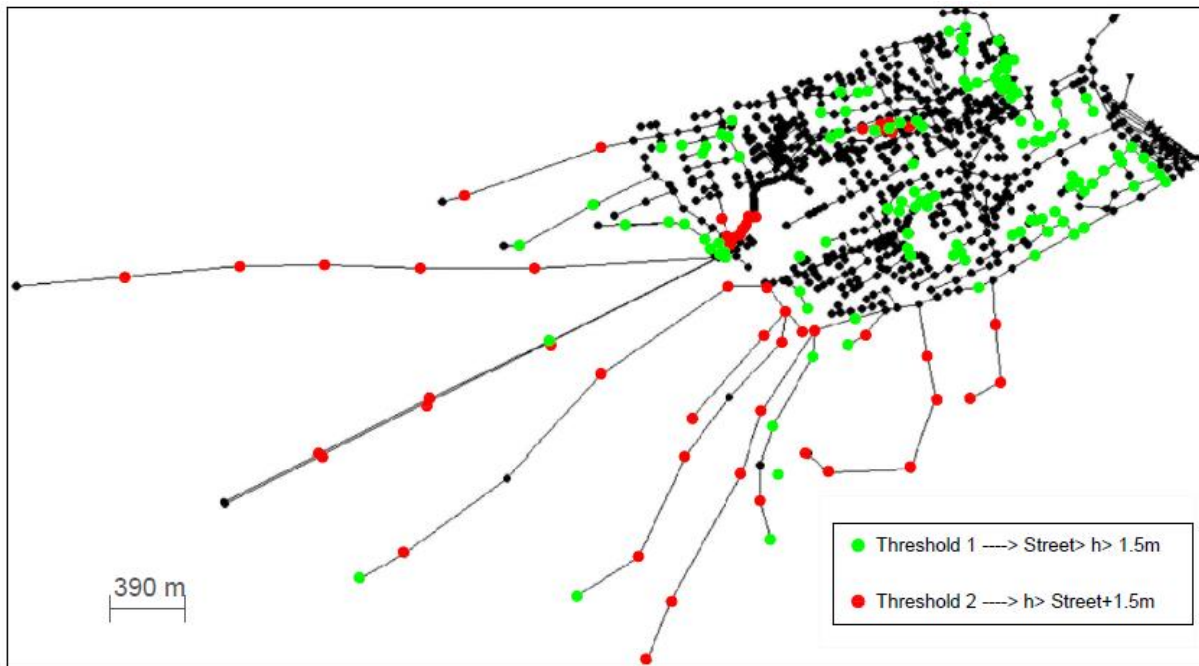


Figure 4.24. Nodes in Palermo centro storico drainage system under 95° percentile series that flood in both scenarios.

By this map it is possible to state that the most common kind of flood in this case is the ordinary one, except that two parts in which red dots are condensed and that are have been resulted as *critical* even by analysis of results of 50° percentile series.

Shown results allow to solve the first issue questioned in the beginning of this section: future rainfalls will cause an higher number of flooded manholes than the current climate and the distribution of *critical points* of the drainage system of Palermo shows an extension of the flooded areas and an increasing of these areas. Moreover, looking only at the *failures* common in both scenarios, the number of *ordinary* floods will be higher in the future for rainfalls that represent both median situations and the highest cases. The number of *extraordinary* floods remains almost the same with a decreasing of about 25% in the future rainfalls coming from median simulations, compared to the current precipitations.

In order to answer to the second point, it is essential to analyze frequencies of flooding for the flooded nodes common in both scenarios and so, for each *failure* it is possible to obtain frequency of threshold exceedances.

For this analysis, only flooded nodes common in both scenarios are considered and, in detail for 50° percentile series, 94 nodes are those that overcome the street level and 58 of these exceed it in both scenarios while 8 show a maximum flood depth that is higher than zero but lower than 1.5m. *Table 4. 7* shows results about frequency obtained on these nodes.

Table 4.7. Comparison of flooded nodes between both scenarios for 50° percentile series

Frequency	h>Street		h>Street+1,5		Street<h<1,5	
#common nodes	94		58		8	
	2100>CUR	CUR>2100	2100>CUR	CUR>2100	2100>CUR	CUR>2100
#nodes	93	1	38	20	8	0

Regarding the 94 nodes that show a flood depth, this study proves that flooding frequency of 93 manholes is higher in 2100 scenario and only in 1 manhole it is higher in Current scenario. Same remark can be stated for the 58 nodes for which water rises the second threshold: 38 of those show frequency in the future higher than Current and 20 nodes show the opposite. Eventually, about 8 nodes that are affected by ordinary floods, all of them show frequency higher in the future condition.

Same consideration can be noted for 95° percentile series, as shown in Table 4.8, but, in this case, there are also node that show frequency in the future equal to the Current one.

Table 4.8. Comparison between both scenarios for 95° Percentile series

Frequency	h>Street			h>Street+1,5			Street<h<1,5		
#common nodes	170			53			116		
	2100>CUR	CUR>2100	2100=CUR	2100>CUR	CUR>2100	2100=CUR	2100>CUR	CUR>2100	2100=CUR
#nodes	78	70	22	24	24	5	45	50	21

Among the 170 nodes that are affected by floods in both scenarios, 78 show flooding frequencies under future rainfalls higher than *Current* one while 70 show the opposite behavior and 22 nodes do not give evidence of changing in terms of frequency.

Among the 53 nodes that generate extraordinary floods, 24 are affected by flooding frequencies higher in the 2100 scenario than the current one while other 24 nodes show the opposite behavior and 5 confirm the same flooding frequency for both scenarios. Going through ordinary floods generated by 116 nodes common in both scenarios, frequency caused by future rainfalls is higher for 45 nodes, while 50 nodes show to floods a larger number of time steps under *Current* conditions and frequency of 21 nodes is equal in both scenarios.

Even in this case it is possible to create some maps (*Figure 4.25* and *Figure 4.26*) that point out the differences and that are able to summarize results coming out by tables.

Figure 4.25 refers to comparison of 50° percentile series and it shows nodes classified according to thresholds. Furthermore, in these classifications it is possible to distinguish nodes according to the comparison between the frequency in both scenarios. By *Table 4.7* it is clear that all manholes affected by ordinary floods are from 2100 scenario. Extraordinary

floods are caused by both scenarios but the map shows a higher number of nodes that produce a future flooding frequency higher than the current scenario.

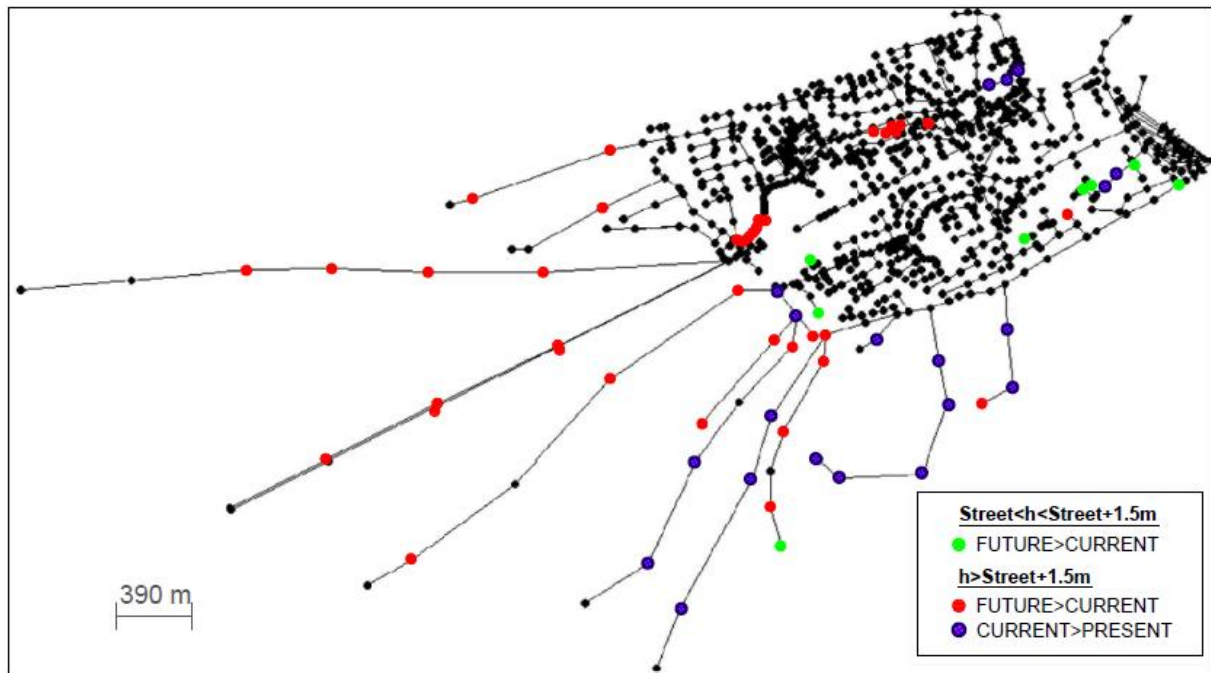


Figure 4.25. Nodes in Palermo centro storico drainage system under 50° percentile rainfall series. Comparison of flooding frequency of exceedance between both scenarios that flood in both scenarios.

Same remarks can be stated about *Figure 4.26*. However, comparison between 95° percentile series shows that differences between the two scenarios are not clear as the previous case because the number of nodes with flooding frequency higher in future scenario is almost the same of those that have opposite behavior and, moreover there are nodes that produce the same flooding frequency in both scenarios.

In this case, the important information extractable is that the hardest rainfalls will probably produce the same flooding frequencies in future as that caused by current scenario. Even in this case, the number of nodes, that produce flooding frequencies of exceedance of threshold 1, is larger than those that overcome threshold 2: it means that the drainage system of Palermo is affected by *ordinary* floods having a frequency of occurrence higher than that related to *extraordinary* floods.

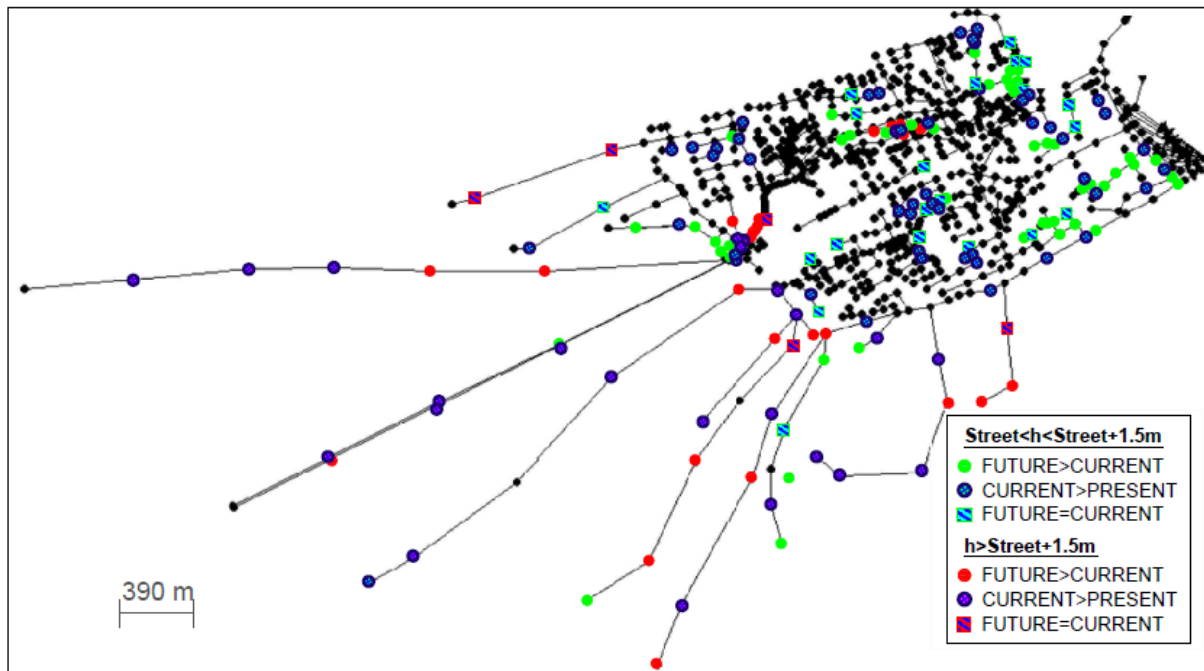


Figure 4.26. Nodes in Palermo centro storico drainage system under 95° percentile rainfall series. Comparison of flooding frequency of exceedance between both scenarios that flood in both scenarios.

Comparing the two maps, it is possible to notice how that generated by comparison between 50° percentile series shows a number of frequency of occurrence related to extraordinary floods larger than that associated to the exceedance of the only threshold 1, while the 95° percentile series show the opposite behavior.

Summarizing results, it is possible to state that according 20-year rainfalls generated stochastically by ensemble of 32 GCMs by the IPCC-5AR and RCP 8.5, future weather could probably produce effects on the drainage system that could likely cause floods.

Outcomes prove that Palermo could likely be affected by floods in several parts of the center that is the part of the city richer in terms of arts and culture. Furthermore some of those flooded areas seem to have a drainage system that, even if it is working well under current climate, could fail in the future, being affected by an increasing of the number of ordinary floods: drainage system of Palermo could be obliged to deal with those, even in parts of the city that seem to work well under current rainfalls.

Another significant result is related to the times that sewer system could fail producing problems in the city because by this study it is possible to notice that the center of the city could be affected by a number of frequency of occurrence that could probably increase making vulnerable streets, transportations and services and all problems that could be seen more often in the future.

Concluding, future for Palermo could see more floods in terms of both density of occurrences in the space and times of occurrences in 20 years.

Conclusion

Many studies show that climate change (CC) is one of the greatest threats to the economic viability, security, environmental health and territorial management of the Earth (Adger et al., 2013). Cities have been identified as among the most vulnerable human habitats to the effects of CC (Stern, 2007; Intergovernmental Panel on Climate Change, 2007). In a world where the consensus view predicts substantial impacts of anthropogenic CC on global water cycle in the near term and distant future (Kundzewicz *et al.*, 2007), hydrological impact analysis has become a thriving area of research.

For urban areas, some of the most significant potential impacts of CC and further urban development are those related to stormwater management (Semadeni-Davies *et al.*, 2008). In fact, CC does not only involve an increase in average temperature, but it also results in changes to natural phenomena such as extreme temperatures, wind, snowfall, rainfall, and an increase in sea level and, with growing urbanization leading to increasingly extensive impervious surfaces and enhanced CC effects on urban drainage, changes in urban runoff are an issue of growing concern (Denault et al. 2006; Semadeni-Davies et al. 2008). This means that floods are going to be an important issue because they can influence many aspects of human life, due to their destructive effects, and create significant expenses on mitigation efforts. Heavy rains and urban development have led to the increasing in the frequency of

flood, that is caused by: the accumulative impervious areas, the reducing of the flow capacity by the canals silting, the infrastructure deficit of micro and macro drainage facilities that are undersized to the current demands (Tucci and Collischonn, 2000).

These occurrences can cause enormous physical and mental damage to a country and its people and, for this reason, countries must be allowed to prepare for adaptation at the country level. In particular, increases in localized intensive rainfall and extreme rainfall events have resulted in a need for diverse research about CC and its effects on urban areas.

This study has intended to analyze CC impacts on the drainage system of Palermo. Being created in 734 A.D., Palermo is today a densely populated city especially in the center area that is full of historic buildings as churches, monuments and palaces separated by narrow streets. In details, the aim has been to analyze if, in future, rainfalls will put the drainage system through the wringer, causing more floods. Therefore, defining *critical points* of the drainage system those where water comes out from manholes this dissertation has tried to answer to two main research questions:

- I. Spatial distribution of *critical points* of the drainage system of Palermo caused by future climate may be different from the one caused by the *Current* precipitation: are these differences going to be remarkable, in terms of number of failing manholes and their location?
- II. Looking at the *critical points* that fail in both scenarios, are floods going to be more frequent in the future than in the *Current* conditions, or *vice versa*?

In order to solve these issues, analyses have been organized in two parts: the first related to characterize heavy rainfalls by exploiting GCMs simulations; the second refers to effects that these precipitations may cause in the drainage system of the city.

In particular, regarding the first part, this dissertation has been focused on two scenarios: the first related to the *Current* condition (*baseline*), the second for simulating the 2081-2100 period (*2100* scenario). For each scenarios, 50 hourly climatic series 20-year long have been generated by a weather generator model (AWE-GEN) that used both observed data from a weather station in Palermo and an ensemble of 32 GCMs based on RCP 8.5. The latter, the worst between those considered by IPCC, is an extreme scenario with an high increase of concentration of greenhouse gasses: concentration of CO₂ at the end of XXIX century is about 940 ppm that is more than double of current values.

Along these 50 series, only precipitation data representing the median (*50° percentile*) and a very high (*95° percentile*) rainfall conditions have been selected to compare the two scenarios.

In this way it has been possible to obtain precipitation depths at 1-hour scale and, because hourly rainfall data are not appropriate to the use of a rainfall-runoff model on an urban catchment, they have been downscaled by a Random Cascade Model.

The Random Cascade Model is able to distribute mass on successive regular subdivisions of an interval in a multiplicative manner. This dissipative process is reminiscent of rainfall disaggregation and multiplicative random cascade models were successfully applied to rainfall modeling (Schertzer and Lovejoy, 1987; Over and Gupta, 1994, 1996; Olsson, 1998; Güntner et al., 2001).

In order to be sure that this model could be useful for the aim of this dissertation, testing its results has been necessary. This test has been carried out using high resolution data (10 minutes) from a weather station: these 10-minutes precipitation depths have been firstly aggregated at 30-minute scale (*observed* series) and then to hourly time steps.

Using Random Cascade model, the hourly time series have been downscaled in 30-minute scale (*downscaled* series). Statistics from *observed* series have been compared to those from *downscaled* series and results showed that the model is able to well maintain characteristics of the precipitation: standard deviation, coefficient of variation, Skewness, Kurtosis and percentage of number of wet time steps of the *downscaled* dataset outcomes are very close to the same indexes of the *observed* dataset. This allow us to use this procedure to disaggregate the hourly 50° and 95° percentile series into 15-minute scale.

Regarding the second part of the study, it is related to the comparison of the effects that these rainfall series could cause on the drainage system of Palermo. Due to these analysis, we have been able to answer to the above mentioned two key issues of this dissertation.

In details, using the four time series (two for each scenario) 20- year long at 15-minute resolution as driving forces of the Epa Swmm model, we have studied the drainage system of the center of Palermo: along the several outputs obtained by Epa Swmm, we focused on the flooding depths above manholes. Floods have been roughly classified according to the flood depths on the street above the manhole defining *ordinary* flood if the depth does not rise 1.5m and *extraordinary* flood if the water overcomes 1.5m, neglecting other important components as, for example, velocity of the water above the streets.

In order to answer to the first questioned point, it is possible to state that, by comparing scenarios, outputs of the 50° percentile series show that 2100 scenario could probably cause a number of flooded nodes higher than *Current* scenario for *ordinary* floods, while *extraordinary* floods are going to affect about the same number of manholes. Regarding the 95° percentile, results show that number of *ordinary* floods will likely be slightly higher in

2100 scenario than *Current* one, while, again, *extraordinary* floods could occur by the same number of manholes.

In order to answer to the second question, we needed to focus only on those nodes that could probably flood in both scenarios and on analysis of flooding *frequency*.

Outputs of the comparison of the 50° percentile series show that flooded nodes with flooding frequencies caused by 2100 scenario could be higher than those caused by *Current* scenario in both *extraordinary* and *ordinary* floods for a number of nodes larger than those affected by opposite situation, while, regarding the 95° percentile series, comparison points out that these numbers are similar in both scenarios.

Summarizing results, it is possible to state that according 20-year rainfalls generated stochastically by ensemble of 32 GCMs by the IPCC-5AR and RCP 8.5, future weather could probably produce effects on the drainage system that could likely cause floods.

Outcomes prove that Palermo could likely be affected by floods in several parts of the center that is the part of the city richer in terms of arts and culture. Furthermore some of those flooded areas seem to have a drainage system that, even if it is working well under current climate, could fail in the future, being affected by an increase of the number of *ordinary* floods.

Another significant result is related to the times that sewer system could fail producing problems in the city because by this study it is clear that the center of the city could be affected by frequencies of occurrence that could probably increase making vulnerable streets, transportations and services and all problems that could be seen more often in the future.

It is well known that it is almost impossible to eliminate floods caused by heavy precipitations in cities, but the research here presented aims to be an incentive to further investigate the interactions between climate change and urban drainage systems. Indeed more efforts could be made in the future to improve design guidelines for urban drainage systems adding low impact development techniques or other integrated approaches that, reducing effects of climate change, could limit damages and restore urban drainage system to current conditions.

Bibliography

- Ackerman F., Stanton E.A., Hope C., Alberth S., Fisher J., Biewald B. (2008) The cost of climate change: what we'll pay if global warming continues unchecked. Natural Resources Defense Council, New York
- Adger N., Barnett J., Brown K., Marsh N. (2013) Cultural dimensions of climate change impact and adaptation. *Nature Climate Change*, 3, 112–117.
- Aerts J., Botzen W., Bowman P. J., Ward P., Dircke P. (Eds.). (2012) Climate adaptation and flood risk in coastal cities. Oxford: Earthscan Climate from Routledge.
- Aerts J.; Major D. C.; Bowman M. J.; Dircke P. Aris Marfai M. (2009) Connecting delta cities: coastal cities, flood risk management and adaptation to climate change.
- Ahmed S., Tsanis I. (2016) Climate Change Impact on Design Storm and Performance of Urban Storm-Water Management System-A Case Study on West Central Mountain Drainage Area in Canada Hydrology: Current Research, OMICS International.
- Ajami N. K., Thompson Jr B. H., Victor D. G. (2014) The path to water innovation The Brookings Institution.
- Albrechts L. (1999) Planners as catalysts and initiators of change: The new structure plan for Flanders. *European Planning Studies*, 7, 587–603.

- Albrechts L. (2004) Strategic (spatial) planning examined. *Environment and Planning B: Planning and Design*, 31, 743–758.
- Amanatidis G. T., Paliatsos A. G., Repapis C. C., Bartzis J. G. (1993) Decreasing precipitation trend in the Marathon area, Greece. *International Journal of Climatology*, 13(2), 191–201.
- Anas A., Arnott R., Small K. A. (1998). Urban spatial structure. In Working paper. University of Buffalo.
- Andreadis K.M., Lettenmaier D.P. (2006) Trends in 20th century drought over the continental United States. *Geophys Res Lett* 33(10):L10403. doi:10.1029/2006GL025711
- Andreásson J., Bergström S., Carlsson B., Graham L.P. Lindström G. (2004) Hydrological change: climate change impact simulations for Sweden. *Ambio* 33, 228–34.
- Ansell C., & Gash A. (2008). Collaborative governance in theory and practice. *Journal of Public Administration Research and Theory*, 18, 543–571.
- Arisz H.; Burrell B.C. (2006) Urban Drainage infrastructure planning and design considering climate change. In *EIC Climate Change Technology, Proceedings of the 2006 IEEE EIC Climate Change Conference*, Ottawa, ON, Canada, 10–12 May 2006; pp. 1–9.
- Arnbjerg-Nielsen K. (2006) Significant climate change of extreme rainfall in Denmark. *Water Science and Technology* 54, 6–7, 1–8.
- Arnbjerg-Nielsen K. (2008) Quantification of climate change impacts on extreme precipitation used for design of sewer systems, *Proceedings of the 11th International Conference on Urban Drainage*.
- Arnbjerg-Nielsen K. (2010) Past, present, and future design of urban drainage systems with focus on Danish experiences. *Water Science and Technology* 63 (3), 527–535.
- Arnbjerg-Nielsen K., Fleischer H. (2009) Feasible adaptation strategies for increased risk of flooding in cities due to climate change. *Water Science and Technology* 60 (2), 273–281.
- Arnbjerg-Nielsen K., Willems P., Olsson J., Beecham S., Pathirana A., Gregersen I. Bü., Madsen H., Nguyen V.-T.-V. (2013) Impacts of climate change on rainfall extremes and urban drainage systems: a review *Water Science and Technology*, IWA Publishing, 68, 16–28
- Arnell N.W. (2000) Thresholds and response to climate change forcing: the water sector. *Climatic Change* 46, 305–16.
- Arnell N.W. (2003a) Effects of IPCC SRES emission scenarios on river runoff: a global perspective. *Hydrology and Earth System Sciences* 7, 619–41.
- Arnell N.W. (2003b) Relative effects of multi-decadal climatic variability and changes in the mean and variability of climate due to global warming: future streamflows in Britain. *Journal of Hydrology* 270, 195–213.

- Arnell N.W. (2008) Climate change and drought. Paper presented at the international conference drought management: scientific and technological innovations, Zaragoza, Spain, June 12–14 2008
- Aronica G., Cannarozzo M., Noto L. (2002) Investigating the changes in extreme rainfall series recorded in an urbanised area. *Water Science and Technology*, 45(2), 49-54.
- Ashley, R., Balmforth, D., Saul, A., Blanskby J. (2005), Flooding in the future predicting climate change, risks and responses in urban areas, *Water Science & Technology*, 52(5), 265-273.
- Augustsson T., Ramanathan V. (1977) Radiative-convective model study of CO₂ climate problem. *J. Atmos. Sci.*, 34, 448–451.
- Bae D., Jung I.W., Chang H. (2008) Potential changes in Korean water resources estimated by high-resolution climate simulation. *Climate Research* 35, 213–26.
- Baguis P., Roulin E., Willems P., Ntegeka V. (2009) Climate change scenarios for precipitation and potential evapotranspiration over central Belgium. *Theoretical and Applied Climatology*. doi:10.1007/s00704-009-0146-5.
- Bahri A. (2012) Integrated Urban Water Management. GWP Technical Background Papers. Global Water Partnership, Stockholm Number 16.
- Baker M.B., Peter T. (2008) Small-scale cloud processes and climate. *Nature* 451, 299–300.
- Bárdossy A., Caspary H.J. (1990) Detection of climate change in Europe by analyzing European atmospheric circulation patterns from 1881 to 1989. *Theoretical and Applied Climatology* 42, 155–167.
- Barrett S., Fudge C. (Eds.). (1981) *Planning and action*. London: Methuen.
- Bates B.C., Kundzewicz Z.W., Wu, S., Palutikof, J.P. (2008) Climate change and water. Technical paper. *Intergovernmental Panel on Climate Change, IPCC Secretariat, Geneva*.
- Beecham S. (2012) Development of multifunctional landuse using water sensitive urban design. Chapter 18. In: *Designing for Zero Waste: Consumption, Technologies and the Built Environment* (S. Lehmann & R. Crocker, eds). Routledge Press, London, UK, pp. 374–384.
- Benestad R.E., Hanssen-Bauer I., Chen D. (2008) Empirical–Statistical Downscaling. World Scientific Publishing Co. Pte. Ltd., Hasensack, New Jersey 981-281-912-6.
- Bengtsson L., Milotti S. (2008) Intensive storms in Malmö (in Swedish). *Vatten* 64, 291–304.
- Beniston M., Stephenson D.B., Christensen O.B., Ferro C.A.T., Frei C., et al. (2007) Future extreme events in European climate: an exploration of regional climate model projections. *Climatic Change* 81: 71-95.
- Benveniste G. (1989). *Mastering the politics of planning*. San Francisco, CA: Jossey-Bass.

- Berggren K. (2008) Indicators for urban drainage system-assessment of climate change impacts. In Proceedings of 11th International Conference on Urban Drainage, Edinburgh International Conference Centre, Scotland: 11 ICUD, Munich, Germany, 31 August–5 September 2008.
- Berggren K. (2014) Urban Stormwater Systems in Future Climates – Assessment and Management of Hydraulic Overloading. Doctoral thesis, Lulea University of Technology, Lulea, Sweden.
- Berggren K., Olofsson M., Viklander M., Svensson G. (2007) Tools for measuring climate change impacts on urban drainage systems. In Proceedings of the NOVATECH 2007: Sixth International Conference on Sustainable Techniques and Strategies in Urban Water Management, Lyon, France, 25–28 June 2007.
- Berggren K., Olofsson M., Viklander M., Svensson G., Gustafsson A. (2012) Hydraulic Impacts on Urban Drainage Systems due to Changes in Rainfall Caused by Climatic Change. *J Hydrol Eng* 17 (1): 92-98.
- Berggren K., Olofsson M., Viklander M., Svensson G., Gustafsson A. (2011) Hydraulic impacts on urban drainage systems due to changes in rainfall caused by climatic change. *J. Hydrol. Eng.* 2011, 17, 92–98.
- Berkhout F., Hertin J., Jordan A. (2002) Socio-economic futures in a climate change impact assessment: using scenarios as ‘learning machines’. *Global Environ. Change, Part A* 12 (2), 83– 95.
- Berry J. (2016) Ecosystem-based Adaptation to Climate Change in Urban Areas: An Evaluation of Rainwater Management Practices in Metro Vancouver SIMON FRASER UNIVERSITY.
- Bi E. G., Monette F., Gachon P., Gaspéri J., Perrodin Y. (2015) Quantitative and qualitative assessment of the impact of climate change on a combined sewer overflow and its receiving water body *Environmental Science and Pollution Research*, Springer, 22, 11905-11921
- Blair A., Sanger D., Holland A.F., White D., Vandiver L., White S. (2011) Stormwater Runoff? Modeling Impacts of Urbanization and Climate Change, Louisville, Kentucky, August 7–10, 2011. American Society of Agricultural and Biological Engineers.
- Blanc J., Hall J.W., Roche N., Dawson R.J., Cesses Y., Burton A., Kilsby C.G. (2012) Enhanced efficiency of pluvial flood risk estimation in urban areas using spatial–temporal rainfall simulations. *Journal of Flood Risk Management* 5, 143-152.
- Blasing T.J. (2013) Recent greenhouse gas concentrations. Carbon Dioxide Information Analysis Center, Oak Ridge National Laboratory, U.S. Department of Energy.
- Boller M. (2004). Towards sustainable urban stormwater management. *Water Science and Technology*. *Water Supply* 4 (1), 55–65.

- Bonaccorso B., Cancelliere A., Rossi G. (2005) Detecting trends of extreme rainfall series in Sicily. *Advances in Geosciences*, 2, 7-11.
- Bouteligier R., Vaes G., Berlamont J., van Assel J., Gordon D. (2001) Water quality model set-up and calibration—a case study, The Autumn WaPUG Conference, Blackpool, UK.
- Bovard B.D., Curtis P.S., Vogel C.S., Su H-B., Schmid H.P. (2005) Environmental controls on sap flow in a northern hardwood forest. *Tree Physiol.*, 25:31-8.
- Braud I., Breil P., Thollet F., Lagouy M., Branger F., Jacqueminet C., Michel K. (2013) Evidence of the impact of urbanization on the hydrological regime of a medium-sized periurban catchment in France. *J Hydrol* 485:5–23.
- Brown C. (2010) The end of reliability. *J Water Resour Plann Manage* 136: 143145.
- Burger M., Meijers E. (2012) Form follows function: Liking morphological and functional polycentricity. *Urban Studies*, 49(5), 1127–1149.
- Burrell B.C., Davar K., Hughes R. (2007) A review of flood management considering the impacts of climate change. *Water Int.* 2007, 32, 342–359.
- Burton G.A., Pitt R.E. (2002) Stormwater effects handbook—a toolbox for watershed managers, scientists, and engineers. Lewis, Boca Raton, p 911
- Busetta A. (2013). *Glistranieri a Palermo: caratteristiche socio-demografiche*, StrumentiRes Anno V n° 3.
- Caissie D., Kurylyk B.L., St-Hilaire A., El-Jabi N., MacQuarrie K.T. (2014) Streambed temperature dynamics and corresponding heat fluxes in small streams experiencing seasonal ice cover. *J Hydrol* 519: 1441–1452
- Caltabiano F. (2012) Costo dell'invarianza idraulica ottenuta mediante sistemi distribuiti di gestione dei deflussi (BMP) nei bacini urbani. University of Palermo. Ph.D.thesis.
- Cannarozzo M. (1985) Analisi statistica delle precipitazioni registrate in Sicilia finalizzata allo studio dei cambiamenti climatici. *Sviluppo Agricolo*, 3(4), 53-64.
- Cannarozzo M., Noto L. V., Viola F (2006) Spatial distribution of rainfall trends in Sicily (1921–2000). *Physics and Chemistry of the Earth, Parts A/B/C*, 31(18), 1201-1211.
- Cantwell, M. (2016) National policy framework to address drought and water security in the United States.
- Carrière A., Barbeau B., Cantin J.F. (2007) Vulnerability of drinking water treatment plants to low water levels in the St. Lawrence River. *J Water Resour Plan Manag* 133(1):33–38
- Carter N. (2007) *The politics of the environment: Ideas, activism policy* (2nd ed.). Cambridge: Cambridge University Press.

- Casadio A., Maglionico M., Bolognesi A., Artina S. (2010) Toxicity and pollutant impact analysis in an urban river due to combined sewer overflows loads. *Water Sci Technol* 61(1):207–215
- Chang H. (2008) Spatial analysis of water quality trends in the Han River basin, South Korea. *Water Research* 42, 3285–304.
- Chen J., Brissette F.P., Leconte R. (2011) Uncertainty of downscaling method in quantifying the impact of climate change on hydrology. *J. Hydrol.* 401 (3–4), 190–202.
- Chiew F.H.S., Harrold T.I., Siriwardena L., Jones R.N., Skrikanthan R. (2003) Simulation of climate change impact on runoff using rainfall scenarios that consider daily patterns of change from GCMs. In *Proceedings of the International Congress on Modelling and Simulation (MODSIM 2003)*, Townsville, 14–17 July 2003.
- Chiplunkar A., Kallidaikurichi S., Cheon K.T. (2012) *Good Practices in Urban Water Management: Decoding Good Practices for a Successful Future*. Asian Development Bank, Mandaluyong City, Philippines.
- Chocat B. (1997) Le rôle possible de l'urbanisation dans l'aggravation du risque d'inondation: l'exemple de l'Yseron à Lyon/The potential role of urbanization in increasing the risk of flooding: the example of the Yzeron in Lyon. *Rev Géogr Lyon* 72(4):273–280
- Chocat B., Bertrand-Krajewski J.L., Barraud S. (2007) *Eaux pluviales urbaines et rejets urbains par Temps de pluie*. Techniques de l'ingénieur, Paris (France). Vol. W2, n W6800. p17
- Christensen J.H., Christensen O.B. (2003) Climate modelling: severe summertime flooding in Europe. *Nature* 421: 805-806.
- Christensen N.S., Wood A.W., Voisin N., Lettenmeier D.P., Palmer R.N. (2004) The effects of climate change on the hydrology and water resources of the Colorado River Basin. *Climatic Change* 62, 337–63.
- Clark S., Grossman T., Przyuski N., Shinn C., Storz D. (nd). *Ecosystem-based Adaptation to Climate Change A Cost-Benefit Analysis*. Bren School of Environmental Science & Management, University of California at Santa Barbara.
- Clifford N.J. (2009) *Globalization: a Physical Geography perspective*. *Progress in Physical Geography* 33, 5–16.
- Climate Change Adaptation (2013) *Recent cases*. Danish Portal for Climate Change Adaptation. <http://en.klimatilpasning.dk/recent/cases.aspx> (accessed 20 February 2013).
- Corbett C.W., Wahl M., Porter D.E., Edwards D., Moise C. (1997) Nonpoint source runoff modeling a comparison of a forested watershed and an urban watershed on the South Carolina coast. *J. Exp. Mar. Biol. Ecol.* 213, 133–149.

- Coulibaly P., Shi X. (2005) Identification of the effect of climate change on future design standards of drainage infrastructure in Ontario. Highway Infrastructure Innovation Funding Program, Ministry of Transportation of Ontario, Canada.
- Cowpertwait P.S.P. (1991) Further developments of the Neyman–Scott clustered point process for modeling rainfall. *Water Resour. Res.*, 27:1431-8.
- Cowpertwait P.S.P. (1994) A generalized point process model for rainfall. *Proc. Roy. Soc. Lond. Ser. A.*, 447:23-7.
- Cowpertwait P.S.P. (1998) A Poisson-cluster model of rainfall: high order moments and extreme values. *Proc. Roy. Soc. Lond. Ser. A.*, 454:885-98.
- Cowpertwait P.S.P. (2004) Mixed rectangular pulses models of rainfall. *Hydrol. Earth Syst. Sci.*, 8:993-1000.
- Cowpertwait P.S.P. (2006) A spatial-temporal point process model of rainfall for the Thames catchment. *J. Hydrol.*, 330:586-95.
- Cowpertwait P.S.P., Isham V., Onof C. (2007) Point process models of rainfall: developments for fine scale structure. *Proc. Roy. Soc. Lond. Ser. A.*, 463(2086):2569-87.
- Cowpertwait P.S.P., Kilsby C., O’Connell P. (2002) A space-time Neyman-Scott model of rainfall: empirical analysis of extremes. *Water Resour. Res.*, 38(8):1-14.
- Cowpertwait P.S.P., O’Connell P., Metcalfe A., Mawdsley J. (1996) Stochastic point process modelling of rainfall: I. Single-site fitting and validation. *J. Hydrol.*, 175:17-46.
- Cox P., Stephenson D. (2007) A changing climate for prediction. *Science* 317 (5835), 207e208.
- Curtis D.C., Eagleson P.S. (1982). Constrained stochastic climate simulation. *Technical report 274, Mass. Inst. of Technol., Dep. of Civ. and Environ. Eng. Ralph M. Parsons Lab., Cambridge, Mass, USA.*
- Dai A. (2011a) Characteristics and trends in various forms of the Palmer Drought Severity Index during 1900–2008. *J Geophys Res* 116(D12):D12115. doi:10.1029/2010JD015541.
- Dai A. (2011b) Drought under global warming: a review. *WIREs Clim Change* 2(1):45–65. doi:10.1002/wcc.81.
- Dale M., Luck B., Fowler H. J., Blenkinsop S., Gill E., Bennett J., Kendon E., Chan S. (2015) New climate change rainfall estimates for sustainable drainage Proceedings of the Institution of Civil Engineers. Engineering Sustainability.
- Davis A.P., Shokouhian M., Sharma H., Christie M. (2006) Water quality improvement through bioretention media: nitrogen and phosphorus removal. *Water Environ. Res.* 284–293.
- de Vries J. (2006) Climate change and spatial planning below sea-level: Water water and more water. *Planning Theory & Practice*, 7, 223–227.

- Deaves D.M., Lines I.G. (1997) On the fitting of low mean windspeed data to the Weibull distribution. *J Wind Eng Indus Aerodynam*, 66:169-78.
- Delpla I., Jung A.V., Baures E., Clement M., Thomas O. (2009) Impacts of climate change on surface water quality in relation to drinking water production. *Environ Int* 35(8):1225–1233
- Denault C., Millar R.G., Lence B.J. (2006) Assessment of possible impacts of climate change in an urban catchment. *Journal of the American Water Resources Association* 42, 685–697.
- Deser C., Phillips A., Bourdette V. (2012) Uncertainty in climate change projections: the role of internal variability. *Climate Dyn* 38: 527-546.
- Devkota J.P., Burian S.J., Tavakol-Davani H., Apul D.S. (2015) Introducing demand to supply ratio as a new metric for understanding life cycle greenhouse gas (GHG) emissions from rainwater harvesting systems, *Journal of Cleaner Production*, Available online 6 November 2015, ISSN 09596526.
- Dibike Y.B., Coulibaly P. (2005) Hydrologic impact of climate change in the Saguenay watershed: comparison of downscaling methods and hydrologic models. *J Hydrol* 307 (1-4): 145-163.
- Dibike Y.B., Gachon P., St-Hilaire A., Ouarda T.B.M.J., Nguyen V.T.V. (2008) Uncertainty analysis of statistically downscaled temperature and precipitation regimes in Northern Canada. *Theoretical and Applied Climatology* 91, 149–170.
- Dingman S. L. (2002) *Physical Hydrology*, 2nd Ed. *Upper Saddle River, New Jersey, Prentice Hall*.
- Dubayah R., Loechel S. (1997) Modeling topographic solar radiation using GOES data. *J. Appl. Meteorol.*, 36:141-54.
- Ducharne A. (2008) Importance of stream temperature to climate change impact on water quality. *Hydrology and Earth System Sciences* 12, 797–810.
- Dufresne J., Quaas J., Boucher O., Denvil S., Fairhead L. (2005) Contrasts in the effects on climate of anthropogenic sulfate aerosols between the 20th and the 21st century. *Geophys. Res. Lett.*, 32, L21703.
- Dufresne J.-L., et al. (2013) Climate change projections using the IPSL-CM5 Earth system model: From CMIP3 to CMIP5. *Clim. Dyn.*, 40, 2123–2165.
- Dunne T., Leopold L. (1978) *Water in environmental planning*. New York: W.H. Freeman and Company.
- Durrans S.R. (2003) *Stormwater Conveyance Modeling and Design*. Haestad Press, Waterbury, CT.

- DWA (2006) Standard DWA-A 118 E, Hydraulic Dimensioning and Verification of Drain and Sewer Systems. DWA, The German Association for Water, Wastewater and Waste, Hennef, Germany.
- Eastern Research Group (2014) Economic Assessment of Green Infrastructure Strategies for Climate Change Adaptation: Pilot Studies in The Great Lakes Region. National Oceanic and Atmospheric Administration Coastal Services Center <http://coast.noaa.gov/digitalcoast/sites/default/files/files/publications/04062014/GLPilots_Final_5-5-14v2.pdf> (Nov. 17 2015).
- Egger C., Maurer M. (2015) Importance of anthropogenic climate impact, sampling error and urban development in sewer system design *Water research*, Elsevier, 73, 78-97 .
- Ekström, M., Fowler H., Kilsby C., Jones P. (2005) New estimates of future changes in extreme rainfall across the UK using regional climate model integrations. 2. Future estimates and use in impact studies. *J. Hydrol.* 2005, 300, 234–251.
- Emerson K., Nabatchi T., Balogh S. (2012) An integrative framework for collaborative governance. *Journal of Public Administration Research and Theory*, 22, 1–29.
- Engström C.-J., Legeby F. (2001) Scenariostudie om framtidsstaden (Scenario studies of future towns – Swedish). Report 2001:1, Chalmers University of Technology, Go`teborg, Sweden.
- Entekhabi D., Rodriguez-Iturbe. I., Eagleson P.S. (1989) Probabilistic representation of the temporal rainfall process by a modified Neyman-Scott rectangular pulses model: parameter estimation and validation. *Water Resour Res*, 25(2):295-302.
- EPA (2007) Innovation and Research for Water Infrastructure for the 21st Century Research Plan. Environmental Protection Agency, Office of Research and Development, Washington DC, USA.
- Esteban-Parra M. J., Rodrigo F. S., Castro-Diez Y. (1998) Spatial and temporal patterns of precipitation in Spain for the period 1880–1992. *International Journal of Climatology*, 18(14), 1557-1574.
- Evans J., Schreider S. (2002) Hydrological impacts of climate change on inflows to Perth, Australia. *Climatic Change* 55, 361–93.
- Fatichi S. (2010) The modeling of hydrological cycle and its interaction with vegetation in the framework of climate change. *PhD thesis, University of Firenze, Italy, and T.U. Braunschweig, Germany.*
- Fatichi S., Ivanov V.Y., Caporali E. (2011) Simulation of future climate scenarios with a weather generator. *Adv. Water Resources*, 34(4), 448-467.

- Fatichi S., Ivanov V.Y., Caporali E. (2012) On the search for vital details of climate change. In: Proceedings of the 9th International Workshop on Precipitation in Urban Areas. St. Moritz, Switzerland, 6e9 December 2012.
- Fatichi S., Ivanov V.Y., Caporali E. (2013) Assessment of a stochastic downscaling methodology in generating an ensemble of hourly future climate time series. *Climate Dynamics*, Volume 40, Issue 7-8, pp 1841-1861. Doi: 10.1007/s00382-012-1627-2.
- Feltmate B., Thistlethwaite J. (2012) Climate Change Adaptation: A Priorities Plan for Canada. Climate Change Adaptation Project, Canada.
- Fiering M.B., Jackson B.B. (1971) Synthetic hydrology. *Water resources monograph*, American Geophysics Union.
- Flood-Site Consortium (2015) Flood risk management Available at http://www.floodsite.net/html/flood_risk.html.
- Forsee W.J., Ahmad S. (2011) Evaluating urban storm-water infrastructure design in response to projected climate change. *J Hydrol Eng* 16 (11): 865-873.
- Fortier C., Mailhot A. (2014) Climate Change Impacts on Combined Sewer Overflows. *J. Water Resour. Plann. Manage.*, 10.1061/(ASCE)WR.1943-5452.0000468.
- Fowler H.J., Blenkinsop S., Tebaldi C. (2007) Linking climate change modeling to impacts studies: Recent advances in downscaling techniques for hydrological modeling. *Int J Climatol* 27 (12): 1547-1578.
- Fowler H.J., Ekström M. (2009) Multi-model ensemble estimates of climate change impacts on UK seasonal precipitation extremes. *Int. J. Climatol.* 29 (3), 385e416.
- Fowler H.J., Kilsby C.G., Stunell J. (2007) Modelling the impacts of potential future climate change on water resources in north-west England. *Hydrology and Earth System Sciences* 11, 1115–26.
- Francesch-Huidobro M. (2015a) Air pollution: Inventories, regional control and institutions. In P. Harris & G. Lang (Eds.), *Routledge handbook of environment and society in Asia*. London & New York: Routledge (ch. 9).
- Francesch-Huidobro M. (2015b) Collaborative governance and environmental authority for adaptive flood risk: Recreating sustainable coastal cities. *Journal of Cleaner Production*, 107, 568–580. <http://dx.doi.org/10.1016/j.jclepro.2015.05.045>.
- Francesch-Huidobro M., Dabrowski M., Tai Y., Chan F., Stead D. (2016) Governance challenges of flood-prone delta cities: Integrating flood risk management and climate change in spatial planning *Progress in Planning*, Elsevier.

- Frazer L. (2005) Paving paradise: the peril of impervious surfaces. *Environ. Health Perspect.* 113 (7), A456–A462.
- Freidenreich S.M., Ramaswamy V. (1999) A new multiple-band solar radiative parameterization for general circulation models. *J. Geophys. Res.*, 104(D24):31389-409.
- Freni G. (1996) Il sistema di drenaggio urbano del centro storico di Palermo: Modello matematico per l'analisi della rete e degli episodi di insufficienza idraulica.
- Friedmann J., Douglas M. (1998) In M. Douglas & J. Friedmann (Eds.), 'Editor's introduction' in cities for citizens. Chichester, Sussex: John Wiley.
- Fujihara Y., Tanaka K., Watanabe T., Nagano T., Kojiri T. (2008) Assessing the impacts of climate change on the water resources of the Seyhan River Basin in Turkey: use of dynamically downscaled data for hydrological simulations. *Journal of Hydrology* 353, 33–48.
- Fussler H. (2007) Adaptation planning for climate change: concepts, assessment approaches, and key lessons. *Sustain Science*, 2:265–275. DOI 10.1007/s11625-007-0032-y.
- Giuffrida A., Conte M. (1989) Long term evolution of the Italian climate outlined by using the standardized anomaly index (SAI). In: Painatuskeskus V (Ed.), Conference on Climate and Water (I). Helsinki, Finland, p. 197.
- Glasbey C., Cooper G., McGechan M. (1995) Disaggregation of Daily Rainfall by Conditional Simulation from a Point-Process Model. *J. Hydrol.* 1995, 165, 1–9.
- Glendenning C.J., Vervoort R.W. (2010) Hydrological impacts of rainwater harvesting (RWH) in a case study catchment: The Arvari River, Rajasthan, India. Part 1: Field-scale impacts. *Agricultural Water Management* 98 (2010) 331–342.
- Gooré Bi. E., Monette F., Gasperi J., Perrodin Y. (2014) Assessment of the ecotoxicological risk of combined sewer overflows for an aquatic system using a coupled Bsubstance and bioassay^ approach. *Environ Sci Pollut Res* 22(6):4460–4474. doi:10.1007/s11356014-3650-9.
- Graham L.P. (2004) Climate change effects on river flow to the Baltic Sea. *Ambio* 33, 235–41.
- Graham L.P., Hagemann S., Jaun S., Beniston M. (2007) On interpreting hydrological change from regional climate models. *Climatic Change* 81, 97–122.
- Granier C., et al. (2011) Evolution of anthropogenic and biomass burning emissions at global and regional scales during the 1980–2010 period. *Clim. Change*, 109, 163–190.
- Gregersen I.B., Arnbjerg-Nielsen K., Madsen H. (2010) Parametric analysis of regional trends in observed extreme rainfall in Denmark. Proceedings of the International Workshop on Advances in Statistical Hydrology, May 23–25, 2010 Taormina, Italy.

- Gregory J. M., et al. (2004) A new method for diagnosing radiative forcing and climate sensitivity. *Geophys. Res. Lett.*, 31, L03205.
- Grossi G., Bacchi B. (2008) A tool to investigate potential climate change effects on the efficiency of urban drainage systems. Proceedings of the 11th International Conference on Urban Drainage, 31 August–5 September 2008, Edinburgh, Scotland.
- Groves D.G., Yates D., Tebaldi C. (2008) Developing and applying uncertain climate change projections for regional water management planning. *Water Resources Research* 44, W12413, DOI: 10.1029/2008WR006964.
- Grum M., Jørgensen A.T., Johansen R.M., Linde J.J. (2006) The effect of climate change on urban drainage: An evaluation based on regional climate model simulations. *Water Sci. Technol.* 2006, 54, 9–15.
- Gueymard C.A. (1989) A two-band model for the calculation of clear sky solar irradiance, illuminance, and photosynthetically active radiation at the Earth's surface. *Solar Energy*, 43:253-65.
- Gueymard C.A. (2001) Parameterized transmittance model for direct beam and circumsolar spectral irradiance. *Solar Energy*, 71:325-46.
- Gueymard C.A. (2008) REST2: High-performance solar radiation model for cloudless sky irradiance illuminance and photosynthetically active radiation validation with a benchmark dataset. *Solar Energy*, 82:272-85.
- Gujer W., Krejci V. (1988) Precipitation and Urban Drainage—From H'orler/Rhein to the Historical Event. Verband Schweizerischer Abwasserfachleute, VSA-Report No. 388, German.
- Güntner A., Olsson J., Calver A., Gannon B. (2001) Cascade-based disaggregation of continuous rainfall time series: the influence of climate. *Hydrol. Earth Syst. Sci.* 5 (2), 145–164.
- Guo Y.P. (2006) Updating rainfall IDF relationships to maintain urban drainage design standard. *J Hydrol Eng* 11 (5): 506-509.
- Gupta V.K., Waymire E.C. (1993) A statistical analysis of mesoscale rainfall as a random cascade. *J. Appl. Meteorol.* 32, 251– 267
- Haines A., Kovats R.S., Campbell-Lendrum D., Corvalan C. (2006) Climate change and human health: Impacts, vulnerability and public health. *Public Health* 120(7):585–596
- Hall J. W., Sayers P. B., Dawson R. J. (2005) National-scale assessment of current and future flood risk in England and Wales. *Natural Hazards*, 36(1-2), 147-164.

- Hall J.W., Meadowcroft I.C., Sayers P.B., Bramley M.E. (2003b) Integrated flood risk management in England and Wales. *Natural Hazards Review* 4, 126-135.
- Hall P., Pain K. (2006) *The polycentric metropolis: Learning from mega-city regions in Europe*. Oxon: Earthscan.
- Hall P., Pfeiffer U. (2000) *Urban future 21*. London, Spon.
- Hallegatte S., Green C., Nicholls R. J., Corfee-Morlot J. (2013) Future flood losses in major coastal cities. *Nature Climate Change*, 3(9), 802–806.
- Hansen J., et al., (1988) Global climate changes as forecast by Goddard Institute for Space Studies 3-dimensional model. *J. Geophys. Res. Atmos.*, 93, 9341–9364.
- Hardy M.J., Kuczera G., Coombes P.J. (2005) Integrated urban water cycle management: the urban cycle model. *Water Sci. Technol.* 52 (9), 1–9.
- Harris P. G. (2012) *Environmental policy and sustainable development in China: Hong Kong in global context*. Bristol: The Policy Press.
- Hatt B., Deletic A., Fletcher T. (2004) *Integrated Stormwater Treatment and Re-Use Systems – Inventory of Australian Practice Technical Report*. Research Centre for Catchment Hydrology, Melbourne.
- Hawkins E., Sutton R. (2011) The potential to narrow uncertainty in projections of regional precipitation change. *Clim. Dyn.* 37 (1e2), 407e418.
- Hibbard K. A., Meehl G. A., Cox P. A., Friedlingstein P. (2007) A strategy for climate change stabilization experiments. *EOS Transactions AGU*, 88, 217–221.
- Hillier J. (2002) *Shadows of power*. London, Routledge.
- Holeton C., Chambers P. A., Grace L., Kidd K. (2011) Wastewater release and its impacts on Canadian waters. *Can. J. Fish. Aquat. Sci.*, 68(10), 1836–1859.
- Huang J., Du P., Ao C., Lei M., Zhao D., Ho M., Wang Z. (2007) Characterization of surface runoff from a subtropics urban catchment. *J. Environ. Sci.* 19 (2), 148– 152.
- Huber W.C., Dickinson R.E. (1988) *Storm Water Management Model—SWMM, Version 4 User’s Manual*. US Environmental Protection Agency, Athens Georgia, USA.
- Huntington T.G. (2006) Evidence for intensification of the global water cycle: review and synthesis. *Journal of Hydrology* 319, 1–4.
- Huong H. T. L., Pathirana A. (2011) Urbanization and climate change impacts on future urban flood risk in Can Tho city, Vietnam. *Hydrology and Earth System Sciences Discussions* 8, 10781–10824.

- Hurt G. C., et al. (2011) Harmonization of land-use scenarios for the period 1500– 2100: 600 years of global gridded annual land-use transitions, wood harvest, and resulting secondary lands. *Clim. Change*, 109, 117–161.
- ICLEI Canada (2015). Finding the Nexus: Exploring Climate Change Adaptation and Planning. http://www.icleicanada.org/images/icleicanada/pdfs/Nexus_Series_Adaptation_Biodiversity_Final_sm.pdf.
- IDA Spildevandskomiteen (2005) Guideline No. 27, Functional Practice for Sewer Systems under Rainfall (Skript 27, Funktionspraksis for afløbssystemer under regn). Ingeniørforeningen i Danmark, IDA Spildevandskomiteen, Denmark (in Danish).
- Im S., Brannan K.M., Mostaghimi S., Kim S.M. (2003) Comparison of HSPF and SWAT models performance for runoff and sediment yield prediction. *Journal of Environmental Science and Health: Part A Toxic/Hazardous Substances and Environmental Engineering* 42, 1561–70.
- Incontrera A. (2014) Development of an early warning system to predict sewer overflow. University of Palermo. Ph.D.thesis.
- Ineichen P. (2006) Comparison of eight clear sky broadband models against 16 independent data banks. *Solar Energy*, 80:468-78.
- Intergovernmental Panel on Climate Change (IPCC) (2013) Climate change: The physical science basis. In: Stocker TF et al (eds) Contribution of working group I to the fifth assessment report of the intergovernmental panel on climate change. Cambridge University Press, Cambridge.
- Intergovernmental Panel on Climate Change (IPCC) (2007) Climate change: Synthesis Report. Contribution of Working Groups I, II and III to the Fourth Assessment Report of the Intergovernmental Panel on Climate Change [Core Writing Team, Pachauri, R.K and Reisinger, A. (eds.)]. IPCC, Geneva, Switzerland, 104 pp.
- Intergovernmental Panel on Climate Change (IPCC) (2012) Climate change: Managing the risks of extreme events and disasters to advance climate change adaptation. A special report of Working Groups I and II of the Intergovernmental Panel on climate change. Cambridge University Press, Cambridge
- Jayaraman K (2010) Bt brinjal splits Indian.
- Intergovernmental Panel on Climate Change (IPCC) (2014) Climate change: Impacts, adaptation, and vulnerability working group II AR5 glossary Available at <http://www.ipcc.ch/report/ar5/wg2/>.
- Istat (2016) Popolazione residente.

- Ivanov V.Y., Bras R.L., Curtis D.C. (2007) A weather generator for hydrological, ecological, and agricultural applications. *Water Resour. Res.* 43 (10), W10406. <http://dx.doi.org/10.1029/2006WR005364>.
- Jenkins K., Surminski S., Hall J., Crick F., et al. (2016) Assessing surface water flood risk and management strategies under future climate change: an agent-based model approach Grantham Research Institute on Climate Change and the Environment.
- Jha M.K. (2005) Hydrological modelling and climate change study in the Upper Mississippi River Basin using SWAT. PhD dissertation, Department of Civil Engineering, Iowa State University.
- Jiang T., Chen Y.D., Xu C., Chen X., Chen X., Singh V.P. (2007) Comparison of hydrological impacts of climate change simulated by six hydrological models in the Dongjiang Basin, South China. *Journal of Hydrology* 336, 316–33.
- Johns T. C., et al., (2011) Climate change under aggressive mitigation: The ENSEMBLES multi-model experiment. *Clim. Dyn.*, 37, 1975–2003.
- Jones H. P., Hole D. G., Zavaleta E. S. (2012) Harnessing Nature To Help People Adapt To Climate Change. *Nature Climate Change*, 2(7), 504-509.
- Kahane J.P., Peyriere J. (1976) Sur certaines mertingales de Benoit Mandelbrot. *Adv. Math.* 22, 131–145.
- Kahinda J.M., Taigbenu A.E., Boroto R.J. (2010) Domestic rainwater harvesting as an adaptation measure to climate change in South Africa. *Physics and Chemistry of the Earth, Parts A/B/C, Volume 35, Issues 13–14, 2010, Pages 742-751, ISSN 1474-7065*.
- Kalra A, Ahmad S (2009) Using Oceanic-atmospheric oscillations for long lead time streamflow forecasting. *Water Resour Res* 45(3): DOI:10.1029/2008WR006855.
- Kalra A., Ahmad S. (2011) Evaluating changes and estimating seasonal precipitation for Colorado River Basin using stochastic nonparametric disaggregation technique. *Water Resour Res* 47: W05555.
- Kang N., Kim S., Kim Y., Noh H., Hong S. J., Kim H. S. (2016) Urban Drainage System Improvement for Climate Change Adaptation Water, Multidisciplinary Digital Publishing Institute, 8, 268
- Kaplan S. (1995) The Restorative Benefits of Nature: Toward an Integrative Framework. *Journal of Environmental Psychology*, 15, n.3 (Sep): 169-1982.
- Kattenberg A., et al., (1996) Climate models—Projections of future climate. In: *Climate Change 1995: The Science of Climate Change. Contribution of WGI to the Second Assessment Report of the Intergovernmental Panel on Climate Change* [J. T. Houghton, L. G. Meira . A.

- Callander, N. Harris, A. Kattenberg and K. Maskell (eds.)). Cambridge University Press, Cambridge, United Kingdom, and New York, NY, USA, pp. 285–357.
- Katz R.W., Parlange M.B. (1998) Overdispersion phenomenon in stochastic modeling of precipitation. *J. Climate*, 11:591-601.
- Kaufmann J. L., Jacobs H. M. (1987) A public planning perspective on strategic planning. *Journal of the American Planning Association*, 62, 460–472.
- Kay A.L., Davies H.N., Bell V.A., Jones R.G. (2009) Comparison of uncertainty sources for climate change impacts: flood frequency in England. *Climatic Change* 92, 41–63.
- Kay A.L., Jones R.G., Reynard N.S. (2006) RCM rainfall for UK flood frequency estimation. II: Climate change results. *Journal of Hydrology* 318, 163–72.
- Khedun C. P., Singh V. P. (2014) Climate change, water, and health: a review of regional challenges *Water Quality, Exposure and Health*, Springer, 6, 7-17
- Kleidorfer M., Moderl M., Sitzenfrei R., Urich C., Rauch W. (2009) A case independent approach on the impact of climate change effects on combined sewer system performance.
- Kleinen T., Petschel-Held G. (2007) Integrated assessment of changes in flooding probabilities due to climate change. *Climatic Change* 81, 283–312.
- Knutti R. (2008) Should we believe model predictions of future climate change? *Philosophical Trans. R. Soc. A* 366, 4647e4664.
- Kundzewicz Z.W., Mata L.J., Arnell N.W., Döll P., Kabat P., Jiménez B., Miller K.A., Oki T., Sen Z., Shiklomanov I.A. (2007) Freshwater resources and their management. In Parry, M.L., Canziani, O.F., Palutikof, J.P., van der Linden, P.J. and Hanson, C.E., editors, *Climate change 2007: impacts, adaptation and vulnerability. Contribution of Working Group II to the Fourth Assessment Report of the Intergovernmental Panel on Climate Change*, Cambridge, UK: Cambridge University Press, 173–210.
- Kundzewicz Z.W., Radziejewski M., Pinskiwar I. (2006) Precipitation extremes in the changing climate of Europe. *Climate Research* 31: 51-58.
- Kundzewicz Z.W., Ulbrich U., Brücher T., Graczyk D., Krüger A., Leckebusch G.C., Menzel L., Pinskiwar I., Radziejewski M., Szwed M. (2005) Summer floods in central Europe – climate change track? *Natural Hazards* 36, 165–89.
- Kunkel K.E., Andsager K., Easterling D.R. (1999) Long-term trends in extreme precipitation events over the conterminous United States and Canada. *J Clim* 12:2515–2527.
- Kutieli H. A. I. M., Maheras P., Guika S. (1996). Circulation and extreme rainfall conditions in the eastern Mediterranean during the last century. *International Journal of Climatology*, 16(1), 73-92.

- Kysely J., Dubrovsky M. (2005) Simulation of extreme temperature events by a stochastic weather generator: effects of interdiurnal and interannual variability reproduction. *Int. J. Climatol.*, 25:251-69.
- Lamarque J., et al., (2010) Historical (1850–2000) gridded anthropogenic and biomass burning emissions of reactive gases and aerosols: Methodology and application. *Atmos. Chem. Phys.*, 10, 7017–7039.
- Lamarque J.-F., et al., (2011) Global and regional evolution of short-lived radiatively active gases and aerosols in the Representative Concentration Pathways. *Clim. Change*, 109, 191–212.
- Lapp D., Eng P. (2005) Engineers and climate change: What you need to know. *Eng. Dimens.*, 26, 51–53.
- Lehner B., Döll P., Alcamo J., Henrichs T., Kaspar F. (2006) Estimating the impact of global change on flood and drought risks in Europe: a continental, integrated analysis. *Climatic Change* 75, 273–99.
- Leith N.A., Chandler R.E. (2010) A framework for interpreting climate model outputs. *Journal of the Royal Statistical Society: Series C (Applied Statistics)* 59, 279–296. doi:10.1111/j.1467-9876.2009.00694.x.
- Leonard M., Lambert M.F., Metcalfe A.V., Cowpertwait P.S.P. (2008) A space–time Neyman–Scott rainfall model with defined storm extent. *Water Resour. Res.*;44(W09402). doi:10.1029/2007WR006110.
- LeRoy P.N., Bledsoe B.P., Cuhaciyan C.O. (2006) Hydrologic variation with land use across the contiguous United States: geomorphic and ecological consequences for stream ecosystems. *Geomorphology* 79 (3), 264–285.
- Levy II H., Horowitz L. W., Schwarzkopf M. D., Ming Y., Golaz J.-C., Naik V., Ramaswamy V. (2013) The roles of aerosol direct and indirect effects in past and future climate change. *J. Geophys.*
- Lindberg S., Nielsen J.B., Carr R. (1989) An integrated PC modelling system for hydraulic analysis of drainage systems, The first Australian Conference on technical computing in the water industry: Watercomp '89, Melbourne, Australia.
- Loukas A., Quick M.C. (1999) The effect of climate change on floods in British Columbia. *Nord Hydrol* 30(3):231–256.
- Loukas A., Vasiliades L., Dalezios N.R. (2002a) Potential climate change impacts on flood producing mechanisms in southern British Columbia, Canada using the CGCMA1 simulation results. *Journal of Hydrology* 259, 163–88.

- Luis M. D., Raventós J., González-Hidalgo J. C., Sánchez J. R., Cortina J. (2000) Spatial analysis of rainfall trends in the region of Valencia (East Spain). *Int. J. Climatol*, 20(12), 1451-1469.
- Madsen H., Arnbjerg-Nielsen K., Mikkelsen P.S. (2009) Update of regional intensity-duration-frequency curves in Denmark: tendency towards increased storm intensities. *Atmospheric Research* 92 (3), 343–349.
- Madsen H., Mikkelsen P.S., Rosbjerg D., Harremoës P. (2002) Regional estimation of rainfall intensity-duration-frequency curves using generalized least squares regression of partial duration series statistics. *Water Resources Research* 38 (11), 1239. doi:10.1029/2001WR001125, 2002.
- Mai Q., Francesch-Huidobro M. (2015) *Climate change governance in Chinese cities*. Abingdon, Oxon: Routledge (Studies in Asia and the Environment).
- Mailhot A., Duchesne S. (2010) Design criteria of urban drainage infrastructures under climate change. *J Water Resour Plann Manage* 136 (2): 201-208.
- Mailhot A., Duchesne S., Caya D., Talbot G. (2007) Assessment of future change in intensity-duration-frequency (IDF) curves for Southern Quebec using the Canadian Regional Climate Model (CRCM). *J Hydrol* 347: 197-210.
- Mailhot A., Duchesne S., Rivard G., Nantel E., Caya D., Villeneuve J. (2006) Climate change impacts on the performance of urban drainage systems for southern Québec. In *Proceeding of the EIC Climate Change Technology Conference*, Ottawa, ON, Canada, 10 May 2006.
- Mailhot A., Rivard G., Duchesne S., Villeneuve J. (2007) *Impacts et Adaptations Liés Aux Changements Climatiques (CC) en Matière de Drainage Urbain au Québec*; Centre Eau, Terre et Environnement: Québec, QC, Canada.
- Mailhot A.; Duchesne S. (2009) Design criteria of urban drainage infrastructures under climate change. *J. Water Resour.*, 136, 201–208.
- Manabe S., Milly P.C.D., Wetherald R. (2004) Simulated long-term changes in river discharge and soil moisture due to global warming. *Hydrological Sciences* 49, 625–42.
- Mandelbrot B.B. (1974) Intermittent turbulence in self-similar cascades: divergence of high moments and dimension of the carrier. *J. Fluid Mech.* 62, 331– 358
- Maraun D., Wetterhall F., Ireson A.M., Chandler R.E., Kendon E.J., Widmann M., Brienen S., Rust H.W., Sauter T., Themel M., Venema V.K.C., Chun K.P., Goodess C.M., Jones R.G., Onof C., Vrac M., Thiele-Eich I. (2010) Precipitation downscaling under climate change: recent developments to bridge the gap between dynamical models and the end user. *Rev. Geophys.* 48, RG3003.

- Mark O., Weesakul S., Apirumanekul C., Aroonnet S. B., Djordjević S. (2004) Potential and limitations of 1D modelling of urban flooding. *Journal of Hydrology*, 299(3), 284-299.
- Maurer M., Herlyn A. (2006) Condition, Costs and Investment Needs of the Swiss Wastewater Infrastructure (Zustand, Kosten und Investitionsbedarf der schweizerischen Abwasserentsorgung). Final report. Eawag, Dübendorf, Switzerland (in German).
- Measham T., Preston B., Smith T., Brooke C., Gorrdard R., Withycombe G., Morrison C. (2011) Adapting to climate change through local municipal planning: barriers and challenges. *Mitig Adapt Strateg Glob Change*, 16:889– 909.
- Meehl G. A., Boer G. J., Covey C., Latif M., Stouffer R. J. (2000) The Coupled Model Intercomparison Project (CMIP). *Bull. Am. Meteorol. Soc.*, 81, 313–318.
- Meehl G. A., et al., (2007b) Global climate projections. In: *Climate Change 2007: The Physical Science Basis. Contribution of Working Group I to the Fourth Assessment Report of the Intergovernmental Panel on Climate Change* [Solomon, S., D. Qin, M. Manning, Z. Chen, M. Marquis, K. B. Averyt, M. Tignor and H. L. Miller (eds.)] Cambridge University Press, Cambridge, United Kingdom and New York, NY, USA, pp. 747–846.
- Meehl G.A., Stocker T.F., Collins W.D., Friedlingstein P., Gaye A.T., Gregory J.M., Kitoh A., Knutti R., Murphy J.M., Noda A., Raper S.C.B., Watterson I.G., Weaver A.G., Zhao Z.C. (2007) Global Climate Projections, in: *Climate Change 2007: The Physical Science Basis, Contribution of Working Group I to the Fourth Assessment Report of the Intergovernmental Panel on Climate Change*, edited by: Solomon, S., Qin, D., Manning, M., Chen, Z., Marquis, M., Averyt, K. B., Tignor, M., and Miller, H. L. *Cambridge University Press, Cambridge, United Kingdom and New York, NY, USA*.
- Meinshausen M., et al., (2011c) The RCP greenhouse gas concentrations and their extensions from 1765 to 2300. *Clim. Change*, 109, 213–241.
- Menabde M., Harris D., Seed A., Austin G., Stow D. (1997) Multiscaling properties of rainfall and bounded random cascades. *Water Resour. Res.* 33 (12), 2823– 2830.
- Menabde M., Sivapalan M. (2000) Modeling of rainfall time series and extremes using the bounded random cascades and Levy-stable distributions. *Water Resour. Res.* 36 (11), 3293–3300.
- Meyer H., Bobbink I., Nijhuis S. (2010) *Delta urbanism: The Netherlands*. Chicago, IL: American Planning Association Available at <http://www.worldcat.org/title/delta-urbanism-the-netherlands/oclc/600991968?page=citationi> .

- Milly P.C.D., Betancourt J., Falkenmark M., Hirsch R.M., Kundzewicz Z.W., Lettenmaier D.P., Stouffer R.J. (2008) Stationarity is dead: whither water management? *Science* 319 (5863), 573e574.
- Milly P.C.D., Dunne K.A., Vecchia A.V. (2005) Global pattern of trends in streamflow and water availability in a changing climate. *Nature* 438, 347–50.
- Milly P.C.D., Wetherald R.T., Dunne K.A., Delworth T.L. (2002) Increasing risk of great floods in a changing climate. *Nature* 415(6871):514–517.
- Mirza M.M., Warrick R.A., Ericksen N.J. (2003) The implications of climate change on floods of the Ganges, Brahmaputra and Meghna Rivers in Bangladesh. *Clim Change* 57(3):287–318. doi:10.1023/A: 1022825915791
- Mishra A.K., Singh V.P. (2010) A review of drought concepts. *J Hydrol* 391(1–2):202–216. doi:10.1016/j.jhydrol.2010.07.012
- Mitchell V.G., Deletic A., Fletcher T.D., Hatt B.E., McCarthy D.T. (2007a) Achieving multiple benefits from stormwater harvesting. *Water Sci. Technol.* 55 (4), 135– 144.
- Mitchell V.G., Diaper C. (2005) UVQ: a tool for assessing the water and contaminant balance impacts of urban development scenarios. *Water Sci. Technol.* 52 (12), 91–98.
- Mitchell V.G., Duncan H., Inman M., Rahilly M., Stewart J., Vieritz A., Holt P., Grant A., Fletcher T., Coleman J., Maheepala S., Sharma A., Deletic A., Breen P. (2007b) Integrated urban water modelling – past, present, and future. Joint 13th International Rainwater Catchment Systems Conference and the 5th International Water Sensitive Urban Design Conference, Conference 21–23 August, 2007, Sydney, Australia.
- Mitchell V.G., McMahon T.A., Mein R.G. (2003) Components of the total water balance of an urban catchment. *Environ. Manag.* 32 (6), 735–746.
- Moglen G.E., Vidal G.E.R. (2014) Climate change impact and storm water infrastructure in the Mid-Atlantic region: design mismatch coming. *J Hydrol Eng* 19 (11): DOI:10.1061/(ASCE)HE.1943-5584.0000967.
- Molnar P., Burlando, P. (2005) Preservation of rainfall properties in stochastic disaggregation by a simple random cascade model. *Atmospheric Research*, 77(1), 137-151.
- Moss R. H., et al., (2008) Towards new scenarios for analysis of emissions, climate change, impacts, and response strategies. In: IPCC Expert Meeting Report: Towards New Scenarios. Intergovernmental Panel on Climate Change, Geneva, Switzerland, 132 pp.
- Moss R.H., Edmonds J.A., Hibbard K.A., Manning M.R., Rose S.K., van Vuuren D.P., Carter T.R., Emori S., Kainuma M., Kram T., Meehl G.A., Mitchell J.F.B., Nakicenovic N., Riahi K., Smith S.J., Stouffer R.J., Thomson A.M., Weyant J.P., Wilbanks T.J. (2010) The next

- generation of scenarios for climate change research and assessment. *Nature* 463, 747–756. <http://dx.doi.org/10.1038/nature08823>.
- Mote P.W., Parson E.A., Hamlet A.F., Keeton W.S., Lettenmaier D., Mantua N., Miles E.L., Peterson D.W., Peterson D.L., Slaughter R., Snover A.K. (2003) Preparing for climatic change: the water, salmon, and forests of the Pacific Northwest. *Climatic Change* 61, 45–88.
- Mott MacDonald (2011) Future Impacts on Sewer Systems in England and Wales. Mott MacDonald, Report produced for Ofwat, Cambridge, UK.
- Muneer T., Gul M.S., Kubie J. (2000) Models for estimating solar radiation and illuminance from meteorological parameters. *J. Solar Energy Eng.*, 122:146-53.
- Myhre G., Highwood E., Shine K., Stordal F. (1998) New estimates of radiative forcing due to well mixed greenhouse gases. *Geophys. Res. Lett.*, 25, 2715–2718.
- Naess L. O., Bang G., Eriksen S., Vevatne J. (2005) Institutional adaptation to climate change: Flood responses at municipal level in Norway. *Global Environmental Change*, 15, 125–138.
- NASA (2014) NASA, NOAA Find 2014 Warmest Year in Modern Record. Retrieved from: <http://www.nasa.gov/press/2015/january/nasa-determines-2014warmest-year-in-modern-record>.
- National Research Council (2011) Global change and extreme hydrology: testing conventional wisdom. The National Academies Press, Washington.
- NCDC (2012) Billion-dollar weather/climate events. <http://www.ncdc.noaa.gov/billions/>.
- Nelder J., Mead R. (1965) A Simplex method for function minimization. *Comput. J.*, 7:308-13.
- Nelson D.R., Adger W.D., Brown K. (2007) Adaptation to environmental change: contributions of a resilience framework. *Annual Review of Environment and Resources* 32, 395–419.
- Nelson Valerie I. (2008) “New approaches in decentralized water infrastructure”, Coalition for Alternative Wastewater Treatment, <<http://sustainablewaterforum.org/new/newappreport.pdf>>
- Neumann J.E., Price J., Chinowsky P., Wright L., Ludwig L., Streeter R., Jones R., Smith J.B., Perkins W., Jantarasami L. (2015) Climate change risks to us infrastructure: Impacts on roads, bridges, coastal development, and urban drainage. *Clim. Chang.* 2015, 131, 97–109.
- Nguyen V.T.V., Desramaut N., Nguyen T.D. (2008) Estimation of urban design storms in consideration of GCM-based climate change scenarios. In: Feyen, J., Shannon, K., Neville, M. (Eds.), Proceedings International Conference on ‘Water & Urban Development Paradigms: Towards an Integration of Engineering, Design and Management Approaches’, Leuven, 15–17 September 2008. CRC Press, Taylor & Francis Group, pp. 347–356.

- Nguyen V.T.V., Desramaut N., Nguyen T.D. (2010) Optimal rainfall temporal patterns for urban drainage design in the context of climate change. *Water Science and Technology* 62 (5), 1170–1176.
- Nicholls R. J., Hanson S., Herweijer C., Patmore N., Hallegatte S., Corfee-Morlot J., et al. (2007) Ranking of the world's cities most exposed to coastal flooding today and in the future. In OECD environment working paper no. 1 (ENV/ WKP(2007)1). Paris: OECD.
- Niemczynowicz J. (1989) Impact of the greenhouse effect on sewerage systems – Lund case study. *Hydrological Sciences Journal* 34, 651–666.
- Nilsen V., Lier J., Bjerkholt J., Lindholm O. (2011) Analysing urban floods and combined sewer overflows in a changing climate, *Journal of water and climate change*, 2(4), 260-271.
- Nirupama N., Simonovic S.P. (2007) Increase of flood risk due to urbanisation: a Canadian example. *Natural Hazards* 40, 25–41.
- Nohara D., Kitoh A., Hosaka M., Oki T. (2006) Impact of climate change on river discharge projected by multimodel ensemble. *Journal of Hydrometeorology* 7, 1076–89.
- Ntegeka V., Willems P., Baguis P., Roulin E. (2008) Climate change impact on hydrological extremes along rivers and urban drainage systems — Phase 1. Development of Climate Change Scenarios for Rainfall and ETo. Summary Report Phase 1 of CCI-HYDR Project by K.U.Leuven and Royal Meteorological Institute of Belgium, for the Belgian Science Policy Office, April 2008. 56 pp.
- O'Hara J.K., Georgakakos K.P. (2008) Quantifying the urban water supply impacts of climate change. *Water Resource Management* 22, 1477–97.
- Oki T., Kanae S. (2006) Global hydrological cycles and world water resources. *Science* 313, 1068–72.
- Olofsson M. (2007) Climate Change and Urban Drainage: Future Precipitation and Hydraulic Impact. Licentiate Thesis, Luleå University of Technology, Luleå, Sweden.
- Olsson J. (1998) Evaluation of a cascade model for temporal rainfall disaggregation. *Hydrol. Earth Syst. Sci.* 2, 19–30.
- Olsson J., Berggren K., Olofsson M., Viklander M. (2009) Applying climate model precipitation scenarios for urban hydrological assessment: a case study in Kalmar City, Sweden. *Atmospheric Research* 92, 364–375.
- Olsson J., Dahné J., German J., Westergren B., von Scherling M., Kjellson L., Ohls F., Olsson A. (2010) A study of future discharge load on Stockholm's main sewer system, SMHI Reports climatology, No. 3, SMHI, Norrköping, Sweden (in Swedish).

- Olsson J., Uvo C.B., Jinno K., Kawamura A., Nishiyama K., Koreeda N., Nakashima T., Morita O. (2004) Neural networks for rainfall forecasting by atmospheric downscaling. *Journal of Hydrologic Engineering* 9, 1–12. doi:10.1061/(ASCE)1084-0699(2004) 9:11.
- Olsson J., Willén U., Kawamura A. (2012) Downscaling extreme short-term regional climate model precipitation for urban hydrological applications Hydrology Research, IWA Publishing
- Onof C., Arnbjerg-Nielsen K. (2009) Quantification of anticipated future changes in high resolution design rainfall for urban areas. *Atmospheric Research* 92 (3), 350–363.
- Onof C., Chandler E., Kakou A., Northrop P., Wheeler H.S., Isham V. (2000) Rainfall modeling using Poisson-cluster processes: a review of developments. *Stochast Environ Res Risk Assess*, 14:384-411.
- Over T.M., Gupta V.K. (1994) Statistical analysis of mesoscale rainfall: dependence of a random cascade generator on large scale forcing. *J. Appl. Meteorol.* 33, 1526–1542.
- Over T.M., Gupta V.K. (1996) A space–time theory of mesoscale rainfall using random cascades. *J. Geophys. Res.* 101 (D21), 26319– 26331.
- Pagliara S., Viti C., Gozzini B., Meneguzzo F., Crisci A. (1998) Uncertainties and trends in extreme rainfall series in Tuscany, Italy: effects on urban drainage networks design. *Water Science and Technology* 37, 195–202.
- Palmer T.N., Räisänen J. (2002) Quantifying the risk of extreme seasonal precipitation events in a changing climate. *Nature* 415, 512–14.
- Papa F., Guo Y., Thoman G. (2004) Urban drainage infrastructure planning and management with a changing climate. In *Proceedings of the 57th Canadian Water Resources Association Annual Congress—Water and Climate Change: Knowledge for Better Adaptation*, Montréal, QC, Canada, 16–18 June 2004.
- Parlange M.B., Katz R.W. (2000) An extended version of the Richardson model for simulating daily weather variables. *J. Appl. Meteorol.*, 39:610-22.
- Passerat J., Ouattara N. K., Mouchel J.-M., Rocher V., Servais P. (2011) Impact of an intense combined sewer overflow event on the microbiological water quality of the Seine River. *Water Res.*, 893-903.
- Patz J.A., Kovats R.S. (2002) Hotspots in climate change and human health. *BMJ* 325(7372):1094–1098. doi:10.1136/bmj.325.7372. 1094.
- Payne J.T., Wood A.W., Hamlet A.F., Palmer R.N., Lettenmeier D.P. (2004) Mitigating the effects of climate change on the water resources of the Columbia River Basin. *Climatic Change* 62, 233–56.

- Pedersen A., Mikkelsen P. S., Arnbjerg-Nielsen K. (2012) Climate change induced impacts on urban flood risk influenced by concurrent hazards. *Journal of Flood Risk Management* 5 (3), 203–214.
- Pierpont L. (2008) Simulation-optimization Framework to Support Sustainable Watershed Development by Mimicking the Pre-Development Flow Regime. North Carolina State University, Raleigh, NC, USA Master's Thesis.
- Piervitali E., Colacino M., Conte M. (1998) Rainfall over the Central-Western Mediterranean basin in the period 1951-1995. Part I: Precipitation trends. *Nuovo cimento della Società italiana di fisica. C*, 21(3), 331-344.
- Pinkham R. (2000) Daylighting: New Life for Buried Streams. Old Snowmass, CO: Rocky Mountain Institute.
- Praskievicz S., Chang H.J. (2009) A review of hydrological modeling of basin-scale climate change and urban development impacts. *Progress in Physical Geography* 33 (5): 650-671.
- Prein A.F., Gobiet A., Truhetz H. (2011) Analysis of uncertainty in large scale climate change projections over Europe. *Meteorol. Z.* 20 (4), 383e395.
- Prudhomme C., Reynard N., Crooks S. (2002) Downscaling of global climate models for flood frequency analysis: Where are we now? *Hydrol. Processes* 16 (6): 1137-1150.
- Quinn J. B. (1980) Strategies for change: Logical incrementalism. Homewood, IL: Dow Jones-Irwin.
- Quirnbach M., Papadakis I., Einfalt T., Langstadtler G., Mehlig B. (2009) Analysis of precipitation data from climate model calculations for North Rhine-Westphalia. CD-ROM Proceedings of the 8th International Workshop on Precipitation in Urban Areas, 10–13 December 2009, St.Moritz, Switzerland, pp. 134–138.
- Ragab R., Bromley J., Rosier P., Cooper J.D., Gash J.H.C. (2003) Experimental study of water fluxes in a residential area: rainfall, roof runoff and evaporation. The effect of slope and aspect. *Hydrol. Process.* 17, 2409–2422.
- Räsänen J. (2007) How reliable are climate models? *Tellus* 59A, 2e29.
- Ramaswamy V., et al., (2001) Radiative forcing of climate change. In: *Climate Change 2001: The Scientific Basis. Contribution of Working Group I to the Third Assessment Report of the Intergovernmental Panel on Climate Change* [J. T. Houghton, Y. Ding, D. J. Griggs, M. Noquer, P. J. van der Linden, X. Dai, K. Maskell and C. A. Johnson (eds.)]. Cambridge University Press, Cambridge, United Kingdom and New York, NY, USA pp. 349-416.
- Rauch W., de Toffol S. (2006) On the issue of trend and noise in the estimation of extreme rainfall properties. *Water Science and Technology* 54, 17–24.

- Refsgaard J.C., Arnbjerg-Nielsen K., Drews M., Halsnæs K., Jeppesen E., Madsen H., Markandya A., Olesen J.E., Porter J.R., Christensen J.H. (2013) The role of uncertainty in climate change adaptation strategies e a Danish water management example. *Mitig. Adapt. Strategies Glob. Change* 18 (3), 337e359.
- Richardson C.W., Wright D.A. (1984) WGEN: a model for generating daily weather variables, *ARS 8, USDA-ARS, 1984*.
- Richardson G.R.A., Otero J. (2012) Land use planning tools for local adaptation to climate change. Ottawa, Ont.: Government of Canada, 38 p.
- Rigon R., Bertoldi G., Over T.M. (2006) GEOtop: a distributed hydrological model with coupled water and energy budgets. *J. Hydrometeorol*, 7:371-387.
- Rodriguez-Iturbe I., Cox D., Isham V. (1987) Some models for rainfall based on stochastic point processes. *Proc. Roy. Soc. Lond. Ser. A.*, 410:269-88.
- Rodriguez-Iturbe I., Cox D., Isham V. (1987) Some Models for Rainfall Based on Stochastic Point Processes. In *Proceedings of the Royal Society of London A: Mathematical, Physical and Engineering Sciences*, London, UK.
- Rodriguez-Iturbe I., Cox D., Isham V. (1988) A Point Process Model for Rainfall: Further Developments. In *Proceedings of the Royal Society of London A: Mathematical, Physical and Engineering Sciences*, London, UK.
- Rodriguez-Iturbe I., Eagleson P.S. (1987) Mathematical models of rainstorm events in space and time. *Water Resour Res.*, 23(1):181-90.
- Rogelj J., Meinshausen M., Knutti R. (2012) Global warming under old and new scenarios using IPCC climate sensitivity range estimates. *Nature Clim. Change*, 2, 248–253.
- Rose, J. B., Epstein P. R., Lipp E. K., Sherman B. H., Bernard S. M., Patz J. A. (2001) Climate variability and change in the United States: potential impacts on water-and foodborne diseases caused by microbiologic agents, *Environmental Health Perspectives*, 109(Suppl 2), 211.
- Rosenzweig C., Solecki W. (Eds.) (2001) *Climate change and the global city: The potential consequences of climate variability and change*, Metro east coast report for the US global change research program. New York, NY: Columbian Earth Institute.
- Rossmann L. A. (2010) Storm water management model user's manual, version 5.0 (p. 276). Cincinnati, OH: National Risk Management Research Laboratory, Office of Research and Development.
- Roy A. H., Paul M. J., Wenger S. J. (2010) Urban Stream Ecology. Chapter 16 in Jacqueline Aitkenhead-Peterson and Astrid Volder, eds. *Urban Stream Ecology*. Agronomy Monograph

55. Madison, WI: American Society of Agronomy, Crop Science of America, Soil Science Society of America.
- Salathé Jr. E.P., Mote P.W., Wiley M.W. (2007) Review of scenario selection and downscaling methods for the assessment of climate change impacts on hydrology in the United States Pacific Northwest. *International Journal of Climatology* 27, 1611–21.
- Sample D. J., Liu J. (2014) Optimizing rainwater harvesting systems for the dual purposes of water supply and runoff capture. *J. Clean. Prod.*, 75, 174-194.
- Saraswat C., Kumar P., Mishra B. K. (2016) Assessment of stormwater runoff management practices and governance under climate change and urbanization: An analysis of Bangkok, Hanoi and Tokyo *Environmental Science & Policy, Elsevier*, 64, 101-117.
- Schanze J. (2006) Flood risk management: A basic framework. In J. Schanze, E. Zeman, & J. Marsalek (Eds.), *Flood risk management: Hazards, vulnerability and mitigation measures*. Springer-Link Available at <http://www.springer.com/us/book/9781402045967i>.
- Schertzer D., Lovejoy S. (1987) Physical modelling and analysis of rain and clouds by anisotropic scaling multiplicative processes. *J. Geophys. Res.* 92, 9693– 9714.
- Schreider S., Smith D. I., Jakeman A. J. (2000) Climate change impacts on urban flooding. *Climatic Change* 47, 91–115.
- Schueler T.R. (1994) Review of pollutant removal performance of stormwater ponds and wetlands. *Watershed Protect. Tech.* 1 (1), 17–18.
- Segond M.-L., Neokleous N., Makropoulos C., Onof C., Maksimovic C. (2007) Simulation and spatial–temporal disaggregation of multi-site rainfall data for urban drainage applications. *Hydrological Sciences Journal* 52 (5), 917–935.
- Semadeni-Davies A., Hernebring C., Svensson G., Gustafsson L. (2005) *The Impacts of Climate Change and Urbanisation on Urban Drainage in Helsingborg; Final Report; Department Water Research Engineering, Lund University: Lund, Sweden.*
- Semadeni-Davies A., Hernebring C., Svensson G., Gustafsson L.-G. (2008) The impacts of climate change and urbanisation on drainage in Helsingborg, Sweden: combined sewer system. *Journal of Hydrology* 350, 100–113.
- Semadeni-Davies A., Hernebring C., Svensson G., Gustafsson L.-G. (2008) The impacts of climate change and urbanisation on drainage in Helsingborg, Sweden: Combined sewer system. *Journal of Hydrology* 350, 100–113.
- Semenov M.A., Brooks R.J., Barrow E.M., Richardson C.W. (1998) Comparison of the WGEN and LARS-WG stochastic weather generators for diverse climates. *Climate Res.*, 10:95-107.

- Semmler T, Jacob D (2004) Modeling extreme precipitation events-a climate change simulation for Europe. *Global and Planetary Change* 44: 119-127.
- Shackley S., Deanwood R. (2002) Stakeholder perceptions of climate change impacts at the regional scale: implications for the effectiveness of regional and local responses. *J. Environ. Plan. Manage.* 45 (3), 381–402.
- Sharpley A.N., Williams J.R. (1990) EPIC-Erosion/Productivity impact calculator: 1. Model documentation. *Technical bulletin 1768, US Department of Agriculture, 235 p.*
- Slingo A. (1989) A GCM parameterization for the shortwave radiative properties of water clouds. *J. Atmos. Sci.*, 46(10):1419-27.
- Smith A., Katz R. (2013) US billion-dollar weather and climate disasters: data sources, trends, accuracy and biases. *Nat Hazards* 67(2):387– 410. doi:10.1007/s11069-013-0566-5.
- Smith S. J., van Aardenne J., Klimont Z., Andres R. J., Volke A., Delgado Arias S. (2011) Anthropogenic sulfur dioxide emissions: 1850–2005. *Atmos. Chem. Phys.*, 11, 1101–1116.
- Sousa P.M., Trigo R.M., Aizpurua P., Nieto R., Gimeno L., Garcia-Herrera R. (2011) Trends and extremes of drought indices throughout the 20th century in the Mediterranean. *Nat Hazards Earth Syst Sci* 11(1):33– 51. doi:10.5194/nhess-11-33-2011.
- Spirn A. W. (1984) *The Granite Garden*. New York: Basic Books.
- Srikanthan R., McMahon T.A. (1982) Simulation of annual and monthly rainfalls a preliminary study at five Australian stations. *J. Appl. Meteorol.*, 21:1472-9.
- Srikanthan R., McMahon T.A. (2001) Stochastic generation of annual, monthly and daily climate data: a review. *Hydrol Earth Syst Sci*, 5:653-70.
- Steimo S. (2001) The new institutionalism. In B. Clark & J. Foweraker (Eds.), *The encyclopaedia of democratic thought*. London: Routledge.
- Stephens G.L. (1978) Radiation profiles in extended water clouds: 2. Parameterization schemes. *J. Atmos. Sci.*, 35(11):2123-32.
- Stephens K., Graham P., Reid D. (2002) *A guidebook for British Columbia: Stormwater Planning*. The Ministry of Land, Air and Water Protection, the Province of British Columbia. Retrieved from: <http://www.env.gov.bc.ca/epd/epdpa/mpp/stormwater/guidebook/pdfs/stormwater.pdf>.
- Stern N. (2007) Stern review: The economics of climate change Available at http://mudancasclimaticas.cptec.inpe.br/_rmclima/pdfs/destaques/sternreview_report_complete.pdf.
- Sundberg C., Svensson G., Söderberg H. (2004) Re-framing the assessment of sustainable stormwater systems. *Clean Technol. Environ. Policy* 6 (2), 120–127.

- Sunyer M.A., Madsen H. (2009) A comparison of three weather generators for extreme rainfall simulation in climate change impact studies. CD-ROM Proceedings of the 8th International Workshop on Precipitation in Urban Areas, 10–13 December 2009, St.Moritz, Switzerland, pp. 109–113.
- Sunyer M.A., Madsen H., Ang P.H. (2012) A comparison of different regional climate models and statistical downscaling methods for extreme rainfall estimation under climate change. *Atmos. Res.* 103 (0), 119e128.
- Tait S. J., Ashley R. M., Cashman A., Blanksby J., Saul A. J. (2008) Sewer system operation into the 21st century, study of selected responses from a UK perspective. *Urban Water Journal* 5 (1), 77–86.
- Takle E.S., Brown J.M. (1978) Note on the use of Weibull statistics to characterize wind-speed data. *J. Appl. Meteorol.*, 17:556-9.
- Tang Z., Engel B.A., Pijanowski B.C., Lim K.J. (2005) Forecasting land use change and its environmental impact at a watershed scale. *Journal of Environmental Management* 76, 35–45.
- Tavakol-Davani H., Burian S.J., Devkota J., Apul D. (2015) Performance and cost-based comparison of green and gray infrastructure to control combined sewer overflows *Journal of Sustainable Water in the Built Environment*. Online Publication Date: 27 Oct 2015, DOI: 10.1061/JSWBAY.0000805.
- Tavakol-Davani H., Goharian E., Hansen C. H., Tavakol-Davani, H., Apul, D., Burian S. J. (2016) How does climate change affect combined sewer overflow in a system benefiting from rainwater harvesting systems? *Sustainable Cities and Society*, Elsevier.
- Tavakol-Davani H., Nasser M., Zahraie B. (2013) Improved statistical downscaling of daily precipitation using SDSM platform and data-mining methods. *Int. J. Climatol.*, 33: 2561–2578. doi:10.1002/joc.3611.
- Taylor K. E., Stouffer R. J., Meehl G. A. (2012) A summary of the CMIP5 experiment design. *Bull. Am. Meteorol. Soc.*, 93, 485–498.
- Tebaldi C., Knutti R. (2007) The use of the multi-model ensemble in probabilistic climate projections. *Philos. Trans. R. Soc. A: Math. Phys. Eng. Sci.* 365 (1857), 2053e2075.
- Thodsen H. (2007) The influence of climate change on stream flow in Danish rivers. *Journal of Hydrology* 333, 226–38.
- Travers A., Elrick C., Kay R., Vestergaard O., Olhoff A., Mills A., Dews G. (2012) Ecosystem-based adaptation guidance: moving from principles to practice. UNEP.

- Tsanis I.K., Koutroulis A.G., Daliakopoulos N.I., Jacob D. (2011) Severe climate-induced water shortage and extremes in Crete: A letter. *Climatic Change* 106 (4): 667-677.
- Tucci C. E. M., Collischonn W. (2000) Drenagem urbana e controle de erosão. Instituto de Pesquisas Hidráulicas. Universidade Federal do Rio Grande do Sul- UFRGS. Porto Alegre.
- U.S. EPA (2013). Energy Efficiency in Water and Wastewater Facilities, EPA state and local climate and energy program, Local government climate and energy strategy Guides, A Guide to Developing and Implementing Greenhouse Gas Reduction Programs <<http://www3.epa.gov/statelocalclimate/documents/pdf/wastewater-guide.pdf>> (Dec,26,2015)
- U.S. EPA. (1999) Combined sewer overflows guidance for monitoring and modeling. EPA-832-B-99-002, <<http://www.epa.gov/npdes/pubs/sewer.pdf>> (Jul. 23, 2015).
- U.S. EPA. (2004) Report to congress: impacts and control of combined sewer overflows (CSOs) and sanitary sewer overflows (SSOs). EPA-833-R-04-001, <http://cfpub.epa.gov/npdes/cso/cpolicy_report2004.cfm> (Jul. 7, 2014).
- U.S. EPA. (2008) Combined sewer overflows: demographics.” <<http://cfpub.epa.gov/npdes/cso/demo.cfm>>.
- UKCIP (2001) Socio-economic scenarios for climate change impact assessment: a guide to their use in the UK Climate Impacts Programme. UKCIP, Oxford.
- UKCIP (2013) Local Authority case studies, UK Climate Impacts Programme. <http://www.ukcip.org.uk/case-studies/la-casestudies/> (accessed 20 February 2013).
- UNDESA (Department of Economic and Social Affairs Population Division) (2014) The World Population Situation in 2014: The Concise Report. UNDESA, New York.
- UNDP (United Nations Development Program) (2006) Human Development Report 2006. Beyond Scarcity: Power, Poverty and the Global Water Crisis. UNDP, New York.
- United Nations Agenda 21 (1992) United Nations Conference on Environment & Development . <https://sustainabledevelopment.un.org/content/documents/Agenda21.pdf>.
- USEPA (2002) U.S. Environmental Protection Agency (USEPA). 2000 National Water Quality Inventory. EPA-841-R-02-001. Office of Water, Washington, DC, pp. 207.
- van Vuuren D. P., et al., (2011) RCP3–PD: Exploring the possibilities to limit global mean temperature change to less than 2°C. *Clim. Change*, 109, 95–116.
- VanRheenen N.T., Wood A.W., Palmer R.N. and Lettenmeier D.P. (2004) Potential implications of PCM climate change scenarios for SacramentoSan Joaquin River Basin hydrology and water resources. *Climatic Change* 62, 257–81.

- Verworn H.-R., Krämer S., Becker M., Pfister A. (2008) The impact of climate change on rainfall runoff statistics in the Emscher-Lippe region. Proceedings of the 11th International Conference on Urban Drainage, 31 August–5 September, Edinburgh, Scotland. 10 pp.
- Verworn H.-R., Krämer S., Becker M., Pfister A. (2008) The impact of climate change on rainfall runoff statistics in the Emscher-Lippe region. Proceedings of the 11th International Conference on Urban Drainage, 31 August–5 September, Edinburgh, Scotland. 10 pp.
- Vohland K., Boubacar B. (2009) A review of in situ rainwater harvesting (RWH) practices modifying landscape functions in African drylands. *Agriculture, Ecosystems and Environment*, 131 (2009) 119–127.
- Vrac M., Marbaix P., Peillard D., Naveau P. (2007b) Non-linear statistical downscaling of present and LGM precipitation and temperatures over Europe. *Climate of the Past* 3, 669–682.
- Walker W.E., Harremoës P., Rotmans J., van der Sluijs J.P., Asselt M.B.A., Janssen P., Krayen von Kraus M.P. (2003) Defining uncertainty. A conceptual basis for uncertainty management in model-based decision support. *Integr. Assess.* 4 (1), 5e17.
- Walling D.E., Webb B.W. (1992) Chapter 3: Water quality. I: Physical characteristics. In Calow, P. and G.E. Pettse, editors, *The rivers handbook: Volume 1*, Oxford: Blackwell, 48–72.
- Walsh C. J., Roy A. H., Feminella J. W., Cottingham P. D., Groffman P. M., Morgan R. P. (2005) The urban stream syndrome: Current knowledge and the search for a cure. *J. N. Am. Benthol. Soc.*, 24(3), 706–723.
- Wang L. (2006) Investigating impacts of natural and human-induced environmental changes on hydrological processes and flood hazards using a GISbased hydrological/hydraulic model and remote sensing data. PhD dissertation, Department of Geography, Texas A&M University.
- Waters D., Watt W. E., Marsalek J., Andreson B. C. (2003) Adaptation of a storm drainage system to accommodate increased rainfall resulting from climate change. *Journal of Environmental Planning and Management* 46, 755–770.
- Watt W.E., Waters D., Mclean R. (2003) Climate variability and urban stormwater infrastructure in Canada: context and case studies. Toronto-Niagara region study report and working paper series. Meteorological Service of Canada, Waterloo
- Werner A.D., Alcoe D.W., Ordens C.M., Hutson J.L., Ward J.D., Simmons C.T. (2011) Current practice and future challenges in coastal aquifer management: flux-based and trigger-level approaches with application to an Australian case study. *Water Resour. Manag.* 25 (7), 1831–1853.

- Whitehead P.G., Wilby R.L., Battarbee R.W., Kernan M., Wade AJ (2009) A review of the potential impacts of climate change on surface water quality. *Hydrol Sci J* 54(1):101–123
- Wilby R.L. (2007) A review of climate change impacts on the built environment. *Built Environ* 33(1):31–45
- Wilby R.L., Dawson C.W., Barrow E.M. (2002) SDSM — a decision support tool for the assessment of regional climate change impacts. *Environmental Modelling & Software* 17, 147–159.
- Wilby R.L., Harris I. (2006) A framework for assessing uncertainties in climate change impacts: low-flow scenarios for the River Thames, UK. *Water Resources Research* 42, W02419, DOI: 10.1029/2005WR004065.
- Wilby R.L., Whitehead P.G., Wade A.J., Butterfield D., Davis R.J., Watts G. (2006) Integrated modelling of climate change impacts on water resources and quality in a lowland catchment: River Kennet, UK. *Journal of Hydrology* 330, 204–20.
- Wilby R.L., Wigley T.M.L. (1997) Downscaling general circulation model output: a review of methods and limitations. *Prog. Phys. Geogr.* 21, 530–548.
- Wilks D.S. (1999) Interannual variability and extreme-value characteristics of several stochastic daily precipitation models. *Agric. Forest Meteorol.*, 93:153-69.
- Wilks D.S., Wilby R.L. (1999) The weather generation game: a review of stochastic weather models. *Prog. Phys. Geograph.*, 23:329-57.
- Wilks D.S., Wilby R.L., (1999) The weather generation game: a review of stochastic weather models. *Prog. Phys. Geogr.* 23 (3), 329e357.
- Willems P. (2011) Revision of urban drainage design rules based on extrapolation of design rainfall statistics. 12th International Conference on Urban Drainage, Porto Alegre/Brazil, 10–15 September 2011.
- Willems P., Arnbjerg-Nielsen K., Olsson J., Nguyen V. (2009) Climate change impact assessment on urban rainfall extremes and urban drainage: methodologies en difficulties Rainfall in the urban context: forecasting, risk and climate change, 149-154
- Willems P., Arnbjerg-Nielsen K., Olsson J., Nguyen V.T.V. (2012) Climate change impact assessment on urban rainfall extremes and urban drainage: Methods and shortcomings. *Atmos. Res.* 2012, 103, 106–118.
- Willems P., Vrac M. (2010) Statistical precipitation downscaling for smallscale hydrological impact investigations of climate change. *Journal of Hydrology* 402, 193–205.

- Willems P., Yiou P. (2010) Multidecadal oscillations in rainfall extremes. *Geophysical Research Abstracts*, Vol. 12, EGU2010-10270, 2010: EGU General Assembly 2010, 2–7 May 2010, Vienna.
- Wilson E.B., Hilferty M.M. (1931) Distribution of Chi-square. *Proc. Natl. Acad. Sci. USA*, 17:684-8.
- Wohl E. E. (2000) *Inland Flood hazard*. Cambridge University Press, Cambridge.
- Wong T. H. F., Brown R. (2009) The water sensitive city: principles for practice. *Water Science and Technology* 60 (3), 673–682.
- Wong T., Brown R. (2008) Transitioning to water sensitive cities: ensuring resilience through a new hydro-social contract. 11th International Conference on Urban Drainage, Edinburgh, Scotland, UK.
- Wood A.W., Leung L.R., Sridhar V., Lettenmeier D.P. (2004) Hydrological implications of dynamical and statistical approaches to downscaling climate model outputs. *Climatic Change* 62, 189–216.
- World Meteorological Organization (WMO). (2014) Draft Statement: Global Features. Retrieved from: https://www.wmo.int/pages/mediacentre/press_releases/documents/1009_Draft_Statement_2014.pdf.
- Young O. (1999) *The effectiveness of environmental regimes: Causal connections and behavioural mechanisms*. Mass: MIT Press.
- Zahmatkesh Z., Burian S., Karamouz M., Tavakol-Davanin H., Goharian E. (2014) Low-Impact Development Practices to Mitigate Climate Change Effects on Urban Stormwater Runoff: Case Study of New York City. *J. Irrig. Drain Eng.*, 10.1061/(ASCE)IR.1943-4774.0000770, 04014043
- Zhou Q. (2014) A review of sustainable urban drainage systems considering the climate change and urbanization impacts. *Water* 2014, 6, 976–992.
- Zhou Q., Mikkelsen P. S., Halsnæs K., Arnbjerg-Nielsen K. (2012) Framework for economic pluvial flood risk assessment considering climate change effects and adaptation benefits. *Journal of Hydrology* 414–415, 539–549.
- Zhu J. (2013) Impact of climate change on extreme rainfall across the United States. *J Hydrol Eng* 18 (10): 1301-1309.
- Zhu J., Stone M.C., Forsee W. (2012) Analysis of potential impact of climate change on intensity-duration-frequency (IDF) relationships for six regions in the United States. *J Water and Climate Change* 3 (3): 185-196.